A PROBABILISTIC REPRESENTATION FOR DRAINED CREEP IN CLAYS

by

Dunstan Dou-Shen Chen, M.Eng.

A thesis submitted to the faculty of Graduate Studies and Research in partial fulfillment of the requirements for the degree of Doctor of Philosophy

Department of Civil Engineering and Applied Mechanics
McGill University
Montreal, Quebec
Canada

October, 1975

RÉSUMÉ

Titre: Représentation probabilistique pour le fluage drainé dans les argiles

---

Thèse de doctorat
par Dunstan Dou-Shen Chen

Département du génie civil et de la mécanique appliquée

Université McGill

octobre, 1975

Nous avons procédé à une série de tests consolidés sur le fluage drainé soumis à des pressions d'étreinte de 30, 60, 120 et 240 au pouce carré et ce dans un appareil triaxial comprenant des niveaux contrôlés de température de 68°, 78°, 88° et 98° F. Les spécimens avaient été préparés en laboratoire et le matériau utilisé était une argile kaolinitique dégénérée.

Les résultats démontrent qu'un certain nombre de particules d'argile tendent à se coaguler entre elles et se comportent comme s'il s'agissait d'une unité de liant d'argile. En vue d'expliquer l'interaction physique et la contribution individuelle de cette unité à la création de fluage, l'unité élémentaire a été définie et utilisée comme modèle de base à l'élaboration d'une théorie probabilistique exposée par cette thèse.

Il est prouvé qu'en appliquant la théorie, on dispose d'une méthode systématique pour l'analyse du fluage drainé qui provoque les distributions non homogènes de la tension, de la dilatation et les caractéristiques de retardation des unités élémentaires dans les sols argileux.

ABSTRACT

A series of consolidated, drained creep tests under confining pressures of 30, 60, 120, and 240 psi were performed in triaxial apparatus with controlled temperature levels of 68°, 78°, 88° and 98°F. Specimens were laboratory prepared, and the material used was a degenerate kaolinitic clay.

Evidences have shown that a number of clay particles tend to floc together and behave as if a unit in a clay soil matrix. To account for the physical interaction and individual contribution of the unit to creep performance, the elementary unit has been defined and utilized as a basic model for the development of probabilistic theory presented in the thesis.

It is shown that with the application of the theory, a consistent method of the drained creep analysis is available which accounts for the non-homogeneous distributions of stress, strain and the retardational characteristics of the elementary unit in the clay soils.

ACKNOWLEDGEMENTS

The writer wishes to express his deep appreciation to

Dr. R.N. Yong, Research Director, for his valuable guidance and unceasing encouragement during the course of the preparation of this thesis;

Mrs. Yong, Mr. R. Poon of Canada Cement and Mr. M. Muckler of Dames & Moore for their proofreading of the thesis;

Mrs. E. L. Foster, for proofreading and typing of the text; and

Elisa, my wife, for typing the test data.

This study was financed through the Department of Supply and Services administered by the Earth Science Division of the Defense Research Establish, Ottawa, Canada.

TABLE OF CONTENTS

TABLE OF CONTENTS (Cont'd)

LIST OF FIGURES

LIST OF FIGURES

LIST OF FIGURES

LIST OF TABLES

ABBREVIATIONS

cm	-	centimeter
cgs	-	centimeter-gram-second (system)
fig.	-	figure
gm	-	gram
min.	-	minute; minimum
mm	-	millimeter
mol.	-	mole
no.	-	number
p.	-	page
pp.	-	pages
psi	-	pounds per square inch
sec.	-	second
vol.	-	volume
e.g.	-	for example, for instance
et al.	-	and others
etc.	-	et cetera, and so forth (on)
i.e.	-	that is, that is to say
vs	-	versus
Appl.	-	Applied
ASCE	-	American Society of Civil Engineers
ASME	-	American Society of Mechanical Engineering
ASTM	-	American Standard of Testing and Materials
Chap.	-	Chapter
Civ.	-	Civil
Co.	-	Company
Conf.	-	Conference
Cong.	-	Congress
Dept.	-	Department
Disc.	-	Discussion
Div.	-	Division
Eng.	-	Engineering
Found.	-	Foundation
Hyd.	-	Hydraulics
HW	-	Highway
ICOSMFE	-	International Conference on Soil Mechanics and Foundation Engineering
Inst.	-	Institute
Int.	-	International
J.	-	Journal
Mech.	-	Mechanics
Nat.	-	National
N.Y.	-	New York
Proc.	-	Proceedings
Sci.	-	Science
STP	-	Special Technique Publications
Symp.	-	Symposium
Trans.	-	Transaction

NOTATIONS

PAGE

g_i = degeneracy..... 35

h = Planck's constant (=6.62x10^{-27} erg-sec)..... 12
= height of a cylindrical speciman..... 50

K = the specific rate of chemical reactions..... 10

^{o}K = degree, Kelvin..... 10

k = Boltzmann's constant
(1.38x10^{-16} erg/^{o}K, cgs)..... 12

L(p) = creep function after Laplace transformation. 7

$\bar{L}(p)$ = relaxation function after Laplace
transformation..... 7

ℓ = slope of strain line in a E-($\sigma_1 - \sigma_3$) plot... 77

m = creep potential.....110

n = porosity.....144

p_i = probability of occurrence
of an elementary unit at energy level E_i.... 33

q = loading intensity..... 44

R = the universal gas constant (=1.98 cal/^{o}K mol.
or = 8.31 erg/^{o}K gm mol.)..... 10

T = absolute temperature, temperature..... 10

t = time..... 28

Δu = net rate of flow in direction
of applied force..... 11

$\bar{v}$ = elementary unit (or ped)..... 33

Δv = volume of porewater extrusion..... 51

Z = thickness of the loaded layer..... 44

ΔZ = total settlement..... 44

ΔZ_p = settlement due to primary consolidation..... 44

PAGE

Δz_s = settlement due to secondary consolidation.. 44

α = value of the slope of the mid-range linear portion of a $\log \dot{\epsilon}$ vs $(\sigma_1 - \sigma_3)$ plot.... 29

α_p = primary compressibility coefficient..... 44

α_s = secondary compressibility coefficient..... 44

β = constant..... 35

γ, α = either 0 or 1..... 29

ϵ = microscopic strain.....144

ϵ^* = microscopic strain fluctuation.....144

$\langle \epsilon \rangle$ = mathematical expectation of strain.....144

ϵ_t = total strain of an elementary unit..... 28

ϵ_i = instantaneous strain of an elementary unit. 28

ϵ_r = retarded strain of an elementary unit..... 28

ϵ_f = constant rate strain of an elementary unit. 28

$\dot{\epsilon}$ = time derivative of strain..... 13

ε_t = total deformation (strain)..... 27

ε_i = instantaneous deformation (strain)..... 27

ε_r = retarded deformation (strain)..... 27

$\varepsilon_{r,u}$ = ultimate retarded deformation (strain)..... 36

ε_f = constant rate deformation (strain)..... 27

ε_{ff} = accelerated deformation (strain)..... 27

σ = macroscopic stress..... 29

$\bar{\sigma}$ = standard deviation..... 90

σ_1 = axial stress..... 47

σ_3 = confining pressure..... 47

δ = distance of translation.....131

PAGE

τ = time of retardation..... 37

λ = the distance between two equilibrium positions in the direction of motion..... 11

λ_2 = the mean distance between two adjacent molecules in the moving layer in the direction at right angle to the direction of motion..... 11

λ_s = the distance between neighboring molecules in the direction of motion..... 12

θ = angular rotation.....131

μ = mean..... 90

$\bar{\Omega}$ = canonical ensemble..... 33

$\omega(E_i)$ = number of states accessible to the systems in the ensemble with one system at state i... 34

χ = average displacement in direction of deformation due to a single surmounting of the energy barrier..... 13

CHAPTER 1

INTRODUCTION

1.1 BACKGROUND OF RHEOLOGICAL STUDIES - A SELECTED HISTORICAL REVIEW

"Rheo" in Greek means flow. Rheology is a branch of science that studies the flow phenomena exhibited by various materials.

With the advance of modern technology and because of the requirements of exactness, accurate measuring instruments were developed. They reveal that many materials previously considered as "rigid" would undergo continuous deformation under a sustained loading. Reiner (1949, 1953, 1954, 1960) studied the rheology of building materials and found that many materials exhibit time dependent relationships which include volume creep under hydrostatic stress conditions. His "Twelve Lectures on Theoretical Rheology" stimulated many early rheological investigations (e.g. Reiner, 1969), and established the foundation of rheological studies.

In geological and metallurgical studies, it has been shown that rocks creep under existing tectonic stress (Haefeli, 1965) and metals flow under high stress or at high temperatures even under moderate loadings, (Dorn, 1954; Finnie, 1959; Oding, 1956; Pao and Martin, 1953; etc.). There are many other materials such as high polymers

(Alfrey, 1948), ceramics (Kingery, 1962; Reiner, 1954), asphalt (Abdel-Hady and Herrin, 1966), soils etc., that are not as fluid as liquid but are not as rigid as metals or rocks, however, they all exhibit rheological characteristics when subjected to loads exceeding a critical loading intensity (Abdel-Hady and Herrin, 1966; Tan, 1957, 1961; Vyalov, 1969, etc.). All studies concerning time effects on the mechanical properties of these materials may be categorized under the realm of rheology. It was soon found that the rheological principles can be applied to different disciplines of material science. Not only civil engineers, but also chemists, electricians, and biologists found that rheological principles can be applied to their own fields successfully to describe the time dependent phenomena of the substances they are investigating (Reiner, 1969).

The early approach to the analysis of the time effects on the stress-strain relationships of these materials invariably involve using the simple mechanical models which were the combinations of springs, dashpots or frictional elements representing respectively the idealized elastic, viscous and frictional properties of the substances. With a proper constant assigned to each element, it was found that the mathematical expression of the stress-strain-time relationships may be derived for different idealized substances, e.g. Hookean, Newtonian, St. Venant, Maxwell, Bingham, etc. (Jaeger, 1962;

Schiffman, 1954; Yong and Warkentin, 1966). Furthermore, combinations of these idealized models give different descriptions for a variety of rheological behavior of materials.

Since Terzaghi rationalized the theory of consolidation and established the science of soil mechanics (Terzaghi, 1943), soils engineers were occupied, for some twenty years, trying to establish the basic principles such as settlement and strength characteristics, pore pressure concept, and permeability (Casagrande, 1961; Terzaghi, 1943; Skempton, 1954) for the immediate use in the field. The elasticity theory and simple state of plastic equilibrium were assumed valid in their stress-strain and stability analysis. Secondary time effects were purposely ignored due to its complexity and hence some discrepancies were found between field observations and theoretical calculations (Tan, 1961).

Only in recent years, considerable attention and research activities have been directed towards the study of rheological effects in frozen and unfrozen soils such as creep (Bishop and Lovenbury, 1969; Chen, 1965; Haefeli, 1953), creep rupture (Haefeli, 1965; Saito and Uezawa, 1961; Singh and Mitchell, 1969), strain hardening (Casagrande and Wilson, 1951; Drucker, Gibson and Henkel, 1957; Vyalov and Meschyan, 1969), and long-term strength (Bishop, 1966; Ladanyi, 1972; Murayama, 1969).

Following are a few examples of the early stage of these rheological studies.

— Casagrande and Wilson (1951), studying the effect of rate of loading on strength of clays and shales, found that creep under sustained loading caused loss of strength of some undisturbed samples whereas some laboratory compacted samples and an unsaturated, undisturbed natural soil tested tended to become stronger and stiffer under sustained loads even though water content was kept constant.

— Field observations of creep processes in natural soils, snow and ice combined with laboratory investigations were intensively studied by Haefeli (1953, 1965). From his vast experience with massive movements of ice and snow, he generalized on some of the factors involved in creep, creep pressure, and creep rupture of ice and soil materials under field situations. It was found that creep deformation, with the ability to cause densification and stress reduction, may offer a general increase in the overall stability, however, it may also cause stress concentrations which will lead to failure.

— Geuze and Tan (1953, 1961) investigated the mechanical behavior of clays during creep and relaxation with oedometer tests. They illustrated that the major discrepancy between the Terzaghi's consolidation theory and the larger observed settlements in practice was

caused by the so-called "secondary time effects" due to volume creep and lateral flow of the clay soil strata.

— By examining the strain hardening phenomenon exhibited during the creep tests, Vyalov (1969) introduced the concept into the Volterra-Boltzmann integral equation. He obtained a rheological equation of states which established the relationships amongst intensities of stresses, strains, average pressure and time. He found that the shear creep curves can have an undampened or dampened character, depending on the applied shear stress which exceeds or is less than a salient point on the stress-strain curve. This stress, he stated, corresponds to the structural strength of the soil, and can be taken as the limiting shear stress as well as the limiting long-term strength. He concluded from his experimental results that the stress-strain relationship may be expressed with sufficient accuracy by a linear law until the structural strength is exceeded; thereafter the relationship becomes non-linear.

Without exception, these efforts helped in gaining an understanding of the rheological behavior of clay soils and made it possible to obtain more insight into economical design and construction of structures. In addition, it is apparent that a more accurate prediction of rheological behavior of clay soils can serve as input to analyze against possible failure of structures or

naturally occurring disasters (Saito, 1965, 1969).

In the development of creep theories for soils, two different paths have been taken over the years (Ladanyi, 1972): one aiming at an engineering theory of creep to be used in design work; the other aiming at a physical theory capable of describing the creep phenomena in terms of already established concepts of physics. The engineering theory of creep can be considered as a collection of laws that are found by experience to adequately describe the observed macroscopic manifestations of creep. Typical examples of such theories are that of viscoelasticity (Gross, 1953) and creep of frozen soils (Haefeli, 1953; Vyalov and Maschyan, 1969). On the other hand, the aim of a physical or micromechanistic theory of creep is to establish a set of laws that would be able to describe the observed phenomena of creep in terms of previously established quantities and laws of physics. An example is the theory of creep which is based on the concept of rate processes developed in statistical mechanics to describe the atomic or molecular diffusion phenomena (Andersland and Douglas, 1970; Glastone, Laidler and Eyring, 1941; Mitchell, Campanella and Singh, 1968; Murayama and Shibata, 1961). Each approach has advantages which depend on the problem to be studied. One may be of value in interpreting material properties from a test; another may be used in the calculation of a time dependent

stress or displacement field in the same material (Scott and Ko, 1969).

Many investigations and discussions (Krizek and Kondner, 1965; Schiffman, 1954) have been directed towards the applicability of viscoelasticity theory in the stress-strain-time relations for soils. They showed the potential use of the theory in the field of soil mechanics due to its mathematical simplicity.

The standard method of viscoelastic stress analysis has been employing the Laplace transform of the equation governing the time dependent stress, strain distributions and the boundary conditions. The solution involves solving the resulting elastic type problem and then taking the Laplace inversion for the desired viscoelasticity solution. However, the body shape and the boundary conditions are assumed not to change with time and that linearity is also given.

Creep or relaxation tests are usually employed to investigate the rheological phenomena of the material when a quasi-static state is assumed in the analysis so that the inertia forces can be neglected. It can be shown that these two types of tests are not independent but, after a simple transformation, there exists a reciprocal relation between creep and relaxation functions;

$$(1 + L(P)) (1 - \bar{L}(P)) = 1$$

where $L(P)$ and $\bar{L}(P)$ are creep and relaxation functions ,

respectively after transformation. The structure of this theory is shown on the next page. (Figure 1-1)

A large variety of practical problems can be solved by this method if the laws governing the creep characteristics, i.e. creep or relaxation functions, are known (Finn and Emery, 1972; Krizek and Kondner, 1965). This has been demonstrated by Finn (1972) who used the finite element method of stress analysis in conjunction with the developed stress-strain-time relationships for soils. The creep of an earth slope was theoretically calculated successfully. With the advance of computing technology, the same technique would certainly find its wide range of applicability.

However, there remains a not-yet completely solved problem: the principle of superposition. Though fundamental for the structure of a mathematical theory of linear viscoelasticity, it has been severely limiting the direct extension of this theory to soils because most soils do not exhibit linear stress-strain-time behavior. Gross (1953) has stated that a non-linear theory may be developed in a form similar to that of the linear one. Although some of the non-linear results are available, (Chao, 1960), much more effort can still be exerted along this line of research in order to establish a convenient and practical method for stress-strain-time calculations for soils.

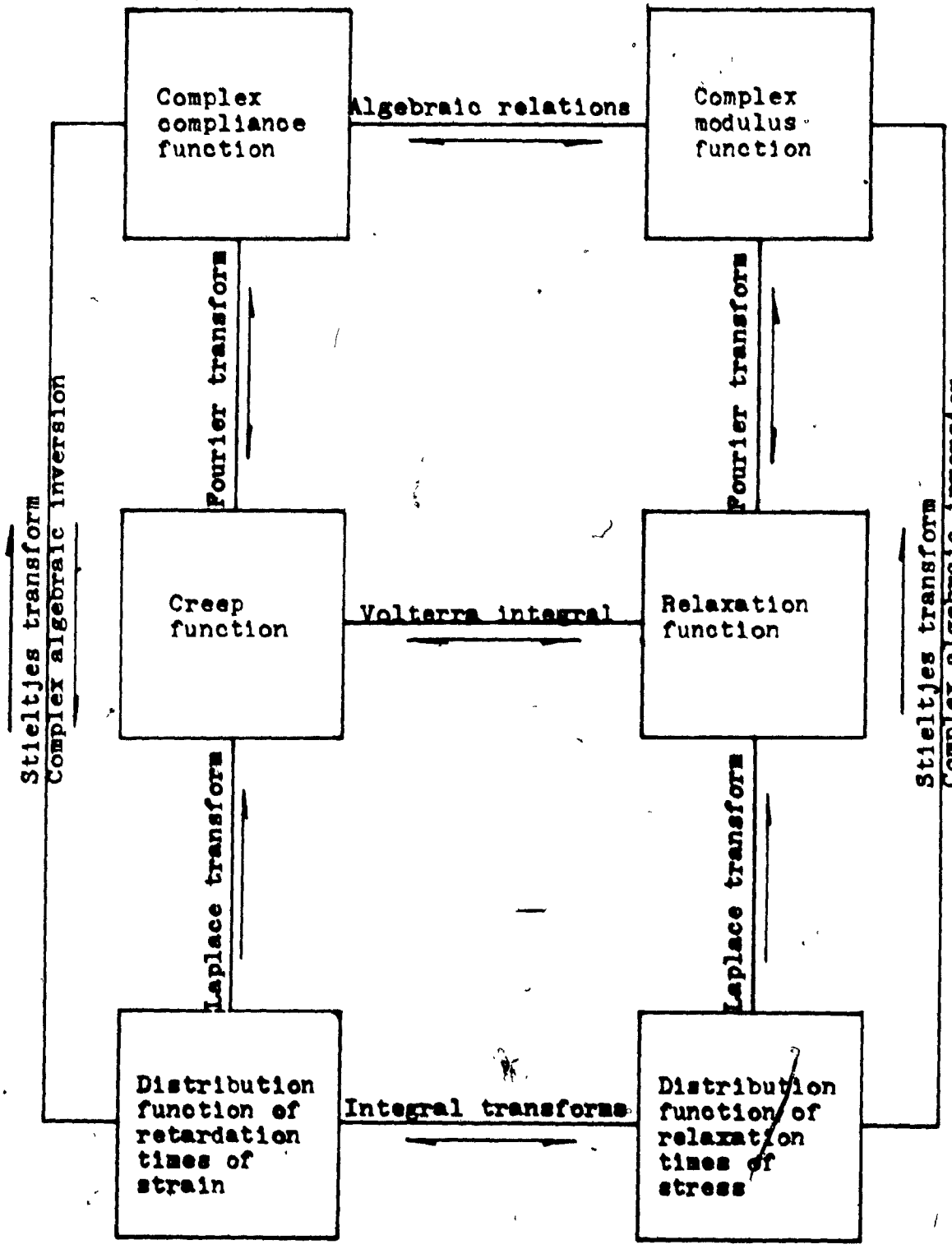

Fig. 1-1 structure of viscoelasticity theory
(B. Gross, 1968)

In order to correlate the rheological properties of soils to the structural configuration of soil particles as well as the influence of temperature on the mechanical behavior of soils, basic physical and chemical properties of soils and various theories potentially applicable to soils are intensively studied by soils researchers. In this regard, the rate process theory is the one among the theories which has received considerable attention in the last decade (Christensen and Wu, 1964; Mitchell, 1961; Murayama and Shibata, 1961; Andersland and Akili, 1967).

The rate process theory, also called absolute reaction rate theory, was developed by Eyring (1941) through statistical mechanics considerations of the following equation proposed by Arhenius:

$$K = Ae^{-\frac{\Delta E}{RT}}$$

K is the specific rate of chemical reactions, A is a frequency factor or collision number, ΔE is termed the "heat of activation" or "energy of activation" of the reaction, R is the universal gas constant = 1.98 cal. $^{o}K^{-1}mole^{-1}$, and T is the absolute temperature. It is generally accepted that a relationship of this kind represents the temperature dependence of the specific rates of most chemical reactions and certain physical processes. Eyring (1941), from the statistical point of

view, considered the exponential factor $e^{-\Delta E/RT}$ in the equation as a measure either of the probability of the occurrence of the activated state or of the fraction of the total number of the reaction elements that possess the requisite activation energy which enables them to take part in reaction. Therefore, the factor A in the equation must have a dimension of a frequency so that the product $Ae^{-\frac{\Delta E}{RT}}$ may give the specific reaction rate. By postulating the existence of "holes" in liquids, he derived an expression for the flow rate in the direction of the applied force f in the following form (Figure 1-2):

$$\Delta u = 2\lambda k \sinh \frac{f\lambda_2\lambda_3\lambda}{2kT}$$

where: $$K = \frac{kT}{h}\frac{F_i}{F}e^{-\frac{\Delta E_0}{kT}}$$

where:

Δu = net rate of flow in the forward direction of the application of the force f,

λ = the distance between two equilibrium positions in the direction of motion,

λ_2 = the mean distance between two adjacent molecules in the moving layer in the direction at right angle to the direction of motion,

λ_s = the distance between neighboring molecules in the direction of motion,

f = applied force in the direction of motion

k = Boltzmann constant = 1.38×1.0^{-16} erg/ ^{o}K,

h = Plank's constant = 6.62×10^{-27} erg-sec,

T = absolute temperature,

$F_{\ddagger}$ = the partition function, for unit volume, of the molecule in the activated states,

F = the partition function, for unit volume, of the molecule in the initial states,

E_o = the energy of activation at 0^{o}K, i.e. the height of energy barrier when no force is acting.

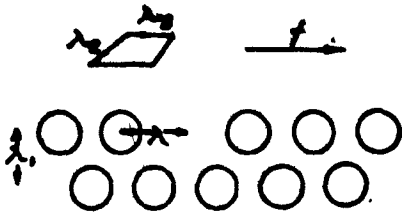

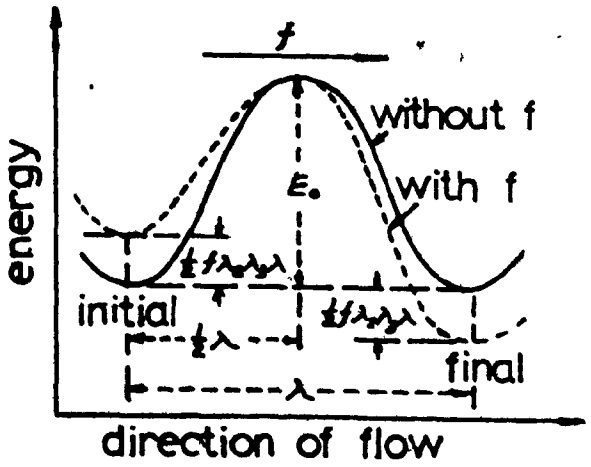

Fig.1-2
energy barrier
(Glasstone, 1941)

After modifications are made (Andersland and Douglás, 1970; Mitchell, 1964), the following practical form is obtained:

$$\dot{\varepsilon} = \chi \frac{kT}{h} e^{-\frac{\Delta E}{RT}}$$

where

$\dot{\varepsilon}$ = rate of strain,

χ = average component of displacement in direction of deformation due to single surmounting of the energy barrier,

ΔE = experimental activation energy.

Details of the derivation of this equation may be found in the literature cited.

Since this theory gives the functional relationship between rate of flow, frequency of mutual exchange of position between reaction elements, applied force, energy barrier to be overcome for a single jump of position, and temperature, it is potentially a powerful theory to describe the creep mechanism in clay soils. Attempts have been made to use this theory to develop an improved understanding of fundamental mechanisms contributing to the shearing resistance of soils and factors controlling time dependent response to stress and strain. Examples of work in this area are Murayama and Shibata (1961, 1964), Mitchell (1964), Christensen and Wu (1964), Andersland and Akili (1967), Mitchell,

Campanella and Singh (1968), Singh and Mitchell (1968) and many others. It has been shown that this theory well describes the functional relationship between rate of flow, stress intensities, and temperature for the undrained creep and the stress relaxation tests they carried out in their investigations. It was also possible for them to evaluate the so-called experimental energy of activation which varies from 2.5×10^{-12} erg for Osaka clay (Murayama and Shibata, 1961, 1964) to 93.6 kcal/mole for the frozen soil tested by Andersland and Akili (1967). This magnitude of the calculated value of the experimental energy of activation is in the range of strength of ionic bonds and, therefore, it was suggested that ionic bonding at contact points between particles is a major controlling mechanism for creep rates of soils.

Although the functional relationships between parameters based on the rate process theory seem to be in conformity with experimental results, there are still some questions remaining unanswered. For example, there is no direct way by which the mechanism of creep in clay soils as postulated in the rate processes theory can be proven. Secondly, the unit of activation energy is expressed as kcal/mole. Since no simple molecular formula can be written for clay soil, it becomes difficult

to explain the physical implications of the value of activation energy thus obtained. Thirdly, it has been shown by Walker (1969), Arulanandan et al. (1971), that in the undrained creep tests, in which the pore pressure was allowed to build up and as high as 90 percent of consolidation pressure was registered, the shear strains are directly related to a gradual but significant increase in excess pore pressure and, hence, reduction in effective confining pressure. Therefore, unless one accounts for the increase in pore pressures during undrained creep, it is unlikely that one will be successful in formulating a generally valid mathematical model for stress-strain-time behavior of fine grained soils based on this type of laboratory testing.

Based on the results of a previous drained creep study (Chen, 1965), where the pore pressure was allowed to dissipate throughout the test, the writer subsequently made a postulate concerning the structure of clay soils as shown on Figure 1-3. In recent years, knowledge gained from theoretical and experimental physico-chemical studies substantiates the fact that both artificial and natural clay soils are indeed made up of clay plates aggregated into peds, crumbs, clusters, or domains (Barden, 1972; Morgenstern, 1969; Sides and Barden, 1971; Yong and McKyes, 1971; Yong and Wakentin, 1975). These lead to the concept of treating the soil mass as a structured material

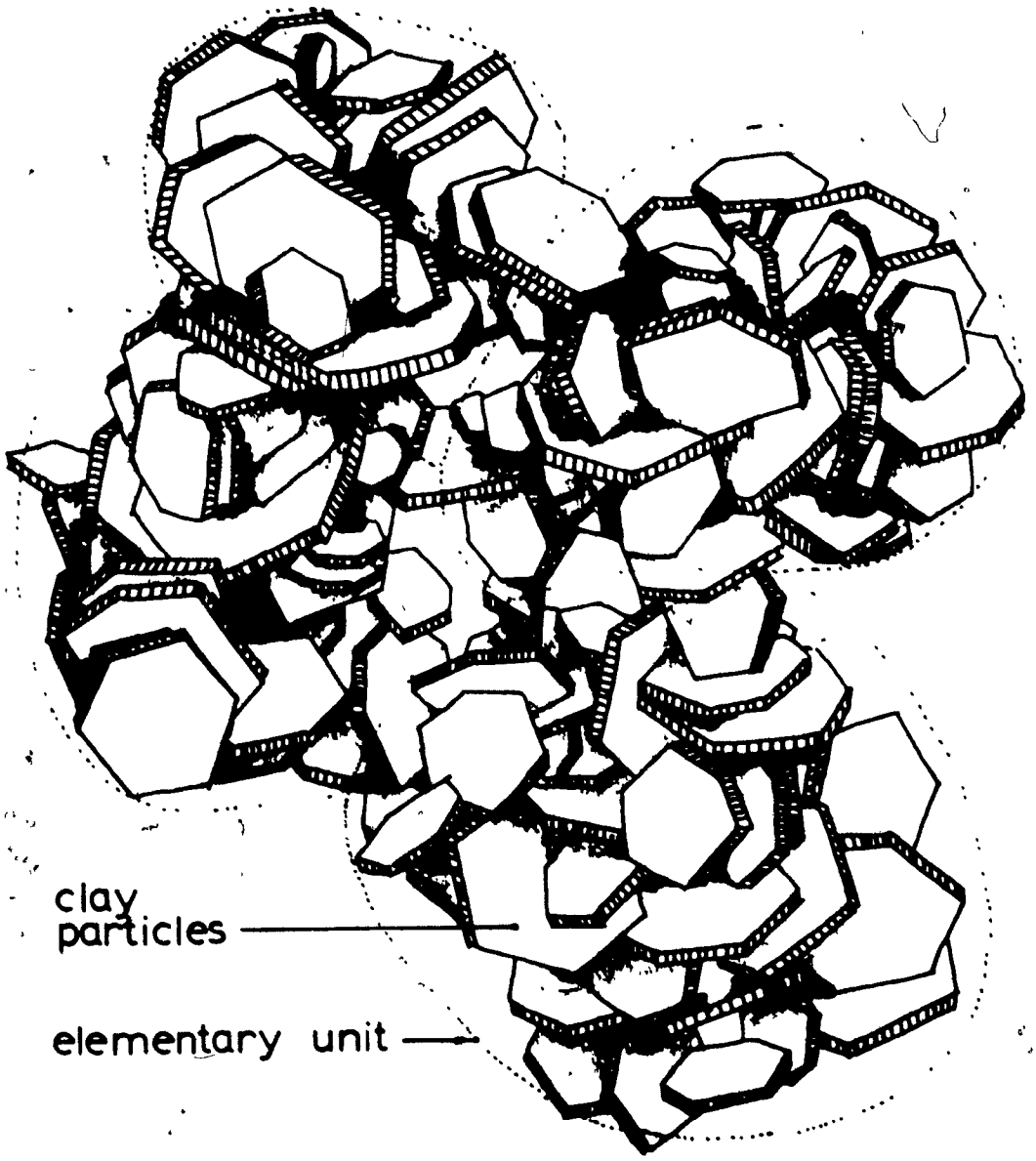

fig.1-3 postulated elementary units

and provide a link between the macro-behavior of soil mass to its micro constituents. New rationale approaches in this regard, especially on rheological and yielding behavior of soils, have been proposed (Axelrad and Yong, 1970; Axelrad, 1971; Barden, 1972; Yong, 1972; Yong and Warkentin, 1975). A random theory of deformation has been developed by Axelrad and Yong (1970) in which they used statistical mechanics and the theory of probability to consider the clay plate aggregate (i.e. ped) as a mesoscopic region and established a first order theory of the rheological behavior of structured media under a delayed impulse function. Yong and Chen (1970, 1972) have experimentally shown that creep of clays may be analyzed by using retardation time distribution methods. They further considered that each ped acts as a unit and is characterized by a retardation time constant. The probability of occurrence of each ped may be evaluated by the distribution of the retardation times. The mathematical expectation of mechanical after effect quantities may, therefore, be obtained.

From the above review of the trend of rheological studies for the past decades in soils, a gradual evolution from field and laboratory identification of rheological behavior of soils towards the theoretical development of a suitable theory which can accurately and practically predict rheological behavior of soils can be observed.

No unanimously accepted theory has yet been established, although a number of equations have been proposed and proven, experimentally, to be accurate enough under prescribed restrictions. A sound engineering theory of rheology, however, as indicated from this review, requires that it has to be based both on an understanding of the physical make-up of the soil mass, e.g. considering a realistic structure of soils and realistic experiments in the field as well as in the laboratory. One example of such an experiment is the long-term drained creep tests carried out by Bishop and Lovenbury (1969) which resembled the conditions that would occur in nature.

Since the basic mechanism involved in the rheological process is not clearly known and due to the lack of convincing experimental results, the endeavour to arrive at a practical engineering theory still needs great efforts from soils researchers and practical engineers for many years to come.

1.2 NEED FOR THE PRESENT STUDY

From the foregoing brief review of the present state of knowledge gained from rheological studies in soil mechanics, it was recognized that it has been considered by many (Krizek and Kondner, 1965; Schiffman, 1954) that the theory of viscoelasticity serves as a convenient tool for the mathematical formulation of phenomenological stress-strain-time relationship while others (Mitchell, 1965; Andersland et. al. 1967, 1970) considered that the rate process theory may be of value in interpreting the mechanism involved in the rheological process in soils. It was also noticed that the lack of linearity between stress and strain severely limited the use of the linear viscoelasticity theory while the integral of the rate of reaction, as given by the rate process theory, does not yield the relationships for the stress-strain-time behavior in creep test (Mitchell, 1964). Such a relationship has been investigated by Singh and Mitchell (1968) by postulating the existence of linear relationships between logarithm of axial strain rate and logarithm of time; logarithm of axial strain rate and stress difference. The functional relationship they obtained are limited to creep deformation under the first application of shear stress. The description of creep behavior for a succession of load increments has not yet been accomplished.

Available literature indicates that most of the creep tests are carried out under undrained conditions. Only a limited number of tests are performed under drained conditions even though they are most consistent with what would occur in nature (Bishop and Lovenbury, 1969). Tests carried out by Arulanandan et al. (1971) and Holzer et al. (1973) have shown that significant pore water pressure was developed in saturated clay samples when creep tests are carried out in an undrained condition. It becomes obvious from the understanding of the influence of effective stress on the strength of soils, unless one accounts for the increase in pore pressures during undrained creep, it is unlikely that one will be successful in formulating a general valid mathematical model for stress-strain-time behavior based on laboratory undrained creep testing. Therefore, in order to maintain a constant effective stress during tests and to simulate the field condition in a long term creep, it will be more desirable if the test is carried out under a fully drained condition. Very little has been done along this line of research, therefore, it is the purpose of this thesis study to obtain both experimental and theoretical background for investigating into a method of deriving such a stress-strain-time relationship for clay soils. The necessity of launching an intensive investigation is clearly indicated.

1.3 SCOPE OF THESIS STUDY

Creep or stress relaxation tests are commonly used in the investigation of rheological behavior of clay soils. For the interest of engineering practice, time dependent deformation under a sustained load, or creep, is one of the behaviors of most man-made structures which causes concern to most engineers. In this thesis study, creep tests on laboratory prepared kaolinitic clay samples were carried out to investigate the fundamental stress-strain-time relationships under fully drained conditions. The triaxial apparatus was chosen for the experimental program because the current methods of deformation and stability analysis call for a range of test data which can be conveniently obtained with such equipment.

The variables used in the investigation include the variation of the confining pressure, temperature, and stress difference. The range of confining pressure chosen was from 30 psi to 240 psi which is within the limit of the general purpose of engineering interest and can be conveniently done in the triaxial apparatus available in the market. Specifically, 30 psi, 60 psi, 120 psi, and 240 psi were used in the tests. The upper limit of 240 psi was chosen by the consideration that the sample consolidation under this confining pressure, the void ratio would be sufficiently low and the volume change due to the application of creep load would be

reduced to a minimum amount. Four different temperature levels (68°, 78°, 88°, and 98°F) were used in this series of tests. For each sample, the temperature was kept constant at one level throughout testing. After consolidating the sample to the desired confining pressure, axial load was applied instantaneously and the sample was allowed to creep until a steady state creep curve was obtained; generally a period of two days was necessary to ensure the attainment of this stage. This was followed by a complete removal of the applied axial load to investigate the recovery behavior of the sample. It was found that 24 hours was needed for the completion of the recovery process. The sample was then loaded to a higher stress-difference level and the above procedure was repeated until the stress reached approximately 80 percent of the unconfined compressive strength of the sample. Each increment of stress difference was approximately 10 percent of the unconfined compressive strength of the sample.

With this test program, it is possible to examine the results in the light of the commonly employed theories such as rate process theory and also to investigate the functional relationships between stress-strain-time and temperature. Little has been done on drained creep tests even though its practical importance is generally recognized. The difference in the rheological behavior

under drained conditions, if any, that can be shown in this study will be of great interest.

1.4 APPROACH OF THESIS STUDY

It is a generally accepted fact that clay soil is a microscopically structured material (Barden, 1972; Tan, 1957; Terzaghi, 1943; Yong and McKyes, 1971; Yong, 1972; Yong and Warkentin, 1975). Almost all physico-chemical theories of clay behavior to date have been based on the interaction of single clay particles. However, there is a growing recognition that both artificial and natural clay soils are made up of clay plates aggregated into peds, crumbs, clusters, or domains (Sides and Barden, 1971; Yong, 1972; Yong and Warkentin, 1975). Yong (1971, 1972) has shown how an orientation macrostructure of aniso-dimensional clay peds can be produced by consolidation or compaction pressures, though the microstructure of these peds may remain essentially random.

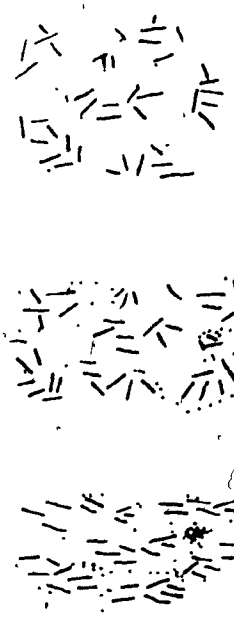

1. initial reorientation of crumbs.
2. accentuated preferred orientation of crumbs.
3. reorientation of crumbs and particles within crumbs

fig. 1-4 Crumb & Particle Orientation under Load (Yong, 1972)

Scanning microscope structure study results by various authors (Barden, 1971, 1972; Morgenstern, 1969; Yong and McKyes, 1971; Yong, 1972) have revealed that almost no single plate "Cardhouse" structure resembles that proposed by Tan (1957), nor that of the honeycomb structure drawn by Terzaghi (1943). In general, the evidence shows the occurrence of a fabric composed of a number of particles tending to floc together with void spaces between flocs (Yong and Warkentin, 1975). These groups of particles are randomly distributed spatially. Therefore, a postulate concerning the fabric of the soil samples was made that the macroscopic body (clay soil sample) possesses a complex three dimensional structure, consisting of a multiplicity of various elementary units (or peds, designated as $\bar{\nu}$). Each unit, in turn, is composed of a number of clay particles. A schematic visualization of particles within elementary units and units interacting to form part of a clay structure is shown in Figure 1-3.

In order to analyze the stress-strain-time behavior of such a heterogeneous structure, the use of a probabilistic treatment of the problem is indicated since the properties of each unit would be as random as structure itself, and the stress-strain distribution among the units will also be highly variable. In previous studies by Axelrad and Yong (1970), the stochastic

approach was applied to obtain a macroscopic yield function based on a viscoelastic model representing a micro volume of clay particles surrounded by fluid (water) matrix. This approach has been under investigation in the last decade at McGill University.

In this thesis study, the basic approach is to accumulate sufficient data which characterizes the drained creep of a laboratory prepared clay soil, the results are examined and discussed in the light of the postulated soil structure and the concepts of various theories. The detail of the proposed approach will be elaborated in Chapter 2, where a probability weighing factor is introduced in the analysis for the derivation of a stress-strain-time relationship. The parameters used in this relationship will be shown in Chapter 5 may be obtained by simple tests carried out in the field or in the laboratory and hopefully this relationship may be used to predict the creep behavior in engineering practice.

CHAPTER 2

THEORETICAL CONSIDERATIONS

2.1 CLASSICAL TREATMENT OF CREEP ANALYSIS

Experimental observations of the creep deformation of materials have shown that many materials which have completely different micro-structures follow a common pattern in their macroscopic behavior during creep deformation.

A typical creep deformation may be conveniently divided into four parts (Figure 2-1):

(a) Instantaneous deformation (designated ε_i)

(b) Retarded deformation (designated ε_r)

(c) Constant rate deformation (designated ε_f)

(d) Accelerated deformation (designated ε_{ff})

or the total deformation (designated ε_t) may be expressed as:

$$\varepsilon_t = \varepsilon_i + \varepsilon_r + \varepsilon_f + \varepsilon_{ff} \qquad \text{.....(2-1-1)}$$

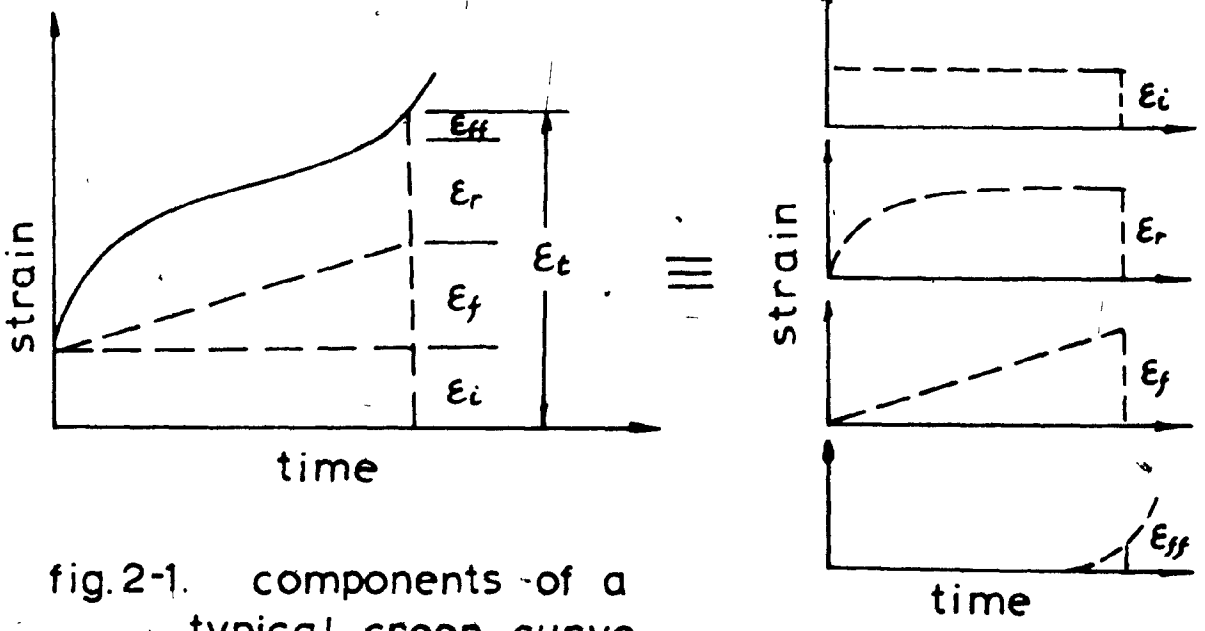

fig. 2-1. components of a typical creep curve

For a moderate loading intensity, ϵ_{ff} is not usually observed for tests carried out in a laboratory, so that for a creep test, the curve obtained may be considered to consist of the first three portions. In a large number of creep tests carried out on many other materials and some granular soils, the constant rate deformation is so small that in their analyses it is usually neglected; however, in clay soils, it may constitute a large portion of the total deformation. Hence, it is of primary importance to take ϵ_f into consideration if a reliable creep analysis is to be obtained for clay soils.

Assuming that this creep pattern applies to the creep performance of an elementary unit designated $\bar{v}$, the deformation of an elementary unit under a sustained load is given by

$$\epsilon_t = \epsilon_i + \epsilon_r + \epsilon_f$$
$$= a\xi + \alpha a' C(t)\xi + \gamma \xi b t \quad \text{.....(2-1-2)}$$

where ϵ_t = total strain of an elementary unit as a function of time t

ϵ_i = instantaneous strain of an elementary unit

ϵ_r = retarded strain of an elementary unit

ϵ_f = constant rate strain of an elementary unit

ξ = microscopic stress acting on the elementary unit

$C(t)$ = creep function depends on t

t = the elapsed time after load application

a', a and b are material constants of the elementary unit and

$\alpha = 0, \gamma = 1$ when ξ is greater than or equal to the yield strength of the elementary unit

$\alpha = 1, \gamma = 0$ when ξ is less than the yield strength of the elementary unit.

The overall creep performance may be expressed in terms of the performance of the elementary units $\bar{v}$ as

$$\varepsilon(t) = \sum_{m \neq \kappa, j} a_m \xi_m + \sum a'_k C_k(t) \xi_k + \sum b_j \xi_j t \quad \text{.....(2-1-3)}$$

where $\varepsilon(t)$ = total strain as a function of time t

ξ_m = stress acting on the unit m

$C_k(t)$ = creep function depends on t and for unit k whose yeild strength is not exceeded

j denotes the unit whose yield strength is attained

m denotes all the existing units in the test sample

a', a_m, b_j are material constants of units.

In terms of the Volterra-Boltzmann relationship

$$\varepsilon(t) = A\sigma + \int_0^t \dot{C}(t-\tau) A' \sigma \, d\tau + B\sigma t \quad \text{.....(2-1-4)}$$

where σ = macroscopic stress

and A, A', B = material constants

In this classical treatment of creep behavior, consideration is given only to the existing units in the test specimen in performing the summation in equation (2-1-3), or the integration in equation (2-1-4). To account for all the accessible units, some statistical treatment is called for. This will be considered in detail in the following section.

2.2 PROPOSED CREEP ANALYSIS

2.2.1 Elementary Unit (Ped) and The Probability of Its Occurrence

The integrity of a saturated, remoulded clay soil is defined by the complex interaction between clay particles and the constituent pore fluids. Clay minerals are alumino-silicates, i.e. oxides of aluminum and silicon with smaller amounts of metal ions substituted within the crystal (Grim, 1953; Yong and Warkentin, 1966). The aluminum oxygen and silicon oxygen combinations are the basic structural units which are bonded together in such a way that sheets of each one result. The stacking of these sheets into layers, the bonding between layers and the substitution of other ions for aluminum and silicon account for the different minerals. This substitution occurs for ions of approximately the same size, and is called isomorphous substitution. Substitution of one for another in the clay crystal lattice and imperfections at the surface, especially at the edges, lead to negative charges on clay particles. It becomes obvious that the presence of clay particle surface forces in a soil water solution would result in complex interactions. Studies (Barden, 1972; Yong, 1972; Yong and Warkentin, 1975) have shown that the flocs or aggregates consisting of a number of particles formed in such a way that they tend to act together as single units are identified herein as elementary units or peds (Figure 1-3).

It is apparent that in a heterogeneous medium such as clay soil, infinite numbers and varieties of elementary units may be formed where interparticle action between elementary units are not necessarily similar. Some form of statistical treatment is necessary if one is to examine and analyze the demonstrated creep behavior of such a soil. It is hence postulated that the macroscopic body (clay soil sample) possesses a complex three dimensional structure, consisting of a multiplicity of various elementary units (each of them in turn composed of a number of particles). Thus, distortion of any unit would involve the physical make-up of each unit as well as the bonding and specific interactions of particles within each unit. The individual performance of each unit, which will be different from other units forming the soil sample, contributes to the overall performance and integrity of a test system. It is further postulated that each elementary unit possesses its own yield strength and deformation characteristic. When the yield strength of any unit is not exceeded, its retardation deformation resembles that of a Kelvin substance and is characterized by a proper retardation time constant. However, when the yield strength of any unit is attained, it would flow in a manner characteristic of a plastic material. Figure 1-3 shows a schematic visualization of particles within elementary units and units interacting to form part of a clay structure. Under external load or by the force

of gravity, local yielding and collapse can occur throughout any one test system. The overall (macroscopic) system stability will hinge on the distribution of representative units. The identification of a representative unit is a matter of direct concern in view of its participation in the definition of system stability and integrity.

Recognizing that the formational characteristics of each elementary unit depend on specific environmental constraints in regard to balance of energy, the probability of occurrence P_m of a ped at a particular level of integrity is a direct function of its energy state E_i, i.e.,

$$P_m = F(E_i) \qquad \text{.....(2-2-1-1)}$$

Whilst several ped structural states may possess the same energy state, the converse does not hold, i.e., there is only one energy state uniquely identified with the structure of any one ped. The necessity for averaging over the energy states, in view of the available spectrum of ped structures, is apparent.

It has been shown by Yong and Chen (1972) that a canonical ensemble of volume Ω (identified as $\bar{\Omega}$) can be constructed such that each ped of volume v (identified as $\bar{v}$) constitutes an elemental system of the ensemble. Eacy system $\bar{v}$ (i.e. ped) of the ensemble $\bar{\Omega}$ may be considered to be in weak thermal interaction with other peds forming the ensemble. Thus, if there exists m peds

or systems in the ensemble $\bar{\Omega}$, each system, together with the other m-1 systems, constitutes a heat reservior (i.e., the ensemble $\bar{\Omega}$ is a heat bath).

The energy of any one system $\bar{\nu}$ is not fixed whilst the energy of $\bar{\Omega}$ is of some constant value between $E^{(o)}$ and $E^{(o)} + \delta E$. It is apparent from the fundamental statistical postulate that, in an equilibrium situation, the probability of occurrence of one system $\bar{\nu}$ in $\bar{\Omega}$ in a state i is a function of the number of states accessible to $\bar{\Omega}$. Thus

$$P_m = c\,\omega(E') \qquad \text{.....(2-2-1-2)}$$

where

$E' = E^{O} - E_i$ = energy of m-1 systems remaining in $\bar{\Omega}$ if any one system has energy E_i,

c = proportionately constant independent of i,

and $\omega(E')$ = number of states accessible to the systems remaining in $\bar{\Omega}$ in view of one system be at state i . (Equation 2-2-1-6).

It follows from the normalization procedure that

$$\Sigma P_m = 1 \qquad \text{.....(2-2-1-3)}$$

where the summation includes all possible states of $\bar{\nu}$. The significance of this statement, in view of the variability of ped structures and its relation to the energy state, should not be minimized.

Since $\bar{\nu} \ll \bar{\Omega}$, it follows that $E_i \ll E^{(o)}$ and thus equation (2-2-1-2) can be approximated by expanding

the logarithm of $\omega(E')$ about the value $E' = E^{(o)}$, giving

$$\log \omega(E^{(o)} - E_i) = \log \omega(E^{(o)}) - \left[\frac{\partial \log \omega}{\partial E'}\right] E_i \qquad \text{.....(2-2-1-4)}$$

Since the term $\left[\frac{\partial \log \omega}{\partial E'}\right]$ is a constant if evaluated at the fixed energy $E' = E^{(o)}$, let this constant be β, equation (2-2-1-4) can now be written as

$$\log \omega(E^{(o)} - E_i) = \log \omega(E^{(o)}) - \beta E_i \qquad \text{.....(2-2-1-5)}$$

Thus

$$\omega(E^{(o)} - E_i) = \omega(E^{(o)}) e^{-\beta E_i} \qquad \text{.....(2-2-1-6)}$$

can be substituted into equation (2-2-1-2) to give

$$P_m = c\, e^{-\beta E_i}\, \omega(E^{(o)}) \qquad \text{.....(2-2-1-7)}$$

Since $\omega(E^{(o)})$ is a constant independent of i, the following expression is obtained

$$P_m = C e^{-\beta E_i} \qquad \text{.....(2-2-1-8)}$$

In view of equation (2-2-1-3),

$$\frac{1}{C} = \sum_m g_i e^{-\beta E_i} \qquad \text{.....(2-2-1-9)}$$

is generally called partition function, hence

$$P_m = \frac{e^{-\beta E_i}}{\sum_m g_i e^{-\beta E_i}} \qquad \text{.....(2-2-1-10)}$$

The particular role of P_m in the overall ensemble stability may be developed in regard to the concept of a "weighing" factor which modifies and contributes to the constitutive performance of the material.

Since there are g_i elementary units which possess the same amount of energy, E_i, therefore the

probability of existence of energy state i is given by

$$P_i = q_i P_m \qquad \text{.....(2-2-1-11)}$$

2.2.2 Stress-Strain-Time Relationship

In equations (2-1-3) and (2-1-4), account is taken only over the existing units in the test specimen in performing the summation in equation (2-1-3) or the integration in equation (2-1-4). To account for all accessible structural states of the ensemble $\bar{\Omega}$, the probability of occurrence of a unit at energy state i, as given by equation (2-2-1-10), which recognizes the availability of q_i unit structural forms, can be introduced into the creep performance evaluation in terms of the mathematical expectation of the total strain $\langle \varepsilon(t) \rangle$. Thus

$$\langle \varepsilon(t) \rangle = \Sigma a_m P_m \xi_m + \Sigma P_k C_k(t) a'_k \xi_k + \Sigma \beta_j b_j \xi_j t \qquad \text{.....(2-2-2-1)}$$

Where m is enlarged to encompass all the accessible states, and similarly for k and j.

In continuous form

$$\langle \varepsilon(t) \rangle = A\sigma + \int_0^t P_k(\tau) \dot{C}_k(t-\tau) A' \sigma \, d\tau + B\sigma t \qquad \text{.....(2-2-2-2)}$$

The second term on the right hand side indicates the anelasticity in an elastic body, i.e. the time delayed effect upon deformation. The ultimate deformation of such a body under a stress increment approaches a finite value (designated ε_{ru}) if sufficient time elapses. The

degree of retardation is determined by the characteristics of the deformed body and is conveniently characterized here by a time constant τ, or so called retardation time.

The retardation time is defined in rheology as the time required for the retarded portion of deformation to reach $(1-e^{-1})$ or 0.632 of its ultimate value under a certain increment of load on a Kelvin substance. Physically, in clay soils, it implies that upon the application of an external load, local pore pressure is induced in the clay soil system. This induced pore pressure dissipates gradually as time elapses. Transfer of stresses from pore fluid to the skeleton formed by the clay particles occurs. This will bring particles closer together and finally this stress increment will be balanced by the solute and matrix potentials and structural bondings. By this time-delayed deforming process, energy is gradually stored in the clay-water system and the rate of the retarded deformation decreases accordingly. Hence, the retardation time thus defined is a characteristic constant of the unit $\bar{v}$ in consideration. The set of retardation times encompassing all units in the ensemble $\bar{\Omega}$ then shows, after normalization, the probability distribution of the existing units and is defined as retardation time distribution. The basic property of this distribution and a method to define the distribution has been developed by T. Alfrey (1954) and further modified by Yong and Chen (1970).

The details of the method are given in Section 2.2.3.

The third term on the right hand side of equations (2-1-3), (2-1-4), (2-2-2-1), and (2-2-2-2) gives the flow strain under the applied sustained-loading. Whenever the stress acting on, or transferring to any unit is equal to or in excess of the strength of the unit, the unit starts to yield and causes continuous dissipation of energy. This explains why the creep process is an irreversible process. However, macroscopically the dissipation of energy and the input of energy, either mechanically or thermally, become equalized and a steady state is achieved. In addition, the breakdown of a strained unit may cause the complete release of the stored strain energy. In the theory of plasticity, this implies that microscopic instability is allowed whilst ensemble performance still maintains the required convex yield surface (Drucker, 1950, 1951, 1959; Hill, 1950; Koiter, 1960).

2.2.3 Retardation Time Distribution Method

At the early stage of rheological studies, tentatives were performed to explain the time-dependent effects of the "anelastic" systems by elementary mechanisms which exhibit superposed elastic and viscous behaviors. All such interpretative theories led to simple exponential laws for stress decay and strain retardation. Comparing with a more complex experimental behavior, one naturally

was led to generalize the theories furthermore by assuming a continuous set of exponential functions with time constants distributed continuously over a finite or infinite interval.

Studying the rheological behavior of high polymers and rubber-like materials, Alfrey (1948) found that the time of retardation is a characteristic property of the molecule of high polymer and the spectrum of the retardation time distribution shows a characteristic distribution of the substance under investigation. Examining the continuous, uniformly increasing creep function represented by the integral:

$$C_r(t) = \int_0^{\infty} f(\tau)(1 - e^{-t/\tau})\, d\tau \qquad \text{.....(2-2-3-1)}$$

in which $f(\tau)$, the distribution function of retardation times of strain, may be graphically evaluated, providing the normalization factor is so determined that

$$\int_0^{\infty} f(\tau)\, d\tau = 1 \qquad \text{.....(2-2-3-2)}$$

The graphical solution, as given by T. Alfrey, consists of the following steps.

1. Plot the retarded portion of strain versus the logarithm of time, thus obtaining an "S" shaped curve.
2. Normalize the curve by dividing the vertical coordinates by $\varepsilon_{r,u}$, the ultimate retarded strain, this gives the accumulative distribution function $F(\tau)$.

For different materials tested, different characteristic distributions of retardation time may be obtained. For high polymers, the retardation time for each molecule is different from other molecules with different structured polymer molecules.

The distribution characteristics may be further extended by the following additional step (Yong and Chen, 1970):

3. The slope at each point on the "S" shaped curve obtained via Step 2 is evaluated and plotted against the logarithm of time, a bell shape distribution curve may thus be obtained.

The bell shape curve obtained in Step 3 is, mathematically, the derivative of $F(\tau)$ with respect to decade of time and is called the distribution density function $f(\tau)$. Since this bell shaped curve shows the distribution of the portion of retarded strain yielded by the molecules characterized by a retardation time τ, it may also physically be interpreted as the distribution of the probability of the occurrence of molecules, where $f(\tau)$ may be regarded as a probability density function identical to $p(\tau)$. Thus, the probability of occurrence of a specific molecular structure with retardation time between $(\tau + \frac{1}{2}d\tau)$ and $(\tau - \frac{1}{2}d\tau)$ may be given by $p(\tau)d\tau$.

The importance of this result is that by this method it will enable one to obtain the probability

weighing factor from series of experimental results. In view of equations (2-2-1-10), (2-2-2-1), and (2-2-2-2), once the term $p(\tau)$ can be defined experimentally, the bridge connecting the theoretical considerations and the observed creep behavior is, therefore, provided. Figure 2-2 shows an example of analyzing the test results by the proposed retardation time distribution method.

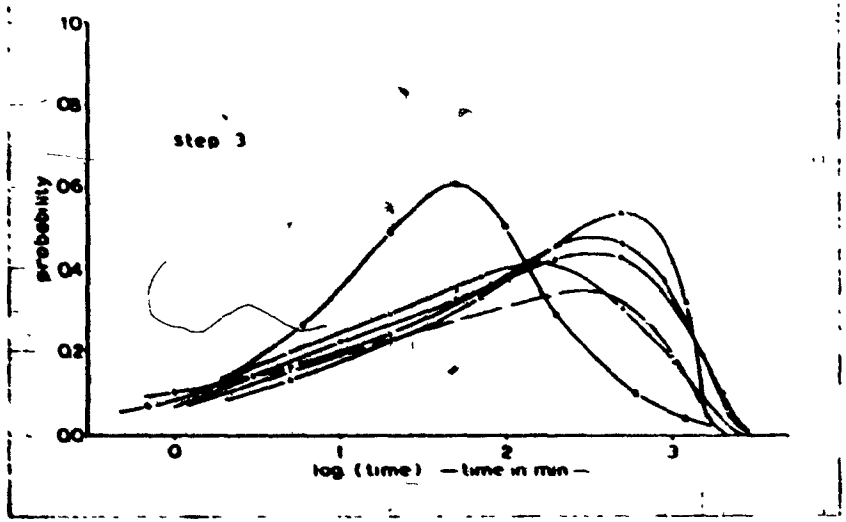

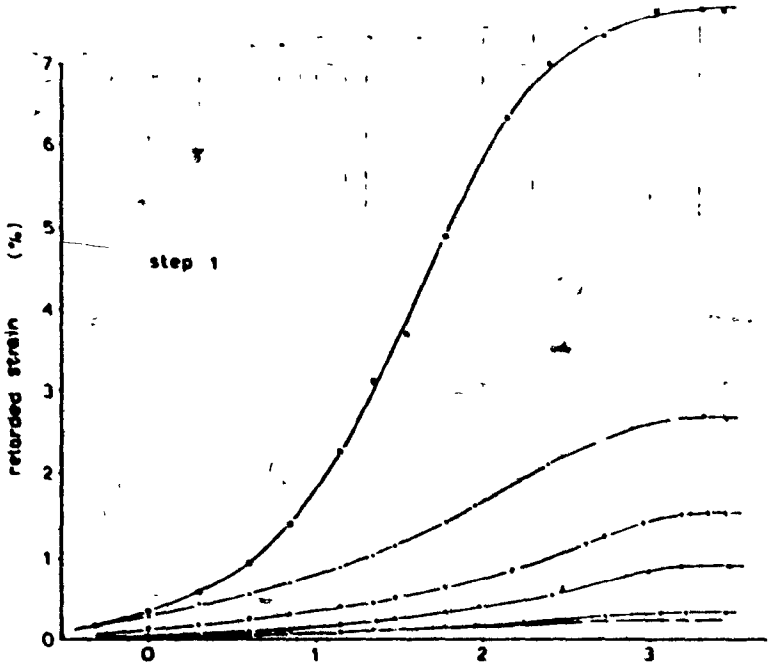

σ_3 = 60 psi T = 98°F

symbol	$(\sigma_1-\sigma_3)$ psi
▲	3.3
●	10.0
■	16.6
◆	23.3
▼	30.0
★	36.6

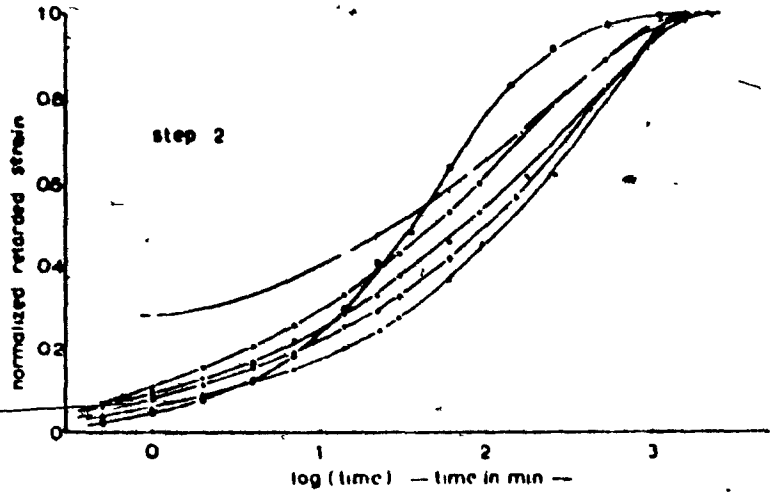

Fig.2-2 retardation time distribution method example

2.3 SUMMARY

In Section 2.1 a typical creep curve is decomposed into three components which represent elastic, retardation and flow characteristics of a creep deformation. Section 2.2 takes into account of the contribution of all the accessible elementary units to the overall creep performance, the probability of occurrence of each unit as given by equation (2-2-1-10) is introduced into the Volterra-Boltzmann relationship, therefore, the mathematical expectation of strain under a sustained load may be expressed by equation (2-2-2-2). The characteristic distribution of probabilities may be evaluated by the proposed "retardation time distribution method" as outlined in Section 2.2.3.

It is seen that the theoretical developments so far are very general in nature. In order to investigate the physical implications of the proposed stress-strain-time relationship, experimental studies of drained creep behavior will be described in the next chapters and the results will be analyzed in the light of the proposed approach as described in this chapter.

CHAPTER 3

VOLUME CHANGE CONSIDERATIONS IN A DRAINED CREEP PROCESS

The consolidation process was initially defined by Terzaghi (1925) as "every process involving a decrease of the water content of a saturated soil without replacement of the water by air", and the end of the consolidation process is when the excess hydrostatic pressure becomes equal to zero. It is seen that the classical theories of consolidation deal primarily with the change of the void ratio accompanying the dissipation of excess pore water pressure and that classical consolidation tests provide measurement and results in terms of the applied effective stresses and the corresponding changes in void ratio of the test specimens.

Observations of the consolidation process demonstrated that volume changes take place long after the pore water pressure has been essentially dissipated. This process is termed secondary consolidation, or secular compression (Buismann, 1936). Buismann appears to be the first to propose a semi-empirical relationship to estimate the amount of secondary consolidation, which is given by:

$$\Delta Z = \Delta Z_p + \Delta Z_s = Z.q\ (\alpha_p + \alpha_s \log t)$$

$$\therefore \quad \Delta Z_s = Z.q.\ \alpha_s \log t \quad \ldots\ldots\ldots (3\text{-}1)$$

where

ΔZ = total settlement

ΔZ_p = settlement due to primary consolidation

ΔZ_s = settlement due to secular compression

Z = thickness of the loaded layer

q = loading intensity

α_p = primary compressibility coefficient

α_s = secular compressibility coefficient

α_p and α_s were considered to be constants, thus demonstrating (by assumption) that secondary consolidation is proportional to the logarithm of time. In fact, these coefficients are functions of pressure, permeability, temperature, etc. (Leonards and Ramiah, 1954), and are not constants. For practical purposes, this relationship has been found to be relatively consistent with respect to correspondence between prediction and experimental observations. It has been found to be valid for the Bell Clay used in this study by a six-month consolidation test (Chen, 1965) (Figure 3-1)

When an additional axial stress, designated $\Delta\sigma_1$, is imposed on a triaxial specimen originally equilibrated under a hydrostatic pressure of σ_3, the test specimen undergoes further consolidation, or anisotropic consolidation, if full drainage is provided. In the case of an

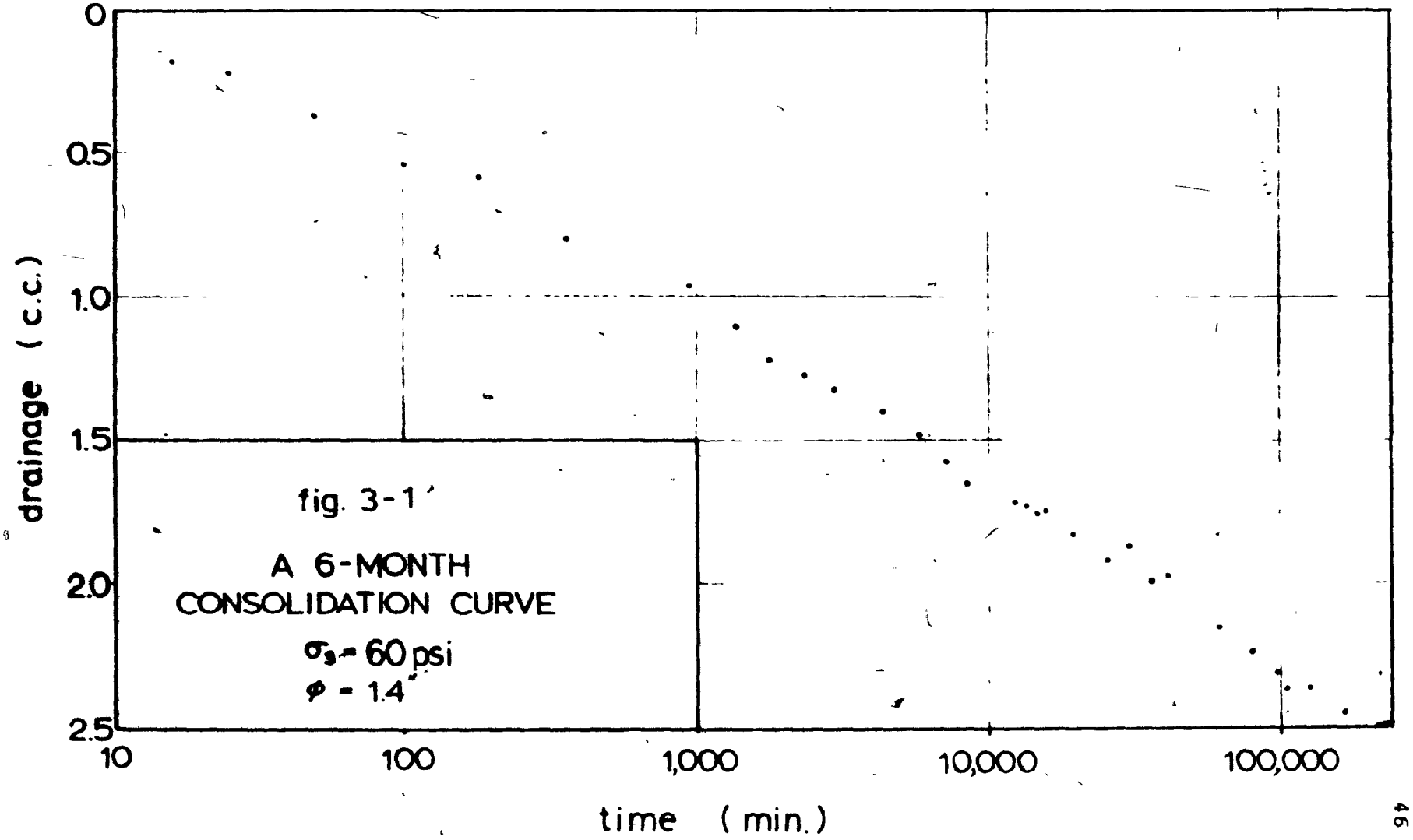
0
0.5
1.0
1.5
2.0
2.5
drainage (c.c.)
10
100
1,000
10,000
100,000
time (min.)
fig. 3-1
A 6-MONTH
CONSOLIDATION CURVE
σ_3 = 60 psi
ϕ = 1.4

undrained test, where the pore water is not allowed to escape, it has been shown that the magnitude of pore water pressure generated by this additional stress depends on a number of factors such as the stress history and the intensity of this additional stress (Skempton, 1954). For a normally consolidated clay and a moderate value of $\Delta\sigma_1$, the magnitude of the pore water pressure generated shortly after stress increment is likely to be approximately equal to the increase in volumetric stress, or 1/3 $\Delta\sigma_1$, i.e. $\frac{1}{3}(\Delta\sigma_1 + \Delta\sigma_2 + \Delta\sigma_3)$ where $\Delta\sigma_2 = \Delta\sigma_3 = 0$. This value has been obtained by Lambe (1969) from a separate consideration of the compressibilities of pore water and the soil skeleton.

If the pore water pressure is allowed to develop further, as in the case of an undrained condition, the magnitude of pore pressure parameter A (defined as $\Delta u/\Delta\sigma_1$), may eventually reach 1/2 to 1 for a normally consolidated clay (Skempton and Bjerrum, 1957), where Δu is the increase in pore water pressure generated by the increase of $\Delta\sigma_1$.

For a creep test carried out under drained conditions, the initially induced pore water pressure due to the application of axial load is allowed to dissipate. However, at the center of the specimen where the drainage path is longest, the generated pore water pressure is expected to take a longer time to be fully dissipated than that would take place at boundaries of the specimen. That

is to say, that creep and consolidation take place simultaneously. It becomes necessary, therefore, to distinguish between axial strain due to creep and the strain due to further extrusion of pore water accompanying the dissipation of pore water pressure.

To delineate the strain due to anisotropic consolidation, especially the secondary portion of the anisotropic consolidation process where the pore water pressure is essentially zero, from the conventional creep strain in this case is conceptually difficult. Because the mechanism of both processes involves the reorientation of clay particles and both may involve the volume change of the clay soil specimen. However, although a creep process at higher stress levels or close to failure stage may cause dilation or contraction of the specimen, for a moderate loading intensity, the volume change involved would be practically insignigicant. This is demonstrated by the observed volume change data obtained from this series of studies which shows that volume change essentially completed six to twelve hours after additional axial load application. Utilizing the conventional concept of consolidation, which is invariably measured in terms of volume change of the soil specimen, and assuming that the volume change is insignificant due to creep, it is suggested in this study that the creep performance be measured in terms of

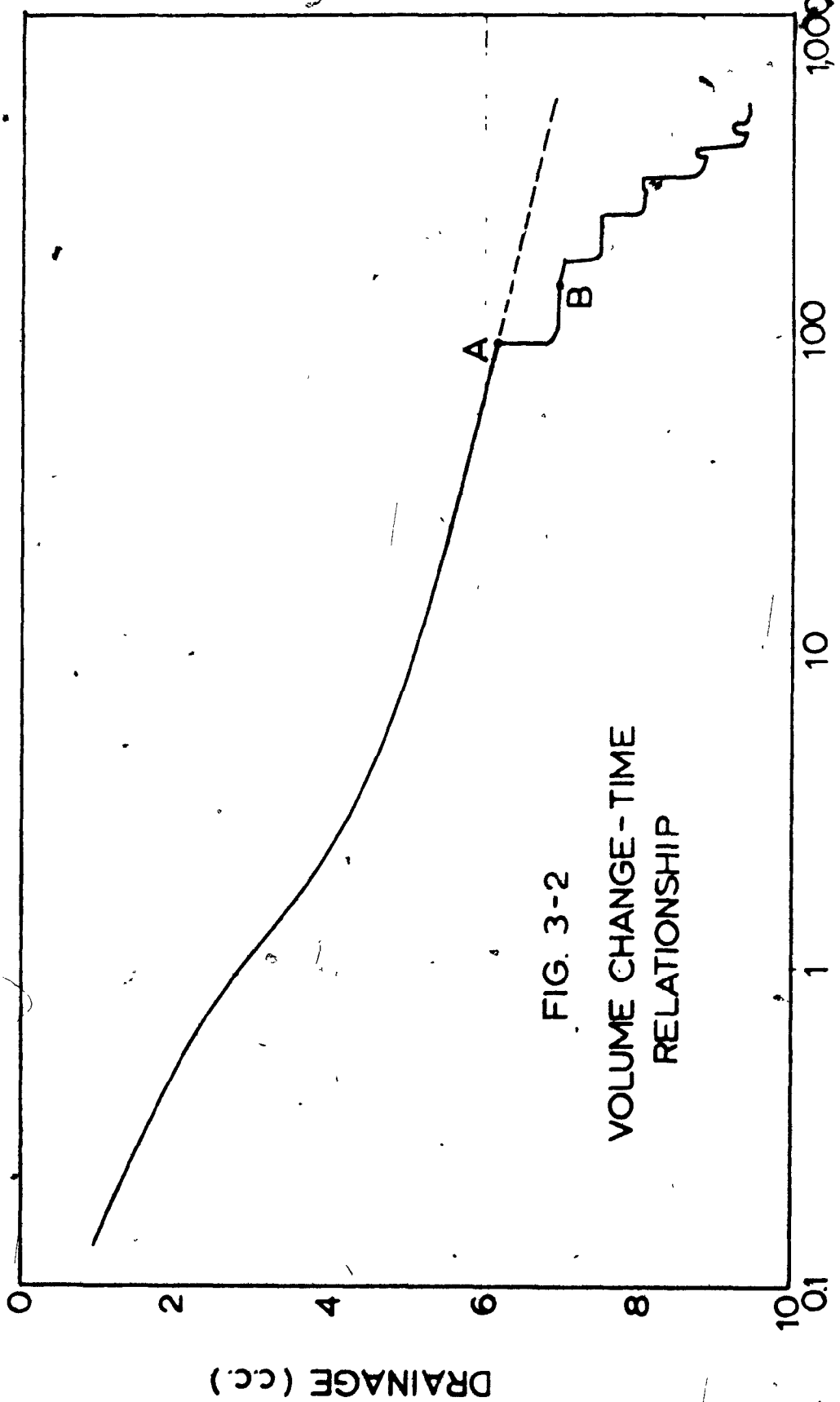

FIG. 3-2
VOLUME CHANGE-TIME
RELATIONSHIP

the axial displacement whereas the consolidation be measured in terms of volume change. The correction for the measured creep displacement for the portion due to consolidation may, therefore, be made by computing the axial strain due to consolidation process from volume change measurements and by comparing that with the measured vertical strain. It is, therefore, possible to distinguish between creep and anisotropic consolidation in a drained triaxial creep test.

Consider Figure 3-2 which shows the volume change versus logarithm of time during consolidation and under additional axial loadings. The sample was consolidated under a designated confining pressure of σ_3 into the secondary stage (i.e. until t_{100} as defined by conventional methods is reached) and a straight line of secondary consolidation curve could be constructed as shown by the dotted line. At the time corresponding to point A, an axial stress increment $\Delta\sigma_1$ was applied instantaneously. Further extrusion of water was measured, as shown by the solid line AB. At the same time, the time dependent vertical deformation of the specimen was also recorded. This vertical deformation obviously consisted of two components, one due to the extrusion of pore water because of the anisotropic consolidation process, and the other due to the time dependent deformation of the specimen without volume change under the sustained loading.

Consider a cylindrical specimen with a diameter d and height h, and with the assumption that the shape

of the cylinder remains cylindrical after volume change, the vertical strain due to the extrusion of pore water of volume ΔV could be evaluated by the following formula:

$$\Delta V = \frac{1}{4}\pi d^2 h - \frac{1}{4}\pi (d-\Delta d)^2 (h-\Delta h)$$

neglect the higher order terms and assumed that $\Delta h = \Delta d$

$$\therefore \left(\frac{\Delta h}{h}\right) = \frac{4\Delta V}{\pi dh(d+2h)} \qquad \ldots\ldots\ldots (3\text{-}2)$$

For a specimen of diameter 1.4-inch and height of 2.8-inch, a volume change of 1 cubic centimeter will result in a vertical strain of 0.00283 inch/inch. As may be seen, this will represent an upper limit because the drainage path in the radial direction is the shortest and it is likely that the contraction in radial direction will be greater than the axial direction if under an increment of all around pressure, while in the calculation $\Delta d = \Delta h$ was assumed.

Figures B-39 to B-42 inclusive in Appendix B show plots of volume change measurements versus logarithm of time for this series of tests carried out under various σ_3 and under axial loads, in steps, up to approximately 80 percent of the unconfined compressive strength of the specimen. For each step, the volume change is approximately 0.5 to 1.0 c.c. Tables B-4a to B-4d inclusive in the same appendix show the detail volume change measurements for each step and the corresponding vertical strains

due to these volume changes. The percentages of total axial strain at each step due to this anisotropic consolidation versus stress levels (percent of unconfined compressive strength) are shown on Figure 3-3. It is seen that at lower stress levels, a significant portion of axial strain is due to anisotropic consolidation; as stress increases to over 40 percent of the unconfined compressive strength of the specimens, the percentage remains relatively constant, within 5 to 10 percent of the total strain.

In general practice, most settlement calculations are based on one dimensional consolidation theory which gives relatively good agreement between prediction and field observation where the thickness of the compressible layer is thin compared to the size of foundation. Whenever there is a thick deposit of compressive layer, either a very low designed pressure is used or resort to other foundation alternatives. However, there are cases where a structure can tolerate large settlements without endangering the structure, for economical reasons, foundations may be built on this thick compressible layer. In such cases, prediction of settlement becomes important. So far no valid theory is available since in this occasion creep would play an important role in the foundation performances.

Since delineation of total settlements into anisotropic consolidation and creep is not conclusive from this study, therefore throughout this study, the analysis is done in terms of the measured total strain and the applied stress. This was thought would provide a means for the total settlement estimation as far as engineering practice is concerned.

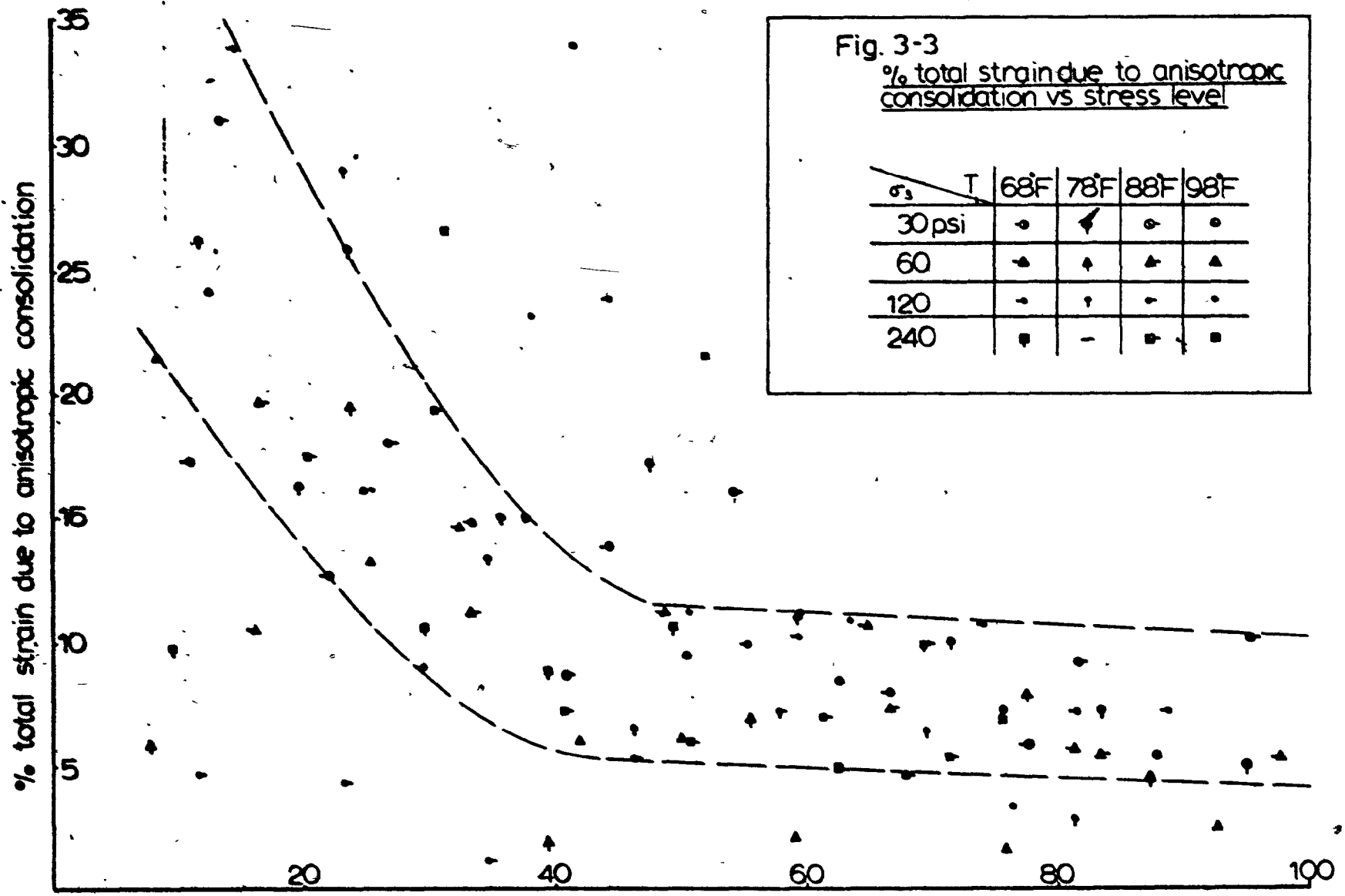

Fig. 3-3
% total strain due to anisotropic consolidation vs stress level

σ_3 \ T	68°F	78°F	88°F	98°F
30 psi	●	◢	○	●
60	▲	▲	▲	▲
120	▬	▮	▬	▬
240	■	–	■	■

CHAPTER 4

EXPERIMENTATION AND TEST RESULTS

Based on the considerations discussed in previous chapters, a series of drained creep testing programs were designed and carried out on laboratory prepared samples with variations of confining pressure, axial load and controlled environmental temperature. A full detailed description of experimentation is given in Appendix A. The following is a brief summary of the test program, material properties, sample preparation and instrumentation used in this experimental study.

4.1 TEST PROGRAM

A total of sixteen kaolinitic clay samples were prepared and tested in this series of drained creep investigations. For each sample five to eight axial loading and unloading steps were applied and a total of ninety-nine creep curves were obtained. Table 4-1 shows a summary of axial loading intensities applied to each sample and the associated confining pressure and temperature used for each test. Test results of Sample Number 14, where leakage was found during the test, were completely discarded.

Confining pressures of 30, 60, 120, and 240 psi were used to consolidate the samples before axial loads were applied to specimens (i.e. dead weights being placed on a loading yoke). For each sample, the consolidation and

Table 4-1 Summary of Test Program

sample no.	1	2	3	4	5	6	7	8	9	10	11	12	13	14	15	16
σ_3	30 psi				60 psi				120 psi				240 psi			
T e-g Fe no. loading	68°F	78°F	88°F	98°F	68°F	78°F	88°F	98°F	68°F	78°F	88°F	98°F	68°F	78°F	88°F	98°F
1	3.3	3.3	3.3	3.3	6.6	3.3	6.6	3.3	13.3	13.3	13.3	13.3	13.3	leakage during test	13.3	13.3
2	6.6	6.6	6.6	6.6	13.3	10.0	13.3	10.0	26.6	26.6	26.6	26.6	26.6		26.6	26.6
3	10.0	10.0	10.0	10.0	20.0	16.6	20.0	16.6	40.0	40.0	40.0	40.0	40.0		40.0	40.0
4	13.3	13.3	13.3	13.3	26.6	23.3	26.6	23.3	53.3	53.3	53.3	53.3	53.3		53.3	53.3
5	16.6	16.6	16.6	16.6	33.0	30.0	33.3	30.0	66.6	66.6	66.6	66.6	66.6		66.6	66.6
6	20.0	20.0	20.0	20.0	40.0	36.6	-	36.6	73.3	80.0	80.0	80.0	80.0		80.0	80.0
7	23.3	23.3	23.3	23.3	-	-	-	-	80.0	93.3	-	-	93.3		93.3	96.7
8	-	26.6	-	-	-	-	-	-	-	-	-	-	-		-	-

creep tests were conducted at a designated temperature level. The temperature levels used in this investigation were 68°, 78°, 88°, and 98°F. Double drainage and slotted filter paper drain, placed around each specimen, were provided. Volume change was measured by using a fine graded burrette to an accuracy of 0.025 cc. After consolidating the sample to the desired confining pressure, axial load was applied instantaneously and the sample was allowed to creep until a steady state was obtained. A period of two days was generally necessary to ensure the attainment of this stage. This was followed by a complete removal of the applied axial load to investigate the recovery behavior of the sample. It was found that 24 hours was generally needed for the completion of the recovery process. The sample was then loaded to a higher stress-difference level with an increment of stress difference equals approximately 10 percent of the unconfined compressive strength of the sample (see the example shown in Figure 4-1). The above procedure was repeated until the stress reached approximately 80 percent of the unconfined compressive strength of the sample. The implied stress paths are shown on Figure 4-2 .

Fig. 4-1
Example of Loading Procedure
σ_3 = 30 psi T = 98°F

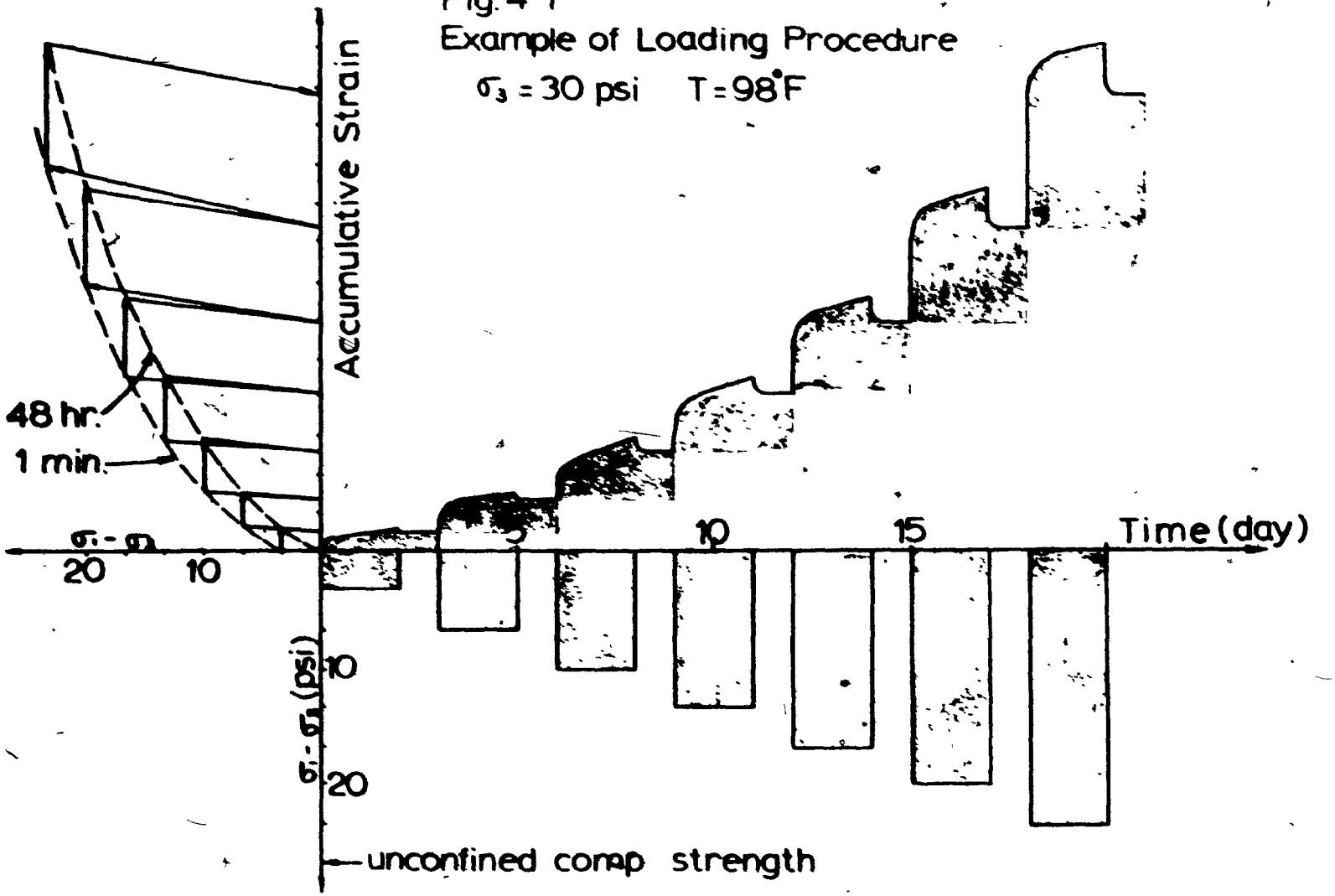

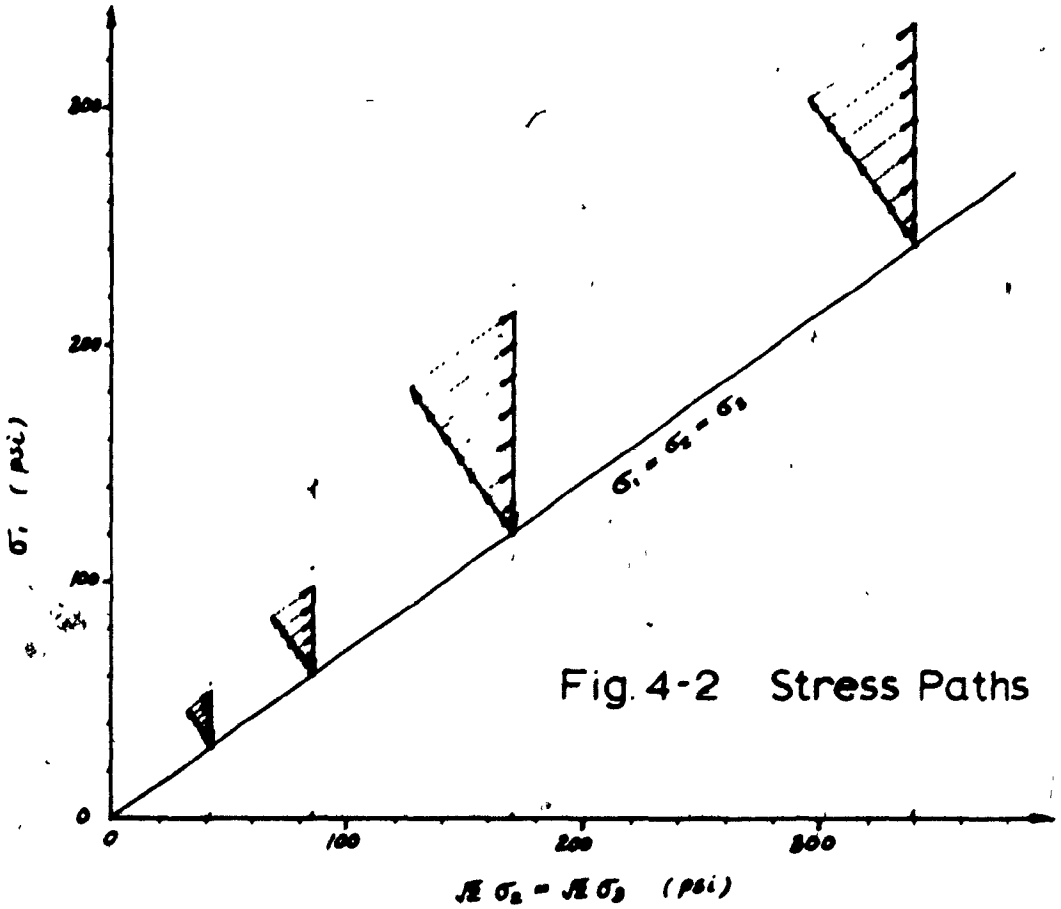

Fig. 4-2 Stress Paths

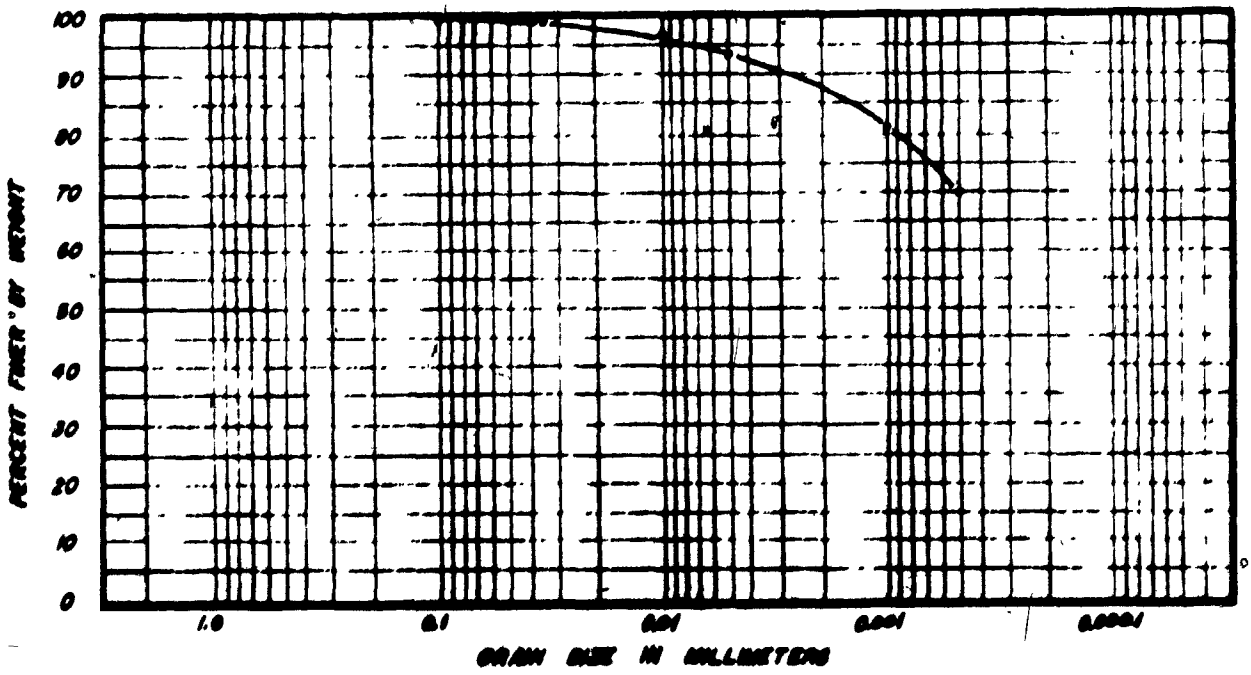

Fig. 4-3 PARTICLE SIZE DISTRIBUTION

4.1.1 Material

The soil selected for this investigation was a finely divided, light brown kaolinitic clay known as Bell Clay; prepared and packaged by Bell Industries, Ltd.

A total of two batches, each weighing approximately 25 pounds (in powder form), of Bell Clay were used in this series of tests. These two batches were shipped directly from Bell Industries, Ltd. on the same order.

The standard hydrometer test (Figure 4-3) showed that all of the particles exhibited an equivalent diameter of less than 0.1 mm with approximately 70 percent by weight of the soil particles remaining in suspension after 72 hours. The major clay mineral component was kaolin, with a trace of the degenerage form of the mineral being present. The non-clay minerals present were quartz and apatite (about 10 percent by weight). The liquid limit and plastic limit were 71 percent and 33 percent, respectively. The specific gravity determined by using distilled water and carbon tetrachloride as pore fluids was found to be 2.52 and 2.72, respectively.

4.1.2 Sample Preparation

Slurry samples of approximately 120 percent moisture content were prepared from clay powders and consolidated in multiple stages in a lucite tube, 3.5 inches in diameter, to an axial pressure of approximately 25 psi to obtain sufficient consistency for handling. The sample was further consolidated isotropically in a triaxial cell under 30 psi of confining pressure. After full consolidation the sample was trimmed to the size of 1.4 inches in diameter and 3.14 inches in length. Usually two such samples could be prepared from each tube sample. The sample was then installed in the triaxial cell and further consolidated to the desired test confining pressures, i.e. 30 psi, 60 psi, 120 psi, and 240 psi.

The homogeneity of the sample was checked by cutting a fully consolidated sample into slices. The maximum variation of the water content of the individual slices from the average value for example σ_3 = 240 psi was found to be less than 0.4 percent. It indicated a good homogeneity within the sample under this relatively high consolidation pressure.

The test sample was allowed to consolidate at the designated confining pressure and at the controlled designated temperature inside a thermally insulated chamber. A

volume change-log t plot was maintained for each sample during consolidation; t_{100} was evaluated by Casagrande construction method. The t_{100} was found ranging from 2.5 to 30 hours, depending on the confining pressures used in the consolidation. However, a consolidation period of four days was found necessary to assure that a considerable portion of the secondary consolidation curve was obtained. Based on Buismann's equation for secondary consolidation, a straight line may be extrapolated on the volume change - log t plot by extending the secondary consolidation curve thus obtained. Therfore, further volume change, due to additional aixial load may be delineated by the method as presented in Chapter 3.

4.1.3 Apparatus

The arrangement and the testing apparatus are schematically represented in Figure 4-4. The triaxial cells used were reinforced to withstand the relatively high cell pressures. Double membranes with vaseline coating between them were used for confining pressures up to 60 psi. For pressures greater than 60 psi, an additional mercury sleeve was used as a jacket and also as a moisture barrier to prevent the transfer of moisture between membrane covered specimens and the surrounding confining fluid. Pressure was applied to the confining fluid in the triaxial cell through a small reservoir which was in hydraulic connection with the cell. The source of the pressure was a compressed nitrogen tank connected to a pressure regulator. After the samples were placed in the triaxial cells, the entire setup was insulated in a styroform cabinet. The temperature inside the cabinet was heated and regulated through a system of combined light bulb-fan system, and a thermal-couple sensor which was able to control the chamber temperature to $\pm 1^{\circ}F$ of the designated level.

The vertical deformation was measured by a dial gauge to an accuracy of 0.5×10^{-4} inch. The volume changes, due to consolidation and the addition of vertical pressure, was measured by burrettes which had an accuracy

of 0.025 cc. The tops of these burrettes were so connected that the vapor pressure in the connecting tube prevented the evaporation of the water in the burrettes.

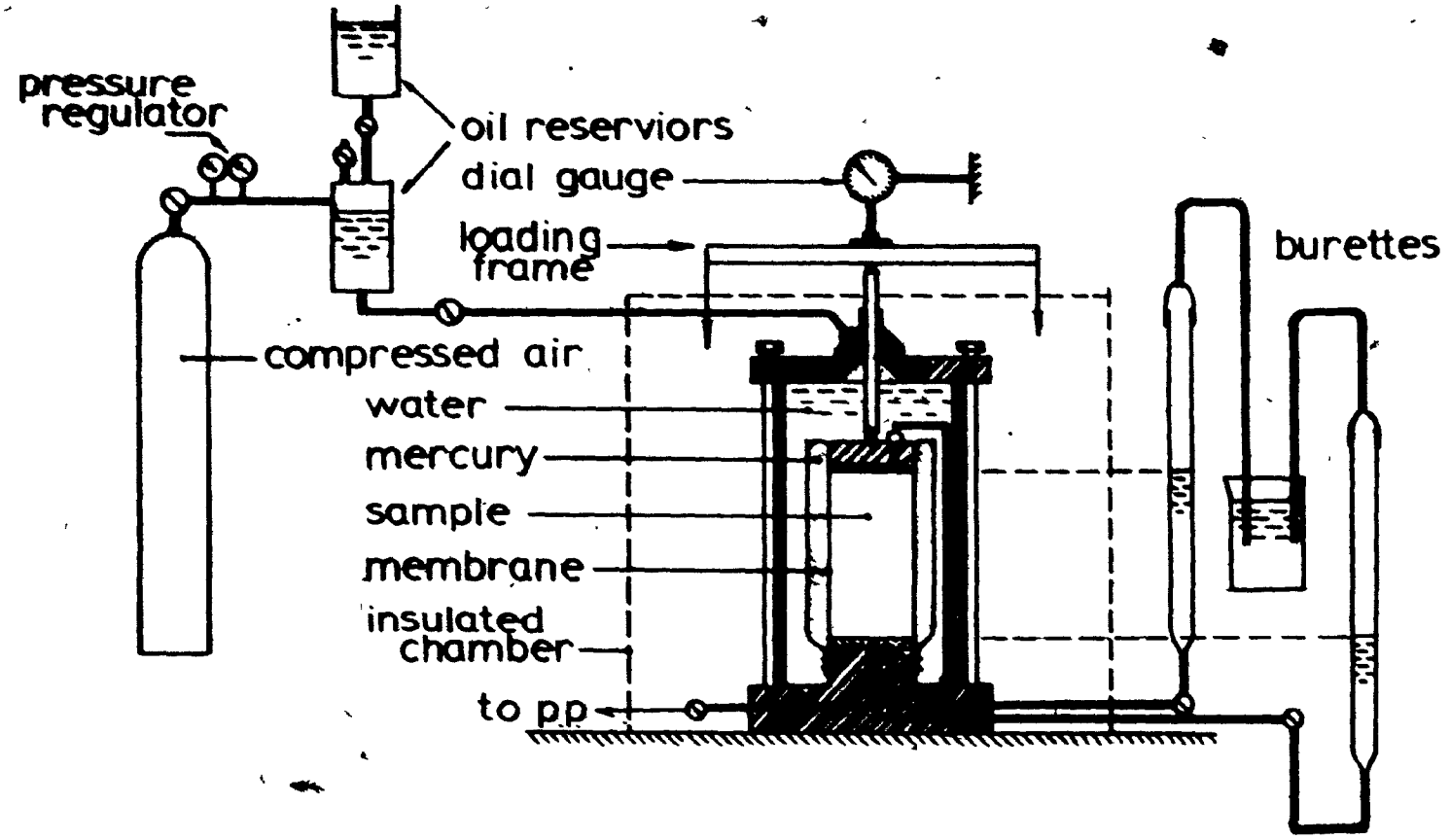

fig. 4-4 schematic representation of the apparati

4.2 TEST RESULTS

4.2.1 Result Presentation

Because of the abundance of test results, a brief summary is provided in this section for the reader. All the graphs and tables are presented in Appendix B.

A. Test Data: Pages B-2 through B-35, inclusive.

B. Family of Creep Curves: Figures B-1 through B-15, inclusive (pages B-36 through B-50).

C. Minimum Flow Rate Variation: Figure B-16 (Page B-51).

D. Unconfined Compressive Strength: Table B-1 (Page B-52).

E. Final Moisture Content: Table B-2 (Page B-52).

F. Stess-Strain Relations: Figure B-17 (Page B-53).

G. Recovered Strain versus Stress Curves: Figure B-18 (Page B-54).

H. Instantaneous Modulus of Elasticity: Figures B-19 through B-22 inclusive, (Pages B-55 through B-58).

I. Relationship Between Stresses and Retarded Strain: Figure B-23 (Page B-59).

J. Probability Distribution Curves: Figures B-24 through B-38 inclusive (Pages B-60 through B-74.)

K. Basic Properties of Probability Distribution Curves: Tables B-3a and B-3b (Pages B-75 and B-76).

L. Drainage Curves: Figures B-39 through B-42 inclusive (Pages B-77 through B-80).

M. Component of Axial Strain due to Anisotropic Consolidation: Table B-4a through B-4d inclusive (Pages B-81 through B-84).

In all the colored graphs, except those specified, the legends used are expressed in the following matrix form:

• 30 psi	black 68°F
• 60 psi	red 78°F
▲ 120 psi	green 88°F
▪ 240 psi	blue 98°F

Thus a black dot denotes confining pressure σ_3 = 30 psi and conducted at a chamber temperature of 68°F; red dot denotes σ_3 = 30 psi, T = 78°F; green dot denotes σ_3 = 30 psi, T = 88°F, blue dot denotes σ_3 = 30 psi, T = 98°F; and so forth.

4.2.2. Typical Results

The above list of results contains approximately eighty three pages of data, tables and graphs. Frequently referenced and typical results are:

1. Figures B-1 through B-15 - Family of Creep Curves.
2. Figure B-16 - Minimum Flow Rate Variation
3. Figure B-17 - Stress-Strain Relations
4. Figure B-18 - Recovered Strain versus stress Curves.
5. Figure B-39 through B-42 - Drainage Curves

From Figures B-1 through B-15, it is seen that these creep curves follow the expected pattern very well,

i.e., each curve consists of an instantaneous strain (strain at 0.1 min. after load application was taken as instantaneous strain), a continuously decreasing rate strain and a constant creep rate strain. The constant creep rate was achieved approximately 24 hours after load application. No progressive creep failure was observed in this series of tests. As expected, Figure B-17 shows that the higher the confining pressure is, the lower is the strain; and the higher the stress difference is, the higher is the resulting strain. A considerable amount of strain was recovered after the load of two days duration was completely removed. This is shown in Figure B-18. A plot of the percent of ratio of recovered strain to total strain versus stress difference (Figure 4-5) shows that, in general, the recoverable strain is in excess of 20 percent of the total strain. With increasing confining pressure and stress difference, the percent of recovery is higher as well.

The most unusual result is revealed in Figure B-16 where the minimum flow rate at steady state was plotted versus the stress difference. It shows that the minimum flow rate does not vary linearly with the increase of stress difference. At higher stress levels, the minimum flow rate fluctuates in magnitude and in some cases the flow rate was lower at higher stress levels. This relationship seems to be consistent with drained creep results obtained by Bishop and Lovenbury (1969) (Figure 4-6); however it

contradicts the undrained creep tests carried out by others (Arulanandan, et al. 1971; Mitchell, et al, 1968; Singh, et al, 1968). They showed that the flow rate at a steady state was seen to increase progressively as the stress-difference approached higher stress levels. The results of logarithm of minimum flow rate plotted against stress difference by Singh, et al. (1968) showed that a linear relationship exists between these two variables. However, no such linearity was observed in the drained creep results of 15 specimens from this series of tests (Figure 4-7). The detailed comparison and discussion between the results obtained from this study and those previously gathered by otheres will be given in Section 5.2, Chapter 5.

Temperature influences on the test results may be recognized from Figures B-16, B-17, and B-18. Especially for confining pressures of 60 psi and 120 psi, it is seen that at a higher temperature, the strain, the strain rate, and the recoverable strain are generally higher as well. In the tests carried out under confining pressures of 30 psi and 240 psi, the temperature effect is not so obvious and no similar conclusion may be drawn.

Figures B-39 through B-42 inclusive show the drainage - time curves at different confining pressures and stress difference levels. The t_{100} evaluated according to the Casagrande construction method varies from 2.5 hours for σ_3 = 30 psi, T = 68°F to 30 hours for σ_3 = 60 psi,

T = 98°F. Generally, the t_{100} is in the range of 5 to 10 hours. For every consolidation curve, the prolonged secondary consolidation portion may be extrapolated by a straight line (dashed portion of the curves). The additional drainages, due to the application and removal of the stress difference $(\sigma_1 - \sigma_3)$ are shown as solid lines. It is seen that this additional drainage at each step of loading varies from approximately 0.2 cc to about 1.0 cc, i.e. the axial strain due to this additional drainage may vary from 0.06 to 0.28 percent as calculated by Equation (3-2). This order of magnitude contributes approximately 10 percent of the total axial strain shown on creep curves of B-1 through B-15 inclusive.

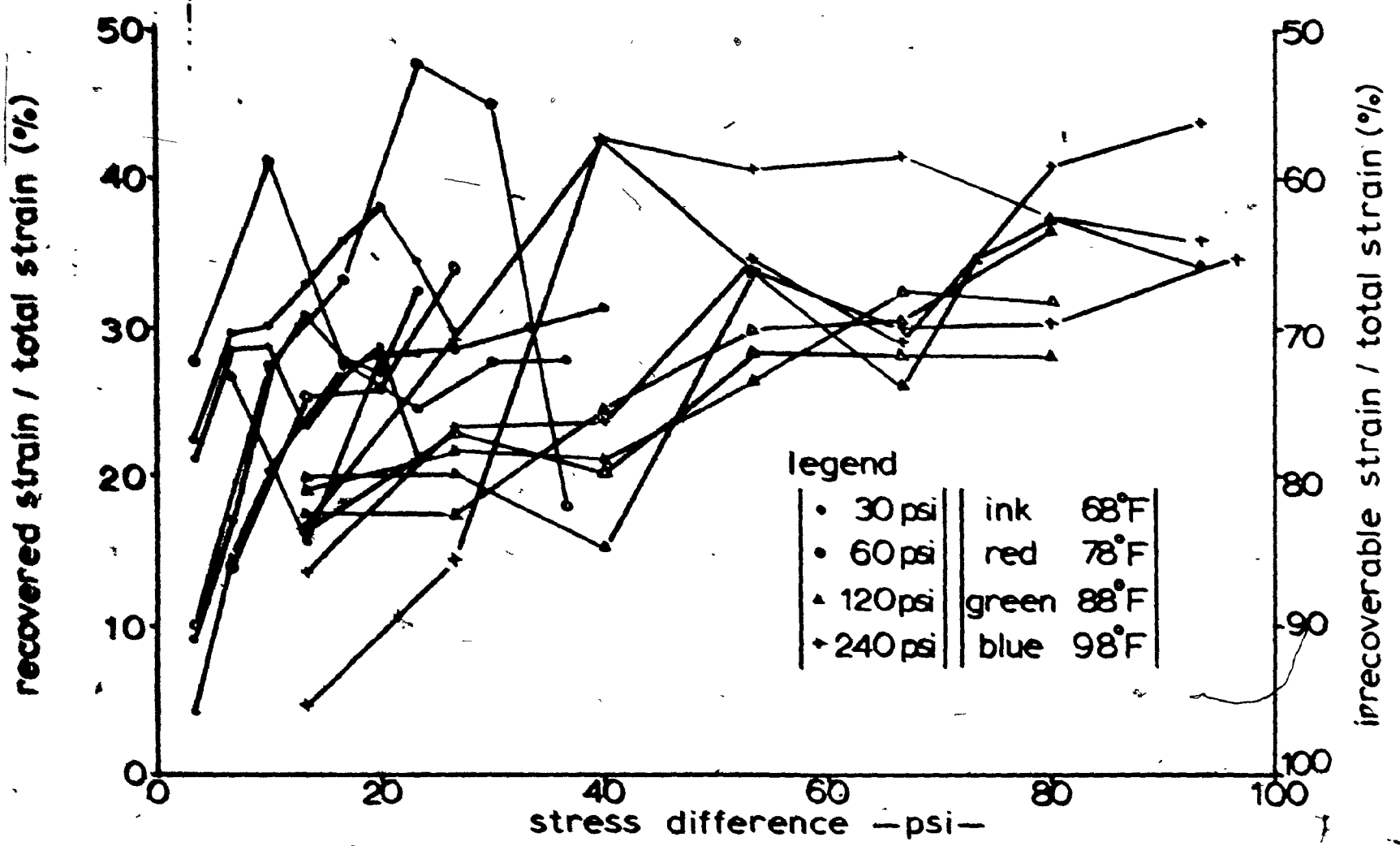

fig. 4-5 percent recovery vs stress levels

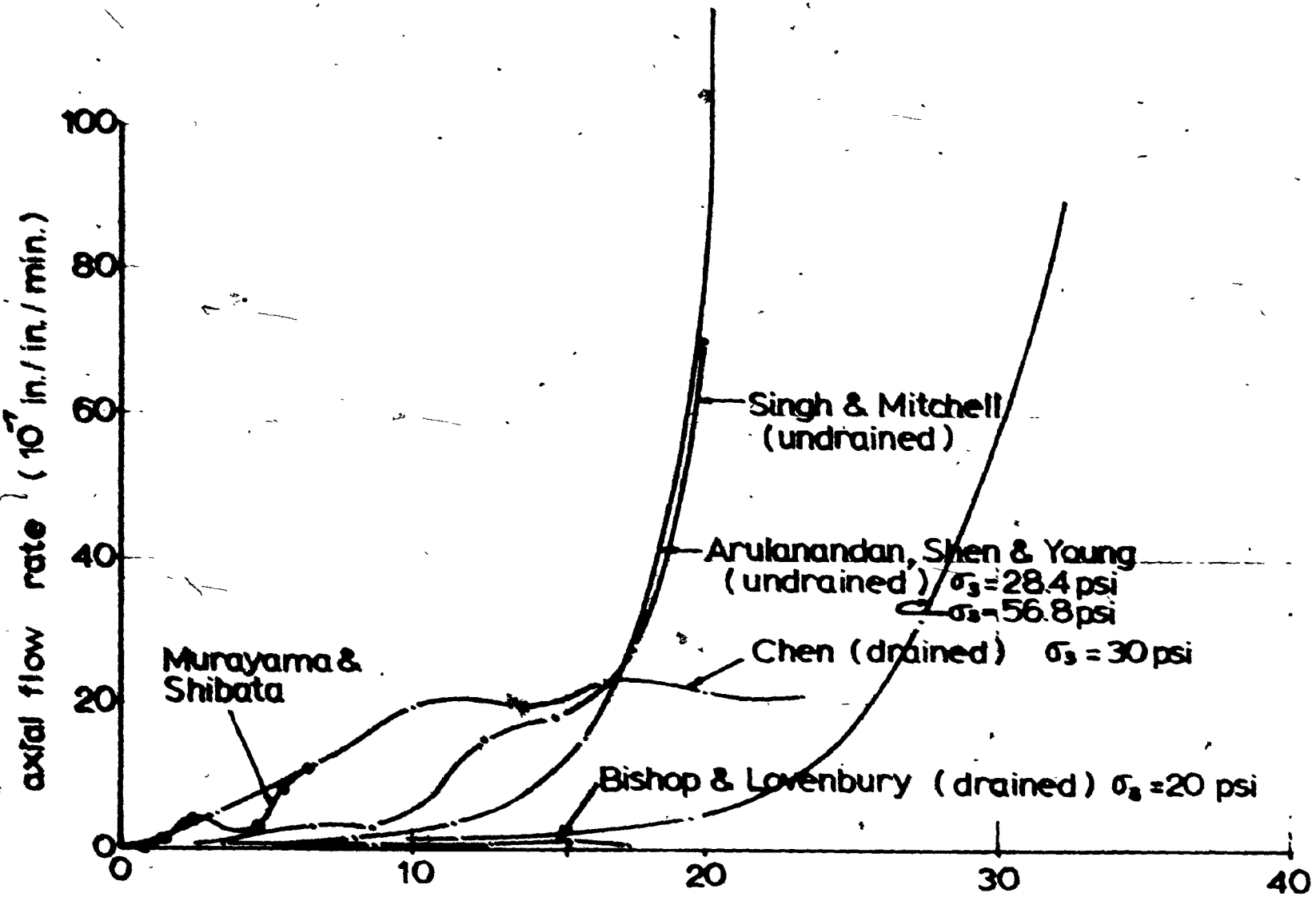

fig. 4-6 min. flow rate-stress relations

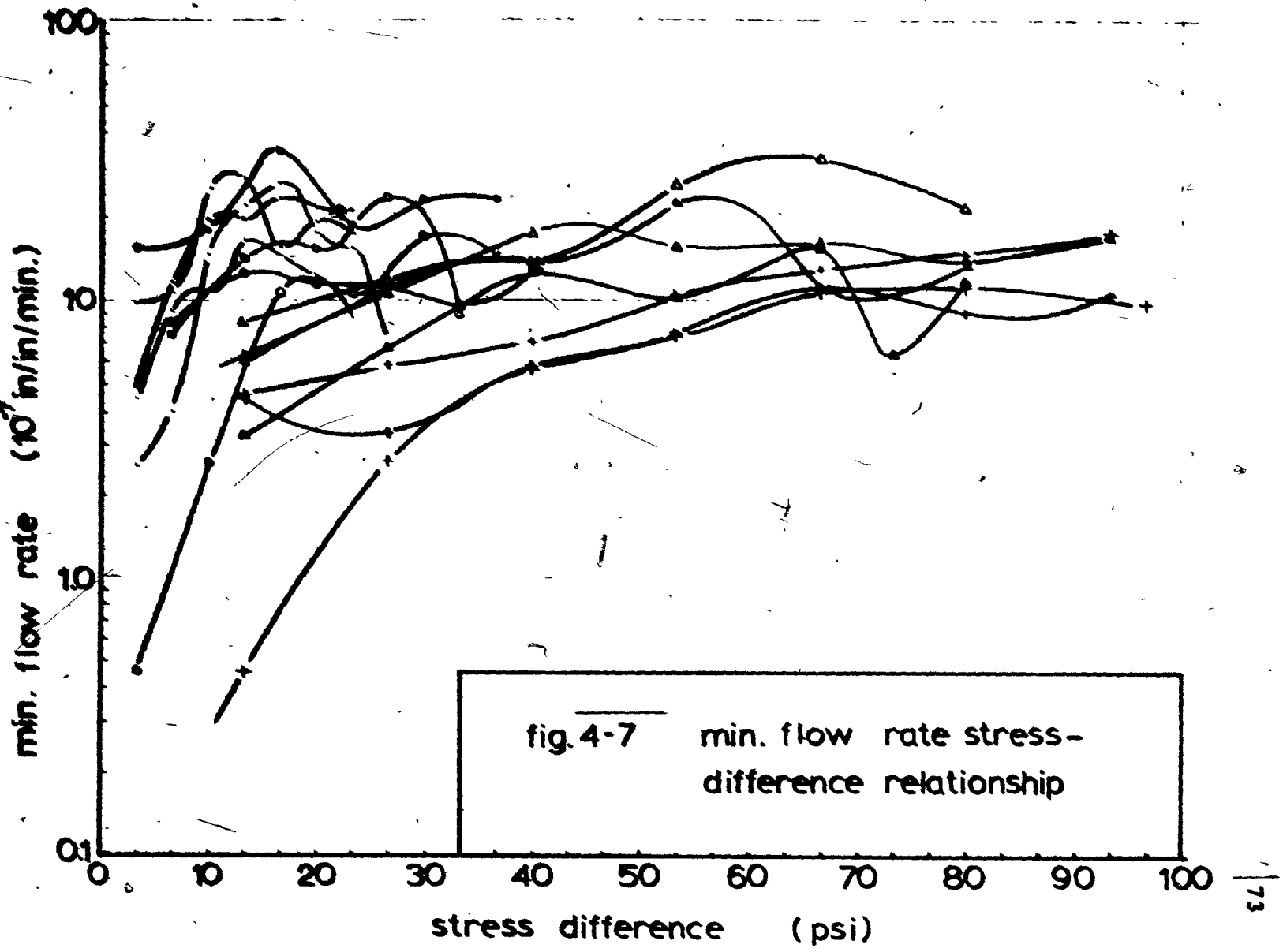

fig. 4-7 min. flow rate stress-difference relationship

CHAPTER 5

ANALYSIS OF RESULTS

In this chapter, results are analyzed by the method of induction in order to obtain a stress-strain-time relationship. This requires that the creep strain may be decomposed into three components, i.e. instantaneous, retarded and flow components as described in Sections 2.1 and 2.2 in Chapter 2. These components may be evaluated separately from the test results and are presented in Sections 5.1, 5.3, and 5.2, respectively. The summation of these three components gives the total stress-strain-time relationship, this is to be presented in Section 5.4. The discussion of the findings will be given in Chapter 6.

5.1 ELASTICITY MODULI AND INSTANTANEOUS DEFORMATION

The axial strain reading taken at 0.1 minute after each load is applied or removed is designated as "instantaneous strain" in this series of study. The ratio of the stress applied (or removed) to this instantaneous strain reading is called instantaneous modulus of elasticity. It is apparent that since the instantaneous strain at loading may contain an irrecoverable component, the instantaneous modulus of elasticity evaluated at unloading would appear to be more representative of the true elastic property of the specimen. However, the use

of the recoverable strain is complicated by the fact that transfer of elastic to plastic strain may take place during the time the load is acting which may result in a strengthening or weakening of the specimen. It appears that cyclic loading method or the methods described, for example, by Mitchell and McConnell (1969) or by Wilson and Dietrich (1960) would provide a better means for the study of the elastic properties of clay soils. Unfortunately, these techniques are beyond the scope of present study.

From results of this investigation, all the calculated instantaneous modulus of elasticity and the instantaneous strain reading are plotted against the stress intensities, and are shown on Figures 5-1A and 5-1B, respectively. On these figures, the strain readings at 1.0 minute and the corresponding modulus of elasticity calculated are also shown for the purpose of comparison.

As shown on Figure 5-1A, instantaneous modulus of elasticity versus stress relationships, it is seen that the modulus of elasticity evaluated at time duration of 1.0 minute is appreciably smaller than that evaluated from 0.1 minute readings. The difference between results obtained from loading and unloading, however, is not clearly shown on this figure. A closer examination of the data presented in Appendix B revealed that for the 0.1 minute readings, 79 out of 99 readings show that recovered strain at unloading is smaller than that obtained at

loading; while for 1.0 minute readings, 87 out of 99 readings show that recovered strain is smaller than that obtained at loading. It is also noticed that two thirds of these inconsistencies occurred at lower confining pressures of 30 psi and 60 psi and at confining pressures of 120 psi and 240 psi, only occasional inconsistencies, i.e. smaller strain readings at loading than at unloading, were recorded.

Allowing the unavoidable experimental scattering of data, results of elastic modulus calculation show that, in general, the instantaneous modulus of elasticity decreases as loading intensity increases. It is apparent that due to the time effect the moduli evaluated at longer time durations are appreciably smaller. The choice of a proper time duration, 0.1 minute in this study, is primarily a result of consideration of the instrumentation and technique used in the test, and therefore is not yet a standard procedure for the instantaneous modulus of elasticity evaluation.

From this series of test results, it is also possible to evaluate the elasticity modulus by evaluating the slope of the stress-strain curves as shown on Figure 5-13. It is seen that the initial portion of the relationship is approximately linear. As the stress-strain intensity reaches about 50 percent of the strength of the specimen, the curve starts to deviate from this straight

line. The remaining portion of the curve may again be approximately represented by another straight line with a milder slope. Values of modulus of elasticity are calculated and are shown on this figure. For example, for σ_3 = 120 psi, the modulus of elasticity evaluated at 0.1 minute after load application is approximately 19,200 psi for stress difference ($\sigma_1 - \sigma_3$) between 0 and 50 psi; 5,300 psi for ($\sigma_1 - \sigma_3$) between 50 and 80 psi. If these slopes are to represent the average elastic modulus of the specimen, then the average modulus of elasticity is again seen to decrease with the increase of stress intensity and, evidently, with the decrease of confining pressure.

To facilitate the calculation of a first order approximation of the instantaneous modulus of elasticity (designated E), the data shown on Figure 5-1A, for each confining pressure, may be represented by a straight line.

$$E = E_o - \ell\,(\sigma_1 - \sigma_3) \qquad \text{.....(5-1-1)}$$

where E_o is the intercept of the vertical axis and ℓ is the slope of the straight line.

A quick estimation of the instantaneous strain (ε_i) may then be obtained by the following equation:

$$\varepsilon_i = \frac{(\sigma_1 - \sigma_3)}{E_o - \ell\,(\sigma_1 - \sigma_3)} \qquad \text{.....(5-1-2)}$$

The numerical values of E_o and ℓ for a particular confining pressure are tabulated below:

σ_3 = 240 psi	E_o = 80 x 10^3 psi	ℓ = 550
= 120 psi	= 36.6 x 10^3 psi	= 255
= 60 psi	= 12.1 x 10^3 psi	= 196
= 30 psi	= 7.67 x 10^3 psi	= 217

Equation (5-1-2) serves only for the calculation of the instantaneous strain component in this series of test. It will be incorporated into the total stress-strain-time relationship in Section 5.4 for total creep strain calculations.

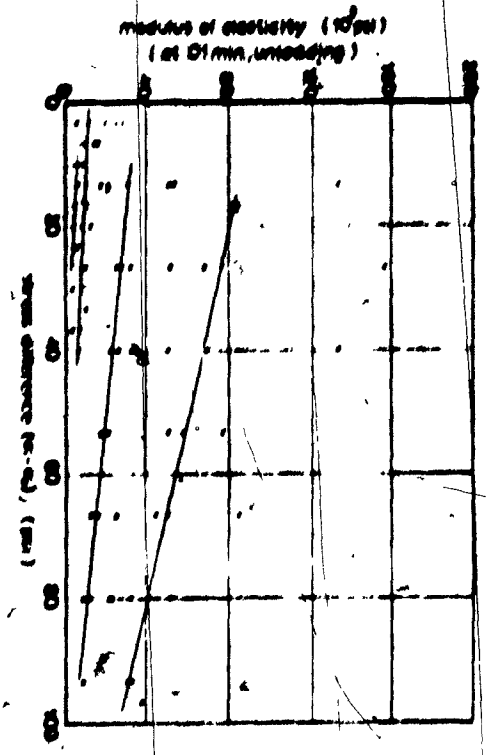
modulus of elasticity (10^3psi)
(at 01 min, unloading)

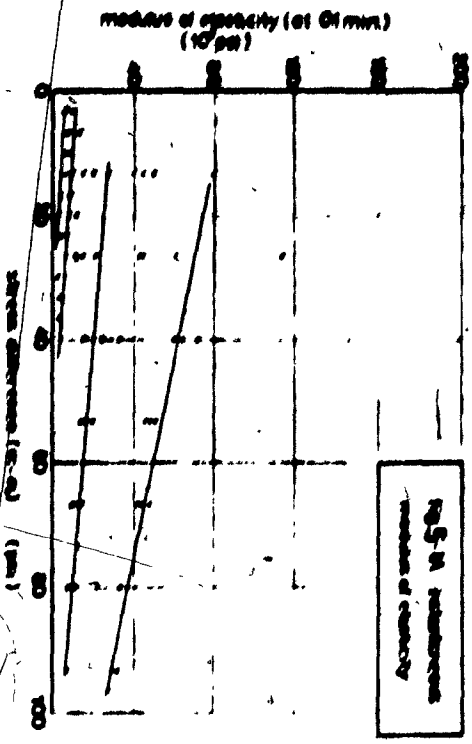
modulus of elasticity (at 01 min.)
(10^3psi)

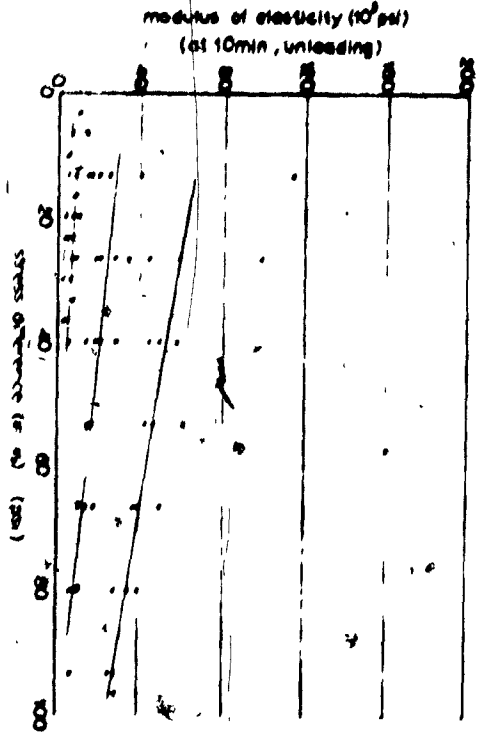
modulus of elasticity (10^3psi)
(at 10min , unloading)

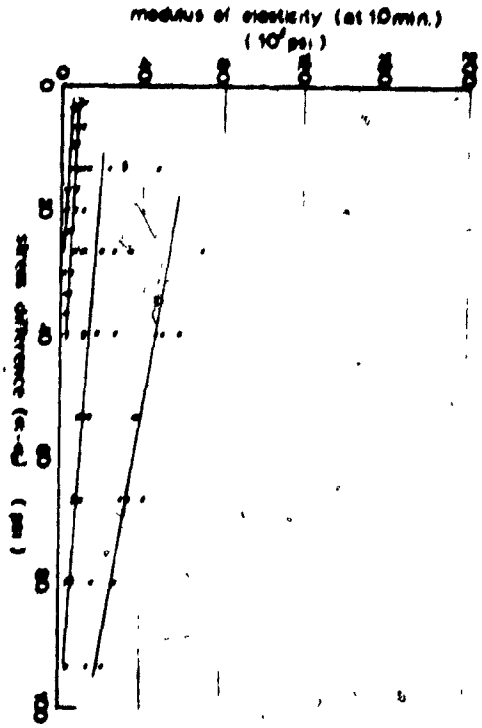
modulus of elasticity (at 10min.)
(10^3psi)

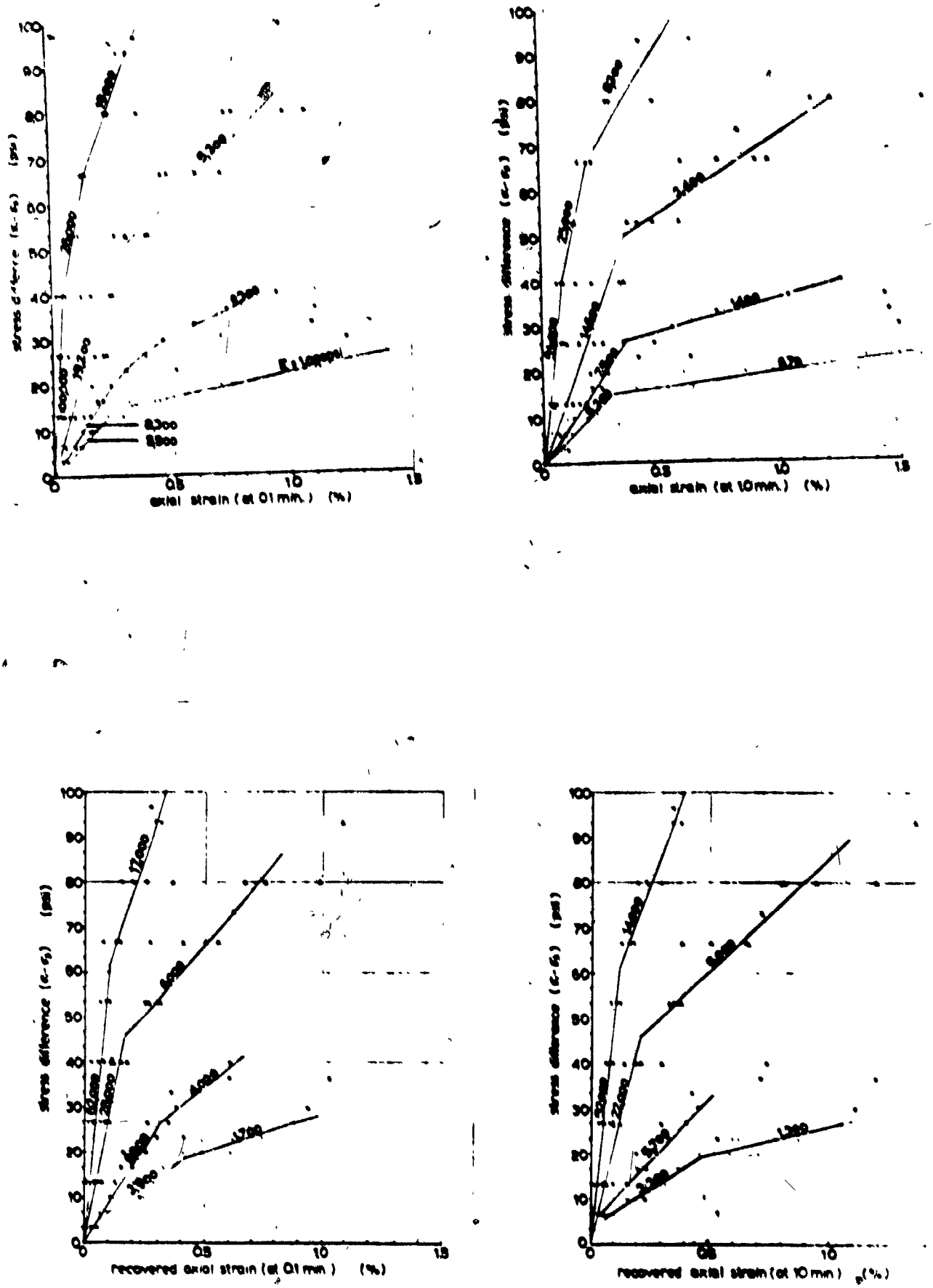

fig 5-18 instantaneous strain stress relationship

Stability of these substances

5.2 MINIMUM CREEP RATE AND FLOW DEFORMATION

Figure 5-2 shows a typical creep curve and the variation of axial strain rate during the creep deformation. It shows that creep rate decreases rapidly and remains essentially a constant after about 24 hours. This steady state is sometimes called secondary creep or constant rate "flow". Depending on the magnitude of this flow rate and the duration of the sustained load, the amount of this flow portion of deformation (designated ε_f) may constitute a large percentage of total deformation (e.g. Vyalov et al. 1957; Haefeli, 1965). Therefore, in the study of rheological phenomena, (especially in clay soils and frozen soils) the variation of creep rate has been investigated in detail by various authors (e.g. Mitchell et al. 1964; Anderaland et al. 1967, 1970). The results of their investigations show that this portion of creep deformation is essentially irreversible and that the creep process at steady state may be considered as a thermally activated process.

To evaluate the flow strain component ε_f, numerically, it is noted that the term $B\sigma t$ in equation (2-2-2-2) applies only for the ideal Newtonian fluid if B takes the form of the reciprocal of the coefficient of viscosity. This form of expression is apparently oversimplified for describing the flow phenomena in clay soils. A plot of the flow strain rate versus stress (Figure B-16)

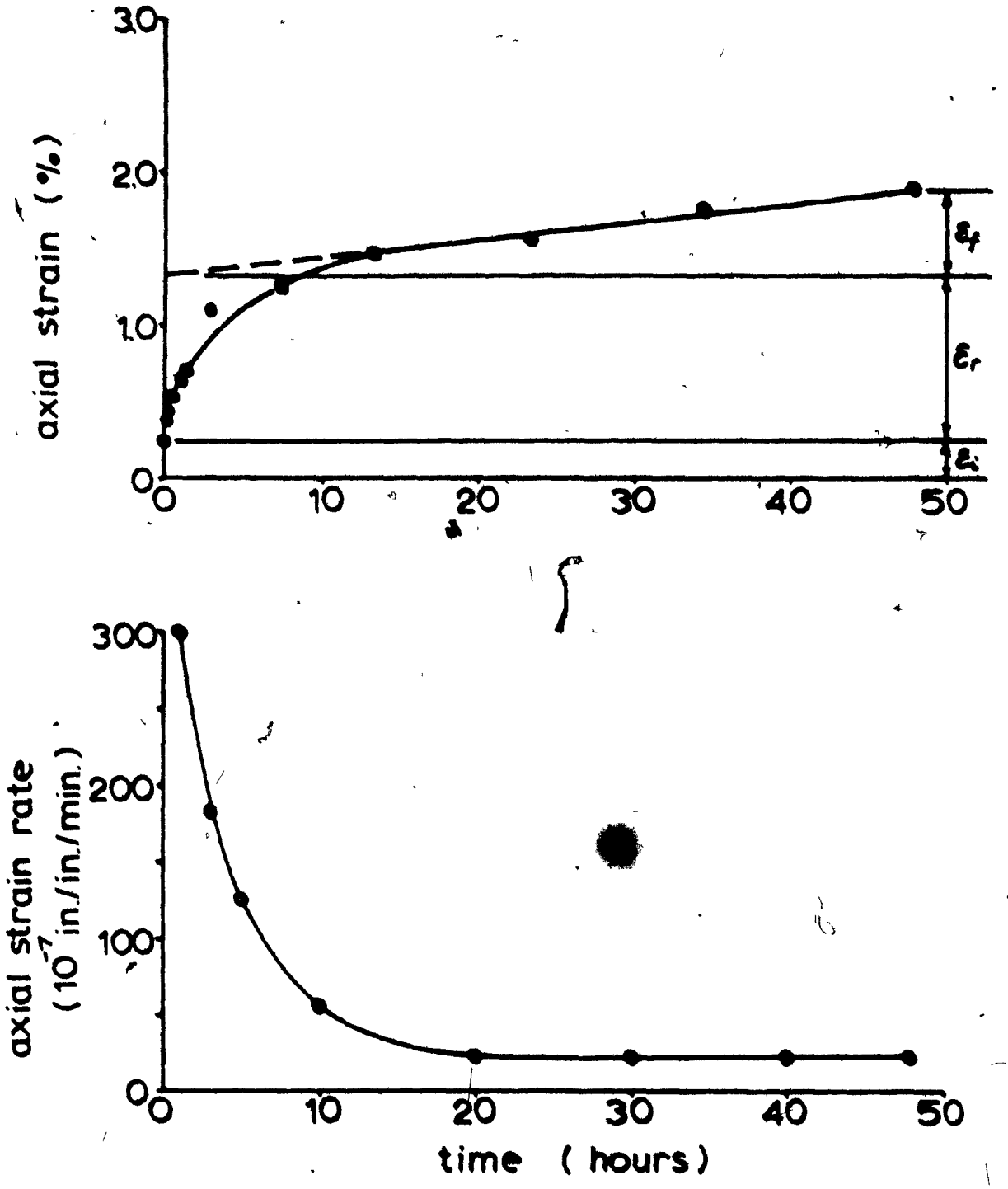

fig. 5-2 axial strain rate variation

shows that the flow rate is not directly proportional to the applied stress and that there is no definite pattern of temperature effect can be found. This may suggest that besides the structural properties of the material itself, temperature, time and stress play important and complex roles in this flow process. Since the flow strain is not directly proportional to the applied stress, the functional form of the term $B\sigma t$ needs some modifications in order to be able to show the relationship between this flow strain component and the stresses. In order to do this, a plot of the average value of flow rate compliances at steady state (i.e. $\dot{\varepsilon}_f/(\sigma_1-\sigma_3)$) versus stress is shown on Figure 5-3 . The variation of this average value is approximately linearly related to the applied stress difference ($\sigma_1 - \sigma_3$). The higher the stress levels, the lower the average compliance value; i.e. at higher confining pressures and higher stress intensities, the flow rate can be produced by the application of a unit stress is smaller. The trend of this variation may be approximately represented by following straight line

$$\frac{\dot{\varepsilon}_f}{\sigma_1 - \sigma_3} = a(\sigma_3) - b\,\sigma_3(\sigma_1 - \sigma_3) \qquad \text{.....(5-2-2)}$$

Integration of equation (5-2-2) gives the flow strain ε_f in the following form

$$\varepsilon_f = [a - b(\sigma_1 - \sigma_3)](\sigma_1 - \sigma_3)\,t \qquad \text{.....(5-2-3)}$$

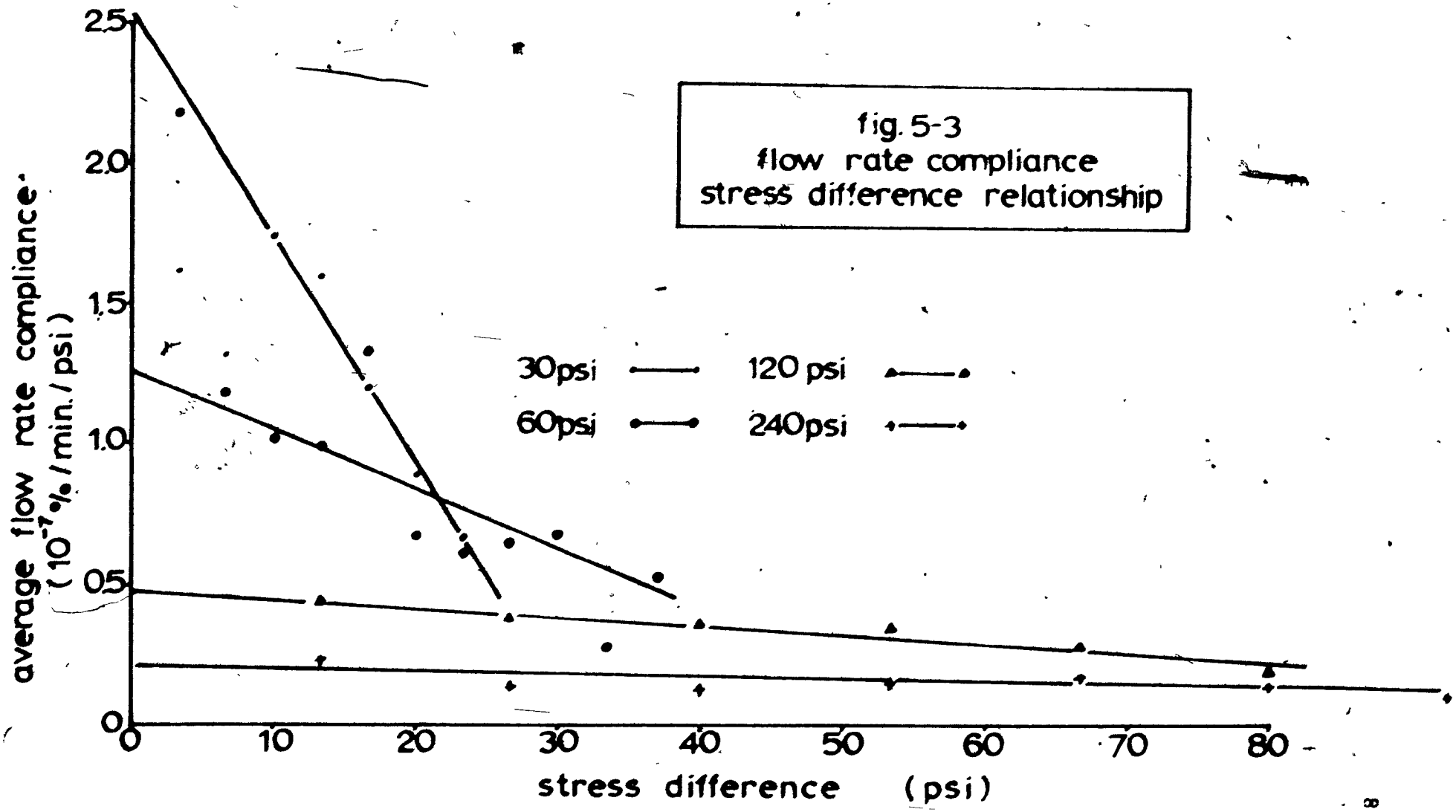
fig. 5-3
flow rate compliance
stress difference relationship
30psi
60psi
120 psi
240psi
average flow rate compliance
(10^{-7} %/min./psi)
2.5
2.0
1.5
1.0
0.5
0
0
10
20
30
40
50
60
70
80
stress difference (psi)

where a is the intercept of the line with the vertical axis at $(\sigma_1 - \sigma_3) = 0$ and is a ficticious creep rate compliance showing the would be rate of flow per unit stress if a near zero stress difference is applied; b is the slope of the line which shows the change of flow rate compliance with the change of stress difference level. The higher is the a value, the more fluid is the sample; and the higher is the b value, the more sensitive is the flow property of the sample to the stress difference changes. Both a and b are a function of confining pressure σ_3. Figure 5-4 shows that the variation of these two coefficients are related to the confining pressure by the following power form

$$a = 154\,\sigma_3^{-1.2}\,10^{-5}$$
$$b = 165\,\sigma_3^{-2.22}\,10^{-5} \qquad \text{.....(5-2-4)}$$

Therefore, the flow portion of strain in this series of tests may be represented by the following formula:

$$\varepsilon_f = [154 - 165\sigma_3^{-1.22}(\sigma_1 - \sigma_3)]\,\sigma_3^{-1.2}(\sigma_1 - \sigma_3)\,t\,10^{-5} \qquad \text{.....(5-2-5)}$$

Differenciation of the equation (5-2-5) gives the creep rate at steady state, i.e.,

$$\varepsilon_f = [154 - 165\sigma_3^{-1.22}(\sigma_1 - \sigma_3)]\,\sigma_3^{-1.2}(\sigma_1 - \sigma_3)\,10^{-5} \qquad \text{.....(5-2-6)}$$

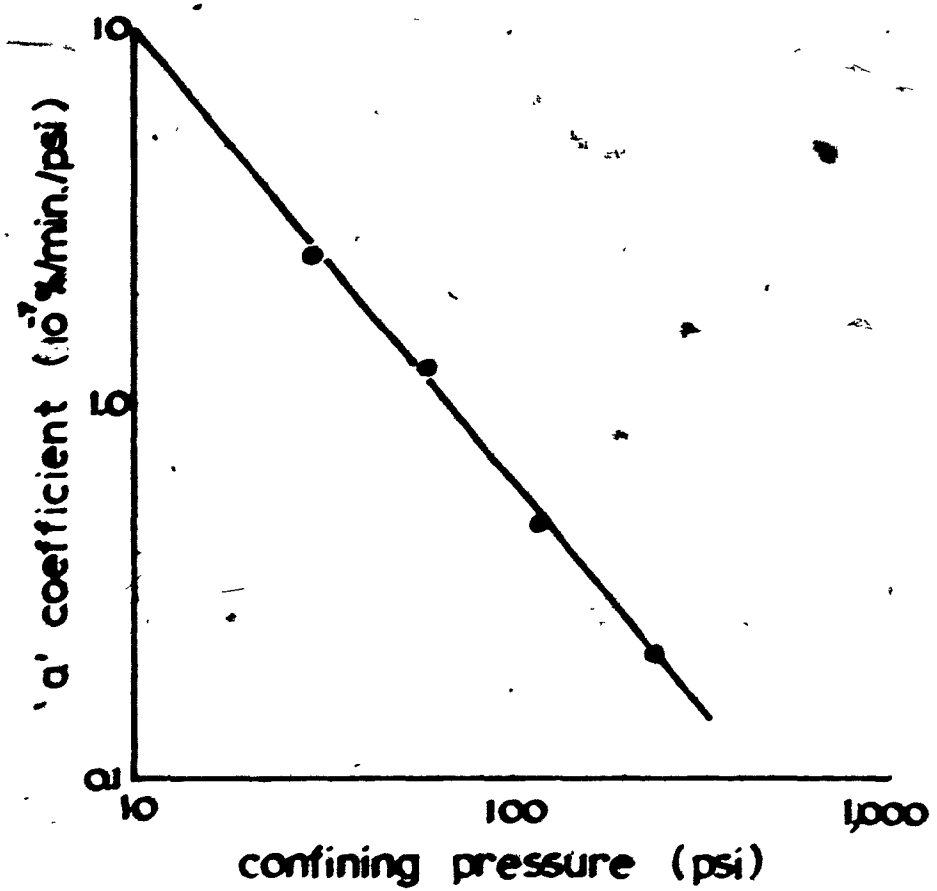

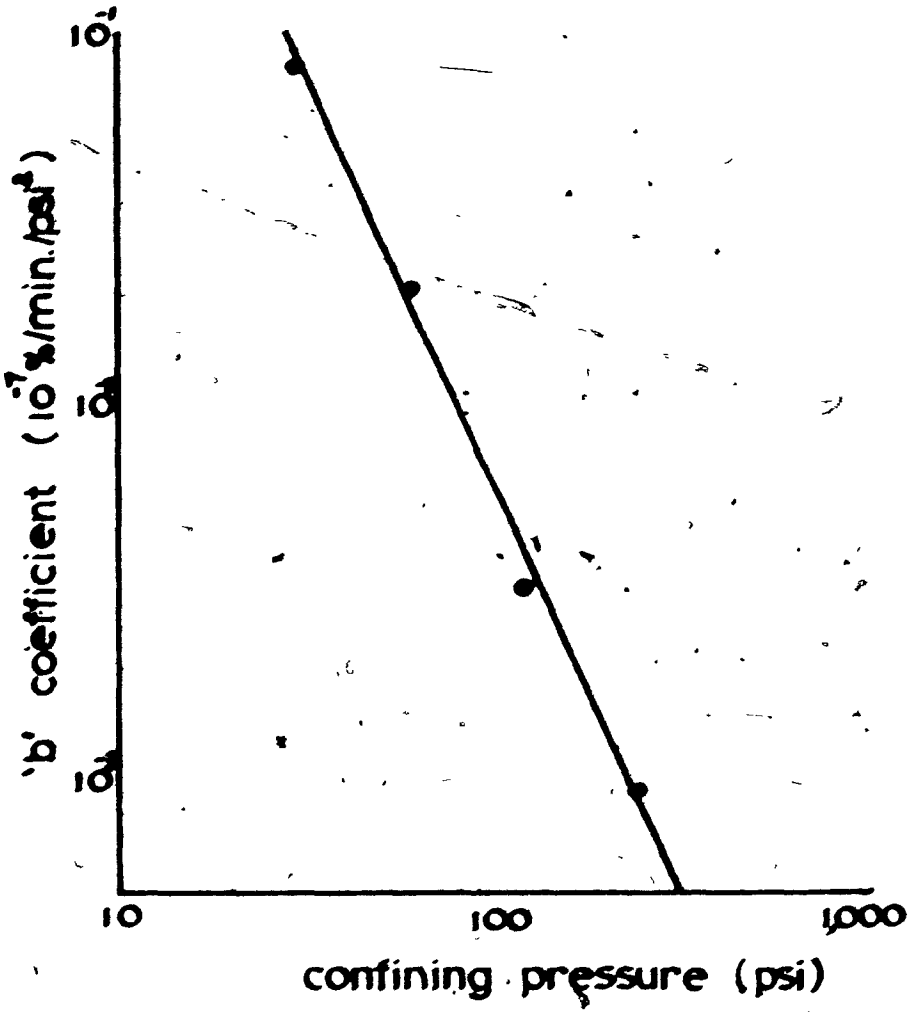

fig. 5-4 coefficients 'a' and 'b'

From these equations, which give the functional relationship between $\dot{\xi}_f$, ξ_f, σ_3, $(\sigma_1 - \sigma_3)$ and time, the flow strain and the flow rate may be evaluated conveniently.

The incorporation of these equations into a total stress-strain-time relationship and the comparison between the experimental results and the results of calculation are given in Section 5.4.

5.3 CREEP RATE VARIATION AND RETARDED DEFORMATION

The portion of creep curve which shows a continuous decrease in strain rate is usually called the primary creep or retarded deformation (designated ε_r). The magnitude of this portion of deformation is determined by subtracting from the total deformation the instantaneous deformation ε_i and the product of minimum flow rate and the elapsed duration, i.e. $\dot{\varepsilon}_f\, t$, i.e. after ε_i and $\dot{\varepsilon}_f$ are evaluated from Sections 5.1 and 5.2, the retarded deformation ε_r may be evaluated by the following equation:

$$\varepsilon_r = \varepsilon_t - \varepsilon_i - \dot{\varepsilon}_f\, t \qquad \text{.....(5-3-1)}$$

The magnitude of this retarded deformation under a certain load increment approaches an ultimate value (designated ε_{ru}) when a steady state is approached. The rate of deformation decreases rapidly from maximum at the moment the load is applied to a minimum creep rate when a steady state flow is attained. Studies (Alfrey, 1949; Yong and Chen, 1970) have shown that this rate changes and the time to attain the full retarded deformation is closely related to the visco-elastic properties of the structure of the material undergoing deformation. If the characteristics of the rate changes can be defined, they could be very useful in the study of the fabric response characteristics.

In order to obtain an expression for the retarded portion of strain at any time over the full range of test duration, all the data obtained are analyzed according to equation (5-3-1). A typical result of retarded strain component versus logarithm time relationship is shown on Figure 5-5, Step 1. Usually an "S" shape curve is obtained for each loading increment and ultimately the retarded strain approaches a finite value ($\varepsilon_{r\infty}$) when the steady state is approached. This curve is further analyzed step by step according to the retardation time distribution method as described in Section 2-2-3. The curve is first normalized by dividing the retarded strain at any time by the ultimate retarded strain $\varepsilon_{r\infty}$ for each loading increment, i.e., $\varepsilon_r/\varepsilon_{r\infty}$. This normalization procedure usually does not change the shape of the original curve and again an "S" shape curve is obtained. The slopes at several convenient points on the curve are evaluated by calculation or by graphically scaling. These slopes are again plotted against logarithm of time and usually a single hump bell shape curve is obtained for each loading increment. All the test results are analyzed by the above procedures and a family of bell-shape curves are obtained for each specimen. These graphs are presented in Appendix B, Figures B-24 through B-38 inclusive. A typical example of procedures used is shown on Figure 5-5.

Examination of all the bell shape curves show that these curves are negatively skewed to a certain degree,

but they approximately represent a normal distribution function with a mean of μ and standard deviation of $\bar{\sigma}$, i.e., the bell shape curves may be described by a density function:

$$f(t) = \frac{1}{\sqrt{2\pi}\,\bar{\sigma}} e^{-\frac{(t-\mu)^2}{2\bar{\sigma}^2}} \qquad \text{.....(5-3-2)}$$

Therefore, the "S" shape curve as shown on Step 2 is an accumulative function. Let this function be F(t), then the following expression for F(t) is obtained:

$$F(t) = \frac{1}{\sqrt{2\pi}\,\bar{\sigma}} \int_{-\infty}^{t} e^{-\frac{(t-\mu)^2}{2\bar{\sigma}^2}} dt \qquad \text{.....(5-3-3)}$$

Since this accumulative function has been normalised, the retarded strain at any time t, $\varepsilon_r(t)$, is given by:

$$\varepsilon_r(t) = \varepsilon_{ru} F(t)$$

$$= \frac{\varepsilon_{ru}}{\sqrt{2\pi}\,\bar{\sigma}} \int_{-\infty}^{t} e^{-\frac{(t-\mu)^2}{2\bar{\sigma}^2}} dt \qquad \text{.....(5-3-4)}$$

In order to use equation (5-3-4) for the retarded strain component calculation, three unknowns, ε_{ru}, $\bar{\sigma}$, and μ, have to be evaluated from the test data. To do this it was found that for a moderately skewed distribution, the distance between the mean and median is one-third of the distance between the mean and the mode (Arkin et al., 1970). From the density function and the accumulative function, mode and median can be easily determined graphically. The mean can therefore also be determined graphically (see example on Figure 5-5). From the

statistical theory (Arkin et al. 1970; Aitken, 1957), if a distance equalling the standard deviation is measured off on the horizontal axis on both sides of the mean in a normal distribution curve, 68.26 percent of the value will be included within the limits indicated. After the mean value is obtained, the standard deviation $\bar{\sigma}$ may then be determined by measuring the distance between the mean and a point which will give a value of 34.13 percent from the mean. By the definition of time of retardation, the time corresponding to 0.368 normalized retarded strain is also evaluated graphically as time of retardation for the sample at the specific loading increment. Results of these evaluations are tabulated on Tables B-3a and B-3b in Appendix B.

To obtain an expression for the $\varepsilon_{r,u}$ values, a plot of the logarithm $(\sigma_1 - \sigma_3)$ versus the logarithm $\varepsilon_{r,u}$ shows that the logarithm of the retarded strain component has an approximate linear relationship with the stress difference and no definite pattern of temperature effect could be clearly defined (Figure 5-6). If the linear relationship is approximated by a straight line, the slope of porportionality is seen to be independent of σ_3 . The magnitude of the retarded strain component, however, is a function of confining pressure σ_3 . This is physically obvious since the compactness of the soil structure will influence the overall retardation performance.

Let the straight line be represented by the following equation:

$$\text{Log } \varepsilon_{ru} = \text{Log } C + \text{Log } (\sigma_1 - \sigma_3)^n$$

where C is the intercept and is a function of σ_3 while the slope n is a constant and is assumed to be independent of σ_3 and temperature. The ultimate retarded strain component ε_{ru} is then given by :

$$\varepsilon_{ru} = C\,(\sigma_1 - \sigma_3)^n \qquad \ldots\ldots\ldots (5\text{-}3\text{-}5)$$

From Figure 5-6 , the slope n equals to 1.5 while the dependency of C on σ_3 may be graphycally evaluated from a plot of logarithm C versus logarithm σ_3 as shown on the sketch on this page. It can be shown that the numerical value of C is given by:

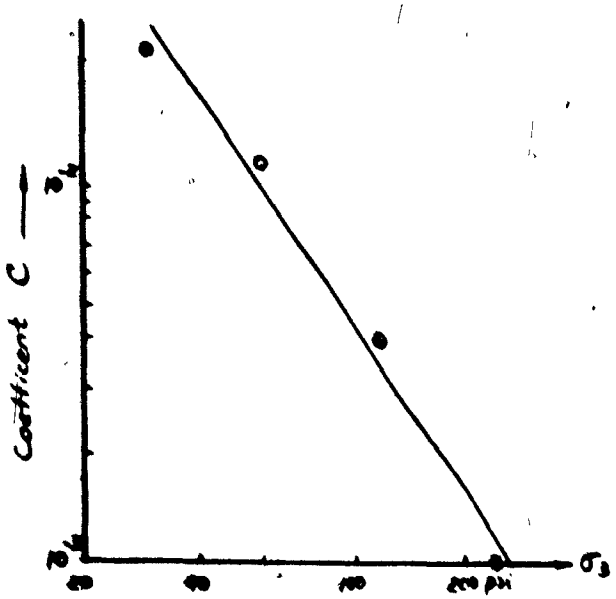

$$C = 52\,\sigma_3^{-1.54}$$

substituting into equation (5-3-5)

$$\varepsilon_{ru} = 52\,\sigma_3^{-1.54}\,(\sigma_1 - \sigma_3)^{1.5} \qquad \ldots\ldots\ldots (5\text{-}3\text{-}6)$$

Again, substituting this value into equation (5-3-4), the numerical value of the retarded strain compo-

nent at any time t is given by:

$$\varepsilon_r(t) = \frac{52\sigma_3^{-1.54}(0.-\sigma_3)^{1.5}}{\sqrt{2\pi}\,\delta}\int_{-\infty}^{t} e^{-\frac{(\tau-\mu)^2}{2\delta^2}}\,d\tau \qquad \text{.....(5-3-7)}$$

From this equation derived for the retarded deformation, Equation (5-2-3) for the flow portion of deformation and Equation (5-1-2) for the instantaneous deformation, a complete stress-strain-time relationship may be obtained by summing up these components. This will be summarized and compared with experimental results in the next section.

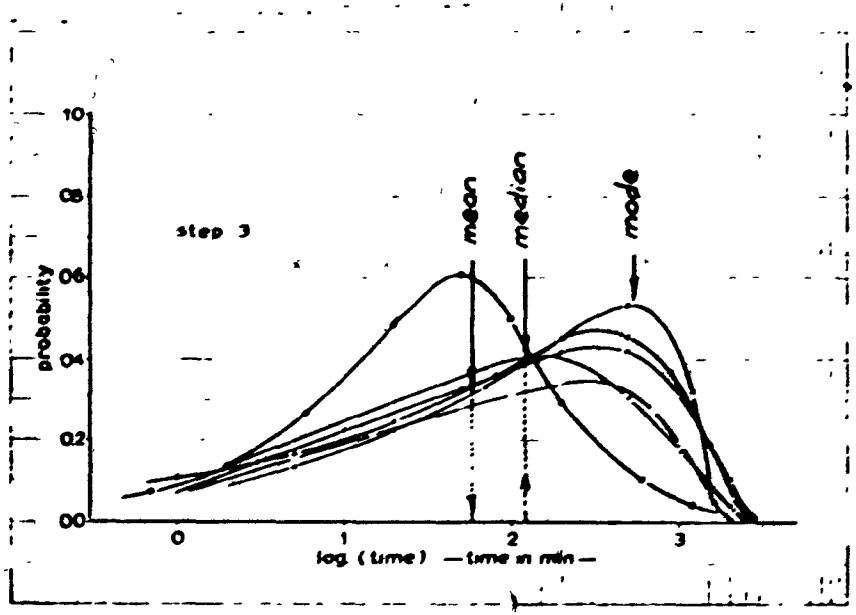

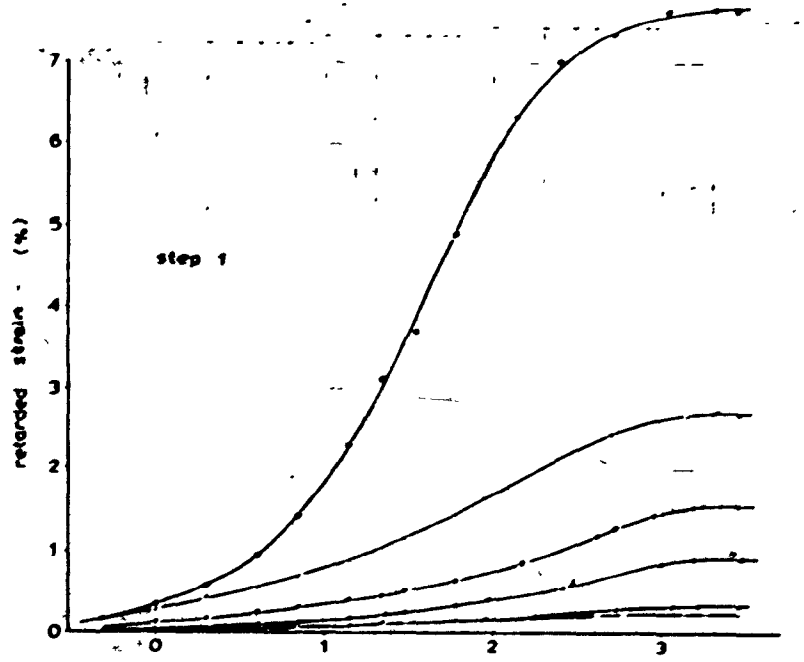

σ_s = 60 psi T = 95°F

symbol	$(\sigma_i - \sigma_s)$ psi
▪	33
•	100
▪	166
•	233
▪	300
•	366

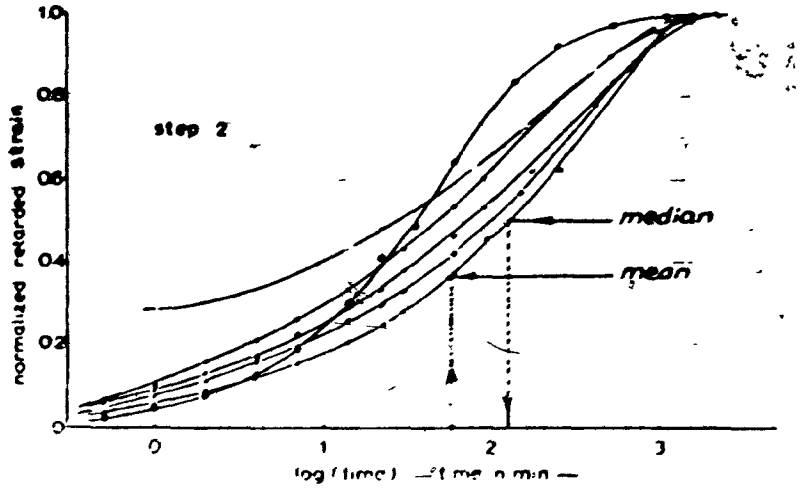

Fig. 5-5 Retardation Time, Standard Deviation and Mean Determination (Example)

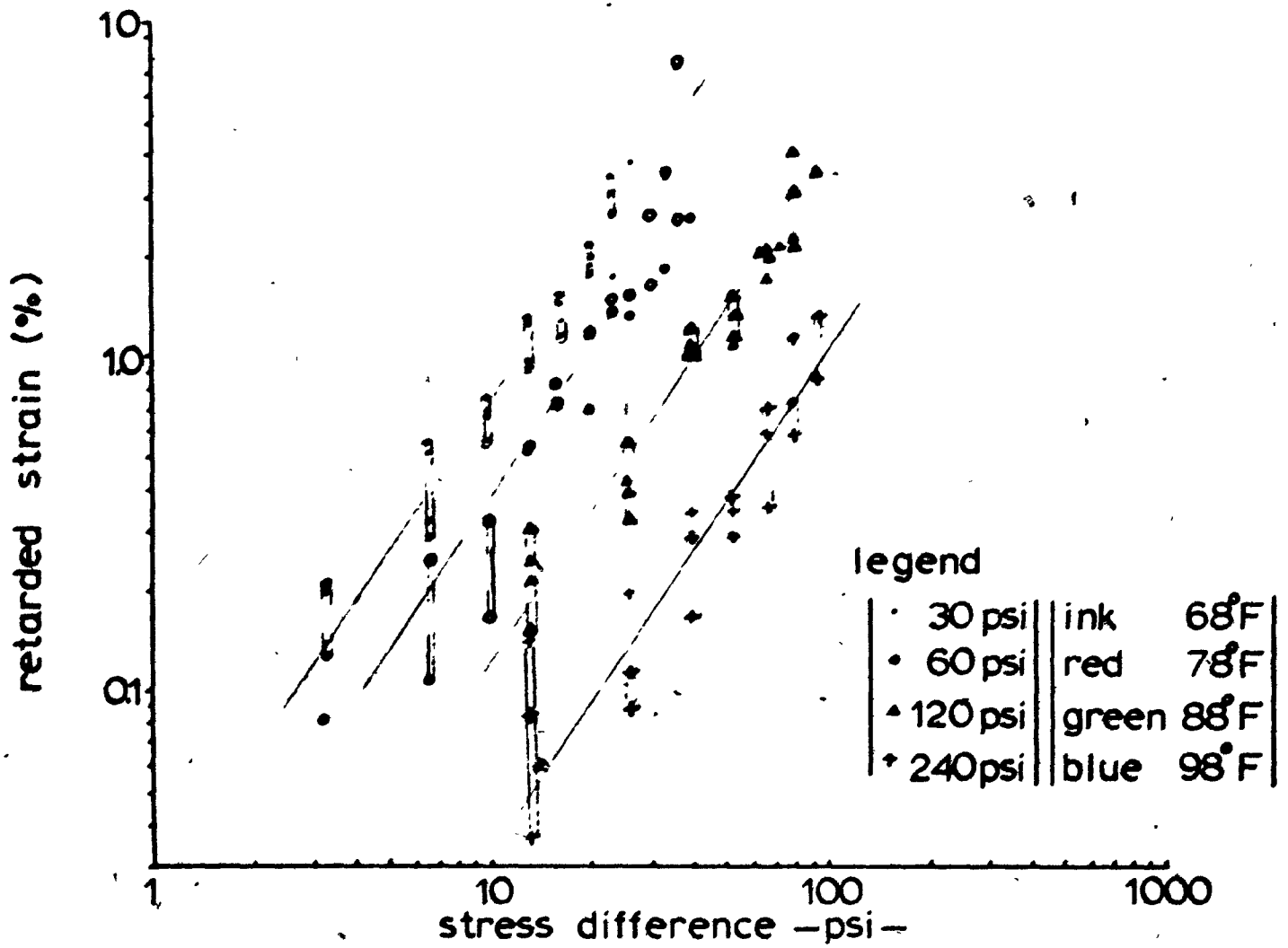

fig. 5-6 relationship between stresses and retarded strain

5.4 STRESS-STRAIN-TIME RELATIONSHIP

From the resulting Equations (5-1-2), (5-3-4), and (5-2-3) for the quantitative representation of instantaneous, retarded and flow strain components respectively, the total strain is then given by the summation of these three components: i.e.

$$\varepsilon_t = \varepsilon_i + \varepsilon_r + \varepsilon_f$$

$$= \frac{(\sigma_1 - \sigma_3)}{E_0 - \ell(\sigma_1 - \sigma_3)} + \frac{\varepsilon_{ru}}{\sqrt{2\pi}\,\delta}\int_{-\infty}^{t} e^{-\frac{(\tau-\mu)^2}{2\delta^2}}\,d\tau$$

$$+ [a - b(\sigma_1 - \sigma_3)](\sigma_1 - \sigma_3)\,t \qquad \text{.....(5-4-1)}$$

Three principal parameters considered in this equation are the confining pressure σ_3 , stress difference ($\sigma_1 - \sigma_3$) and time t.

In the first term, $E_0 - \ell(\sigma_1 - \sigma_3)$ shows the variation of instantaneous elastic moduli with the variation of stress difference level, where E_0 is an extrapolated value of elastic modulus at $\sigma_1 - \sigma_3 = 0$ and ℓ shows the rate of change of elastic modulus with the change of stress difference ($\sigma_1 - \sigma_3$).

The second term on the right hand side of equation (5-4-1) shows the accumulative retarded strain up to time t; in this term, ε_{ru} is the ultimate retarded strain (or inelastic strain) component under a certain increment of load ($\sigma_1 - \sigma_3$) and a certain confining pressure σ_3 ; $\bar{\sigma}$ and μ are the standard deviation and mean values respectively

which characterize the distribution of the retardation time τ . The method of determination of these coefficients in this term is described in Section 5.3.

At higher stress difference levels and longer time durations, the third term on the right hand side of equation (5-4-1) starts to give a significant magnitude of flow strain component. In this term, a-b $(\sigma_1 - \sigma_3)$ gives the flow rate compliance or fluidity of the specimen at stress difference level of $(\sigma_1 - \sigma_3)$, in which a is the initial fluidity of the specimen or the would be rate of flow per unit stress if a near zero stress difference is applied and b shows the change of flow rate compliance with the change of $(\sigma_1 - \sigma_3)$.

All the coefficients in equation (5-4-1) may be evaluated by carrying out a creep test program which is designed to meet the specific conditions of each project such as drainage condition, confinement, and the expected range of stress difference which the specific soil would encounter. Ideally, two soil samples consolidated at two different confining pressures, creep tests at two stress difference levels carried out on each sample will provide sufficient information to evaluate all the coefficients in equation (5-4-1). The resulting equation then may be used to predict the possible creep strain which may take place under the specific stress conditions.

From the test data obtained in this series of study, coefficients in equation (5-4-1) are evaluated and the exact procedures are illustrated in previous sections. Following quantitative representation of all the test results was obtained by summing up equation (5-1-2), (5-2-6), and (5-3-7):

$$\varepsilon(t) = (\sigma_1 - \sigma_3)\left\{\frac{100}{(E_0 - \ell(\sigma_1 - \sigma_3)} + 52\sigma_3^{-.154}(\sigma_1 - \sigma_3)^{.65}\frac{1}{\sqrt{2\pi}\delta}\int_{-\infty}^{t} e^{-\frac{(t-\mu)^2}{2\delta^2}}dt\right.$$

$$\left. + \left[.154 - .165\,\sigma_3^{-.102}(\sigma_1 - \sigma_3)\right]\sigma_3^{-.12}\, t\, 10^{-5}\right\} \qquad \ldots\ldots\ldots (5\text{-}4\text{-}2)$$

All the stress quantities are expressed in psi, strain in percent (%) and time in minute. All the results of calculation based on equation (5-4-2) (using E_0 and ℓ values shown on tha last page of Section 5.1; μ and $\bar{\sigma}$ values on Tables B-3a and B-3b in Appendix B) are shown as solid lines in Figures 5-7A, 5-7B, 5-7C, and 5-7D; the experimental results are also shown using different notations denoting results obtained at various stress difference levels.

The merits of this equation are that it takes into account not only the complicated non-linear relationship between σ_3, $(\sigma_1 - \sigma_3)$ and time, which hindered most of the classical treatment of creep behavior and made the application of principle of superposition impossible, but also consider the basic elastic, non-elastic characteristics of the creep behavior. It is also obvious from the procedure of evaluation that the linear relationship as reported

by others is only a special case and may be treated similarly by the proposed method. Because of the inclusion of non-linear flow components in the equation, it is the author's opinion that this solution could not be obtained by solving a linear differential equation and hence the result of this series of creep tests could not be superimposed linearly. This result is consistent with the results obtained by the author in a previous investigation (Chen, 1965).

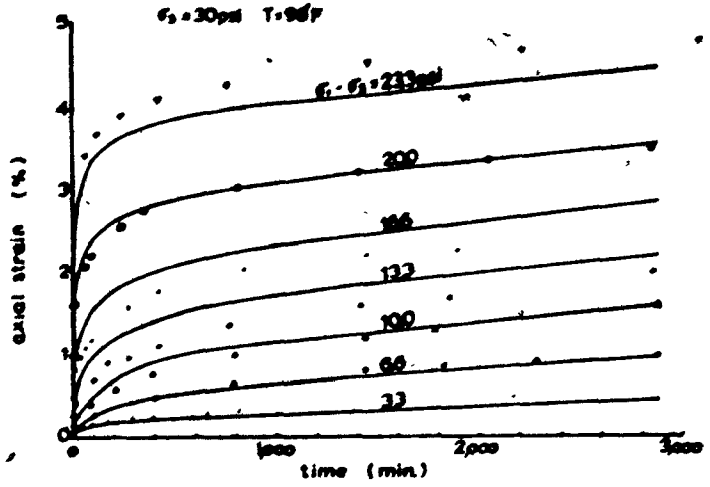

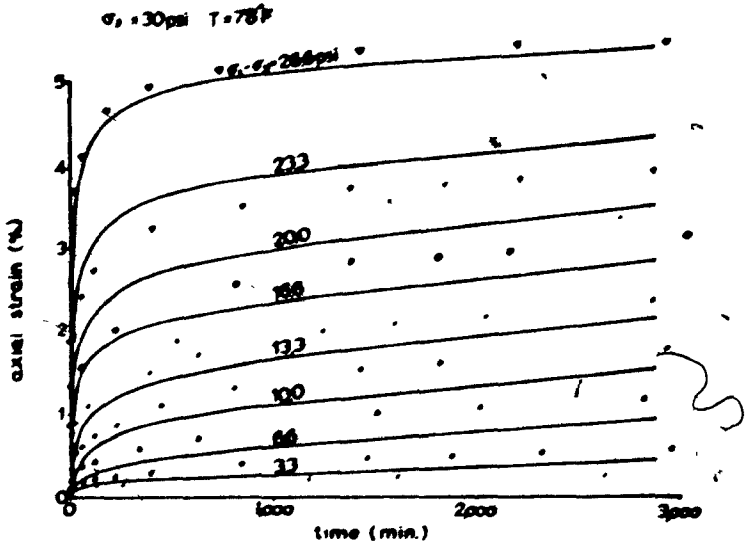

Fig. 5-7A
Comparison Between Theoretical and Experimental Results

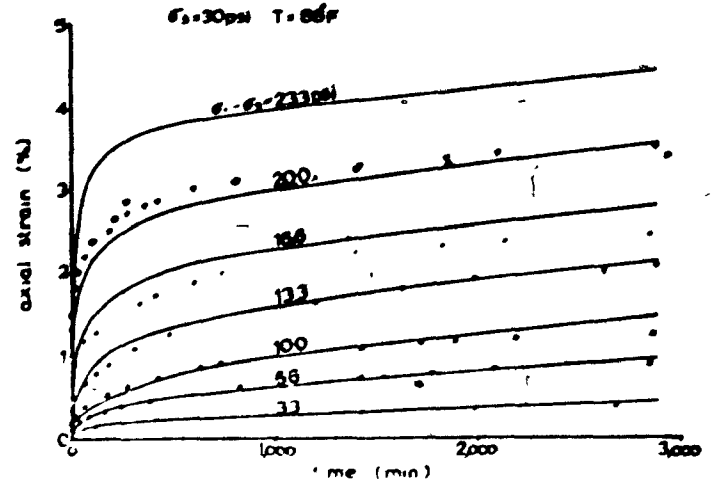

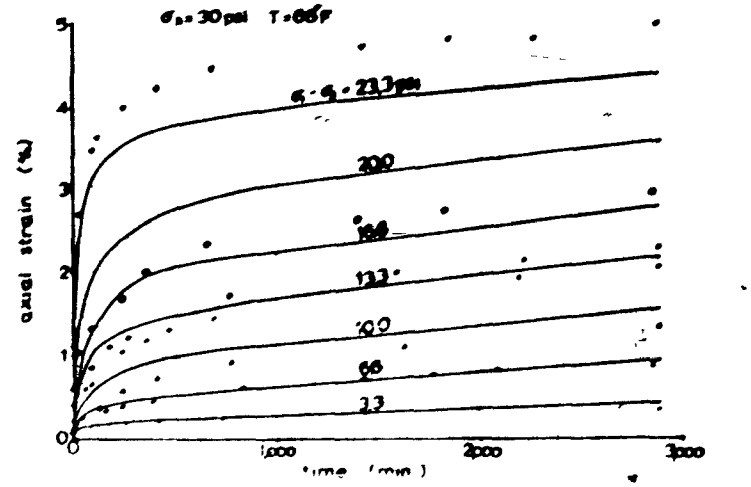

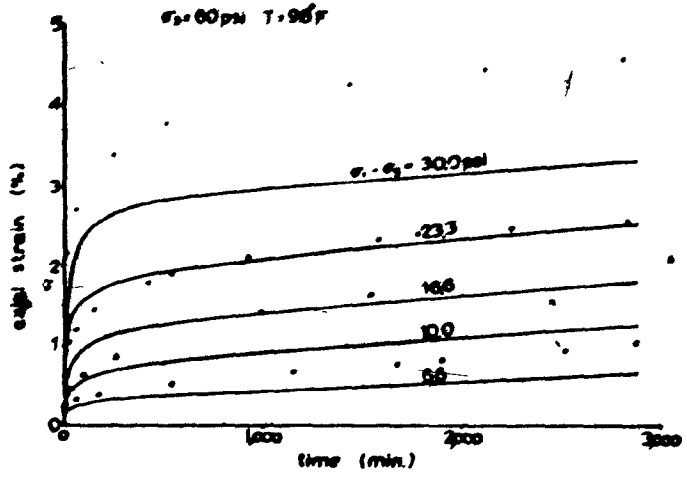

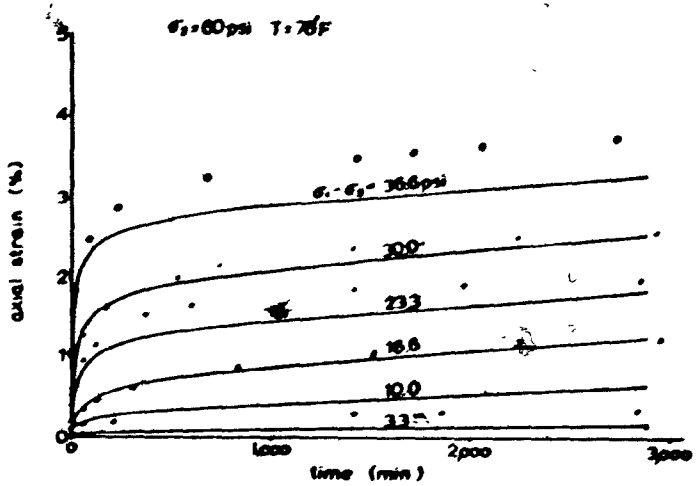

Fig. 5-7B
Comparison Between Theoretical and Experimental Results

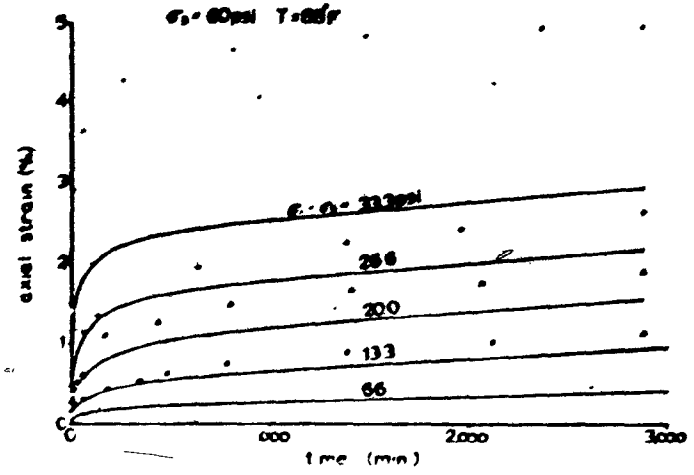

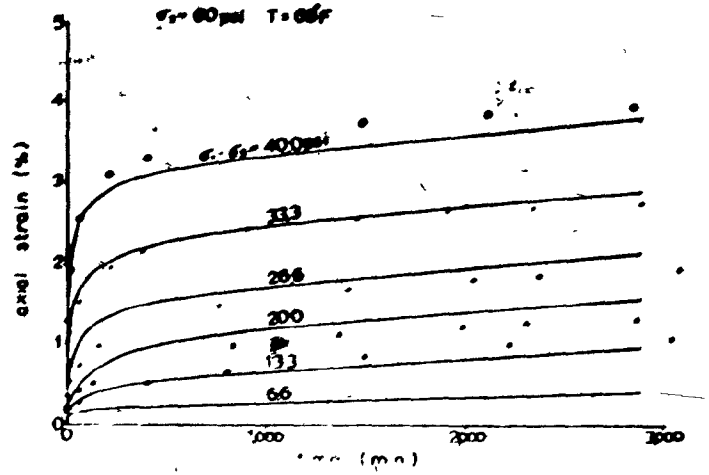

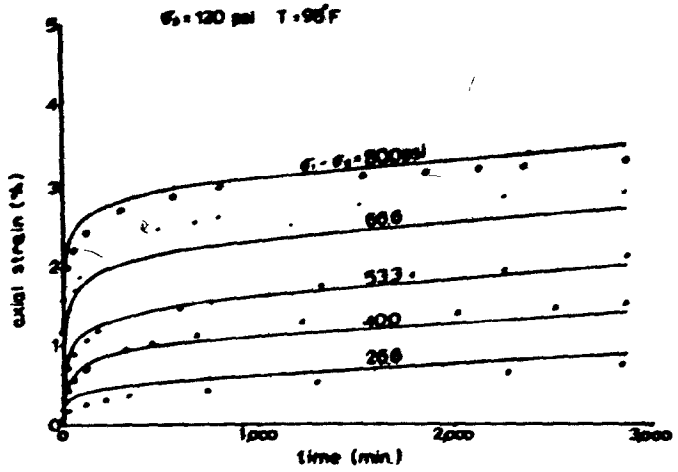

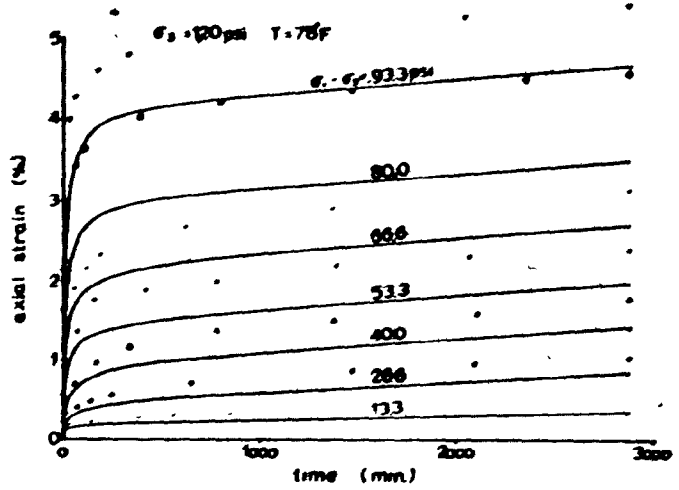

Fig. 5-7C
Comparison Between Theoretical and Experimental Results

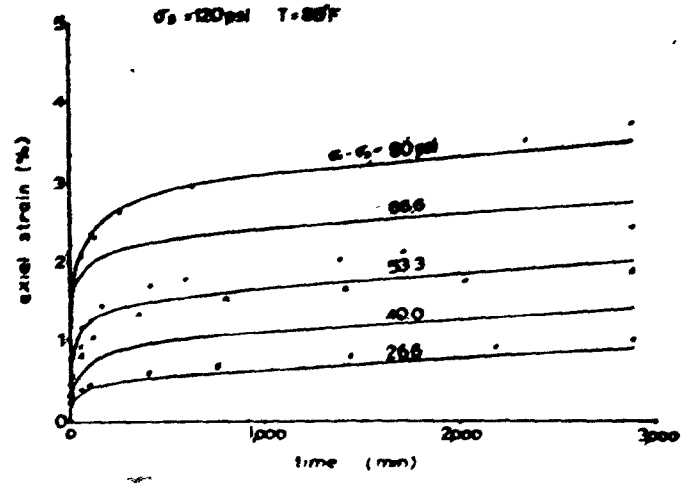

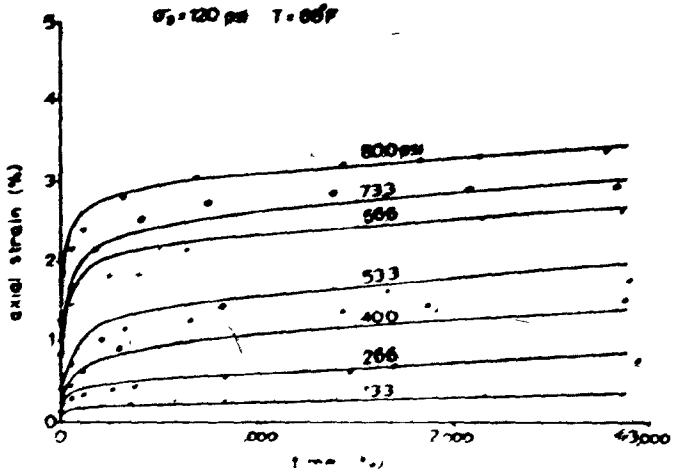

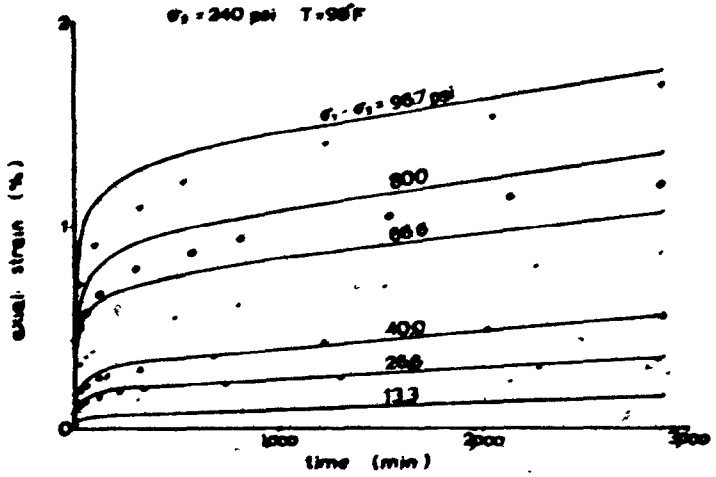

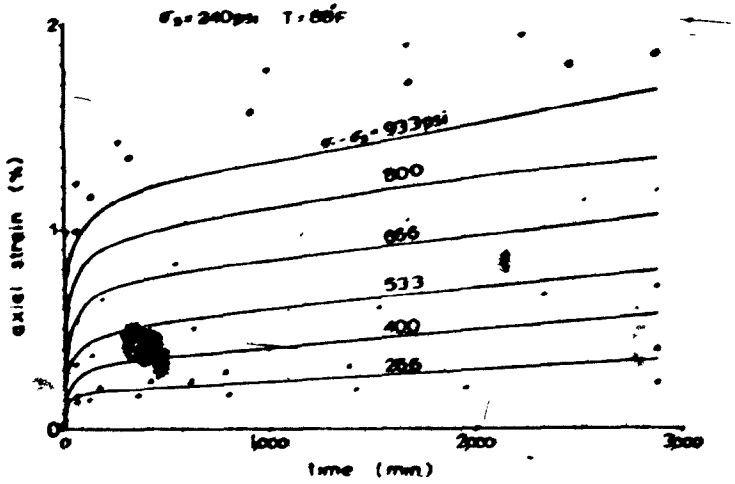

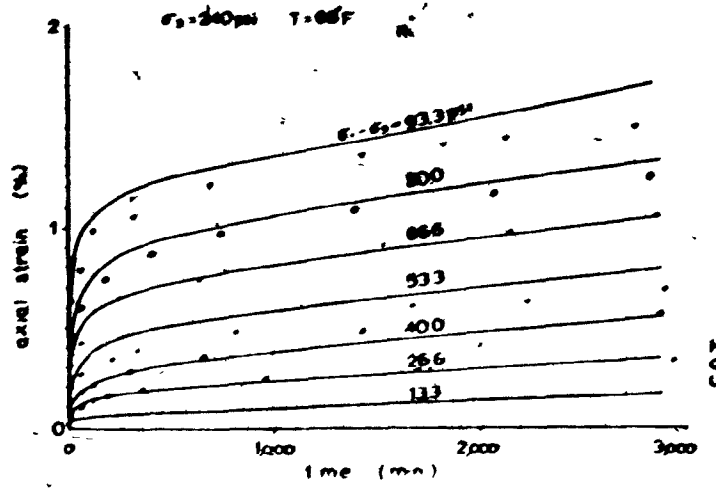

Fig. 5-7D
Comparison Between Theoretical and Experimental Results

CHAPTER 6

DISCUSSION, CONCLUSION AND [illegible] RESEARCH

6.1 DISCUSSION OF RESULTS

Drained creep tests on fifteen specimens were carried out and a total of ninety nine creep curves were obtained from this study. The wide ranges of confining pressure (from 30 psi to 240 psi) and stress difference (from 10 to 80 percent of specimen strength) used in the investigation made it possible to arrive at a stress-strain-time relationship which takes into account the elastic, anelastic and flow characteristics of clay soils. Retarded after effect under each individual load was assumed a priori to be viscoelastic which enables the probability distribution function of micro-structures to be analyzed and introduced into the stress-strain-time relationship. Tests were carried out under controlled temperatures. Levels of 68°F, 78°F, 88°F, and 98°F were arbitrarily chosen in this series of investigation which will enable one to examine the drained creep test results in the light of rate process theory. All the analytical and experimental results presented in previous chapters will be discussed in this chapter.

The discussions in this chapter include the following four points:

(a) comparison of known stress-strain-time

relationship, their merits and descrepancies;

(b) applicability of rate process theory to this series of tests;

(c) a possible creep mechanism (elementary unit interaction) as depicted from drained creep characteristics observed from test results; and

(d) discussion of using distribution function as a bridge to correlate the macroscopic phenomena to the micro structural units in the material.

6.1.1 Stress-Strain-Time Relationships

The stress-strain-time relationships given by Equations (2-2-2-1) and (2-2-2-2) considered the creep performance as the accumulative performances of each elementary unit. The probability of occurrence of each unit then serves as a weighing factor which theoretically assesses not only the existence of each unit but also the contributing performances of each unit. Equation (5-4-1) considered the integrity of the stress-strain-time behavior and introduces the probability density function into the analysis. The spectrum of the distribution function was used to bridge the micro-structure characteristics to the overall performances of the specimen.

These relationships are derived on the basis that a creep strain may be considered as composed of three components: i.e. instantaneous, retarded, and flow components. By numerical evaluation of the terms in these equations, Equation (5-4-2) is obtained which gives a complete description of the creep behavior in this series of drained creep studies.

$$\varepsilon(t) = (\sigma_1 - \sigma_3)\left\{ \frac{100}{E_0 - 1(\sigma_1 \sigma_3)} + 5.2\,\sigma_3^{-1.54}(\sigma_1 - \sigma_3)^{0.5} \frac{1}{\sqrt{2\pi}\,\sigma} \int_{-\infty}^{t} e^{-\frac{(\tau-\mu)^2}{2\sigma^2}} d\tau \right.$$
$$\left. + \left[159 - 165\,\sigma_3^{-0.02}(\sigma_1 - \sigma_3) \right] \sigma_3^{-1.2}\, t\, 10^{-5} \right\} \quad \ldots\ldots\ldots (5\text{-}4\text{-}2)$$

Ideally, numerical evaluation of this equation includes the following steps:

1. A series of creep test on two samples to be performed at upper and lower confining pressure ranges. For each effective confining pressure level, two creep tests to be carried out, one at, say, 10 percent of the strength of the specimen, another at, say, 50 percent of the strength or the expected highest stress to be imposed on the soil in-situ. The tests should be carried out at controlled temperatures and with a duration long enough to obtain steady state creep.
2. Apparent instantaneous modulus of elasticity are evaluated and a relationship between σ_3, $\sigma_1 - \sigma_3$ and modulus of elasticity is obtained as described in Section 5.1 Expression for the prediction of instantaneous strain may be obtained by Equation (5-1-2).
3. The steady state creep rate compliances are plotted versus stress difference levels. Intercepts and slopes of two lines obtained from these two series of tests are evaluated and are plotted as shown on Figure 5-4.

The relationships between a, b, and σ_3 are established. Therefore, the quantitative equations for flow and flow rate similar to (5-2-5) and (5-2-6) may be obtained.

4. Retarded strain at any time after load application may be evaluated according to Equation (5-3-1). This retarded component of deformation is then plotted against logarithm of time and analyzed according to the retardation time distribution method as described in Section 2.2.3 and example given on Figure 5-5. The basic properties of the distribution curves are obtained. Logarithm of the retarded strain components are also plotted against logarithm of ($\sigma_1 - \sigma_3$), a figure similar to Figure 5-6 will be obtained. The "C" value in Equation (5-3-5) in terms of σ_3, may be evaluated, therefore, the ultimate retarded strain may be expressed in terms of σ_3, $\sigma_1 - \sigma_3$ as shown in Equation (5-3-6).
5. With these three components evaluated, a complete stress-strain-time relationship for the soil tested may be obtained by summing up these three terms.

The above procedure of deriving a complete stress-strain-time relationship was deducted for the loading procedure used in this series of tests, i.e. several loading-unloading steps were applied to one sample rather than one loading on one sample as usually used in creep investigation. It remains to be verified whether the proposed procedure can be applied to other test conditions such as undrained creep tests with loading-unloading programs or step loadings. It is the author's opinion that this procedure might be applicable provided that the relationships such as Equations (5-1-1), (5-2-2), (5-3-5) etc. could be verified by a third sample tested under an intermediate confining pressure level and an additional intermediate loading was applied to each sample.

Equation (5-4-2) and results of calculations as shown on Figures 5-7A to 5-7D, indicate that relationships between stress, strain, and time may be predicted satisfactorily by the proposed method even if the relationships are non-linear. In view that soil conditions may vary from one location to another, it is a general practice that for a site which calls for a creep investigation, the stress-strain-time relationships be investigated by an intensive field and laboratory testing program. Because the magnitude of creep at a specified

time duration, or the time duration required to reach a tolerable creep deformation may affect the decision for some construction procedure, the proposed creep analysis which provides separate account of short term (instantaneous and retarded) and long term (flow) strains may be of help in making such a decision. Since there is no unique standard method for creep predictions, it is considered that the proposed method which gives a satisfactory prediction of drained creep behavior for this series of tests might be of practical importance in engineering practice such as settlement of tanks founded in thick compressive soils, in anchor construction, open cuts and other settlement and stability problems.

In recent years, a significant development in the stress-strain-time relationship investigation is the result published by Singh and Mitchell (1968, 1969). A semi-empirical formula was proposed which is in fact the integration of Equation (4-3-2):

$$\varepsilon(t) = a + \frac{A}{1-m} e^{\alpha(\sigma_1 - \sigma_3)} t^{1-m} \qquad \text{.....(6-1-1)}$$

where "a" is an integration constant and in each case the value of "a" must be chosen to give the best fit between observed and predicted behavior; "A" is the projected strain rate at t = 1 minute and ($\sigma_1 - \sigma_3$) = 0 from a

plot of $\log \dot{\varepsilon}$ versus ($\sigma_1 - \sigma_3$) as shown on Figure 6-1: "m" is the slope of the straight lines of a plot of $\log \dot{\varepsilon}$ versus log t; and " α " is the slope of the mid-range linear portion of a plot of $\log \dot{\varepsilon}$ versus ($\sigma_1 - \sigma_3$), all values of $\dot{\varepsilon}$ are corresponding to a certain time duration after load application.

The basic assumptions used in their formulation are the existence of linear relationships between

1. $\log \dot{\varepsilon}$ and $\sigma_1 - \sigma_3$ at a certain time after load application,
2. $\log \dot{\varepsilon}$ and log t at a ($\sigma_1 - \sigma_3$) level.

A sample calculation, using $\alpha = 0.21$, $m = 0.53$, $A = 2 \times 10^{-3}$ for $\sigma_3 = 30$ psi, $T = 88^{\circ}F$ and at different stress levels (Figure 6-2), shows that Equation (6-1-1) fits well for first few loading intensities. But at higher stress levels, the prediction deviates from the experimental results to an untolerable amount; this behavior was also observed by Singh and Mitchell. Examination of the possible source of error for this deviation revealed that it is likely that α and m are functions of time and stress levels. As seen from Figure 6-1-, the slope of the mid-range segment, if straight line portion does exist, becomes milder at longer time durations and higher stress levels, i.e., " α " becoming smaller in value at longer time durations and higher stress levels.

While Figure 6- 3 shows that the assumption of a linear relationship is approximately correct, however, the slope is seen to become slightly steeper, i.e. m value slightly higher, at higher stress difference levels. Therefore, the value of $\frac{A}{1-m}$ becomes slightly smaller at higher $(\sigma_1 - \sigma_3)$ levels. The combined effect of "m" and "α" might be counted for the observed deviation of experimental and theoretical results based on Equation (6-1-1).

Results of calculations based on Equation (5-4-2) developed in this study are also shown on Figure 6- 2. A better agreement between the observed performance and prediction is obvious. Since the three terms in Equation (5-4-2) consider, physically, the basic properties of a stress-strain-time behavior, i.e. elastic, anelastic and flow of the material, it is considered logical in the stress-strain-time relationship formulation to take into separate account of these behaviors. Although this might imply a slightly time consuming in its analysis process, however, it is firmly believed that the method developed in this study would result in a more accurate prediction of the creep behavior, therefore, serve a better interest in engineering practice. The time spent in the calculation would certainly receive immediate reward.

However, some minor discrepancies, other than the usual experimental scattering of data, were observed:

1. usually at the last increment of load, which approaches the unconfined compressive strength of the specimen, the experimental data frequently greater than the calculated results; and
2. there is a gap between theoretical and experimental results in the primary creep portion of deformation.

Because of (1), it is considered that the proposed method should not be applied to the loadings that approach the unconfined compressive strength of the soil. Otherwise may result in the under estimate of the ultimate deformation.

The gap between the theoretical and experimental results as stated in (2), there may be two reasons causing this discrepancy: (a) the distribution of the retarded portion of deformation is generally negatively skewed, while a normal distribution was assumed in the formulation of Equation (5-4-2); (b) the portion of deformation due to drainage is not taken into account and therefore is hidden in the term ε_r evaluated.

Generally, the difference between the theoretical and experimental results are seldom exceeded 0.5 percent for stresses less than 50 percent of the unconfined compressive strength of the specimen. In view of this single compact form of equation could represent well most of the ninety nine experimental curves, especially for stresses below 50 percent of the unconfined compressive strength of the specimens, it is considered that the results of this investigation is rather encouraging and the proposed method of result analysis may be of practical importance in engineering practice due to its simplicity and accuracy in predicting creep strain for a reasonable range of stress levels.

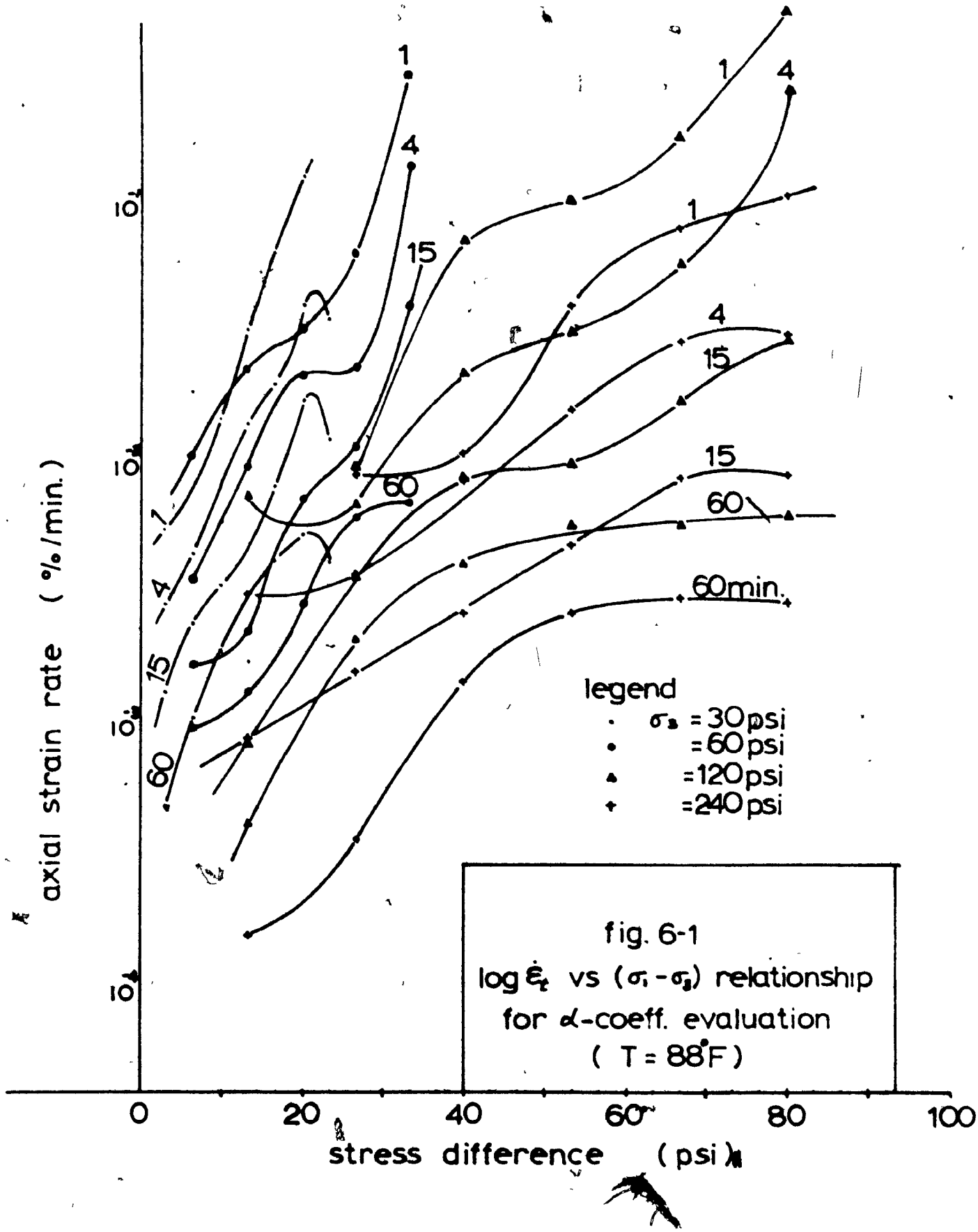

fig. 6-1
log $\dot{\varepsilon}_t$ vs $(\sigma_1 - \sigma_3)$ relationship
for α-coeff. evaluation
(T = 88°F)

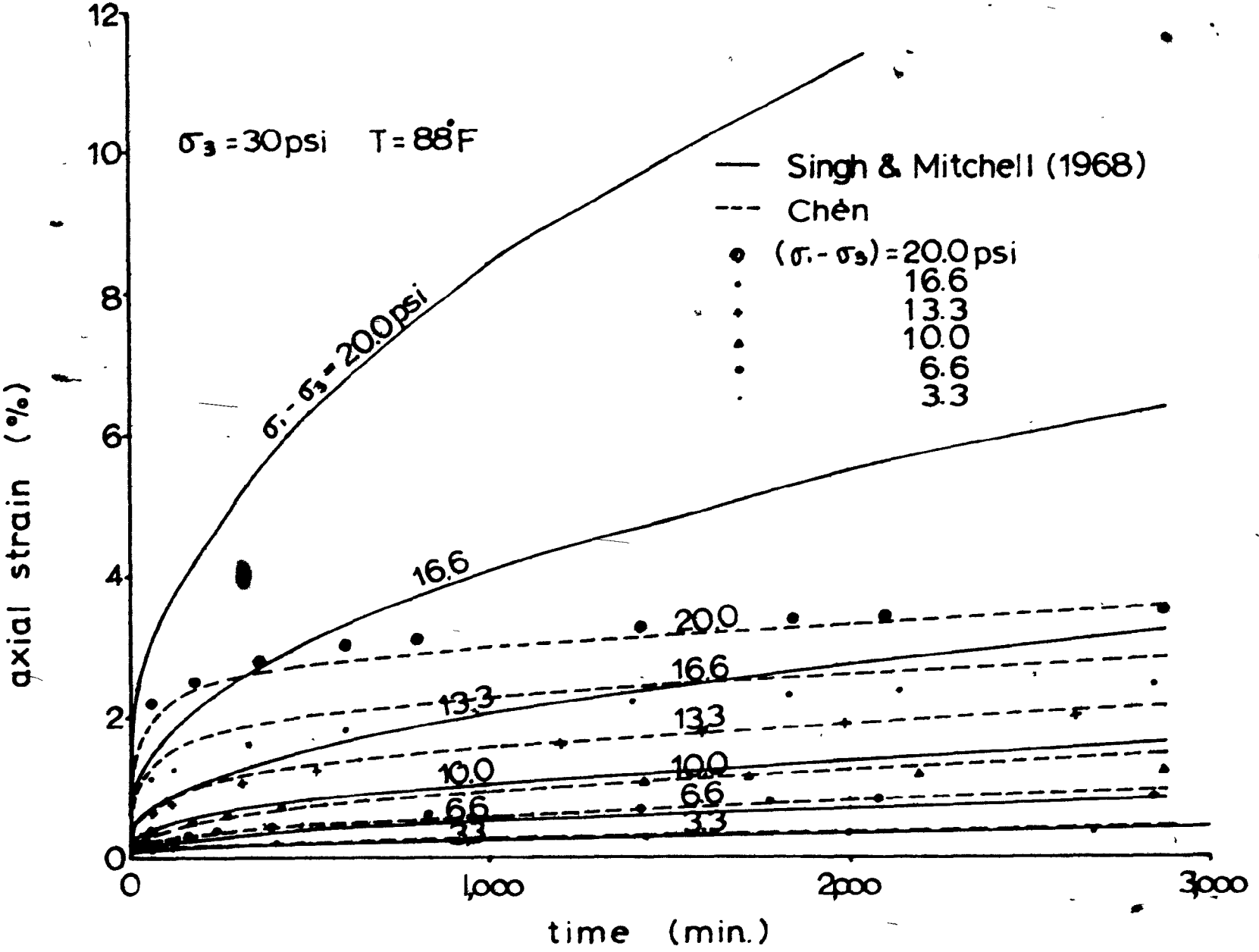

fig. 6-2 comparison between experimental and theoretical results

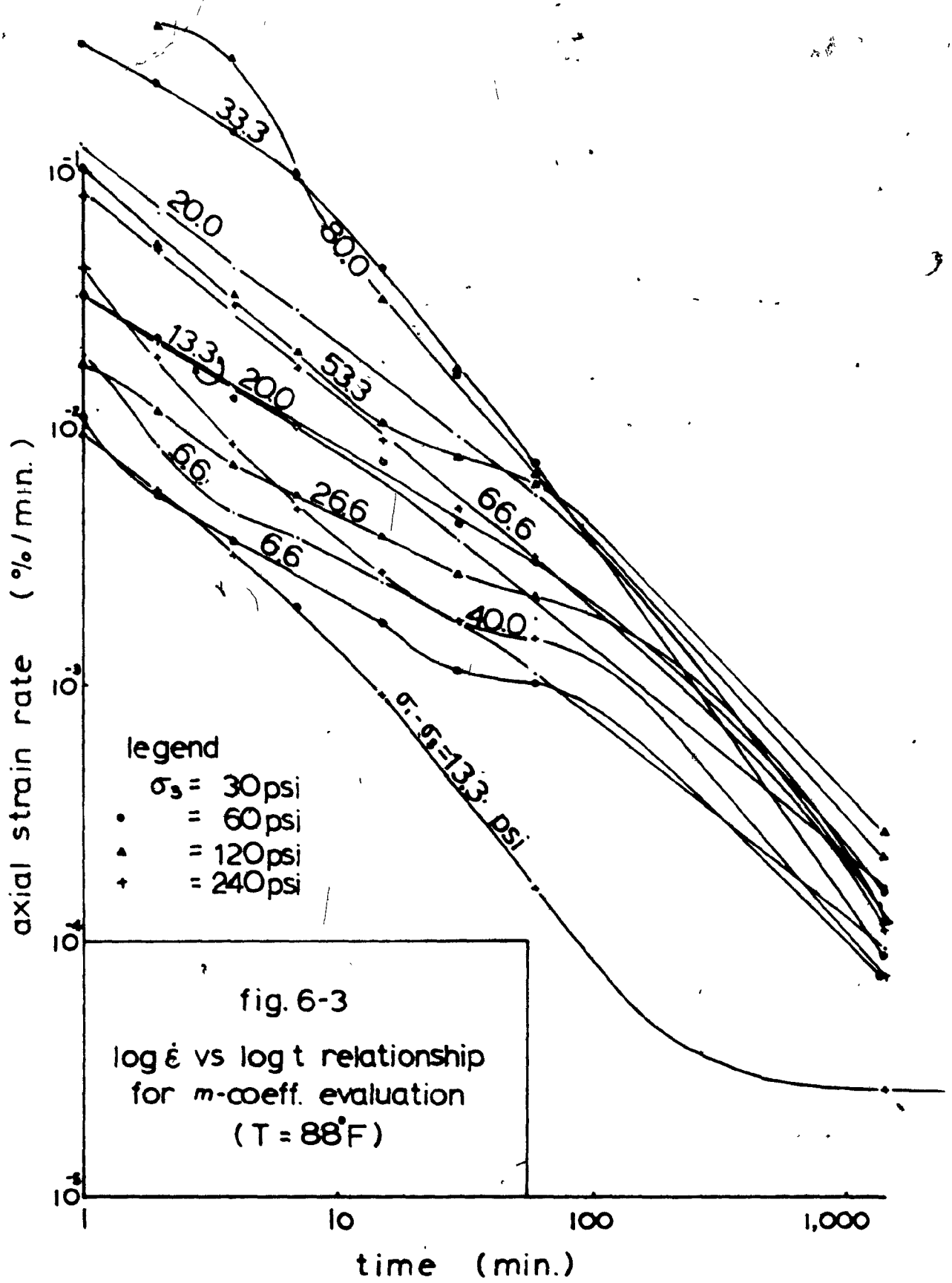

fig. 6-3

log $\dot{\epsilon}$ vs log t relationship for *m*-coeff. evaluation (T = 88°F)

6.1.2 Temperature Effects and Rate Process Theory

It is now generally recognized that carefully controlled temperature surrounding the test sample is necessary in certain types of soil investigations such as consolidation, tests with pore water pressure measurements, physico-chemical studies, etc., because engineering properties of soils can be significantly influenced by temperature variations. Studies of flow and deformation characteristics of clay soils by Mitchell (1964), Andersland (1967), and others demonstrated that the difference in temperature control is also necessary in order to evaluate the so-called "experimental energy of activation".

It is a generally accepted fact that the absorbed double layer on the particle surface behaves differently from that of normal water in the free state (Lambe, 1958; Martin, 1962; Rosenquist, 1962). Atoms of water and clay are in a constant state of thermal agitation with an intensity determined by the environmental temperature. Higher temperatures may increase the probability that an atom, at particle to particle contact points, moves from one equilibrium position to another, giving rise to the observed temperature effect on configuration and mechanical behavior of clay soils. Thus, the thermal actions may be considered as one type of forcing function which will give

rise to a proper response function. However, special control of the temperature and other properties of the test specimen is necessary since the temperature effect may be easily offset by the variation of other influential factors, such as structure, water content, strain, and stresses.

From this series of test results, the temperature effects on stress-strain relationships are not so obvious at high and low confining pressures as at medium confining pressures of 60 psi and 120 psi. At σ_3 = 30 psi, where the fabric are probably in a more random state, the factor of specimen heterogeneity might dominate the test results. While at σ_3 = 240 psi, the specimens are in such a well compacted state that the deformation characteristics are probably primarily controlled by the stress intensities, therefore, the variation of temperature from 68°F to 98°F is probably not sufficient to induce the thermal effect clearly.

The effect of temperature on stress-strain behavior is, therefore, analyzed by examining the results of tests carried out at confining pressures of 60 psi and 120 psi. In Figure B-17, if a horizontal line is drawn through an axial strain of, say 2 percent, this line would intercept the curves representing σ_3 = 120 psi, T = 68°F and 88°F at points with coordinates of (2 percent, 58 psi),

(2 percent, 48 psi) and (2 percent, 43 psi) respectively. The differences in stresses of 10 psi and 15 psi are due to the variation of test temperatures from 68°F to 78°F and 68°F to 88°F respectively.

If these differences in stress are defined as the "stress equivalence" and similarly "strain equivalence", then a plot of stress equivalence versus log ε shows that the stress equivalence increases linearly with the increase of logarithm of strain; while a plot of strain equivalence versus stress difference shows that the strain equivalence increases progressively with increase of stress (Figures 6-4 and 6-5). It is seen that at 3 percent of strain, a difference of 20°F in temperature, from 68°F to 88°F, is equivalent to the effect of 15 psi difference in stress for σ_3 = 120 psi. At stress of 20 psi, the difference in temperature, from 68°F to 88°F, produces an effect equivalent to 0.6 percent in strain. These results indicate that temperature does influence the stress-strain relationship to a measurable amount and can not be ignored in a scrupulous investigation.

The other object of the temperature control in the test was to examine the results in the light of the rate process theory. The original formation of the rate process theory was derived for viscous flow and diffusion process (Glastone, et al, 1941). The temperature

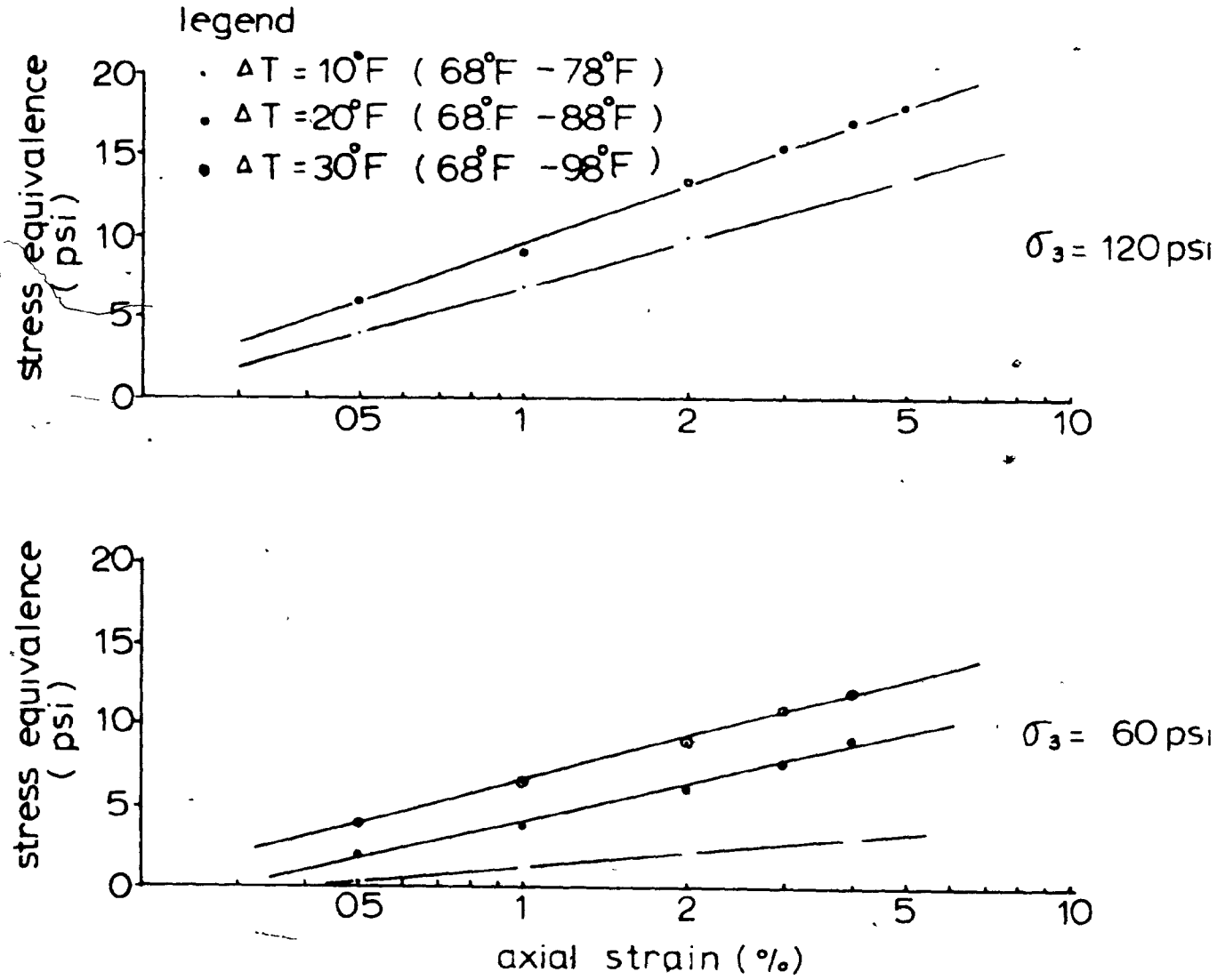

fig. 6-4 temperature effects

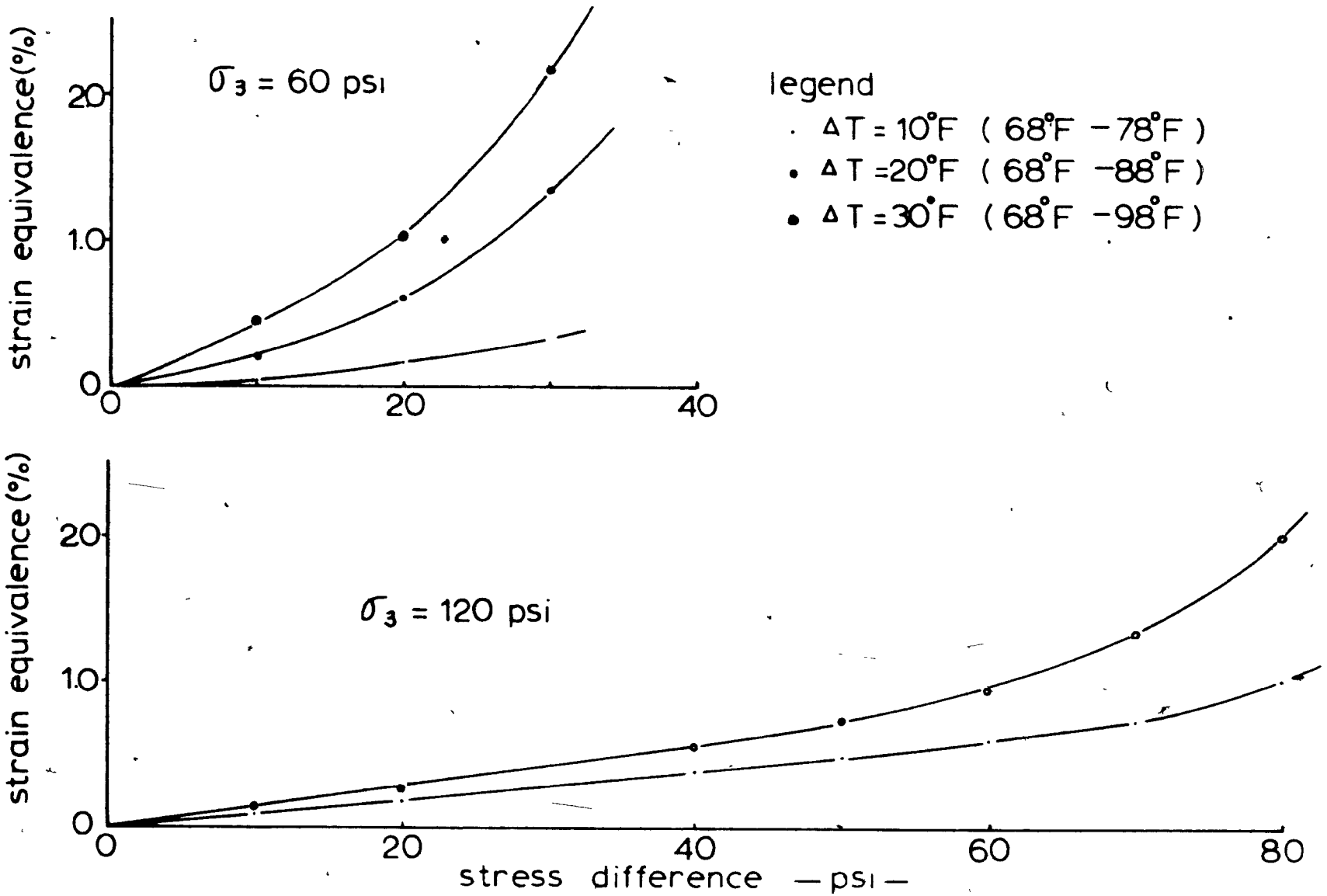

fig 6-5 temperature effects

dependency of reaction rate was expressed by the following functional relationship:

$$\dot{\epsilon} = X e^{-\frac{\Delta E_x}{RT}} \qquad \text{.....(6-2-1)}$$

where $\dot{\epsilon}$ is the reaction rate

X is a parameter relating activation frequency to strain rate

ΔE_x is the experimental activation energy

R is the gas constant equal to 1.987 cal./deg. mol.

T is the absolute temperature in ^{o}K

After partial differentiation, the following relationship between $\log (\dot{\epsilon}/T)$ and $1/T$ is obtained:

$$\frac{\partial \log (\dot{\epsilon}/T)}{\partial (1/T)} = -\frac{\Delta E_x}{R} \qquad \text{.....(6-2-2)}$$

Considering the soil creep process as a thermally activated rate process, Mitchell, Campenella and Singh(1968), after observing the steady state creep rate at several temperature levels, plotted $\log (\dot{\epsilon}/T)$ against $1/T$ for several soils and established that the relationship was linear as predicted by the equation (6-2-2). The slope of the line gives the value of $-\frac{\Delta E_x}{R}$. The experimental activation energy may, therefore, be evaluated; e.g. San Francisco Bay mud consolidated at

$1^{kg}/cm^2$ and at ($\sigma_1 - \sigma_3$) of $0.45^{kg}/cm^2$, experimental activation energy of $\Delta E_x = 31.4^{k.cal}/mol.$ was evaluated; and for remoulded illite, $\Delta E_x = 43.5^{k.cal}/mol.$ A number of other researchers have also used the rate process theory and have obtained various experimental energy of activation values for various materials. Some of their results are listed on Table 6-1. (Mitchell, 1968)

TABLE 6-1

ACTIVATION ENERGIES

Material	Activation Energy 1,000 Cal/K°/Mole	Reference
Water	4-5	Glasstone, Laidler and Eyring
Plastics	7-14	Ree and Eyring
Asphalt	14-20	Herrin and Jones
Soils	25-45	Mitchell, Campanella and Singh
		Ripple and Day
	23-27	Christensen and Wu
	1-76	Chen
Concrete	54	Polivka and Best
Metals	50+	Finnie and Heller
Frozen Soils	93.6	Andersland and Akili

To examine the applicability of rate process theory to this series of drained creep tests, the creep rates at steady states obtained in this series of investigations are plotted against stress difference as shown on Figure B-16. Results show that, in this plot, the creep rate-stress difference relationship is non-linear. At confining pressure of 30 psi, the creep rate increases as stress difference increases to about 50 percent of the strength of the specimen. The creep rate then begins to fluctuate and shows a tendency toward a decrease in magnitude as stress intensity increases. At higher confining pressures of 60, 120, and 240 psi, the creep rate increases as stress intensity increases to about 50 percent of the strength of the specimen and then fluctuates with a tendency toward an increase in magnitude. This result is compared with a number of selected results by others shown on Figure 4- 6. It is shown in this figure that for the undrained creeps carried out by Singh et al., the creep rate increases exponentially as stress difference increases. Whereas in the drained creep test carried out by Bishop et al, the increase in creep rate and stress difference are approximately proportional. It is interesting to note that at last loading of Bishop's results, a slightly smaller creep rate was also obtained.

In order to examine the applicability of the functional relationship of Equation (6-2-2), data obtained

in this series of investigations are plotted in the form of $\log \dot{\varepsilon}/T$ versus $1/T$ as shown on Figure 6-6. As expected, after knowing the fact that the creep rate fluctuates with the change of stress intensity, no linear relationship between $\log \dot{\varepsilon}/T$ and $1/T$ was observed; although in a few instances three points may occasionally form a straight line; most of them do not exhibit such a linear relationship. However, by applying the Equation (6-2-2) to any two points on the same curve in Figure 6-6, which will give a positive ΔE_x, a number of the experimental activation energies may be evaluated for each stress level. A range of values varying from 1,000 cal./^{o}K/mole to 76,000 cal./^{o}K/mole was obtained. Some typical values are shown on the corresponding segments in this figure.

However, by averaging the obtained activation energy values for each stress level, as plotted on Figure 6-7, it is seen that the activation energies at lower stress difference levels are greater in magnitude and decreases rapidly to a relatively constant value at higher stress intensities. At higher confining pressures, the activation energies evaluated by this method are also higher; except for σ_3 = 120 psi the evaluated energy of activation is the highest at higher stress levels.

This result is similar to that observed by Andersland and Akili (1967) in their creep test results

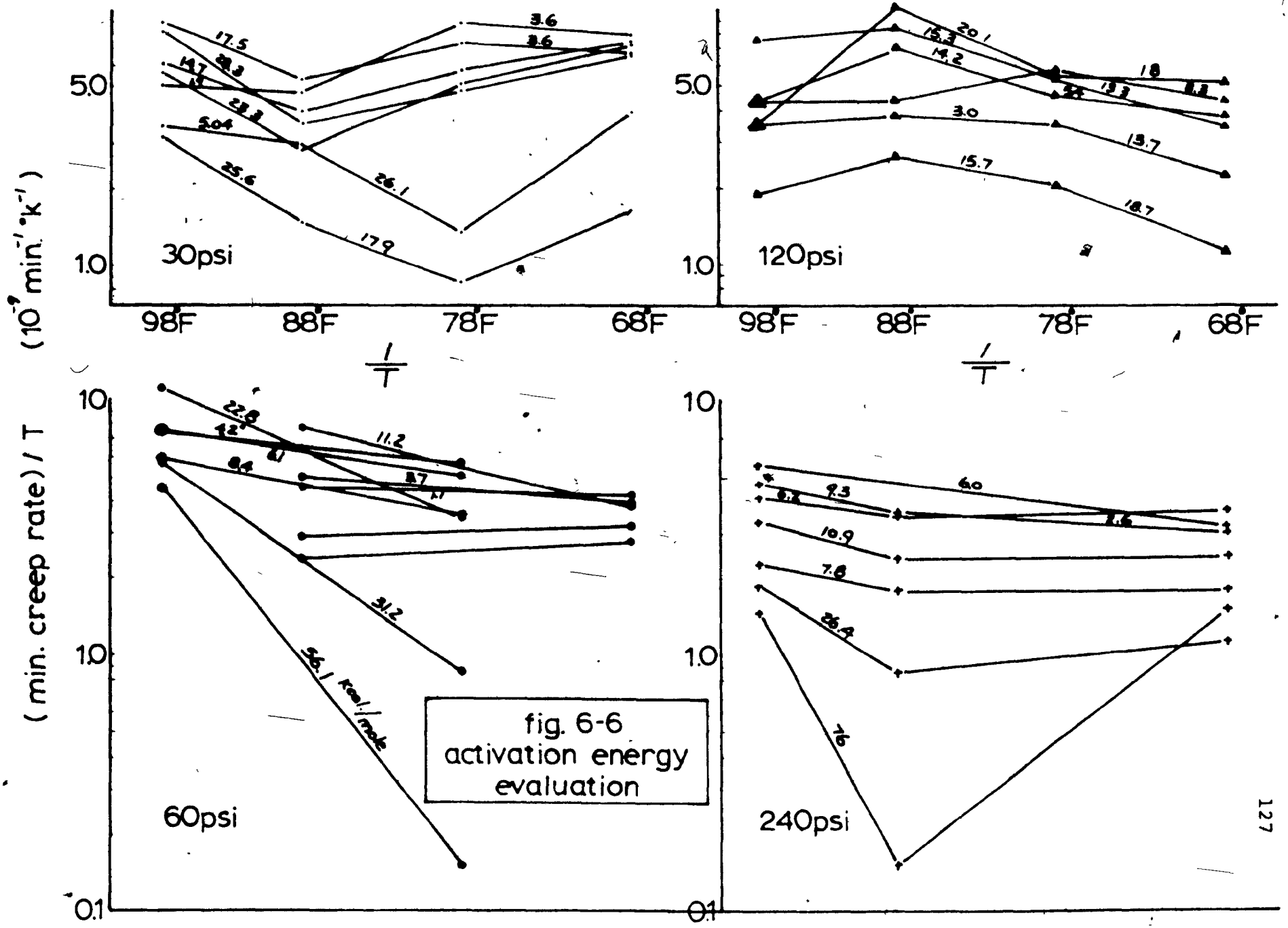

fig. 6-6
activation energy
evaluation

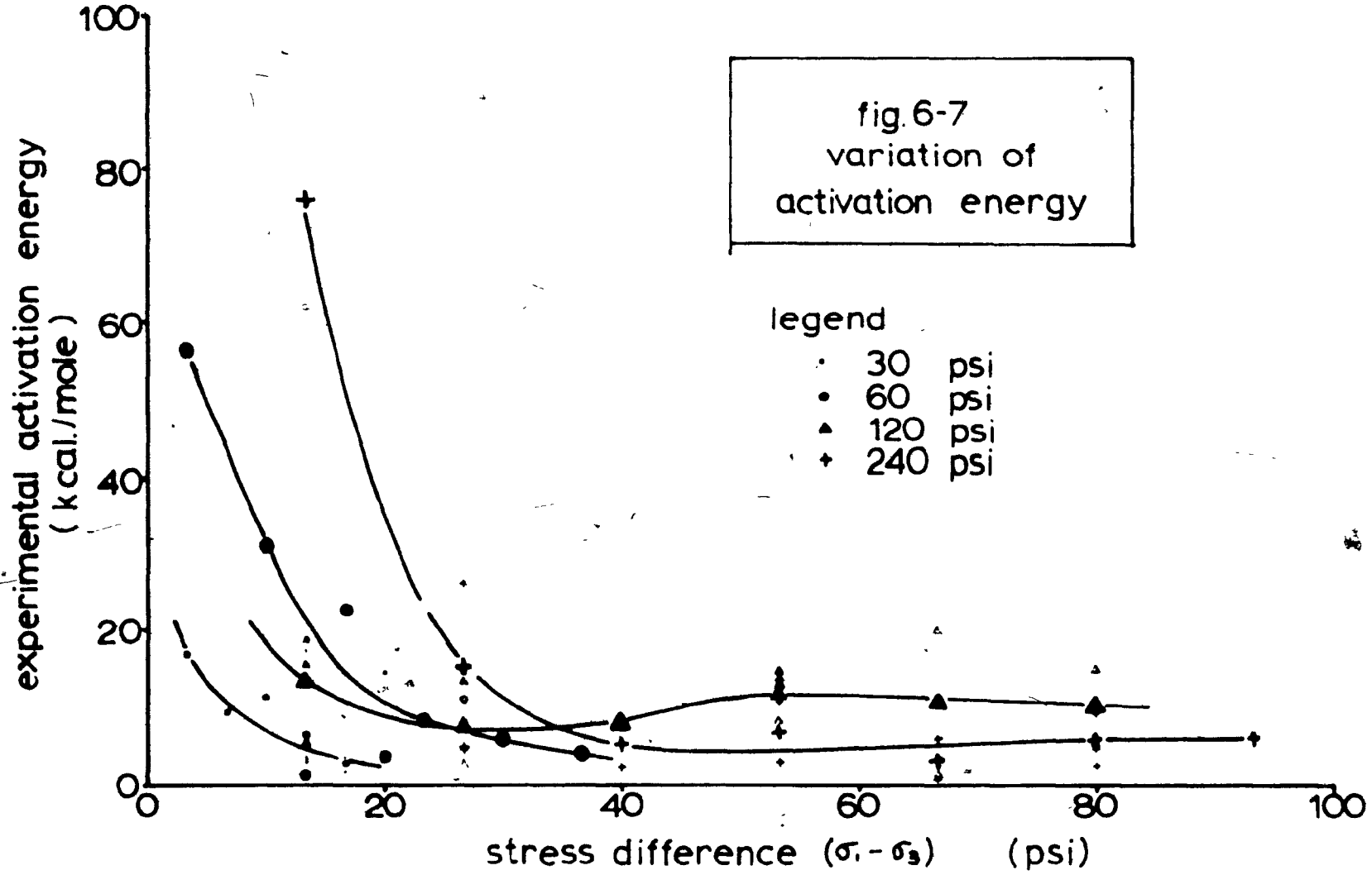

fig. 6-7
variation of
activation energy

carried out on frozen Sault St. Marie Clay. Their observed data also indicated that the energy of activation decreases with the increase of axial stress and approaches a relatively constant value at higher stress levels. They attributed this variation to the different dominant mechanisms such as flow of particle and/or ice contact points at various levels of stress.

Considering the wide range of experimental activation energy values obtained, it is the author's opinion that there may be several possible contributing factors:

(a) Applicability of rate process theory to this series of drained creep tests is questionable. As shown on Figure 6-6, there are a number of segments jointing experimental points by which no positive experimental activation energy could be evaluated. This fact is not consistent with the concept of rate process theory.

(b) Samples tested at two different temperature levels are not identical. Therefore, the response to an applied stress, even if the stress level is kept the same, does not follow the rules predicted by rate process theory.

(c) The rate of creep is dictated by the interactions of the elementary units within the

sample and which is further a result of the interaction of the strain and stress distributions within the samples. Since these distributions are random in nature, the response behavior is expected to fluctuate and deviate from the expectation. A more elaborate consideration in this respect will be discussed in Sections 6-1-3 and 6-1-4 after considering the drained creep characteristics and the possible mechanism involved.

(d) The experimental energy of activation is not only a measure of thermally activation effect, but also measures the energy required by a mechanical activation process, of the participating constituents in a creep process, and this mechanical activation energy is affected by the temperature difference.

If the energy of activation may be regarded as an indication of the energy requirement for the postulated elementary unit to undergo a unit "jump" of a flow unit, then the wide range of activation energies obtained might serve to indicate that a large variety of elementary units with a corresponding wide range of strengths have participated in the deforming process, and that the dominant mechanism involved in the process is not as simple as that suggested

by the model described in the rate process theory. A considerable amount of mechanically activated process, in addition to the thermally activated process, was probably involved in the deformation. As an example, Figure 6-8 shows a cubic block resembling an elementary unit, with dimension dxdxd, acted upon by a stress f and rotates an angular rotation of θ combined with a translation of δ. The work (or energy) required to produce such a deformation may be shown to be:

$$\Delta E = \frac{1}{2} \cdot f \cdot d^2 \cdot (\delta + \frac{1}{2} d \cdot \theta)$$

Assuming

$f = 1{,}000\ g/cm^2$ (14 psi)

$d = 20{,}000\text{Å}, 30{,}000\text{Å}, 50{,}000\text{Å}$ (i.e. 2, 3, 5 clay particle diameters)

$\theta = \frac{\pi}{2}, \pi$

$\delta = d, 2d$

Results of the calculations are plotted on Figure 6-8 which shows that the energy required increases rapidly as the size of the elementary unit increases.

In order to reach a state that these free rotation and translation may take place, it is recognized also that the bonding at contacts between elementary units must be broken. Therefore, the evaluated energies for the translation and rotation are only part of the activation energy necessary to complete a "jumping" process of the elementary unit. From the envisaged mechanism, significant

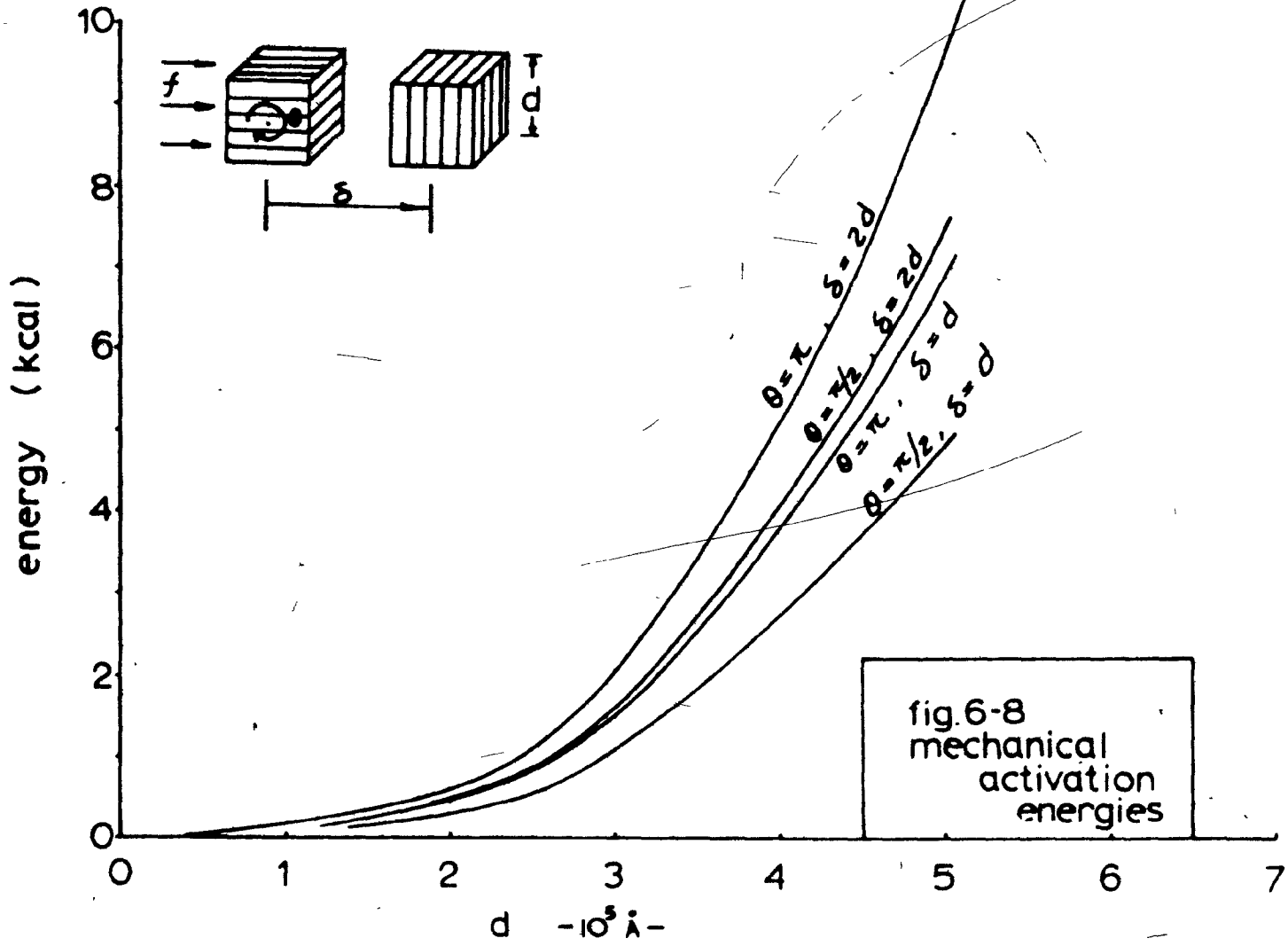

fig.6-8
mechanical
activation
energies

translation and rotation can only take place during the first few loadings when the specimen is relatively loose and has ample, randomly distributed voids in the macro-pores to permit significant displacements. The evaluated high energy of activation during the first few loadings may imply that significant mechanical activation process have taken place along with that of thermal activation process as described by rate process theory.

6.1.3 Drained Creep Characteristics - A Time Dependent Deformation Mechanism

It has been shown by Walker (1969) and Arulanandan et al. (1971) that in an undrained creep test, significant pore water pressures are generated in the specimen tested. Creep strain and pore pressure are shown to be directly related (Walker, 1969), and the magnitude of pore water pressure build-up was shown to be consolidated pressure, time and structure dependent (Arulanandan, et. al., 1971). A pore water pressure as high as 90 percent of the consolidation pressure may be generated at high stress levels and, therefore, considerably reduced the effective stresses acting on the soil skeleton.

In a drained creep test, the pore water pressure built up by the application of additional axial stress is allowed to dissipate. It is, therefore, reasonable to expect that the creep under drained conditions should show a significantly different behavior from that of undrained characteristics.

Consider the postulated elementary units as shown on Figure 1-3 and the schematic picture drawn by Yong (1971) and the possible subsequent behavior under stresses as shown on Figure 6-9 ; the elementary units are expected to become closer after consolidation and reach an equilibrium position when elementary units are in direct contact (B). Upon the application of an additional external force f at

point A, the elementary unit which f acts upon is displaced a distance δ and stresses are redistributed and transmitted to other elementary units (C). A transient pore water pressure gradient may build up within the specimen and local pore water pressure may build up in both micropores within the elementary units and macropores between units. This pore pressure may, however, dissipate to the vicinity macropores which are stressed by lower pore water pressures. Through this redistribution and dissipation process, stress concentration is built up somewhere else on the elementary units and causes continuous deformation as manifested in the measurable macro-deformation process.

The above mechanism is obviously very much simplified. The actual process is three dimensional and probably involves the translation, rotational and distortional deformations. The breaking of structure of the units may also take place in the deforming process. However, the concept of this mechanism was envisaged from the drained creep characteristics observed throughout this series of drained creep tests. In the following paragraphs, the characteristic creep behavior which manifested the proposed mechanism will be described.

The following phenomena are observed from results of this series of drained creep tests:

1. the steady state creep rate decreases at higher stress levels (Figure B-16);

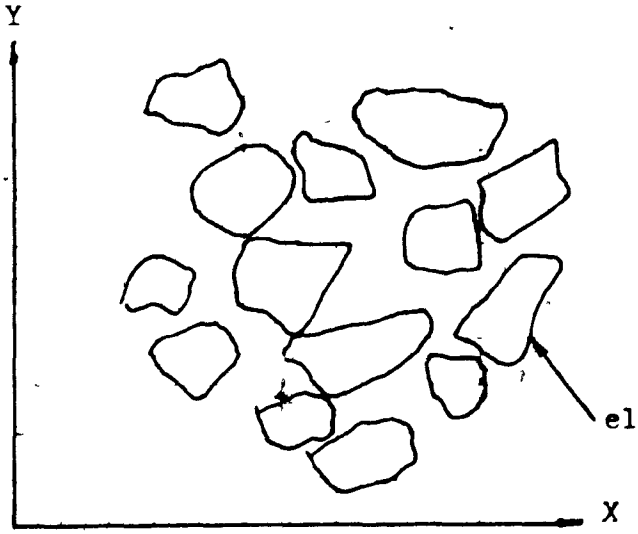

fig. 6-9
creep mechanism

A. before consolidation

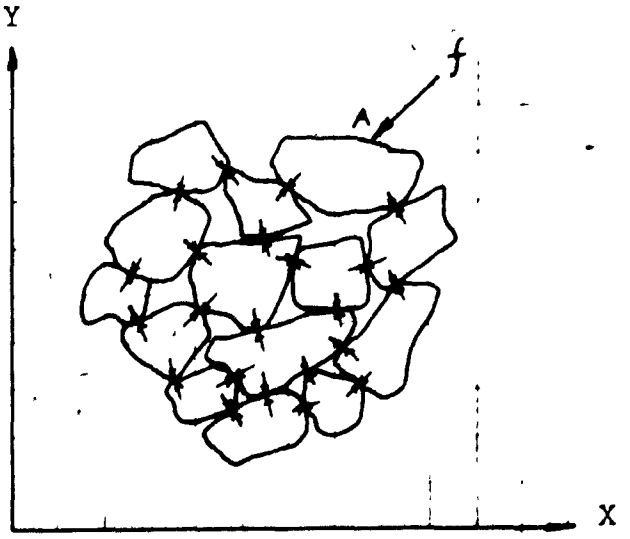

B. after consolidation, before shear

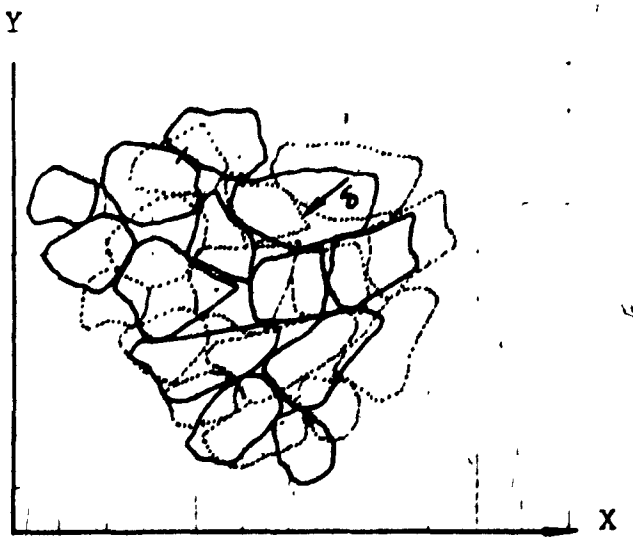

C. after shear

2. the time of retardation for the anelastic deformation decreases at higher stress levels (Tables B-3a and B-3b);
3. the percent of recoverable strain is higher at higher stress levels.

These behaviors indicate that specimens seem to harden under drained conditions due to the reduction of voids within the specimens. Depending on the σ_3 used in the consolidation, the voids between elementary units have different volumes within the sample at the end of consolidation processes. As first shear stress is applied, rotation of elementary units take place and tend to fill the voids within the specimen and causes the majority of the deformation to be irreversible (Figure B-18). This, for the first loading, the creep rate compliance, i.e., the creep rate that a unit stress can produce, is higher (Figure 5-3). As loading intensity increases, the voids are reduced considerably and hence the creep rate compliance decreases accordingly. This reduction in voids brings the elementary units closer together and enables the soil assembly to behave more elastically.

Besides these hardening manifestations, it was found that:

4. the instantaneous modulus of elasticity decreases as stress difference increases to higher levels (Figure 5-1A);

5. the energy of activation decreases as stress difference increases to higher levels (Figure 6-7).

These behaviors seem to contradict the hardening concept at first glance. However, from microscopic pictures of the soil structure, it is possible that at lower stress levels the stress is carried by the more rigid elementary units. This is reflected in the relatively high modulus of elasticity measured and higher energy of activation at first loadings (Figure 5-1A). A continuous increase in the modulus of elasticity at lower stress range was observed due to the fact that the soil mass continues to be more compact because of the reduction in voids. However, as load increases to about 30 percent of the sample strength, the voids are sufficiently reduced and the highest modulus of elasticity measured indicates that the stress might be taken primarily by the most rigid elementary units in the specimen. Due to the random distribution of the stresses and the elementary units, it may be envisaged that at this state some elementary units may not be stressed and some may be stressed to their full strength.

Further loading beyond this stage may cause the instability of these highly stressed elementary units since they are at their highest strain energy states. Adjustment takes place within the specimen so that stresses are more and more evenly distributed among all existing units by bringing into action the lower strength units. The measured lower

modulus of elasticity, the lower activation energy, the relatively high recoverable strain at higher stress levels, all indicate that these units coming into action now are less rigid and most of them are stressed within their elastic limits.

This explanatory mechanism seems, in general, consistent with the observed trend of variation of quantities evaluated from this series of tests. However, it should be emphasized that this does not serve as direct proof of the proposed mechanism. To prove the existence of such a creep mechanism, it is recognized that extensive further theoretical and experimental studies are required. In this regard, one of the most important experimental techniques involved in the research probably is the scanning electron microscopy which was studied and carried out by Barden (1971, 1972), Morgenstern (1969) and Yong (1972). The theoretical development in this thesis study of probabilistic approach may prove to be plausible in view of the observed fluctuation of the quantities and the random nature of the soil specimen. Therefore, the distributions of stress, strain and the elementary units in relation to the observed creep behavior, as will be discussed in the next section, is a direct concern in the theoretical studies.

6.1.4 Distribution of Stress, Strain, and Elementary Units

The size of a typical kaolinite particle is in the order of 10,000 Å in diameter by 1,000 Å in thickness (e.g. Grim, 1953; Lambe, 1958; Yong and Warkentin, 1966). With a test specimen of 1.5 inches by 3.0 inches and a void ratio of 0.8, it is estimated that there are approximately 6.6×10^{14} particles within each test sample. A number of these particles tend to floc together to act as if a single unit (called elementary unit in this thesis study). There are even a greater number of possible elementary units that may be formed from the combination of these constituent particles. Hence, it is not practical, if not impossible, to consider the characteristics of each elementary unit. It would be more sensible if the distribution of certain characteristics of the elementary units may be evaluated and this distribution may further be correlated to the mechanical behavior of the material.

Viscoelastic behavior of high polymers was intensively studied by T. Alfrey (1948) and it was found that the time of retardation is a characteristic property of the high polymer molecules, and the spectrum of retardation times from the creep function may in fact reflect the distribution of the polymer molecules. This method of analysis was employed and further modified by Yong

and Chen (1970) to describe the probability of occurrence of the proposed elementary units in soils. The details of the modified method were presented in Section 2.2.3.

Results of tests are analyzed by using this method. The distribution curves so obtained are plotted on Figures B-24 through B-38 inclusive in Appendix B. A typical result of analysis was shown on Figure 2-2. Some properties of the distribution such as mean, mode, standard deviation and the represented time of retardation, together with the probability of occurrence at this retardation time, are also tabulated on Tables B-3a and B-3b in Appendix B.

Some interesting results are indicated from these graphs and tables:

1. The distribution curves are generally skewed and the values of mean, mode and retardation time shift from the high time decades to the lower ones as loading increases and ultimately the bell shape curve approaches that of a normal distribution.
2. At higher confining pressures and at lower temperatures, the values of mean, mode, and retardation time also generally shift from the high time decades to the lower decades (Tables B-3a and B-3b).

For the samples tested, the representative retardation time is approximately 40 to 400 minutes. It is interesting to note that for a material exhibiting ideal flow, the retardation time approaches ∞ (Figure 6-10), while for a nearly perfect elastic material this retardation time is close to zero. Therefore, it is expected that increasing the material elasticity and rigidity will produce a corresponding decreasing in the retardation time values. This concept is obviously consistent with the results observed: i.e. the observed lower values of mean, mode, and retardation time at higher consolidation pressures indicate that the specimens, which are known to be more compact, have a higher rigidity and behave more elastically; the observed shifting toward lower values of mean, mode, and time of retardation at higher stress levels indicates that the specimens have become more elastic.

(1) elastic
(2) soil
(3) viscous

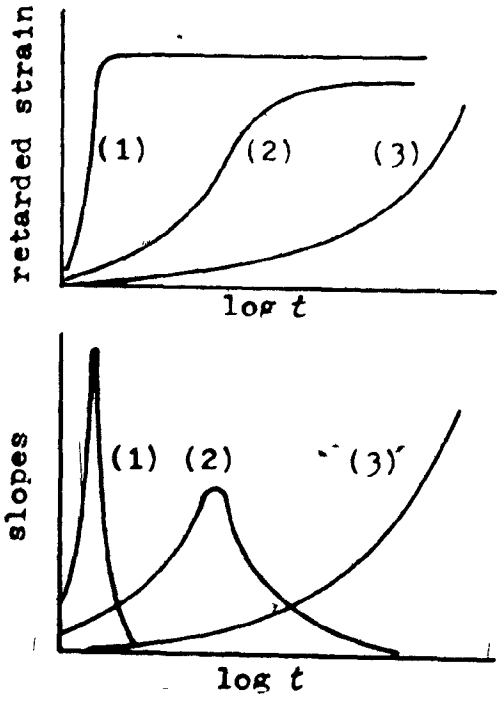

Fig. 6-10
Retarded Strains and Their Distributions for Representative Ideal Materials

From the exhibited creep phenomena, e.g. change of creep rate with time and stress (Figure 5-2), change of steady creep rate with stress (Figure B-16), change of modulus of elasticity (Figure 5-1A), etc., it is probably that the redistribution of stress and strain within the sample has taken place with a mechanism probably like that shown on Figure 6-9 . With this mechanism, it is also obvious that in some of the elementary units, which are so highly stressed, that yielding has occurred. Meanwhile, some of the elementary units may only be stressed slightly or stressed to a fraction of their strengths. Thus, at microscopic level according to the concept of the random distribution of stress and the elementary units, the stress acting on the elementary units may vary from practically zero to the yield strength of the unit. The strains of the elementary units, therefore, may vary from practically zero to that of a continuous plastic flow.

According to this concept, the conventional way of expressing the total stress-strain relationship as shown on Figure 6-11 is no more than mathematical expectations of these quantities. On this figure, the stress is expressed in terms of the conventional engineering definition of stress divided by (1-n) if one takes porosity of the specimen into account, where n is the porosity. Since in a fully consolidated soil, the pore pressure is

dissipated, and the voids do not take stress at all.

It is, hence, plausible to express the variation of stress and strain in the microscopic level in the following forms (Axelrad, 1963; Axelrad and Yong, 1966, 1970).

$$\xi = \langle \xi \rangle + \xi^*$$
$$\epsilon = \langle \epsilon \rangle + \epsilon^* \qquad \text{.....(6-1-4-1)}$$

where ξ = micro stress acting on the unit

ϵ = micro strain of the unit

$\langle \xi \rangle$ = expected stress acting on the unit

$\langle \epsilon \rangle$ = expected strain of the unit

ξ^* = variation of the actual stress from expected stress

ϵ^* = variation of the actual strain from the expected strain

and the expected values of stress and strain are given by the following expressions:

$$\langle \xi \rangle = \frac{\sigma}{1-n}$$
$$\langle \epsilon \rangle = \varepsilon \qquad \text{.....(6-1-4-2)}$$

where σ = the convention stress (load divided by the area upon which the load acts)

ε = the conventional strain (engineering strain or true strain)

n = porosity

If one assumes that the stress and strain distributions in the material are also normally distributed

(Goldstein, 1965), the microscopic stress and strain distributions relating to the macroscopic stress-strain relation may be shown diagrammatically in Figure 6-11.

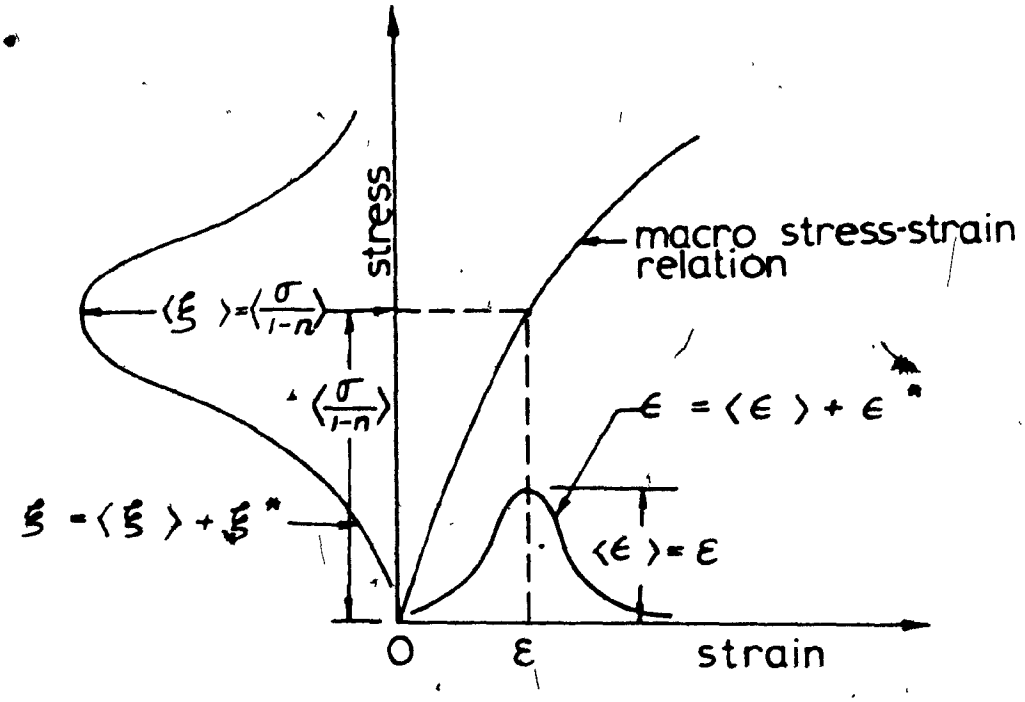

fig.6-11 micro stress strain distributions

The interaction of these two distributions gives rise to the observable macroscopic measurements. In other words, where micro stress equals to or exceeds the strength of the unit, flow takes place, and where the micro stress is less than the strength of the unit it is also acting upon, the unit will undergo definite elastic

and anelastic deformations proportional to the stress. Because of the randomness in the distributions of stress and strain, according to statistical concepts, the distribution which shows the probability distribution of the units being stressed within their yield limits might be considered as the random samples taken from the entire ensemble, therefore, might also be considered as representative distribution of all the elementary units in the specimen (Tien and Lienhard, 1971).

To evaluate the probability distribution functions, one may compare equation (5-4-3) with the theoretical results of equation (2-2-2-2) developed in Chapter 2, let $t \to \infty$ in creep function C(t), then the ultimate value of the second term in this equation is equal to ε_{ru}, i.e.

$$\lim_{t\to\infty} C(t)\Delta\sigma = C(\infty)\Delta\sigma = \varepsilon_{ru} \qquad \text{.....(6-1-4-3)}$$

therefore

$$\int_{-\infty}^{t} p(\tau)d\tau = F(t) \qquad \text{.....(6-1-4-4)}$$

or the probability weighing factor $P_k(\tau)d\tau$ is equal to the density function $f(t)$ which may be evaluated by the retardation time distribution method; and for a normal distribution is given by:

$$P(\tau)d\tau = f(\tau)d\tau = \frac{1}{\sqrt{2\pi}\,\bar{\sigma}} e^{-\frac{(\tau-\mu)^2}{2\bar{\sigma}^2}} d\tau \qquad \text{.....(6-1-4-5)}$$

The probability of occurrence of a unit at a particular level of energy i as given in equation (3-2-1-11) hence may be rewritten as:

$$P_i = \frac{g_i}{\sqrt{2\pi}\,\bar{\sigma}} e^{-\frac{(\tau-\mu)^2}{2\bar{\sigma}^2}} d\tau \qquad \text{.....(6-1-4-6)}$$

The equivalence of these two equations, one derived from thermodynamic concept, the other a consequence of viscoelastic consideration, indicates that there does exist a functional relationship between the specific environmental constraints in regard to the balance of energy and the retardational characteristics of the resulting elementary units. Though, rigorously, it is not necessarily that there exists a one-one correspondence between the particular energy level of integrity and a particular retardation time, i.e., at a particular energy level, there may be g_i units which do not necessarily have the same retardation time. The characteristics of the time of

retardation and the retarded strain may be obtained experimentally while the exact energy level for the formation of the clay soil elementary unit remains unknown due to the complex interactions between soil particles and between soil particles and the constituent fluids. It is also because of this inherent difficulty in the evaluation of exact energy level, that it imposes a problem in the evaluation of the exact value of the partition function, although it may be seen from Equation (6-1-4-5) that the partition function is probably proportional to $\sqrt{2\pi}\,\tilde{\sigma}$, however, the proportional constant is not clear at this stage of the investigation.

6.2 CONCLUSION

The techniques now available have provided evidence that in a clay soil matrix, a number of particles tend to floc together and behave as if a unit; here defined as elementary unit or ped. These peds further define the overall structure and stability of clays. To account for the mechanism of the physical interaction and individual contribution of the unit to the creep performance, the elementary unit has been defined and utilized as a basic model for the development of a probabilistic theory presented in the thesis. It is shown that with the application of the theory, a consistent method of the drained creep analysis is available which accounts for the non-homogeneous distributions of stress, strain, and the physical makeup of the elementary units in the clay soils.

The following conclusions may be drawn from this study:

1. Drained creep behavior can not be predicted by the available creep theories derived from undrained creep behavior. No linear relationship exists between $\log \dot{\varepsilon}$ versus $(\sigma_1 - \sigma_3)$ and no definite pattern of temperature effect may be defined

although higher temperature seems to increase the creep deformation and creep rate. Therefore, no unique energy of activation may be evaluated and the rate process theory can not be applied to drained creep test analysis without significant limitations.

2. The stress-strain-time relationship obtained by separating the deformation into elastic, anelastic and flow components and by introducing the probabilistic weighing function into the analysis provides an excellent prediction of creep strain at any time for given confining pressures and stress difference levels not exceeding 50 percent of the unconfined compressive strength of the specimen.
3. In a drained creep test, the axial strain resulting from anisotropic consolidation was found constituting approximately 5 to 15 percent of the total creep strain. However, at higher confining pressures and at lower stress difference levels, a significant portion of strain is due to anisotropic consolidation.

4. A creep mechanism, based on the postulated elementary units, which is a group of clay particles acting as if a unit, may be utilized to explain the observed drain creep characteristics. The distributional characteristics used in the analysis may provide a theoretical basis for the further probabilistic approach to the creep analysis for clay soils.

6.3 FURTHER RESEARCH

The following are a few examples of further research which will be beneficial to the understanding of rheological characteristics of clay soils:

1. Semi-drained conditions - test results indicate drained creep behavior is significantly different from that of undrained results. However, to simulate the field conditions, both short term (undrained) and long term (drained) behaviors are of interest to engineering practice. Therefore, a research program involves tests on large samples or full scale field tests will be most desirable. The tests should be carried out with free drainage at boundary while pore water pressure be measured at several locations of the specimen or the soil mass in the field. With this program, the influence of pore water pressure build-up and dissipation on the creep pattern may be examined.

2. Applications - with the stress-strain-time relationship for drained creep obtained from this study, it will be interesting to see its practical application to slope stability analysis of open cuts, long inclined slopes, settlement of tanks on soft soils, etc. The program will involve test borings on several predetermined locations to obtain the information on soil stratigraphy, groundwater conditions. Several piezometers, inclinometer

and settlement gauges should be installed for pore water pressure measurements and movement detections, respectively. Stress-strain-time relationship similar to Equation 5-4-2 may be obtained by creep tests on samples obtained from test boreholes. Appropriate σ_3 , $\sigma_1 - \sigma_3$ should be chosen so that they would represent the stress conditions in the field. With this information and boundary conditions, the finite element method of analysis may be used to calculate the predicted creep movement of the soil mass and results may be compared to the field observations.

3. Soil fabric studies - physicochemical studies on soil fabric will include the studies on variations of soil fabric at different stages during the deformation process. The most effective technique probably is the scanning electron microscopy technique. However, this will also involve standardizing the method and procedure, so that a direct comparison can be made and the interpretation of the results will not be hindered by the laboratory conditioning of the specimens. With the increasing understanding of soil fabirc, the mechanism involved in the deformation can be properly envisaged. Therefore, an appropriate physical theory (or theories) may be adopted for the interpretation of observed behavior and it may further be used as a tool for the prediction of the stress-strain-time behavior for soils.

BIBLIOGRAPHY

1. Abdel-Hady M. and Herrin M. (1966)
   Characteristics of Soil-Asphalt as a Rate Process
   J. of the Highway Div.
   Proc. ASCE, HWI, Vol.92, pp.49-69

2. Aitken A. (1957)
   Statistical Mathematics
   Interscience Publishers, Inc. N. Y.

3. Alfrey T. (1948)
   Mechanical Behaviour of High Polymers
   International Publishers. N. Y.

4. Andersland O.B. and Akili W. (1967)
   Stress Effect on Creep Rate of a Frozen Clay Soil
   Geotechnique, Vol.17, No.1, pp.27-39

5. Andersland O.B. and Douglas A.G. (1970)
   Soil Deformation Rates and Activation Energies
   Geotechnique, Vol.20, No.1, pp.1-16

6. Arkin H. and Colton R. (1970)
   Statistical Methods
   Barnes and Noble, Inc. N. Y.

7. Arulanandan K. Shen C.K. and Young R.B. (1971)
   Undrained Creep Behavior of a Coastal Organic Silty Clay
   Geotechnique, Vol.21, No.4, pp.359-375

8. Axelrad D. R. (1963)
   On the Deformation of 2-Phase Systems at High Temperature
   J. Soc. Mat. Sci., Japan, Vol.12, pp.322-325

9. Axelrad D. R. (1965)
   On the Thermo-Rheology of 2-Phase Systems
   J. Soc. Mat. Sci., Japan, Vol.14, pp.367-371

10. Axelrad D. R. and Yong R. N. (1966)
    On an Isothermal Flow Function for a Heterogeneous Medium
    Mod. Develop in the Mechanics of Continua
    Academic Press, Inc. N. Y.

11. Axelrad D. R. and Yong R. N. (1970)
    Micro-Rheology of the Yielding of a Heterogeneous Medium
    Proc. 5th Int. Cong. on Rheology, Vol.2, pp.309-314

12. Axelrad D. R. (1971)
Rheology of Structured Media
Archieves of Mechanics, Vol.23, No.1, pp.131-140

13. Barden L. and Sides G. (1971)
Sample Disturbance in the Investigation of Clay Structure
Geotechnique, Vol.21, No.3, pp.211-222

14. Barden L. (1972)
The Influence of Structure on Deformation and Failure in Clay Soil
Geotechnique, Vol.22, No.1, pp.159-163

15. Bishop A. W. and Henkel D. J. (1957)
The Measurement of Soil Properties in Triaxial Test
Edward Arnold Publishers Ltd., London

16. Bishop A. W. (1966)
The Strength of Soils as Engineering Materials
Geotechnique, Vol.12, No.2, pp.91-130

17. Bishop A. W. and Lovenbury H. T. (1969)
Creep Characteristics of Two Undisturbed Clays
7th ICOSMFE (International Conference on Soil Mechanics and Foundation Engineering)
Vol.1, pp.29-37

18. Casagrande A. and Wilson S. (1951)
Effect of Rate of Loading on Strength of Clays and Shales at Constant Water Content
Geotechnique, Vol.2, No.3, pp.251-263

19. Coates D. F. and McRostie G. C. (1963)
Some Deficiencies in Testing Leda Clay
ASTM STP No.361: Laboratory Shear Testing of Soils
pp.459-470

20. Companella R. G. and Mitchell J. K. (1968)
Influence of Temperature Variations on Soil Behaviour
J. Soil Mech. & Found. Div. Proc. ASCE, SM3,
pp.709-734

21. Chao T. W. (1960)
A Study of the Non-Linear Theory of Creep.
Scientia Sinica, Vol.9, No.5, pp.652-663

22. Chaplin T. K. (1969)
Inner and Outer Plastic Yield Surfaces in Clays
7th ICOSMFE, Vol.1, pp.73-80

23. Chen D. S. (1965)
Investigation into a Method for Creep Determination in Clay Soils
M. Eng. Thesis, McGill University

24. Christensen R. W. and Wu T. H. (1964)
Analysis of Clay Deformation as a Rate Process
J. Soil Mech. & Found. Div. ASCE Proc. Paper 4147
pp.125-157

25. Churchill R. V. (1958)
Operational Mathematics
McGraw-Hill, New York

26. Dorn J. E. (1954)
Some Fundamental Experiments on High Temperature Creep
J. Mech. Phys. Solids, Vol.3, pp.85-116

27. Drucker D. C. (1950)
Some Implications of Work Hardening and Ideal Plasticity
Quarterly Applied Mathematics, Vol.7, No.4, pp.411-418

28. Drucker D. C. (1951)
A More Fundamental Approach to Plastic Stress-Strain Relations
Proceedings of the First U.S. National Congress of Applied Mechanics, ASME, pp.487-491

29. Drucker D. C. (1954)
Coulomb Friction, Plasticity, and Limit Loads
J. Appl. Mech., Vol.21, Trans. ASME, Vol.76, pp.71-74

30. Drucker D. C., Gibson R. E. and Henkel D. J. (1957)
Soil Mechanics and Work-Hardening Theories of Plasticity
Transactions ASCE, Vol.122, pp.338-346

31. Drucker D. C. (1959)
A Definition of Stable Inelastic Material
J. Appl. Mech., Vol.26, Trans. ASME, Vol.81, Series E. pp.101-106

32. Eisenschitz R. (1958)
Statistical Theory of Irreversible Processes
Oxford University Press

33. Findley W. N. (1958)
Prediction of Stress Relaxation from Creep Tests of Plastics
Proc. 3rd. U.S. Nat. Cong. of Appl. Mech., pp.521-526

34. Finn W. D. L. and Emery J. J. (1972)
Time-Dependent Behaviour of Earth Slopes
24th Internation Geological Congress, Section 13
Engineering Geology, pp.117-123

35. Finnie I. and Heller W. R. (1959)
Creep of Engineering Materials
McGraw-Hill Book Company Inc., N. Y.

36. Geuze E. C. W. A. and Tan. T. K. (1953)
The Mechanical Behaviour of Clays
Proc. 2nd. Int. Cong. on Rheology, Oxford, pp.247-259

37. Geuze E. C. W. A. (1957)
Soil Properties and Their Measurement (Disc.)
Proc. 4th. ICOSMFE Vol.3, pp.90-91

38. Gibbs J. W. (1960)
Elementary Principles in Statistical Mechanics
Dover Publications, Inc. N.Y. N. Y.

39. Glastone S., Laidler K. and Eyring H. (1941)
The Theory of Rate Process
McGraw-Hill Book Co., Inc., N. Y.

40. Goldstein M. N. and Ter-Stepanian G. (1957)
The Long Term Strength of Clays and Depth Creep of Slopes
Proc. 4th ICOSMFE, Vol.2, pp.311-314

41. Goldstein M. N., Misumsky V. A. and Lapidus L. S. (1961)
The Theory of Probability and Statistics in Relation
to the Rheology of Soils
Proc. 5th ICOSMFE, Vol.1, pp.123-126

42. Goldstein M. N., Lapidus L. and Misumsky V. (1965)
Rheological Investigation of Clays and Slope Stability
Proc. 6th ICOSMFE, Vol.2, pp.482-485

43. Grim R. E. (1953)
Clay Mineralogy, Chap.2
McGraw Hill Book Co. Inc., N. Y. pp.11-26

44. Gross B. (1953)
Mathematical Structure of the Theories of Viscoelasticity
Hermann, Paris

45. Haefeli R. Schaerer C. and Amberg (1953)
The Behaviour Under the Influence of Soil Creep
Pressure of the Concrete Bridge Built at Klosters
by the Rhaetian Railway Company, Switzerland
Proc. 3rd ICOSMFE, Vol.2, pp.175-179

46. Haefeli R. (1953)
Creep Problems in Soils, Snow and Ice
Proc. 3rd ICOSMFE, Vol.3, pp.238-251

47. Haefeli R. (1965)
Creep and Progressive Failure in Snow, Soil, Rock and Ice
Proc. 6th ICOSMFE, Vol.3, pp.134-148

48. Hill R. (1950)
The Mathematical Theory of Plasticity
Oxford University Press.

49. Holzer T. L., Hoeg K. and Arulanandan K. (1973)
Excess Pore Pressures during Undrained Clay Creep
Canadian Geotechnical Journal
Vol.10, No.1, pp.12-24

50. Hvorslev M. J.
Soil Properties and Their Measurement (Disc.)
Proc. 4th ICOSMFE, Vol.3, pp.105-107

51. Jaeger J. C. (1962)
Elasticity, Fracture and Flow
John Wiley and Sons, Inc. N. Y.

52. Kingery W. D. (1962)
A Review of the Stress-Strain-Time-Temperature Behaviour of Ceramics
Symp. on Stress-Strain-Time-Temperature Relationships in Materials ASTM STP No.325, pp.19-34

53. Koiter W. T. (1953)
Stress-Strain Relations, Uniqueness and Variational Theorems for Elastic-Plastic Materials with a Singular Yield Surface
Quarterly Applied Mathematics, Vol.XI, No.3, pp.350-354

54. Koiter W. T. (1960)
Chapter 4, Progress in Solid Mechanics, Vol.1, Sneddon and Hill

55. Krizek R. J. and Kondner R. L. (1965)
Viscoelastic Principles and Techniques Applied to Soil Mechanics
Behaviour of Soil Under Stress
Proc. 5th Sym. of the Civ. and Hyd. Eng. Dept. Indian Inst. of Sci., Bangalore India. pp.B2/1-B2/23

56. Ladanyi B. (1972)
An Engineering Theory of Creep of Frozen Soils
Canadian Geotechnical Journal, Vol.9, No.1, pp.63-80

57. Laguros J. (1969)
Effect of Temperature on Some Engineering Properties of Clay Soils
Highway Research Board Special Report 103, pp.186-193

58. Lambe T. W. (1958)
The Structure of the Compacted Clay
J. Soil Mech. & Found. Div. SM2, Proc. ASCE 84 pp.1-34

59. Martin R. T. (1962)
Adsorbed Water on Clay: A Review
Proc. of the 9th. Nat. Conf. on Clays and Clay Minerals
Pergamon Press Ltd. N. Y. pp.28-70

60. Mitchell J. K. and Campanella R. G. (1963)
Creep Studies on Saturated Clays
Symp. on Laboratory Shear Testing of Soils
ASTM-NRC, STP. No.361
Ottawa, Canada

61. Mitchell J. K. (1964)
Shearing Resistance of Soils as a Rate Processes
Journal of the Soil Mechanics and Foundations Division ASCE, Vol.90, No.SMI, pp.29-61

62. Mitchell J. K. and McConnell J. R. (1965)
Some Characteristics of the Elastic and Plastic Deformation of Clay on Initial Loading
Proc. 6th ICOSMFE, Vol.1, pp.313-317

63. Mitchell J. K., Campanella R. G. and Singh A. (1968)
Soil Creep as a rate Process
Journal of the Soil Mechanics and Foundation Division
Proc. of ASCE, SMI, pp.231-253

64. Mitchell J. K. (1969)
Temperature Effect on the Engineering Properties and Behaviour of Soils
Highway Research Board Special Report 103 pp.9-28

65. Morgenstern N. R. (1969)
Structural and Physical-Chemical Effects on the Properties of Clays
Proc. 7th ICOSMFE, Vol.3, pp.455-471

66. Murayama S. and Shibata T. (1961)
Rheological Properties of Clays
Proc. 5th ICOSMFE, Vo.1, pp.269-273

67. Murayama S. and Shibata T. (1964)
Flow and Stress Relaxation of Clays
Proc. Rheology and Soil Mech. Symp. of the Int. Union of Rheoretical and Appl. Mech.
Grenoble, France, pp.99-129

68. Murayama S. (1969)
Stress-Strain-Time Behaviour of Soils Subjected to Deviatoric Stress
Proc. 7th, ICOSMFE, Vol.1, pp.297-305

69. Murayama S. (1969)
Effect of Temperature on Elasticity of Soils
Highway Research Board Special Report 103
pp.194-203

70. Oding I. A. (1965)
Creep and Stress Relaxation in Metals
Oliver and Boyd Ltd.
Edingburgh, London

71. Palmer A. C., Maier G. and Drucker D. C. (1967)
Normality Relations and Convexity of Yield Surfaces for Unstable Materials or Structural Elements
Journal Applied Mechanics, Transaction ASME
Vol.34, Series E, No.2, pp.464-469

72. Pao Y. H. and Martin J. (1953)
An Analytical Theory of the Creep Deformation of Materials
Trans. ASME, Vol.75, pp.245-252

73. Reiner M. (1949)
Twelve Lectures on Theoretical Rheology
Pitman

74. Reiner M. (1953)
Volume Rheology
Proc. 2nd Int. Cong. on Rheology
London, pp.310-315

75. Reiner M. (1954)
Building Materials: Their Elasticity and Inelasticity
Interscience Publishers, N. Y.

76. Reiner M. (1960)
Lectures on Theoretical Rheology
North Holland Publishing Co. Amsterdam

77. Reiner M. (1969)
Contributions to Mechanics:
M. Reiner Eightieth Anniversary Volume
Editor: D. Abir
Pergamon Press

78. Rosenqvist I. T. (1962)
The Influence of the Physico-Chemical Factors upon the Mechanical Properties of Clays
Proc. of the 9th, Nat. Conf. on Clays and Clay Minerals
Pergamon Press Ltd. N. Y. pp.12-27

79. Rowe P. W. (1957)
C_e= 0 Hypothesis for Normally Loaded Clays at Equilibrium
Proc. 4th ICOSMFE, Vol.1, pp.89-192

80. Saito M. and Uezawa H. (1961)
Failure of Soil Due to Creep
Proc. 5th ICOSMFE, Vol.1, pp.315-318

81. Saito M. (1965)
Forecasting the Time of Occurance of a Slope Failure
Proc. 6th ICOSMFE, Vol.2, pp.537-541

82. Saito M. (1969)
Forecasting Time of Slope Failure by Tertiary Creep
Proc. 7th ICOSMFE, Vol.2, pp.677-683

83. Schiffman R. L. (1954)
The use of Visco-Elastic Stress-Strain Laws in Soil Testing
ASTM Special Technique Publication No.254, pp.131-155

84. Scott R. F. (1963)
Principles of Soil Mechanics
Addison-Wesley Publishing Comp. Inc., Reading, Mass.

85. Scott R. F. and Ko H. Y. (1969)
Stress-Deformation and Strength Characteristics
Proc. 7th ICOSMFE, State of the Art Volume, pp.1-47

86. Shibata T. and Karube D. (1969)
Creep Rate and Creep Strength of Clays
Proc. 7th ICOSMFE, Vol.1, pp.361-367

87. Sides, G. and L. Barden (1971)
The Microstructure of Dispersed and Flocculated Samples of Kaolinite, Illite, and Montmorillonite
Canadian Geotechnical Journal, Vol.8, No.3, pp.391-399

88. Singh A. and Mitchell J. K. (1968)
General Stress-Strain Time Function for Soils
Journal of the Soil Mechanics and Foundation Division ASCE, Vol.94, No.SMI, pp.21-46

89. Singh A. and Mitchell J. K. (1969)
Creep Potential and Creep Rupture of Soils
Proc. 7th ICOSMFE, Vol.1, pp.379-384

90. Skempton A. W. (1954)
The Pore Pressure Coefficients A and B
Geotechnique, Vol.4, pp.143-147

91. Smith T. L. (1962)
Stress-Strain-Time-Temperature Relations for Polymers
Symp. on Stress-Strain-Time-Temperature Relationships in Materials
ASTM STP No.325, pp.60-89

92. Suklje L. (1961)
A Landslide due to Long-Term Creep
Proc. 5th ICOSMFE, Vol.2, pp.727-735

93. Tan T. K. (1957)
Soil Properties and Their Measurement (Disc.)
Proc. 4th, ICOSMFE, Vol.3, pp.87-89

94. Tan T. K. (1961)
Consolidation and Secondary Time Effect of Homogeneous Anisotropic, Saturated Clay Strata
Proc. 5th, ICOSMFE, Vol.1, pp.367-373

95. Tan T. K. (1961)
Soil Properties and Their Measurement (Disc.)
Proc. 5th, ICOSMFE, Vol.3, pp.141-143

96. Ter-Stepanian G. (1963)
On the Long-Term Stability of Slopes
Norwegian Geotechnical Institute Publication 52, pp.1-14

97. Ter-Stepanian G. (1965)
In-Situ Determination of the Rheological Characteristics of Soils on Slopes
Proc. 6th, ICOSMFE, Vol.2, pp.575-577

98. Terzaghi K. (1943)
Theoretical Soil Mechanics
John Wiley and Sons, Inc., N. Y.

99. Tien C. L. and Lienhard J. H. (1971)
Statistical Thermodynamics
Holt, Rinehart and Winston, Inc. N.Y.

100. Vyalov S. S. and Skibisky A. M. (1957)
Rheological Processes in Frozen Soils and Dense Clays
Proc. 4th ICOSMFE, Vol.1, pp.120-124

101. Vyalov S. S. and Skibisky A. M. (1961)
Problems of the Rheology of Soils
Proc. 5th ICOSMFE, Vol.1, pp.387-391

102. Vyalov S. S. (1965)
Plasticity and Creep of a Cohesive Medium
Proc. 6th ICOSMFE, Vol.1, pp.402-406

103. Vyalov S. S. and Meschyan S. R. (1969)
Creep and Long Term Strength of Soils Subjected to Variable Load
Proc. 7th ICOSMFE, Vol.1, pp.423-431

104. Walker L. K. (1969)
Undrained Creep in a Sensitive Clay
Geotechnique, Vol.19, No.4, pp.515-529

105. Warkentin B. P. (1963)
Physical and Chemical Properties of Clays
Soil Mechanics Series No.7, McGill University

106. Wu T. H., Rosendiz D. and Neukirchner R. J. (1966)
Analysis of Consolidation by Rate Process Theory
J. of Soil Mech. and Found. Div.
Proc. ASCE, SM6, Vol.92, pp.229-248

107. Yen B. C. (1969)
Stability of Slopes Undergoing Creep Deformations
J. Soil Mech. & Found. Div. SM4, Proc. ASCE 95, pp.1075-1096

108. Yong R. N. (1964)
The Effect of Time Rate of Strain on Clay Soil Strength Part One--Preliminary Considerations
Soil Mechanics Series No.9, McGill University

109. Yong R. N. (1972)
Soil Technology and Stabilization
Proc. 4th Asian Regional Conference on Soil Mechanics and Foundation Engineering
Vol.2, pp.111-124

110. Yong R. N. and Chen D. S. (1970)
Analysis of Creep of Clays Using Retardation Time Distribution
Proc. 5th International Congress on Rheology,
Vol.2, pp.501-512

111. Yong R. N. and Chen D. S. (1972)
A Probabilistic After-Effect Analysis of Relaxation in Clays
Proc. 6th International Congress on Rheology
Vol.2, pp.309-314

112. Yong R. N., Japp R. D. and Leitch H. C. (1964)
Strain Rate Effects on Clay Soil Strength
Soil Mechanics Series No.12, McGill University

113. Yong R. N. and McKyes E. (1971)
Yield and Failure of a Clay Under Triaxial Stresses
J. of Soil Mech. and Found. Div. Proc. ASCE. SM1,
Vol.97, pp.159-176

114. Yong R. N. and Warkentin B. P. (1966)
Introduction to Soil Behaviour
MacMillan Co., N. Y.

115. Yong R. N. and Warkentin B. P. (1975)
Soil Properties and Behaviour
Elsevier Scientific Publishing Co., N. Y.

116. Zaretskii Yu. K. and Vyalov S. S. (1971)
Structural Mechanics of Clay Soils
Translated from Osnovaniya, Fundamenty i Mekhanika Gruntov, No.3, pp.1-5

117. Zemansky M. W. (1966)
Basic Engineering Thermodynamics
McGraw-Hill Book Co., N. Y.

APPENDIX A

EXPERIMENTATION

A-1. Material

A-2. Sample Preparation

A-3. Apparatus and Test Procedure

In this series of investigations, degenerated kaoline was selected for testing on the ground as it has a relatively high specific surface due to the poor development of its crystal structure, and it has a considerable abount of isomorphous substitution within the lattice. Under sustained loading, these properties might lead to some unexpected behavior of the material when the specimen is subjected to different environmental conditions such as different confining pressures, temperatures, and time durations. In view of the relatively high confining pressure used in this series of studies and the necessity of temperature control, special sample preparation devices were set up. Conventional triaxial cells were modified. Instrumentation and testing procedures were designed so that meaningful data could be obtained. All the samples tested and the temperature, confining pressure and stress difference levels applied to each sample are shown on Table 4-1.

A.1 MATERIAL (Yong et al., 1964)

The clay soil used in this series of tests was Bell Clay which is a finely divided, kaolinitic clay, light brown in color, and prepared and packaged by Bell Industries, Ltd. From standard hydrometer tests, all of the particles exhibiting an equivalent diameter of less than 0.10 mm while approximately 70 percent by weight of the soil particles remained in suspension after 72 hours.

The X-ray diffraction analysis of the coarse fraction of the soil confirmed that the major clay mineral component was kaolin. However, along with the usual well crystallized form (characterized by a lattice spacing of 7.12 Å), a form with a lattice spacing of 4.63 Å was also recorded; indicating that a poorly developed, or degenerated version of the mineral was also present. Perhaps the most striking feature of the X-ray diffraction trace was an extremely sharp peak corresponding to a lattice spacing of 3.11 Å, typical of the non-clay mineral quartz. The sharpness of this peak is not due to the relative abundance of this mineral but to the well developed cyrstallinity usually associated with it. A secondary quartz spacing of 4.24 Å serves to confirm the presence of this mineral in the sample. Traces of a second non-clay mineral, apatite, were identified by the positive results of chemical tests for the elements calcium and phosphorous.

Following the procedure outlined by ASTM, the liquid limit of Bell Clay was found to be 75 percent and plastic limit 30 percent.

Using distilled water as the displacement fluid, the average specific gravity of Bell Clay was found to be 2.52, an unusually low figure when considering that both quartz and apatite, known to be present in the soil, possess specific gravities considerably higher than that. With carbon tetrachloride as the displacement fluid, a value of 2.72 was obtained. This figure is considered to be

more representative of the material, and the lower figure obtained in water can be considered as an additional indication of the activity of the clay mineral fraction of the soil.

In addition to these more or less routine tests, several non-standard tests were carried out. They included hydrometer analysis in unconditioned, distilled water (the grain size analysis quoted above used sodium metaphosphate as a dispersion agent) and in 10^{-2}, 10^{-3}N solutions of sodium chloride. The results of the tests conducted in distilled water agreed very closely with those of the test cited above indicating that the soil, in its natural state, was not significantly flocculated. In both of the sodium chloride solutions, evaluation of the hydrometer results were different since the clay flocculated immediatly. Such behavior would seem to indicate that the long and short range forces of interaction present in the system were free to act, except where modified by the cautions of the sodium chloride solutions. Consequently, they will play a significant role in determining the characteristics of any soil containing appreciable quantities of Bell Clay.

This hypothesis was confirmed by the evaluation of the consistency limits of the soil with sodium metaphosphate, with 10^{-2} and 10^{-3}N sodium chloride solutions being the fluid phase. Although these tests are in no way standard, the differing results obtained indicate that the

behavior of Bell Clay may be considerably modified by the variation of the exchangeable ion concentration and that the ion exchange capacity is considerably higher than that normally associated with kaolinitic clays. In the degenerate form, degenerated kaoline would act as an amorphous material, and due to the poor development of the crystal structure, a considerable amount of isomorphous substitution within the lattice can be expected. It is likely that this mineral shown in the X-ray diffraction analysis is responsible for much of the unusual behavior of Bell Clay. This, together with the high specific surface inplicit in the small particle size, would lead to the unexpected activity of the mineral.

A.2 SAMPLE PREPARATION

In order to ensure the uniformity of the sample used, and to eliminate the effect of pore air, it is desirable to prepare a high degree of saturation in the sample to obtain a two-phase system.

The sample preparation apparatus is shown in Figure A-1, and the procedure is outlined as follows: when thoroughly mixed slurry of Bell Clay powder and distilled water (water content of 120 percent) was placed in the slurry reservoir and allowed to season for at least 24 hours, a uniform, creamy and consistent slurry was obtained. The sedimentation column and consolidation tube (3.5 inches in diameter) were then filled with distilled water which was subsequently deaired under vacuum. The slurry was drawn under vacuum into deaired water in the sedimentation column and allowed to fall into the consolidation tube which was vibrated to break down the structure of the slurry. When sufficient slurry to produce a test specimen had accumulated in the consolidation tube, it was removed and subjected to a uniaxial loading with top and bottom drainages provided. The loading procedure, prior to the removal of the sample from the tube, follows the incremental technique with low initial loads. A time of approximately ten days was required to reach the axial consolidation pressure of 30 psi. Because of the side friction, this preliminary consolidation pressure was

estimated to be around 25 psi. Following this treatment, the specimen was extruded, cut into six or seven inch lenghts and placed in the traixial cell. This specimen was further isotropically consolidated with a confining pressure of 30 psi for four days. Filter paper side drainage, single rubber sleve (TESTLAB) and 0 rings were used in accordance with the standard practice. After this process, the specimen was trimmed to 1.4 inches in diameter and 3.14 inches in length. This sample was then placed in the triaxial with double membrane and side drainage, and consolidation to the desired confining pressure with an initial consolidation pressure of 30 psi and subsequent incremental pressure of 60 psi. The consolidation period for each increment was four days to ensure that the internal pore water pressure was completely dissipated. Volume change due to consolidation was measured in terms of the water extruded and this observation was checked by a determination of the loss in sample weight. Volume change and axial shortening, due to consolidation, were used to calculate the resultant corss-sectional area of the specimen by assuming that the shape remained cylindrical. The degree of saturation was checked by the use of pore pressure parameter B (Skempton, 1954). Results indicated that the degree of saturation was excellent. The homogeneity of the sample was checked by cutting the fully consolidated sample into slices, the maximum variation of the water content of the individual

slices from the average value for σ_3 = 240 psi was found to be less than 0.4 percent, indicating a good homogeneity within the sample under this relatively high consolidation pressure.

A.3 APPARATUS AND TEST PROCEDURES

The arrangement and the testing apparatus are schematically represented in Figure 4-4. The triaxial cells were reinforced to withstand the relatively high confining pressures. In previous investigations, (Chen, 1965) preliminary tests showed that the membranes were not able to prevent the transfer of moisture between membrane covered specimens and the surrounding confining fluid under pressure higher than 60 psi when water was used as confining medium. Thus, mercury was used as a jacket and moisture barrier for pressures greater than 60 psi. Since the sample had been consolidated to 60 psi prior to the trimming process, the effect of the difference of hydrostatic head between top and bottom of the test sample, in this case calculated to be 1.3 psi, was found negligible.

The pressure source unit was a pressurized nitrogen tank connected to a pressure regulator which can be adjusted to the desired confining pressures. Under relatively constant room temperature, the variation of the pressure was not registered during the loading period.

After the samples were placed in the traixial cells, the entire set-up was insulated in a styroform cabinet. The temperature inside the cabinet was regulated by a light bulb-fans and thermo-couple systems which was designated to control the temperature within $\pm 0.5^{\circ}F$. A periodic check of the temperature inside the cabinet,

however, indicated that $\pm 1^{\circ}F$ was being registered.

Four different confining pressures of 30, 60, 120, and 240 psi were used in this series of tests. The volume change, due to consolidation and the addition of stress difference, were measured by burettes which has an accuracy of 0.025 cc. These burettes were so arranged and adjusted from time to time, that the water levels in them were kept at the same levels as those of the corresponding tops and bottoms of the samples, in order to avoid hydrostatic head differences. The tops of these burettes were so connected that the vapor pressure in the line would prevent the evaporation of the water in the burettes.

After the sample was consolidated to the desired confining pressure, constant loading was then applied instantaneously. Both deviatoric and volumetric stresses were induced to cause shear strain and volume change of the sample. The vertical deformations were measured by dial gauges to an accuracy of 0.5×10^{-4} inch. The guages were firmly attached to the triaxial cells to prevent the possible error due to relative movement. The readings of the deformation were taken at proper time intervals during the retarded deformation stage; intervals of 6 to 8 hours during constant rate flow stage. This was to ensure that the creep curve readings were not to be interrupted by the night. This constant loading was maintained for 48 hours until a constant flow curve was observed.

This was followed by a complete removal of the loading leaving the stress difference acting on the sample to zero. Upon the removal of the loading, the amount of rebound was also recorded at proper time intervals so that a smooth strain-time curve was obtained. The rebound process was found to terminate within 24 hours. Therefore, the sample was kept unloaded for 24 hours before the application of the next higher step of loading which was again followed by complete removal of the load. This procedure was repeated until the loading reached approximately 80 percent of its unconfined compressive strength.

After the last loading, the apparatus was dismantled quickly and the sample was subjected to an unconfined compression test, and the final water content was taken subsequently.

1. slurry reservior
2. feeding line
3. deairing column
4. consolidation tube (28")
5. consolidation tube (14")
6. vacuum line
7. trap
8. vacuum tank
9. vacuum pump
10. pressure gauge

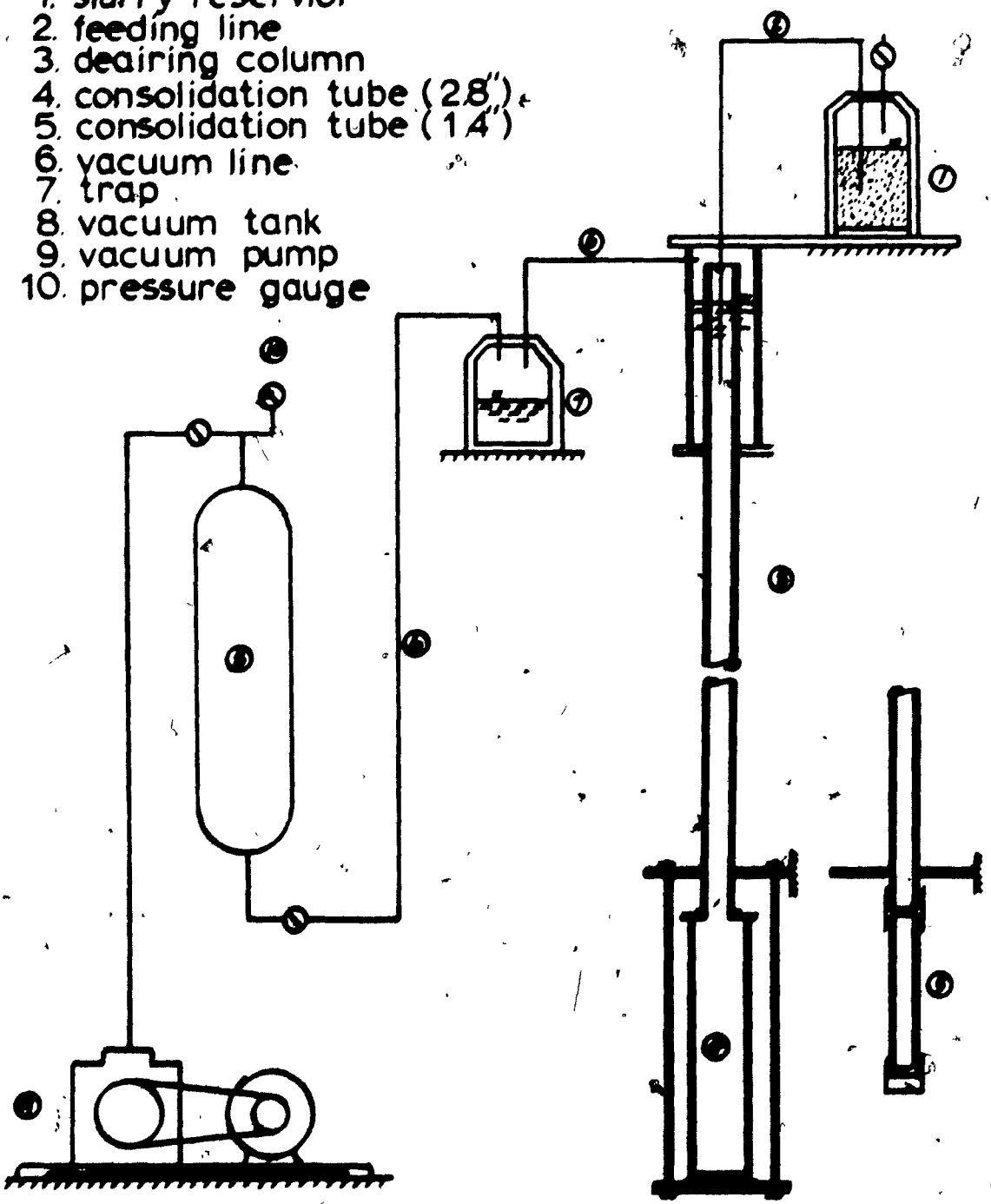

fig.A-1 vacuum sedimentation system

APPENDIX B

EXPERIMENTAL RESULTS

σ_3 = 30 psi T = 98°F

$\sigma_1 - \sigma_3$ = 3.3 psi		$\sigma_1 - \sigma_3$ = 6.6 psi		$\sigma_1 - \sigma_3$ = 10.0 psi	
time (min)	strain (%)	time (min)	strain (%)	time (min)	strain (%)
0.1	0.0670	0.1	0.0770	0.1	0.1430
0.5	0.0770	0.5	0.0851	0.5	0.1531
1.0	0.0788	1.0	0.0901	1.0	0.1632
2.0	0.0821	2.0	0.0968	2.0	0.1733
4.0	0.0887	4.0	0.1068	4.0	0.1901
7.0	0.0937	7.0	0.1151	7.0	0.2052
15.0	0.1069	15.0	0.1335	15.0	0.2389
30.0	0.1235	30.0	0.1635	30.0	0.2776
60.0	0.1499	60.0	0.2036	60.0	0.3415
90.0	0.1665	100.0	0.2520	90.0	0.3920
165.0	0.1946	170.0	0.3070	120.0	0.4391
330.0	0.2459	280.0	0.3838	210.0	0.5619
390.0	0.2558	400.0	0.4689	340.0	0.6981
660.0	0.3021	790.0	0.6441	390.0	0.7503
810.0	0.3203	1440.0	0.7976	790.0	0.9891
1410.0	0.4146	1830.0	0.8526	1440.0	1.1977
2170.0	0.4709	2280.0	0.8977	1785.0	1.2835
3160.0	0.5850	2880.0	0.9511	2880.0	1.5611
		stress difference = 0			
0.0	0.5850	0.0	0.9511	0.0	1.5611
0.1	0.5734	0.1	0.8843	0.1	1.4114
0.5	0.5728	1.0	0.8793	0.5	1.3979
15.0	0.5685	2.0	0.8777	1.0	1.3945
30.0	0.5668	4.0	0.8676	2.0	1.3828
120.0	0.5632	7.0	0.8626	4.0	1.3710
160.0	0.5628	15.0	0.8526	7.0	1.3609
510.0	0.5602	30.0	0.8409	15.0	1.3468
1140.0	0.5602	60.0	0.8309	30.0	1.3313
		90.0	0.8293	60.0	1.3172
		120.0	0.8236	90.0	1.3020
		220.0	0.8209	135.0	1.2936
		400.0	0.8143	750.0	1.2717
		1430.0	0.8126	1340.0	1.2701
				2020.0	1.2448

σ_3 = 30 psi T = 98°F

$\sigma_1 - \sigma_3$ = 13.3 psi		$\sigma_1 - \sigma_3$ = 16.6 psi		$\sigma_1 - \sigma_3$ = 20.0 psi	
time (min)	strain (%)	time (min)	strain (%)	time (min)	strain (%)
0.1	0.2231	0.1	0.4160	0.1	0.7434
0.5	0.2436	0.5	0.4505	0.5	0.8700
1.0	0.2623	1.0	0.4816	1.0	0.9754
2.0	0.2879	2.0	0.5368	2.0	1.1125
4.0	0.3134	4.0	0.6162	3.0	1.2074
7.0	0.3475	7.0	0.6904	4.0	1.2742
15.0	0.4020	15.0	0.7957	7.0	1.4183
30.0	0.4701	30.0	0.9165	15.0	1.6257
60.0	0.5723	60.0	1.0701	30.0	1.8331
100.0	0.6643	90.0	1.1651	45.0	1.9544
170.0	0.7836	140.0	1.3014	60.0	2.0458
270.0	0.9318	275.0	1.5569	75.0	2.1143
420.0	1.0946	420.0	1.7329	90.0	2.1723
660.0	1.2673	840.0	2.0108	150.0	2.3621
770.0	1.3440	1450.0	2.1903	240.0	2.5432
1420.0	1.5688	1895.0	2.2455	390.0	2.7488
1860.0	1.6608	3330.0	2.4820	810.0	3.0212
2860.0	1.9664			1410.0	3.2023
				2055.0	3.3393
				2860.0	3.4800

stress difference = 0

0.0	1.9664	0.0	2.4820	0.0	3.4114
0.1	1.7654	0.1	2.1575	0.1	3.0037
0.5	1.7467	0.5	2.1299	0.5	2.9158
1.0	1.7331	1.0	2.1144	1.0	2.8877
2.0	1.7194	2.0	2.0954	2.0	2.8560
3.0	1.7092	3.0	2.0833	3.0	2.8367
4.0	1.7041	4.0	2.0677	4.0	2.8226
7.0	1.6803	7.0	2.0470	7.0	2.7892
15.0	1.6571	15.0	2.0125	15.0	2.7358
30.0	1.6257	30.0	1.9814	30.0	2.6767
60.0	1.6036	60.0	1.9383	45.0	2.6381
90.0	1.5729	80.0	1.9210	60.0	2.6170
120.0	1.5695	160.0	1.8796	75.0	2.6012
180.0	1.5593	370.0	1.8399	90.0	2.5801
390.0	1.5372	1010.0	1.7968	120.0	2.5590
650.0	1.5201			240.0	2.5361
1440.0	1.5082			410.0	2.5010
				770.0	2.4781
				1420.0	2.4553
				2230.0	2.4553

σ_3 = 30 psi T = 98°F

$\sigma_1 - \sigma_3$ = 23.3 psi		$\sigma_1 - \sigma_3$ = 3.3 psi		$\sigma_1 - \sigma_3$ = 6.6 psi	
time (min)	strain (%)	time (min)	strain (%)	time (min)	strain (%)
0.1	1.1239	0.1	0.048	0.1	0.108
0.5	1.3905	0.5	0.053	0.5	0.112
1.0	1.5814	1.0	0.056	1.0	0.116
2.0	1.8264	2.0	0.058	2.0	0.122
3.0	1.9813	4.0	0.063	4.0	0.133
4.0	2.1055	7.0	0.070	7.0	0.146
7.0	2.3667	15.0	0.088	15.0	0.172
15.0	2.7486	30.0	0.106	30.0	0.202
30.0	3.1034	60.0	0.125	50.0	0.231
60.0	3.4042	90.0	0.135	80.0	0.255
120.0	3.6707	120.0	0.144	160.0	0.321
240.0	3.9157	180.0	0.165	240.0	0.379
420.0	4.0994	410.0	0.208	390.0	0.458
740.0	4.2669	1430.0	0.309	825.0	0.616
1460.0	4.4813	1990.0	0.336	1420.0	0.730
2220.0	4.6434	2680.0	0.365	1770.0	0.779
3090.0	4.7664			2080.0	0.821
				2850.0	0.877

stress difference = 0

0.0	4.7664	0.0	0.365	0.0	0.877
0.1	4.1498	0.1	0.352	0.1	0.807
0.5	4.0418	1.0	0.351	0.5	0.802
1.0	3.9913	4.0	0.343	1.0	0.800
2.0	3.9337	30.0	0.333	2.0	0.797
3.0	3.9085	1410.0	0.332	4.0	0.792
4.0	3.8905			7.0	0.784
7.0	3.8509			15.0	0.781
15.0	3.7806			30.0	0.763
30.0	3.6996			60.0	0.754
45.0	3.6581			120.0	0.744
60.0	3.6365			250.0	0.733
90.0	3.6023			420.0	0.728
180.0	3.5447			610.0	0.728
360.0	3.4906			1430.0	0.728
540.0	3.4654				
1470.0	3.4204				

σ_3 = 30 psi T = 88°F

σ_3 = 30 psi T = 88°F

$\sigma_1 - \sigma_3$ = 10.0 psi		$\sigma_1 - \sigma_3$ = 13.3 psi		$\sigma_1 - \sigma_3$ = 16.6 psi	
time (min)	strain (%)	time (min)	strain (%)	time (min)	strain (%)
0.1	0.178	0.1	0.294	0.1	0.597
0.5	0.186	0.5	0.320	0.5	0.617
2.0	0.198	1.0	0.337	1.0	0.640
4.0	0.212	2.0	0.359	2.0	0.695
7.0	0.235	4.0	0.392	4.0	0.753
15.0	0.269	7.0	0.431	7.0	0.799
30.0	0.312	15.0	0.485	15.0	0.882
60.0	0.376	30.0	0.559	30.0	0.986
90.0	0.421	60.0	0.645	60.0	1.117
170.0	0.521	120.0	0.781	120.0	1.286
270.0	0.618	180.0	0.889	330.0	1.628
420.0	0.728	310.0	1.078	410.0	1.714
630.0	0.842	480.0	1.256	600.0	1.850
730.0	0.884	1200.0	1.630	740.0	1.976
1430.0	1.083	1590.0	1.792	1400.0	2.231
1720.0	1.145	1985.0	1.895	1830.0	2.317
1890.0	1.169	2625.0	1.993	2140.0	2.362
2190.0	1.198	2880.0	2.040	2850.0	2.440
2870.0	1.238				

stress difference = 0

0.0	1.238	0.0	2.040	0.0	2.440
0.1	1.093	0.1	1.725	0.1	2.115
0.5	1.086	0.5	1.715	0.5	2.075
1.0	1.077	1.0	1.704	1.0	2.045
2.0	1.067	2.0	1.681	2.0	2.017
4.0	1.052	4.0	1.652	4.0	1.994
7.0	1.039	7.0	1.627	7.0	1.966
15.0	1.017	15.0	1.601	15.0	1.939
30.0	1.010	30.0	1.568	30.0	1.883
70.0	0.970	60.0	1.542	60.0	1.847
120.0	0.957	90.0	1.523	75.0	1.837
140.0	0.945	220.0	1.500	150.0	1.797
335.0	0.929	390.0	1.477	1440.0	1.760
680.0	0.916	430.0	1.477		
1670.0	0.903	465.0	1.472		
		1475.0	1.444		

σ_3 = 30 psi T = 88°F σ_3 = 30 psi T = 78°F

$\sigma_1 - \sigma_3$ = 20.0 psi		$\sigma_1 - \sigma_3$ = 23.3 psi		$\sigma_1 - \sigma_3$ = 3.3 psi	
time (min)	strain (%)	time (min)	strain (%)	time (min)	strain (%)
0.1	1.153	0.1	1.360	0.1	0.0598
0.5	1.247	0.5	1.429	0.5	0.0664
1.0	1.327	1.0	1.498	1.0	0.0681
2.0	1.413	2.0	1.557	2.0	0.0731
4.0	1.524	4.0	1.649	4.0	0.0797
7.0	1.624	7.5	1.754	7.0	0.0830
15.0	1.811	15.0	1.896	15.0	0.0913
30.0	1.990	30.0	2.033	30.0	0.1013
60.0	2.199	60.0	2.191	60.0	0.1163
110.0	2.395	100.0	2.381	130.0	0.1345
180.0	2.508	210.0	2.641	260.0	0.1545
270.0	2.716	270.0	2.846	1190.0	0.2225
360.0	2.797	810.0	3.083	1610.0	0.2425
420.0	2.856	1400.0	3.213	2630.0	0.2591
600.0	2.993	1860.0	3.275		
800.0	3.092	2940.0	3.369		
1425.0	3.273				
1845.0	3.357				
2100.0	3.401				
2880.0	3.482				

stress difference = 0

0.0	3.482	0.0	3.369	0.0	0.2591
0.1	2.993	0.1	2.887	0.1	0.2425
0.5	2.939	0.5	2.804	0.5	0.2408
1.0	2.901	1.0	2.773	4.0	0.2392
2.0	2.878	2.0	2.742	7.0	0.2358
4.0	2.829	4.0	2.690	15.0	0.2309
7.0	2.793	7.0	2.658	30.0	0.2159
15.0	2.755	15.0	2.596	100.0	0.2126
30.0	2.716	30.0	2.549	395.0	0.1910
60.0	2.682	60.0	2.492	770.0	0.1960
120.0	2.643	125.0	2.454	1430.0	0.2010
310.0	2.588	180.0	2.439		
660.0	2.561	465.0	2.368		
810.0	2.552	570.0	2.357		
1440.0	2.542	1255.0	2.328		
		1480.0	2.321		

σ_3 = 30 psi T = 78°F

$\sigma_1 - \sigma_3$ = 6.6 psi		$\sigma_1 - \sigma_3$ = 10.0 psi		$\sigma_1 - \sigma_3$ = 13.3 psi	
time (min)	strain (%)	time (min)	strain (%)	time (min)	strain (%)
0.1	0.1148	0.1	0.1988	0.1	0.2914
0.5	0.1248	0.5	0.2122	0.5	0.3217
1.0	0.1315	1.0	0.2188	1.0	0.3402
2.0	0.1381	2.0	0.2289	2.0	0.3587
4.0	0.1448	4.0	0.2422	4.0	0.3992
7.0	0.1498	7.0	0.2556	7.0	0.4227
15.0	0.1598	15.0	0.2807	15.0	0.4699
30.0	0.1747	30.0	0.3141	30.0	0.5272
60.0	0.1914	60.0	0.3625	45.0	0.5710
120.0	0.2180	90.0	0.3993	60.0	0.6030
220.0	0.2563	120.0	0.4260	120.0	0.7158
390.0	0.2979	340.0	0.5747	230.0	0.8775
840.0	0.3994	630.0	0.7000	445.0	1.0998
1460.0	0.4643	1510.0	1.0107	810.0	1.3188
1880.0	0.4943	2020.0	1.0842	1430.0	1.5276
2320.0	0.5242	2830.0	1.1677	1820.0	1.6051
2960.0	0.5592			2940.0	1.7600
		stress difference = 0			
0.0	0.5592	0.0	1.1677	0.0	1.7600
0.1	0.4643	0.1	0.9940	0.1	1.4805
0.5	0.4593	0.5	0.9806	0.5	1.4569
1.0	0.4560	1.0	0.9739	1.0	1.4434
2.0	0.4526	2.0	0.9658	2.0	1.4282
4.0	0.4510	4.0	0.9556	4.0	1.4097
7.0	0.4460	7.0	0.9455	7.0	1.3946
15.0	0.4410	15.0	0.9272	15.0	1.3693
22.0	0.4393	30.0	0.9088	30.0	1.3423
30.0	0.4360	60.0	0.8871	45.0	1.3221
45.0	0.4343	90.0	0.8720	60.0	1.3087
140.0	0.4044	130.0	0.8603	80.0	1.2952
380.0	0.3961	180.0	0.8537	325.0	1.2329
1440.0	0.3844	290.0	0.8386	565.0	1.2177
1560.0	0.3828	510.0	0.8319	755.0	1.2177
		1260.0	0.8152	1710.0	1.1958

σ_3 = 30 psi T = 78°F

$\sigma_1 - \sigma_3$ = 16.6 psi		$\sigma_1 - \sigma_3$ = 20.0 psi		$\sigma_1 - \sigma_3$ = 23.3 psi	
time (min)	strain (%)	time (min)	strain (%)	time (min)	strain (%)
0.1	0.4380	0.1	0.6971	0.1	1.1168
0.5	0.4960	0.5	0.8009	0.5	1.2403
1.0	0.5301	1.0	0.8597	1.0	1.3638
2.0	0.5710	2.0	0.9323	2.0	1.5084
4.0	0.6187	4.0	1.0188	4.0	1.6072
7.0	0.6647	7.0	1.1087	7.0	1.7731
14.0	0.7448	14.0	1.2264	14.0	1.9283
22.0	0.8130	22.0	1.3232	22.0	2.0659
30.0	0.8675	30.0	1.3959	30.0	2.1612
45.0	0.9425	45.0	1.4927	45.0	2.3165
60.0	1.0039	60.0	1.5654	60.0	2.4258
90.0	1.0959	90.0	1.6795	90.0	2.5987
120.0	1.1641	220.0	2.0065	120.0	2.7258
390.0	1.5015	405.0	2.2607	290.0	3.1104
630.0	1.7129	820.0	2.5721	400.0	3.2445
1240.0	1.9788	1385.0	2.8315	850.0	3.5197
1600.0	2.0776	1815.0	2.8800	1380.0	3.7490
2050.0	2.1730	2170.0	2.9491	1850.0	3.7931
2870.0	2.3600	3040.0	3.1200	2220.0	3.8545
				2880.0	3.9396

stress difference = 0

0.0	2.3600	0.0	3.1200	0.0	3.9396
0.1	1.8833	0.1	2.5133	0.1	3.1986
0.5	1.8458	0.5	2.4510	0.5	3.0998
1.0	1.8254	1.0	2.4199	1.0	3.0680
2.0	1.8015	2.0	2.3853	2.0	3.0222
4.0	1.7742	4.0	2.3507	5.0	2.9692
7.0	1.7538	7.0	2.3247	7.0	2.9516
14.0	1.7231	14.0	2.2884	14.0	2.9092
22.0	1.6958	22.0	2.2573	22.0	2.8740
30.0	1.6754	30.0	2.2348	30.0	2.8457
45.0	1.6481	50.0	2.1915	45.0	2.8105
60.0	1.6294	70.0	2.1639	60.0	2.7858
90.0	1.6038	690.0	2.0047	90.0	2.7487
120.0	1.5867	1780.0	1.9563	120.0	2.7240
220.0	1.5458			240.0	2.6693
600.0	1.4947			400.0	2.6340
1220.0	1.4657			750.0	2.5987
				1470.0	2.5740

σ_3 = 30 psi T = 78°F

$\sigma_1 - \sigma_3$ = 26.6 psi		$\sigma_1 - \sigma_3$ = 3.3 psi		$\sigma_1 - \sigma_3$ = 6.6 psi	
time (min)	strain (%)	time (min)	strain (%)	time (min)	strain (%)
0.1	1.4070	0.1	0.0464	0.1	0.0515
0.5	1.6968	0.5	0.0464	0.5	0.0598
1.0	1.8670	1.0	0.0514	1.0	0.0731
2.0	2.1060	2.0	0.0613	2.0	0.0881
4.0	2.4273	4.0	0.0795	4.0	0.0947
7.0	2.7580	7.0	0.0911	7.0	0.1180
14.0	3.1853	15.0	0.1011	15.0	0.1229
22.0	3.4859	30.0	0.1259	30.0	0.1346
30.0	3.7213	60.0	0.1425	60.0	0.1578
45.0	3.9784	90.0	0.1491	120.0	0.1960
60.0	4.1305	120.0	0.1491	240.0	0.2492
90.0	4.3116	255.0	0.1707	300.0	0.2725
190.0	4.6303	420.0	0.2005	765.0	0.4021
390.0	4.9146	735.0	0.2320	1440.0	0.5084
740.0	5.1410	1440.0	0.2585	2880.0	0.6745
1430.0	5.3800	2880.0	0.3281		
2210.0	5.4561				
2950.0	5.4851				
3600.0	5.7422				

stress difference = 0

0.0	5.7422	0.0	0.3281	0.0	0.6745
0.1	4.8658	0.1	0.2751	0.1	0.5848
0.5	4.7499	0.5	0.2734	0.5	0.5832
1.0	4.6955	15.0	0.2651	1.0	0.5798
2.0	4.6521	720.0	0.2585	2.0	0.5782
4.0	4.6050			4.0	0.5682
8.0	4.5525			7.0	0.5649
14.0	4.5000			17.0	0.5483
22.0	4.4493			30.0	0.5150
30.0	4.4167			60.0	0.4984
45.0	4.3768			90.0	0.4918
60.0	4.3442			270.0	0.4885
90.0	4.3007			380.0	0.4868
230.0	4.2048			630.0	0.4835
380.0	4.1559			1410.0	0.4818
860.0	4.0961				
1640.0	4.0599				
2880.0	4.0237				

σ_3 = 30 psi T = 68°F

$\sigma_1 - \sigma_3$ = 10.0 psi		$\sigma_1 - \sigma_3$ = 13.3 psi		$\sigma_1 - \sigma_3$ = 16.6 psi	
time (min)	strain (%)	time (min)	strain (%)	time (min)	strain (%)
0.1	0.0835	0.1	0.1753	0.25	0.3134
0.5	0.0901	0.5	0.1854	0.5	0.3339
1.0	0.0968	1.0	0.2023	1.0	0.4024
2.0	0.1269	2.0	0.2292	2.0	0.4264
4.0	0.1386	4.0	0.2596	4.0	0.4624
7.0	0.1536	7.0	0.3000	7.0	0.4915
15.0	0.1903	15.0	0.3557	15.0	0.5669
30.0	0.2337	30.0	0.4433	30.0	0.7004
60.0	0.3055	60.0	0.5866	60.0	0.7672
105.0	0.3873	90.0	0.6658	90.0	0.8546
240.0	0.5759	240.0	1.0417	180.0	1.1114
405.0	0.7195	360.0	1.1917	270.0	1.2262
780.0	0.9315	470.0	1.3181	765.0	1.7126
1635.0	1.1102	690.0	1.4749	1590.0	1.9797
2880.0	1.3422	2190.0	1.9215	1830.0	2.0242
		2880.0	2.0564	2220.0	2.1407
				2880.0	2.2777

stress difference = 0

0.0	1.3422	0.0	2.0564	0.0	2.2777
0.1	1.0985	0.1	1.7799	0.25	1.9369
0.5	1.0951	0.5	1.7799	0.5	1.9232
2.0	1.0801	1.0	1.7631	1.0	1.9061
4.0	1.0634	2.0	1.7429	2.0	1.8804
9.0	1.0467	4.0	1.7243	4.0	1.8530
15.0	1.0250	7.0	1.7108	7.0	1.8444
30.0	1.0100	15.0	1.6822	15.0	1.8187
60.0	0.9933	30.0	1.6569	30.0	1.8136
120.0	0.9866	60.0	1.6384	60.0	1.7742
180.0	0.9783	120.0	1.6148	90.0	1.7588
540.0	0.9699	240.0	1.6030	240.0	1.7280
1230.0	0.9566	420.0	1.5760	390.0	1.7057
		810.0	1.5743	800.0	1.6903
		1440.0	1.5777	1440.0	1.6663

σ_3 = 30 psi. T = 68°F

$\sigma_1 - \sigma_3$ = 20.0 psi		$\sigma_1 - \sigma_3$ = 23.3 psi	
time (min)	strain (%)	time (min)	strain (%)
0.25	0.5312	0.25	0.8788
0.5	0.5695	0.5	0.9855
1.0	0.6009	1.0	1.1136
2.0	0.6531	2.0	1.2773
4.0	0.7158	4.0	1.5192
7.0	0.7785	7.0	1.7860
15.0	0.8969	15.0	2.2272
30.0	1.0345	30.0	2.7146
60.0	1.2017	60.0	3.2056
90.0	1.3254	90.0	3.4582
240.0	1.6911	120.0	3.6183
360.0	1.9889	250.0	4.0043
660.0	2.3529	410.0	4.2373
1410.0	2.6350	680.0	4.4579
1830.0	2.7448	1420.0	4.7016
2850.0	2.9485	1850.0	4.8013
		2270.0	4.8528
		2880.0	5.0094

stress difference = 0

0.0	2.9485	0.0	5.0094
0.25	2.5584	0.25	4.5433
0.5	2.5096	0.5	4.4793
1.0	2.4887	1.0	4.4188
2.0	2.4539	2.0	4.3654
4.0	2.4121	4.0	4.3227
7.0	2.3808	7.0	4.2836
15.0	2.3320	15.0	4.2124
30.0	2.2745	30.0	4.1555
60.0	2.2310	60.0	4.1093
120.0	2.1962	90.0	4.0772
240.0	2.1578	120.0	4.0630
330.0	2.1439	270.0	4.0203
650.0	2.1160	420.0	3.9954
1500.0	2.0986	840.0	3.9616
		1440.0	3.9385

σ_3 = 60 psi T = 98°F

$\sigma_1 - \sigma_3$ = 3.3 psi		$\sigma_1 - \sigma_3$ = 10.0 psi		$\sigma_1 - \sigma_3$ = 16.0 psi	
time (min)	strain (%)	time (min)	strain (%)	time (min)	strain (%)
0.1	0.0329	0.1	0.1615	0.1	0.2069
0.5	0.0690	0.5	0.1813	1.0	0.2570
1.0	0.1018	1.0	0.1911	2.0	0.2854
2.0	0.1117	2.0	0.2043	4.0	0.3137
7.0	0.1183	4.0	0.2192	7.0	0.3455
14.0	0.1380	7.0	0.2373	14.0	0.3972
22.0	0.1511	14.0	0.2603	23.0	0.4406
30.0	0.1585	22.0	0.2768	30.0	0.4706
60.0	0.1807	30.0	0.2933	60.0	0.5641
80.0	0.1938	60.0	0.3263	95.0	0.6509
160.0	0.2283	90.0	0.3559	260.0	0.8611
410.0	0.2973	175.0	0.3988	990.0	1.4169
590.0	0.3515	540.0	0.5372	1530.0	1.6388
780.0	0.4074	1155.0	0.6921	3050.0	2.0861
1380.0	0.4599	1670.0	0.7909		
1710.0	0.4928	1900.0	0.8338		
2880.0	0.6571	2520.0	0.9343		
		2880.0	1.0100		

stress difference = 0

0.0	0.6571	0.0	1.0100	0.0	2.0861
0.1	0.6012	0.1	0.7843	0.1	1.9325
0.5	0.5979	0.5	0.7794	1.0	1.8524
2.0	0.5946	1.0	0.7777	2.0	1.8324
22.0	0.5914	2.0	0.7761	4.0	1.8074
1160.0	0.5914	4.0	0.7728	7.0	1.7823
		14.0	0.7613	14.0	1.7490
		22.0	0.7530	22.0	1.7206
		60.0	0.7481	30.0	1.6972
		90.0	0.7431	70.0	1.6388
		270.0	0.7365	145.0	1.5887
		440.0	0.7316	350.0	1.5437
				1440.0	1.3918

σ_3 = 60 psi T = 98°F

$\sigma_1 - \sigma_3$ = 23.3 psi		$\sigma_1 - \sigma_3$ = 30.0 psi		$\sigma_1 - \sigma_3$ = 36.6 psi	
time (min)	strain (%)	time (min)	strain (%)	time (min)	strain (%)
0.1	0.5178	0.1	1.2375	0.1	1.0987
0.5	0.5741	0.5	1.4123	0.5	1.2818
1.0	0.6337	1.0	1.5066	1.0	1.4466
2.0	0.6882	2.0	1.6570	2.0	1.6883
4.0	0.7597	4.0	1.7968	4.0	2.0582
7.0	0.8177	7.0	1.9436	7.0	2.5197
14.0	0.9199	14.0	2.1429	14.0	3.4059
22.0	0.9744	22.0	2.2914	22.0	4.2300
30.0	1.0289	30.0	2.4050	35.0	4.8049
60.0	1.1754	60.0	2.6952	60.0	5.9952
150.0	1.4215	90.0	2.8944	140.0	7.4967
420.0	1.7920	245.0	3.4153	250.0	8.1743
540.0	1.8976	510.0	3.7858	530.0	8.6247
920.0	2.1123	1430.0	4.2438	1090.0	8.9653
1580.0	2.3218	2120.0	4.4395	1780.0	9.1484
1780.0	2.3882	2810.0	4.5619	2060.0	9.2107
2250.0	2.4632			2540.0	9.2931
2835.0	2.5518			2770.0	9.3572

stress difference = 0

0.0	2.5518	0.0	4.5619	0.0	9.3572
0.1	2.1395	0.1	3.6285	0.1	8.3317
0.5	2.0714	0.5	3.5237	0.5	8.2145
1.0	2.0203	1.0	3.4538	1.0	8.1633
2.0	1.9726	2.0	3.3664	2.0	8.0827
4.0	1.9181	4.0	3.2790	4.0	8.0241
7.0	1.8738	7.0	3.1951	7.0	7.9875
14.0	1.8125	14.0	3.1642	14.0	7.9618
22.0	1.7682	22.0	3.0413	22.0	7.9289
30.0	1.7341	30.0	2.9958	30.0	7.9051
60.0	1.6558	60.0	2.8997	60.0	7.8520
90.0	1.6115	120.0	2.7791	180.0	7.7549
180.0	1.5399	300.0	2.6637	680.0	7.6872
420.0	1.4888	560.0	2.5973	1470.0	7.6615
820.0	1.4547	1250.0	2.5134		

σ_3 = 60 psi T = 88°F

$\sigma_1 - \sigma_3$ = 6.6 psi		$\sigma_1 - \sigma_3$ = 13.3 psi		$\sigma_1 - \sigma_3$ = 20.0 psi	
time (min)	strain (%)	time (min)	strain (%)	time (min)	strain (%)
0.1	0.0488	0.1	0.1570	0.1	0.2440
0.5	0.0537	0.5	0.1668	0.5	0.2671
1.0	0.0651	1.0	0.1831	1.0	0.2780
2.0	0.0700	2.0	0.1929	2.0	0.3232
4.0	0.0782	4.0	0.2060	4.0	0.3462
7.0	0.0879	7.0	0.2158	7.0	0.3809
14.0	0.0993	14.0	0.2338	14.0	0.4419
22.0	0.1091	22.0	0.2551	22.0	0.4930
30.0	0.1172	30.0	0.2714	30.0	0.5309
45.0	0.1351	45.0	0.2943	45.0	0.5870
60.0	0.1498	60.0	0.3205	60.0	0.6414
140.0	0.2051	180.0	0.4480	80.0	0.7007
400.0	0.3354	260.0	0.5101	170.0	1.1014
1210.0	0.4136	350.0	0.5739	430.0	1.2432
1830.0	0.4591	480.0	0.6540	795.0	1.4707
2000.0	0.4657	790.0	0.7734	1405.0	1.6620
2620.0	0.4884	1390.0	0.9042	2065.0	1.7411
		2120.0	1.0170	2880.0	1.8862
		2880.0	1.1118		

stress difference = 0

0.0	0.4884	0.0	1.1118	0.0	1.8862
0.1	0.4429	0.1	0.9778	0.1	1.6373
1.0	0.4396	0.5	0.9581	0.5	1.6175
2.0	0.4380	1.0	0.9516	1.0	1.6076
7.0	0.4347	2.0	0.9434	2.0	1.5944
30.0	0.4315	4.0	0.9402	4.0	1.5845
60.0	0.4249	7.0	0.9352	7.0	1.5713
125.0	0.4233	14.0	0.9173	14.0	1.5449
200.0	0.4217	22.0	0.9091	22.0	1.5284
1440.0	0.4201	30.0	0.8960	30.0	1.5185
		45.0	0.8911	40.0	1.5087
		60.0	0.8846	120.0	1.4147
		90.0	0.8764	1440.0	1.3916
		1440.0	0.8339		

σ_3 = 60 psi T = 88°F

$\sigma_1 - \sigma_3$ = 26.6 psi		$\sigma_1 - \sigma_3$ = 33.3 psi	
time (min)	strain (%)	time (min)	strain (%)
0.1	0.3812	0.1	1.0857
0.5	0.4414	0.5	1.2928
1.0	0.4782	1.0	1.4964
2.0	0.5217	2.0	1.7286
4.0	0.5886	4.0	2.0571
7.0	0.6253	7.0	2.3821
14.0	0.7390	14.0	2.8785
22.0	0.8260	22.0	3.1571
30.0	0.9029	30.0	3.3214
60.0	1.1203	60.0	3.6464
125.0	1.3376	120.0	3.9178
195.0	1.4915	260.0	4.2678
630.0	1.9496	400.0	4.4303
750.0	2.0148	810.0	4.6857
1380.0	2.2573	1480.0	4.8392
1920.0	2.4078	2370.0	4.9392
2880.0	2.6048	2880.0	4.9642

stress difference = 0

0.0	2.6084
0.1	2.2640
0.5	2.2305
1.0	2.2004
2.0	2.1753
4.0	2.1569
7.0	2.1302
14.0	2.1001
22.0	2.0767
30.0	2.0650
40.0	2.0432
65.0	2.0165
195.0	1.9262
910.0	1.7724
1440.0	1.7155

σ_3 = 60 psi T = 78°F

$\sigma_1 - \sigma_3$ = 3.3 psi		$\sigma_1 - \sigma_3$ = 10.0 psi		$\sigma_1 - \sigma_3$ = 16.6 psi	
time (min)	strain (%)	time (min)	strain (%)	time (min)	strain (%)
0.1	0.0469	0.1	0.1240	0.1	0.1864
0.5	0.0502	0.5	0.1274	0.5	0.1948
2.0	0.0519	1.0	0.1290	1.0	0.2116
4.0	0.0536	2.0	0.1307	2.0	0.2200
7.0	0.0553	4.0	0.1341	4.0	0.2318
14.0	0.0569	7.0	0.1391	7.0	0.2519
22.0	0.0603	14.0	0.1475	14.0	0.2754
60.0	0.0653	26.0	0.1575	22.0	0.2973
90.0	0.0686	45.0	0.1642	30.0	0.3208
150.0	0.0753	60.0	0.1709	60.0	0.3796
410.0	0.0988	210.0	0.2045	90.0	0.4249
1410.0	0.1373	345.0	0.2246	125.0	0.4736
1830.0	0.1440	1425.0	0.3117	185.0	0.5357
2880.0	0.1440	1855.0	0.3385	305.0	0.6449
		2200.0	0.3503	390.0	0.7054
		2835.0	0.3637	830.0	0.8901
				1520.0	1.0497
				1870.0	1.1000
				2240.0	1.1454
				2950.0	1.2126

stress difference = 0

0.0	0.1440	0.0	0.3637	0.0	1.2126
0.1	0.1138	0.1	0.2480	0.1	1.0144
0.5	0.1105	0.5	0.2464	0.5	1.0110
1.0	0.1088	2.0	0.2447	1.0	1.0660
60.0	0.1055	4.0	0.2430	2.0	1.0010
1440.0	0.1038	7.0	0.2413	4.0	0.9909
		14.0	0.2380	7.0	0.9808
		30.0	0.2363	14.0	0.9674
		60.0	0.2296	22.0	0.9606
		90.0	0.2263	30.0	0.9539
		120.0	0.2246	45.0	0.9405
		220.0	0.2212	60.0	0.9338
		680.0	0.2195	130.0	0.9170
		1430.0	0.2078	405.0	0.8968
				705.0	0.8867
				1350.0	0.8784

σ_3 = 60 psi T = 78°F

$\sigma_1 - \sigma_3$ = 23.3 psi		$\sigma_1 - \sigma_3$ = 30.0 psi		$\sigma_1 - \sigma_3$ = 36.6 psi	
time (min)	strain (%)	time (min)	strain (%)	time (min)	strain (%)
0.1	0.3101	0.1	0.4611	0.1	0.7293
0.5	0.3507	0.5	0.5196	0.5	0.8976
1.0	0.4151	1.0	0.5575	1.0	1.0449
2.0	0.4558	2.0	0.6228	2.0	1.2097
4.0	0.5100	4.0	0.7106	4.0	1.4166
7.0	0.5676	7.0	0.7846	7.0	1.5989
14.0	0.6523	14.0	0.9016	14.0	1.8286
22.0	0.7167	22.0	0.9910	22.0	1.9688
30.0	0.7743	30.0	1.0564	30.0	2.0688
45.0	0.8709	45.0	1.1597	45.0	2.2291
60.0	0.9454	60.0	1.2526	60.0	2.3212
90.0	1.0674	80.0	1.3575	90.0	2.4685
120.0	1.1318	170.0	1.6036	120.0	2.5947
245.0	1.4012	280.0	1.8083	230.0	2.8788
370.0	1.5436	530.0	2.0509	470.0	3.1593
600.0	1.6655	740.0	2.1507	680.0	3.2767
1420.0	1.8689	1410.0	2.3623	1430.0	3.5117
1970.0	1.9265	1760.0	2.4346	1680.0	3.5783
2860.0	1.9959	2240.0	2.5051	2060.0	3.6519
3160.0	2.0197	2930.0	2.5757	2730.0	3.7378

stress difference = 0

0.0	2.0197	0.0	2.5757	0.0	3.7378
0.1	1.7198	0.1	2.1989	0.1	3.1347
0.5	1.6994	0.5	2.1386	0.5	3.0541
1.0	1.6893	1.0	2.1163	1.0	3.0260
2.0	1.6808	2.0	2.0974	2.0	3.0015
4.0	1.6723	4.0	2.0819	4.0	2.9594
7.0	1.6571	7.0	2.0629	7.0	2.9349
14.0	1.6401	14.0	2.0010	14.0	2.8928
22.0	1.6215	22.0	1.9890	22.0	2.8647
30.0	1.6147	30.0	1.9821	30.0	2.8507
60.0	1.5893	45.0	1.9649	45.0	2.8332
150.0	1.5774	60.0	1.9545	60.0	2.8174
530.0	1.5436	80.0	1.9425	120.0	2.7858
1160.0	1.5232	160.0	1.9287	260.0	2.7525
		300.0	1.9012	430.0	2.7350
		525.0	1.8702	800.0	2.7175
		1440.0	1.8616	1540.0	2.6964

σ_3 = 60 psi T = 68°F

$\sigma_1 - \sigma_3$ = 6.6 psi		$\sigma_1 - \sigma_3$ = 13.3 psi		$\sigma_1 - \sigma_3$ = 20.0 psi	
time (min)	strain (%)	time (min)	strain (%)	time (min)	strain (%)
0.1	0.0831	0.1	0.1269	0.1	0.1616
0.5	0.0879	0.5	0.1439	1.0	0.1779
1.0	0.0911	1.0	0.1519	4.0	0.1955
2.0	0.0926	2.0	0.1615	7.0	0.2100
4.0	0.0990	4.0	0.1662	14.0	0.3200
7.0	0.1070	7.0	0.1760	22.0	0.3424
14.0	0.1150	14.0	0.1902	30.0	0.3636
22.0	0.1182	22.0	0.2046	45.0	0.3924
30.0	0.1247	30.0	0.2190	60.0	0.4200
50.0	0.1327	60.0	0.2655	90.0	0.4700
100.0	0.1534	230.0	0.4315	125.0	0.5170
140.0	0.1662	400.0	0.5350	260.0	0.6540
290.0	0.1950	800.0	0.6870	540.0	0.8445
470.0	0.2110	1490.0	0.8360	830.0	0.9770
1310.0	0.2908	2220.0	0.9940	1360.0	1.0990
2100.0	0.3562	3040.0	1.0290	1980.0	1.1740
2640.0	0.3760			2300.0	1.2220
				2860.0	1.2680

stress difference = 0

0.0	0.3760	0.0	1.0290	0.0	1.2680
0.1	0.3350	0.1	0.9665	0.1	1.1060
0.5	0.3285	0.5	0.9440	0.5	1.0840
1.0	0.3252	1.0	0.9345	1.0	1.0710
2.0	0.3237	2.0	0.9280	2.0	1.0590
6.0	0.3220	4.0	0.9215	4.0	1.0520
14.0	0.3174	7.0	0.9185	7.0	1.0400
22.0	0.3110	14.0	0.9140	20.0	1.0200
30.0	0.3061	22.0	0.9085	30.0	1.0130
60.0	0.3045	30.0	0.9030	45.0	1.0020
120.0	0.3013	45.0	0.8895	60.0	0.9985
260.0	0.3000	60.0	0.8860	210.0	0.9660
870.0	0.3000	90.0	0.8830	540.0	0.9400
		150.0	0.8800	880.0	0.9225
		440.0	0.8755	1500.0	0.9100
		730.0	0.8670		

σ_3 = 60 psi T = 68°F

$\sigma_1 - \sigma_3$ = 26.6 psi		$\sigma_1 - \sigma_3$ = 33.3 psi		$\sigma_1 - \sigma_3$ = 40.0 psi	
time (min)	strain (%)	time (min)	strain (%)	time (min)	strain (%)
0.1	0.2290	0.1	0.5890	0.1	0.9445
0.5	0.2818	0.5	0.6790	0.5	1.1560
1.0	0.3537	1.0	0.7485	1.0	1.2700
2.0	0.3994	2.0	0.8155	2.0	1.3900
4.0	0.4480	4.0	0.8955	4.0	1.5340
7.0	0.4810	7.0	0.9660	7.0	1.6710
14.0	0.5330	15.0	1.1225	14.0	1.8990
22.0	0.5745	22.0	1.2130	22.0	2.0800
30.0	0.6120	30.0	1.3050	30.0	2.2190
45.0	0.6745	45.0	1.4210	45.0	2.4120
60.0	0.7230	60.0	1.5005	60.0	2.5350
160.0	0.9620	220.0	1.9620	90.0	2.7180
760.0	1.4630	380.0	2.1510	210.0	3.1000
1410.0	1.6680	420.0	2.1920	400.0	3.3450
2040.0	1.7960	900.0	2.4260	460.0	3.4000
2370.0	1.8410	1450.0	2.5600	1480.0	3.7500
3080.0	1.9130	1910.0	2.6260	2110.0	3.8500
		2340.0	2.6750	2840.0	3.9240
		2880.0	2.7180		
		stress difference = 0			
0.0	1.9130	0.0	2.7180	0.0	3.9240
0.1	1.6590	0.1	2.3880	0.1	3.3220
0.5	1.6320	0.5	2.3190	0.5	3.2350
1.0	1.6140	1.0	2.2900	1.0	3.1910
2.0	1.5930	2.0	2.2450	2.0	3.1300
4.0	1.5760	4.0	2.2080	4.0	3.0780
7.0	1.5570	7.0	2.1640	7.0	3.0400
14.0	1.5310	14.0	2.1360	14.0	2.9650
22.0	1.5190	22.0	2.1210	22.0	2.9400
30.0	1.5090	30.0	2.1080	30.0	2.9210
45.0	1.4930	45.0	2.0850	45.0	2.9030
60.0	1.4850	60.0	2.0740	60.0	2.8620
85.0	1.4720	140.0	2.0180	120.0	2.8250
210.0	1.4340	300.0	1.9850	420.0	2.7600
620.0	1.3840	540.0	1.9500	740.0	2.7300
1160.0	1.3665	660.0	1.9440	1440.0	2.6920
		1620.0	1.8970		

σ_3 = 120 psi T = 98°F

$\sigma_1 - \sigma_3$ = 13.3 psi		$\sigma_1 - \sigma_3$ = 26.6 psi		$\sigma_1 - \sigma_3$ = 40.0 psi	
time (min)	strain (%)	time (min)	strain (%)	time (min)	strain (%)
0.1	0.0490	0.1	0.0623	0.1	0.1666
0.5	0.0735	0.5	0.0885	0.5	0.1929
1.0	0.0980	1.0	0.1016	1.0	0.2192
2.0	0.1078	2.0	0.1081	2.0	0.2555
4.0	0.1290	4.0	0.1245	4.0	0.2900
7.0	0.1470	7.0	0.1393	7.0	0.3180
14.0	0.1699	14.0	0.1573	14.0	0.3772
22.0	0.1748	22.0	0.1737	22.0	0.4135
30.0	0.1846	30.0	0.1884	30.0	0.4530
60.0	0.1879	60.0	0.2392	60.0	0.5730
120.0	0.2140	120.0	0.2769	120.0	0.7200
310.0	0.2516	220.0	0.3293	160.0	0.7805
580.0	0.2532	340.0	0.3785	320.0	0.9440
1270.0	0.2761	740.0	0.4408	450.0	1.0300
2130.0	0.3153	1300.0	0.5342	680.0	1.1220
2900.0	0.3724	2270.0	0.6374	1220.0	1.2840
		2850.0	0.7046	1670.0	1.3800
				2020.0	1.4060
				2520.0	1.4610
				2880.0	1.5220

stress difference = 0

0.0	0.3724	0.0	0.7046	0.0	1.5220
0.1	0.3463	0.1	0.6653	0.1	1.3710
0.5	0.3414	0.5	0.6423	0.5	1.3380
2.0	0.3120	1.0	0.6259	1.0	1.3280
4.0	0.3104	2.0	0.6358	2.0	1.3060
1440.0	0.3071	4.0	0.6341	4.0	1.2920
		7.0	0.6325	7.0	1.2800
		14.0	0.6259	14.0	1.2670
		22.0	0.6210	22.0	1.2570
		30.0	0.6128	33.0	1.2460
		60.0	0.6046	60.0	1.2330
		190.0	0.5932	150.0	1.2090
		690.0	0.5800	360.0	1.1890
		1440.0	0.5817	830.0	1.1640
				1480.0	1.1480

σ_3 = 120 psi T = 98°F

$\sigma_1 - \sigma_3$ = 53.3 psi		$\sigma_1 - \sigma_3$ = 66.6 psi		$\sigma_1 - \sigma_3$ = 80.0 psi	
time (min)	strain (%)	time (min)	strain (%)	time (min)	strain (%)
0.1	0.2705	0.1	0.4875	0.1	0.7300
0.5	0.3500	0.5	0.6565	1.0	1.1550
1.0	0.3770	1.0	0.7580	2.0	1.2780
3.0	0.4470	2.0	0.8665	4.0	1.4270
4.0	0.4735	4.0	0.9780	7.0	1.5665
7.0	0.5300	7.0	1.0845	14.0	1.7395
14.0	0.6100	14.0	1.2265	22.0	1.8870
22.0	0.6735	22.0	1.3420	30.0	1.9900
30.0	0.7265	30.0	1.4500	45.0	2.1140
60.0	0.8765	60.0	1.7250	60.0	2.2040
120.0	1.0460	90.0	1.8730	120.0	2.4140
180.0	1.1690	490.0	2.4640	300.0	2.6950
600.0	1.4640	680.0	2.5430	570.0	2.8560
760.0	1.5530	800.0	2.6100	810.0	2.9550
1320.0	1.7410	1520.0	2.7600	1540.0	3.1200
1790.0	1.8650	2260.0	2.8520	1860.0	3.1720
2260.0	1.9280	2870.0	2.9080	2130.0	3.2050
2880.0	2.0940			2360.0	3.2340
				2880.0	3.3000

stress difference = 0

0.0	2.0940	0.0	2.9080	0.0	3.3000
0.1	1.8310	0.1	2.4980	0.1	2.9360
1.0	1.7450	0.5	2.4320	1.0	2.5000
2.0	1.7165	1.0	2.3990	2.0	2.4640
4.0	1.6835	2.0	2.3720	4.0	2.4220
7.0	1.6530	4.0	2.3390	7.0	2.3720
14.0	1.6350	7.0	2.3050	15.0	2.3390
22.0	1.6135	14.0	2.2650	30.0	2.2900
30.0	1.5980	22.0	2.2410	60.0	2.2380
60.0	1.5605	30.0	2.2280	120.0	2.1950
120.0	1.5320	45.0	2.1940	230.0	2.1630
380.0	1.5000	60.0	2.1720	450.0	2.1480
800.0	1.4700	120.0	2.1150	510.0	2.1220
1440.0	1.4640	270.0	2.0880	660.0	2.1140
		510.0	2.0680	870.0	2.1020
		1230.0	2.0220	1550.0	2.0850

σ_3 = 120 psi T = 88°F

$\sigma_1 - \sigma_3$ = 13.3 psi		$\sigma_1 - \sigma_3$ = 26.6 psi		$\sigma_1 - \sigma_3$ = 40.0 psi	
time (min)	strain (%)	time (min)	strain (%)	time (min)	strain (%)
0.1	0.0655	0.1	0.2232	0.1	0.2488
0.5	0.1310	0.5	0.2527	0.5	0.2985
2.0	0.2669	1.0	0.2658	1.0	0.3416
4.0	0.2702	4.0	0.2790	2.5	0.4080
7.0	0.2751	7.0	0.2987	4.0	0.4644
14.0	0.2849	14.0	0.3315	7.0	0.5108
22.0	0.2915	22.0	0.3643	14.0	0.5804
30.0	0.2980	30.0	0.3807	22.0	0.6401
60.0	0.3144	60.0	0.4267	30.0	0.6965
100.0	0.3406	100.0	0.4726	60.0	0.8342
270.0	0.3701	410.0	0.6170	120.0	1.0116
470.0	0.3914	760.0	0.6925	360.0	1.3317
600.0	0.3996	1440.0	0.7975	800.0	1.5290
830.0	0.4192	2190.0	0.8730	1420.0	1.6650
1435.0	0.5044	2880.0	0.9682	2030.0	1.7446
1845.0	0.5306			2880.0	1.8640
2880.0	0.6157				

stress difference = 0

0.0	0.6157	0.0	0.9682	0.0	1.8640
0.1	0.5404	0.1	0.8632	0.1	1.6849
0.5	0.5371	0.5	0.8369	0.5	1.6518
1.0	0.5338	1.0	0.8205	1.0	1.6473
30.0	0.5240	2.0	0.7975	2.0	1.6286
60.0	0.5224	4.0	0.7877	4.0	1.6020
1440.0	0.5175	30.0	0.7713	7.0	1.5937
		60.0	0.7581	14.0	1.5755
		1440.0	0.7450	22.0	1.5622
				30.0	1.5473
				60.0	1.5357
				310.0	1.4992
				1440.0	1.4859

σ_3 = 120 psi T = 88°F

$\sigma_1 - \sigma_3$ = 53.3 psi		$\sigma_1 - \sigma_3$ = 66.6 psi		$\sigma_1 - \sigma_3$ = 80.0 psi	
time (min)	strain (%)	time (min)	strain (%)	time (min)	strain (%)
0.1	0.3165	0.1	0.7162	0.1	1.0836
0.5	0.4175	0.5	0.8062	0.5	1.7074
1.0	0.4848	1.0	0.9691	1.0	1.9470
2.0	0.5421	2.0	1.1218	2.0	2.2094
4.0	0.6128	4.0	1.2864	4.0	3.0218
7.0	0.7020	7.0	1.4305	7.0	3.5857
14.0	0.8047	14.0	1.5952	14.0	3.8852
22.0	0.8787	22.0	1.7444	22.0	4.1812
30.0	0.9427	30.0	1.8473	30.0	4.3010
60.0	1.1481	60.0	2.0600	60.0	4.5548
90.0	1.2323	135.0	2.3087	90.0	4.7186
170.0	1.4326	260.0	2.6312	185.0	4.9354
420.0	1.6935	635.0	2.9502	550.0	5.1997
600.0	1.7911	1535.0	3.2658	1165.0	5.4781
790.0	1.8585	2335.0	3.4967	1685.0	5.5908
1390.0	2.0134	2880.0	3.6981	1910.0	5.6507
1710.0	2.1110			2530.0	5.7706
2880.0	2.4005				

stress difference = 0

0.0	2.4005	0.0	3.6981	0.0	5.7706
0.1	2.0908	0.1	3.1458	0.1	4.7838
0.5	2.0504	0.5	3.0772	0.5	4.6164
1.0	2.0184	1.0	3.0429	1.0	4.5830
2.0	1.9898	2.0	3.0154	2.0	4.5283
4.0	1.9628	4.0	2.9742	4.0	4.4700
7.0	1.9325	7.0	2.9399	7.0	4.4332
14.0	1.9006	14.0	2.9125	14.0	4.3839
22.0	1.8753	22.0	2.8765	22.0	4.3504
30.0	1.8686	30.0	2.8610	30.0	4.3257
60.0	1.8299	60.0	2.8336	60.0	4.2799
90.0	1.8164	580.0	2.7050	90.0	4.2517
240.0	1.7794	720.0	2.6758	280.0	4.1883
540.0	1.7440	1440.0	2.6535	570.0	4.1460
1440.0	1.7204				

σ_3 = 120 psi T= 78°F

$\sigma_1 - \sigma_3$ = 13.3 psi		$\sigma_1 - \sigma_3$ = 26.6 psi		$\sigma_1 - \sigma_3$ = 40.0 psi	
time (min)	strain (%)	time (min)	strain (%)	time (min)	strain (%)
0.1	0.0875	0.1	0.1773	0.1	0.2575
0.5	0.1069	0.5	0.2066	0.5	0.3165
1.0	0.1231	1.0	0.2245	1.0	0.3542
2.0	0.1345	2.0	0.2375	2.0	0.3837
4.0	0.1523	4.0	0.2651	4.0	0.4280
7.0	0.1685	7.0	0.2944	7.0	0.4641
14.0	0.1782	14.0	0.3172	14.0	0.5264
30.0	0.2057	30.0	0.3644	30.0	0.6248
105.0	0.2398	65.0	0.4245	60.0	0.7363
180.0	0.2624	140.0	0.5026	170.0	0.9823
390.0	0.3078	250.0	0.5839	340.0	1.1692
560.0	0.3224	650.0	0.7303	470.0	1.2512
850.0	0.3467	1470.0	0.8832	780.0	1.3939
1530.0	0.3888	2090.0	0.9613	1380.0	1.5267
3030.0	0.4828	2880.0	1.0329	2110.0	1.6169
3180.0	0.4957			2880.0	1.7875

stress difference = 0

0.0	0.4957	0.0	1.0329	0.0	1.7875
0.1	0.4326	0.1	0.9385	0.1	1.6727
0.5	0.4303	0.5	0.9158	0.5	1.6087
1.0	0.4277	1.0	0.9028	1.0	1.5776
2.0	0.4261	2.0	0.8946	2.0	1.5612
4.0	0.4245	4.0	0.8881	4.0	1.5382
7.0	0.4180	7.0	0.8800	7.0	1.5284
14.0	0.4115	14.0	0.8735	14.0	1.5185
30.0	0.4115	30.0	0.8637	30.0	1.4907
60.0	0.4083	60.0	0.8523	60.0	1.4612
90.0	0.4066	120.0	0.8475	90.0	1.4464
1090.0	0.4018	190.0	0.8344	1440.0	1.4103
		360.0	0.8214		
		670.0	0.8052		
		1480.0	0.8100		

σ_3 = 120 psi T = 78°F

$\sigma_1 - \sigma_3$ = 53.3 psi		$\sigma_1 - \sigma_3$ = 66.6 psi		$\sigma_1 - \sigma_3$ = 80.0 psi	
time (min)	strain (%)	time (min)	strain (%)	time (min)	strain (%)
0.1	0.3992	0.1	0.6096	0.1	0.9878
0.5	0.5389	0.5	0.7619	0.5	1.4030
1.0	0.5905	1.0	0.9177	1.0	1.6383
2.0	0.6587	2.0	1.0633	2.0	1.8543
4.0	0.7419	4.0	1.1819	4.0	2.3269
14.0	0.9281	7.0	1.2919	7.0	2.5725
30.0	1.1011	14.0	1.4714	14.0	2.8632
45.0	1.1976	22.0	1.5950	22.0	3.0500
70.0	1.3390	45.0	1.8134	45.0	3.3406
160.0	1.7765	60.0	1.9133	60.0	3.4444
420.0	1.8946	120.0	2.1538	110.0	3.6520
785.0	2.0626	185.0	2.3180	250.0	3.9219
1390.0	2.2089	620.0	2.6837	390.0	4.0396
2065.0	2.3121	1370.0	2.9157	800.0	4.2229
2880.0	2.3952	2880.0	3.1595	1470.0	4.3856
				2360.0	4.5101
				2880.0	4.5759

stress difference = 0

0.0	2.3952	0.0	3.1595	0.0	4.5759
0.1	2.1457	0.1	2.6549	0.1	3.8147
0.5	2.0659	0.5	2.5330	0.5	3.7005
1.0	2.0276	1.0	2.5025	1.0	3.6382
2.0	2.0060	2.0	2.4382	2.0	3.5586
4.0	1.9727	4.0	2.3976	4.0	3.5206
7.0	1.9561	7.0	2.3688	7.0	3.4721
14.0	1.9195	14.0	2.3332	14.0	3.4280
30.0	1.8796	30.0	2.2824	30.0	3.3683
1440.0	1.7632	60.0	2.2469	60.0	3.3164
		185.0	2.1758	130.0	3.2611
		890.0	2.1284	210.0	3.2178
		1440.0	2.1267	660.0	3.1434
				1460.0	3.1192

σ_3 = 120 psi T = 78°F

$\sigma_1 - \sigma_3$ = 93.3 psi		$\sigma_1 - \sigma_3$ = 13.3 psi		$\sigma_1 - \sigma_3$ = 26.6 psi	
time (min)	strain (%)	time (min)	strain (%)	time (min)	strain (%)
0.1	1.3839	0.1	0.0262	0.1	0.1280
0.5	1.7053	0.5	0.0295	1.0	0.1330
1.0	2.1339	1.0	0.0426	2.0	0.1510
2.0	2.5518	2.0	0.0655	4.0	0.1822
4.0	2.9375	4.0	0.0753	7.0	0.2036
7.0	3.2518	7.0	0.0966	14.0	0.2101
14.0	2.2286	14.0	0.1146	30.0	0.2561
30.0	3.9910	30.0	0.1473	45.0	0.2692
60.0	4.2821	45.0	0.1539	60.0	0.2889
95.0	4.4410	90.0	0.1686	120.0	0.3382
180.0	4.6053	195.0	0.1899	270.0	0.4252
330.0	4.7803	360.0	0.2357	380.0	0.4596
690.0	4.9785	585.0	0.2799	840.0	0.5746
1245.0	5.1517	840.0	0.2930	1470.0	0.6566
2050.0	5.2946	1410.0	0.3208	1700.0	0.7125
2880.0	5.4285	2160.0	0.3470	2940.0	0.7551
		2865.0	0.3683		

stress difference = 0

0.0	5.4285	0.0	0.3683	0.0	0.7551
0.1	4.3393	0.1	0.3257	0.1	0.6731
0.5	4.1428	0.5	0.3241	0.5	0.6698
1.0	4.0750	1.0	0.3143	1.0	0.6583
2.0	4.0143	2.0	0.3037	2.0	0.6566
4.0	3.9535	4.0	0.3012	60.0	0.6337
7.0	3.8982	7.0	0.2995	315.0	0.6238
14.0	3.8393	1440.0	0.2946	585.0	0.6107
30.0	3.7893			1440.0	0.6025
60.0	3.7357				
80.0	3.7053				
620.0	3.5893				
1440.0	3.5714				

σ_3 = 120 psi T = 68°F

σ_3 = 120 psi T = 68°F

$\sigma_1 - \sigma_3$ = 40.0 psi		$\sigma_1 - \sigma_3$ = 53.3 psi		$\sigma_1 - \sigma_3$ = 66.6 psi	
time (min)	strain (%)	time (min)	strain (%)	time (min)	strain (%)
0.1	0.1222	0.1	0.3949	0.1	0.4571
0.5	0.1387	0.5	0.4116	0.5	0.5688
1.0	0.1470	1.0	0.4200	1.0	0.6027
2.0	0.1602	2.0	0.4752	2.0	0.6704
5.0	0.1949	4.0	0.4986	4.0	0.8007
7.0	0.2180	7.0	0.5287	7.0	0.9000
15.0	0.2659	14.0	0.5722	14.0	1.0327
30.0	0.3468	30.0	0.6358	30.0	1.2252
60.0	0.4624	60.0	0.7260	60.0	1.4522
120.0	0.6507	90.0	0.8065	245.0	1.9182
300.0	0.9249	215.0	1.0006	640.0	2.1500
660.0	1.2387	330.0	1.1277	1550.0	2.4445
1440.0	1.3873	820.0	1.4289	2150.0	2.5360
1875.0	1.4435	1670.0	1.6347	2860.0	2.6172
2880.0	1.5244	2900.0	1.7602		

stress difference = 0

0.0	1.5244	0.0	1.7602	0.0	2.6172
0.1	1.4038	0.1	1.4657	0.1	2.3531
0.5	1.3939	0.5	1.4390	0.5	2.2549
1.0	1.3906	1.0	1.4289	1.0	2.2329
2.0	1.3774	2.0	1.3821	2.0	2.2160
4.0	1.3642	4.0	1.3620	4.0	2.1805
7.0	1.3444	7.0	1.3453	7.0	2.1584
15.0	1.3245	15.0	1.3151	14.0	2.1178
30.0	1.3229	30.0	1.2817	30.0	2.0721
60.0	1.3146	60.0	1.2516	60.0	2.0281
90.0	1.3113	820.0	1.1645	200.0	1.9807
410.0	1.2932	1440.0	1.1645	330.0	1.9570
1440.0	1.2932			1440.0	1.9299

σ_3 = 120 psi T = 68°F

$\sigma_1 - \sigma_3$ = 73.3 psi		$\sigma_1 - \sigma_3$ = 80.0 psi	
time (min)	strain (%)	time (min)	strain (%)
0.1	0.6111	0.1	0.7674
0.5	0.7941	0.5	0.9927
1.0	0.8459	1.0	1.2321
2.0	0.9322	2.0	1.4081
4.0	1.0150	4.0	1.5841
7.0	1.0806	7.0	1.6968
15.0	1.1808	14.0	1.8341
30.0	1.2843	30.0	1.9890
60.0	1.6468	60.0	2.1474
80.0	1.7815	120.0	2.3868
180.0	2.1406	320.0	2.7846
410.0	2.5100	690.0	3.0662
750.0	2.7137	1440.0	3.2492
1390.0	2.8621	1830.0	3.2985
2080.0	2.9036	2130.0	3.3302
2830.0	2.9519	2760.0	3.4041

stress difference = 0

0.0	2.9519	0.0	3.4041
0.1	2.3322	0.1	2.7388
1.0	2.2372	0.5	2.6402
2.0	2.2044	1.0	2.5980
4.0	2.1561	2.0	2.5698
7.0	2.1336	4.0	2.5346
15.0	2.1216	7.0	2.5029
30.0	2.0784	14.0	2.4572
60.0	2.0473	30.0	2.4008
90.0	2.0335	60.0	2.3516
180.0	2.0111	110.0	2.3164
390.0	1.9800	240.0	2.2812
830.0	1.9489	590.0	2.1791
1510.0	1.9282	1400.0	2.1333

σ_3 = 240 psi T = 98°F

$\sigma_1 - \sigma_3$ = 13.3 psi		$\sigma_1 - \sigma_3$ = 26.6 psi		$\sigma_1 - \sigma_3$ = 40.0 psi	
time (min)	strain (%)	time (min)	strain (%)	time (min)	strain (%)
0.1	0.0334	0.1	0.0436	0.1	0.0555
0.5	0.0468	0.5	0.0620	0.5	0.0706
1.0	0.0569	1.0	0.0771	1.0	0.0807
2.0	0.0702	2.0	0.0805	2.0	0.0891
4.0	0.0736	4.0	0.0838	4.0	0.1126
7.0	0.0752	7.0	0.0939	7.0	0.1311
14.0	0.0803	14.0	0.0989	14.0	0.1395
30.0	0.0870	30.0	0.1123	30.0	0.1748
60.0	0.0970	60.0	0.1324	60.0	0.1967
120.0	0.1204	120.0	0.1475	120.0	0.2404
310.0	0.1438	220.0	0.1710	160.0	0.2471
580.0	0.1605	340.0	0.1827	320.0	0.2841
1270.0	0.1956	740.0	0.2078	680.0	0.3563
2130.0	0.2174	1300.0	0.2447	1220.0	0.4269
2900.0	0.2525	2270.0	0.2900	2020.0	0.4891
		2850.0	0.3235	2880.0	0.5496
		stress difference = 0			
0.0	0.2525	0.0	0.3235	0.0	0.5496
0.1	0.2475	0.1	0.3218	0.1	0.5194
0.5	0.2425	0.5	0.3034	0.5	0.4790
2.0	0.2408	1.0	0.2967	1.0	0.4690
1440.0	0.2408	2.0	0.2917	2.0	0.4454
		14.0	0.2900	4.0	0.4269
		30.0	0.2866	7.0	0.4152
		60.0	0.2816	14.0	0.3933
		1440.0	0.2766	33.0	0.3647
				60.0	0.3513
				150.0	0.3278
				360.0	0.3244
				830.0	0.3227
				1480.0	0.3160

σ_3 = 240 psi T = 98°F

$\sigma_1 - \sigma_3$ = 53.3 psi		$\sigma_1 - \sigma_3$ = 66.6 psi		$\sigma_1 - \sigma_3$ = 80.0 psi	
time (min)	strain (%)	time (min)	strain (%)	time (min)	strain (%)
0.1	0.1163	0.1	0.1389	0.1	0.2383
0.5	0.1298	0.5	0.1558	1.0	0.2894
1.0	0.1433	1.0	0.1626	2.0	0.3234
3.0	0.1770	2.0	0.1897	4.0	0.3455
7.0	0.2125	4.0	0.2066	7.0	0.3745
14.0	0.2377	7.0	0.2337	14.0	0.4119
30.0	0.2698	14.0	0.2642	30.0	0.4902
60.0	0.3018	30.0	0.3031	60.0	0.5685
120.0	0.3457	60.0	0.3489	120.0	0.6570
180.0	0.3861	90.0	0.3760	300.0	0.7947
600.0	0.4536	490.0	0.5521	570.0	0.8681
1320.0	0.5531	800.0	0.6080	810.0	0.9413
1790.0	0.5902	1520.0	0.6943	1540.0	1.0553
2260.0	0.6374	2260.0	0.7909	2130.0	1.1507
2810.0	0.6947	2870.0	0.8569	2870.0	1.2085

stress difference = 0

0.0	0.6947	0.0	0.8569	0.0	1.2085
0.1	0.5885	0.1	0.7790	0.1	1.0519
1.0	0.5699	0.5	0.7384	1.0	1.0043
2.0	0.5547	1.0	0.7231	2.0	0.9821
4.0	0.5413	2.0	0.7096	4.0	0.9566
7.0	0.5295	4.0	0.6909	7.0	0.9311
14.0	0.5109	7.0	0.6689	15.0	0.8936
22.0	0.4991	14.0	0.6452	30.0	0.8613
30.0	0.4890	22.0	0.6232	60.0	0.8255
60.0	0.4755	30.0	0.6097	120.0	0.8051
120.0	0.4687	60.0	0.5826	230.0	0.7898
380.0	0.4620	120.0	0.5690	450.0	0.7864
800.0	0.4418	270.0	0.5436	1440.0	0.7830
1440.0	0.4317	510.0	0.5301		
		1230.0	0.5081		

σ_3 = 240 psi T = 98°F

σ_3 = 240 psi T = 98°F

$\sigma_1 - \sigma_3$ = 96.7 psi		$\sigma_1 - \sigma_3$ = 13.3 psi		$\sigma_1 - \sigma_3$ = 20.6 psi	
time (min)	strain (%)	time (min)	strain (%)	time (min)	strain (%)
0.1	0.2951	0.1	0.0299	0.1	0.0[illegible]
0.5	0.3362	0.5	0.0332	0.5	0.0[illegible]4
2.0	0.4323	1.0	0.0431	1.0	0.0[illegible]
4.0	0.5009	14.0	0.0498	2.5	0.0[illegible]
7.0	0.5524	22.0	0.0531	4.0	0.0963
15.0	0.6262	60.0	0.0564	7.0	0.1029
30.0	0.7051	100.0	0.0631	14.0	0.1128
45.0	0.7634	1440.0	0.0664	30.0	0.1295
100.0	0.9058	2880.0	0.0730	60.0	0.1328
170.0	0.9847			120.0	0.1428
320.0	1.0997			360.0	0.1594
530.0	1.2283			800.0	0.1644
1230.0	1.4016			1420.0	0.1860
2050.0	1.5371			1950.0	0.2009
2880.0	1.6881			2880.0	0.2242

stress difference = 0

0.0	1.6881	0.0	0.0730	0.0	0.2242
0.1	1.4239	0.1	0.0631	0.1	0.1843
0.5	1.3621	0.5	0.0614	0.5	0.1828
1.0	1.3450	1.0	0.0614	1.0	0.1793
2.0	1.3158	7.0	0.0614	4.0	0.1760
4.0	1.2832			14.0	0.1743
7.0	1.2626			22.0	0.1694
14.0	1.2215			60.0	0.1660
30.0	1.1734			1060.0	0.1594
60.0	1.1237				
90.0	1.1014				
550.0	1.0808				

σ_3 = 240 psi T = 88°F

$\sigma_1 - \sigma_3$ = 40.0 psi		$\sigma_1 - \sigma_3$ = 53.3 psi		$\sigma_1 - \sigma_3$ = 66.6 psi	
time (min)	strain (%)	time (min)	strain (%)	time (min)	strain (%)
0.1	0.0665	0.1	0.1040	0.1	0.1608
0.5	0.0765	0.5	0.1100	0.5	0.1943
1.0	0.0865	1.0	0.1450	1.0	0.2248
2.0	0.0898	2.0	0.1634	2.0	0.2578
4.0	0.1031	4.0	0.1950	4.0	0.3014
7.0	0.1130	7.0	0.2117	7.0	0.3333
14.0	0.1300	14.0	0.2367	14.0	0.3818
30.0	0.1497	30.0	0.2800	30.0	0.4605
60.0	0.1630	60.0	0.3234	60.0	0.5295
90.0	0.1829	135.0	0.3734	90.0	0.5791
170.0	0.2095	260.0	0.4217	185.0	0.6436
420.0	0.2395	635.0	0.5000	550.0	0.8234
790.0	0.2794	1535.0	0.6017	1165.0	0.9717
1390.0	0.3110	2335.0	0.6567	1680.0	1.0483
1710.0	0.3293	2880.0	0.7001	2530.0	1.1353
2880.0	0.3925			2880.0	1.1755

stress difference = 0

0.0	0.3925	0.0	0.7001	0.0	1.1755
0.1	0.3127	0.1	0.6067	0.1	1.0248
0.5	0.3060	0.5	0.5967	0.5	1.0047
1.0	0.3010	1.0	0.5867	1.0	0.9913
2.0	0.2910	2.0	0.5817	2.0	0.9779
4.0	0.2860	4.0	0.5701	4.0	0.9578
7.0	0.2794	7.0	0.5584	7.0	0.9411
14.0	0.2727	14.0	0.5434	14.0	0.9244
30.0	0.2628	30.0	0.5150	30.0	0.8925
60.0	0.2495	60.0	0.5017	60.0	0.8724
240.0	0.2428	590.0	0.4800	90.0	0.8590
1230.0	0.2262	720.0	0.4634	260.0	0.8440
1440.0	0.2262	1440.0	0.4634	570.0	0.8289
				1440.0	0.8239

σ_3 = 240 psi T = 88°F σ_3 = 240 psi T = [illegible]°F

$\sigma_1 - \sigma_3$ = 80.0 psi		$\sigma_1 - \sigma_3$ = 93.3 psi		$\sigma_1 - \sigma_3$ = 13.[illegible] psi	
time (min)	strain (ε)	time (min)	strain (ε)	time (min)	strain (ε)
0.1	0.3715	0.1	0.3660	0.1	0.01[illegible]
1.0	0.4863	1.0	0.6568	0.5	0.021[illegible]
2.0	0.5471	2.0	0.7320	1.0	0.028[illegible]
4.0	0.6214	4.0	0.8210	2.0	0.0383
7.0	0.6957	7.0	0.8928	4.0	0.0450
14.0	0.7733	14.0	0.9817	7.0	0.05[illegible]
22.0	0.8341	30.0	1.1015	14.0	0.06[illegible]
60.0	0.9962	60.0	1.2178	30.0	0.08[illegible]
130.0	1.1516	95.0	1.3101	60.0	0.0[illegible]
320.0	1.3441	260.0	1.4264	120.0	0.1200
905.0	1.5669	990.0	1.7685	380.0	0.151[illegible]
1680.0	1.7054	1670.0	1.8917	840.0	0.2000
2465.0	1.7898	2230.0	1.9464	1810.0	0.2401
2880.0	1.8371	3050.0	2.0114	2865.0	0.2867

stress difference = 0

0.0	1.8371	0.0	2.0114	0.0	0.2867
0.1	1.5872	0.1	1.7001	0.1	0.2617
1.0	1.5433	1.0	1.6317	0.5	0.2584
2.0	1.5180	2.0	1.6077	1.0	0.2534
4.0	1.4960	4.0	1.5804	2.0	0.2467
7.0	1.4724	7.0	1.5462	7.0	0.2484
14.0	1.4487	14.0	1.5154	1440.0	0.2484
30.0	1.4099	30.0	1.4692		
60.0	1.3812	70.0	1.4316		
140.0	1.3542	145.0	1.4059		
230.0	1.3339	350.0	1.3666		
480.0	1.3069	760.0	1.3101		
800.0	1.2951	1480.0	1.3101		
1300.0	1.2799				

σ_3 = 240 psi T = 68°F

$\sigma_1 - \sigma_3$ = 26.6 psi		$\sigma_1 - \sigma_3$ = 40.0 psi		$\sigma_1 - \sigma_3$ = 53.3 psi	
time (min)	strain (%)	time (min)	strain (%)	time (min)	strain (%)
0.1	0.0234	0.1	0.0620	0.1	0.1110
0.5	0.0301	0.5	0.0687	0.5	0.1178
1.0	0.0384	1.0	0.0687	1.0	0.1380
2.0	0.0468	2.0	0.0787	2.0	0.1413
4.0	0.0501	5.0	0.0905	4.0	0.1481
7.0	0.0568	7.0	0.0955	7.0	0.1615
14.0	0.0652	15.0	0.1139	14.0	0.1868
30.0	0.0953	30.0	0.1391	30.0	0.2255
60.0	0.1120	60.0	0.1659	60.0	0.2625
195.0	0.1521	120.0	0.2027	90.0	0.2827
360.0	0.1822	300.0	0.2798	215.0	0.3399
960.0	0.2395	660.0	0.3636	330.0	0.3709
1700.0	0.2841	1440.0	0.4792	820.0	0.4677
2940.0	0.3259	2880.0	0.5562	1670.0	0.5973
				2230.0	0.6192
				2900.0	0.6680

stress difference = 0

0.0	0.3259	0.0	0.5562	0.0	0.6680
0.1	0.2741	0.1	0.4976	0.1	0.5990
0.5	0.2707	0.5	0.4909	0.5	0.5855
1.0	0.2657	1.0	0.4875	1.0	0.5805
2.0	0.2640	2.0	0.4842	2.0	0.5653
4.0	0.2590	4.0	0.4741	4.0	0.5586
7.0	0.2574	7.0	0.4574	7.0	0.5519
315.0	0.2540	30.0	0.4540	15.0	0.5418
585.0	0.2524	60.0	0.4423	30.0	0.5283
1440.0	0.2507	90.0	0.4339	60.0	0.5099
		410.0	0.4239	820.0	0.4357
		1440.0	0.4239	1440.0	0.4358

σ_3 = 240 psi T = 68°F

$\sigma_1 - \sigma_3$ = 66.6 psi		$\sigma_1 - \sigma_3$ = 80.0 psi		$\sigma_1 - \sigma_3$ = 93.3 psi	
time (min)	strain (ε)	time (min)	strain (ε)	time (min)	strain (ε)
0.1	0.1538	0.1	0.2427	0.1	0.3271
0.5	0.1842	0.5	0.2769	0.5	0.4025
1.0	0.2011	1.0	0.3042	1.0	0.4390
2.0	0.2214	2.0	0.3384	2.0	0.4826
4.0	0.2518	4.0	0.3692	4.0	0.5302
7.0	0.2721	7.0	0.2999	7.0	0.5643
14.0	0.3093	15.0	0.4512	14.0	0.6197
30.0	0.3633	30.0	0.5093	30.0	0.6955
60.0	0.4242	60.0	0.5913	60.0	0.7814
245.0	0.6400	80.0	0.6238	120.0	0.9830
640.0	0.7334	180.0	0.7281	320.0	1.0501
1550.0	0.9109	410.0	0.8614	690.0	1.1999
2150.0	0.9768	750.0	0.9690	1440.0	1.3565
2860.0	1.0524	1390.0	1.0887	1830.0	1.3979
		2080.0	1.1604	2130.0	1.4375
		2830.0	1.2271	2760.0	1.4925

stress difference = 0

0.0	1.0524	0.0	1.2271	0.0	1.4925
0.1	0.9193	0.1	1.0323	0.1	1.2051
0.5	0.9024	1.0	0.9912	0.5	1.1723
1.0	0.8821	2.0	0.9673	1.0	1.1500
2.0	0.8754	4.0	0.9519	2.0	1.1190
4.0	0.8602	7.0	0.9366	4.0	1.0880
7.0	0.8517	15.0	0.9143	7.0	1.0777
14.0	0.8348	30.0	0.8887	14.0	1.0587
30.0	0.8078	60.0	0.8579	30.0	1.0295
60.0	0.7875	125.0	0.8323	60.0	1.0036
200.0	0.7672	180.0	0.8169	110.0	0.9761
330.0	0.7452	390.0	0.7776	240.0	0.9399
1440.0	0.7452	830.0	0.7417	360.0	0.9090
		1510.0	0.7246	590.0	0.8780
				1400.0	0.8401

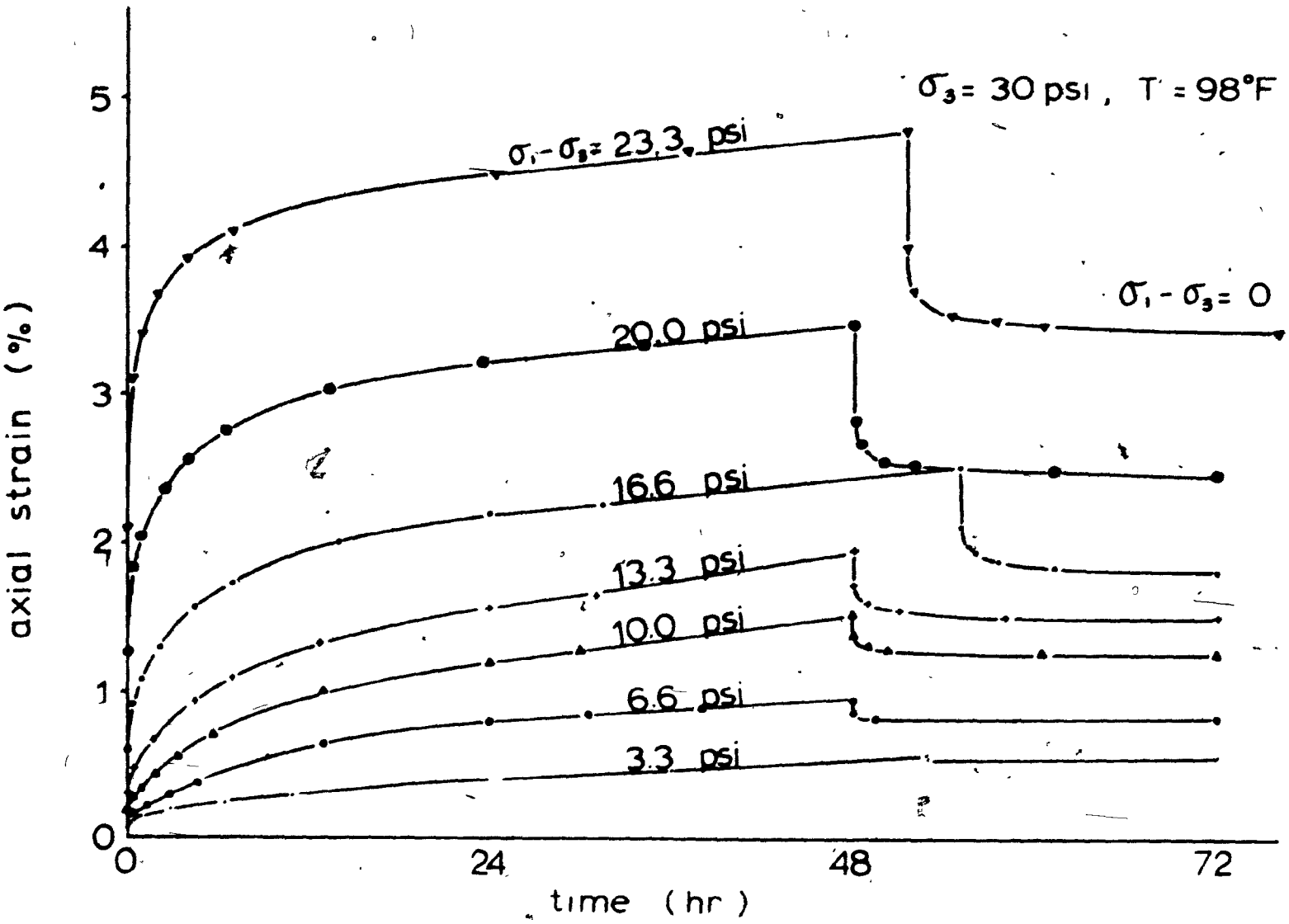

fig B-1 family of creep curves

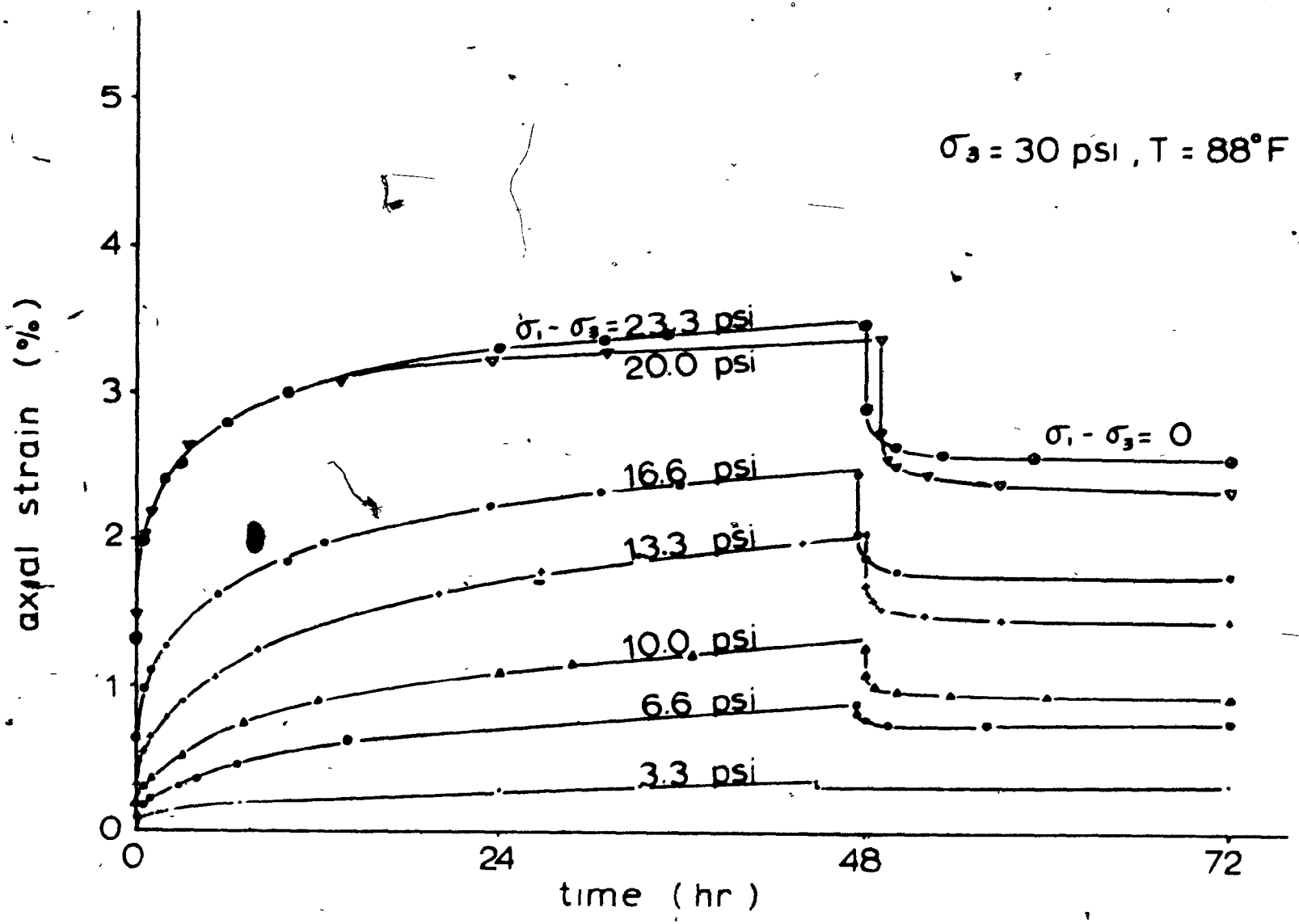

fig B-2 family of creep curves

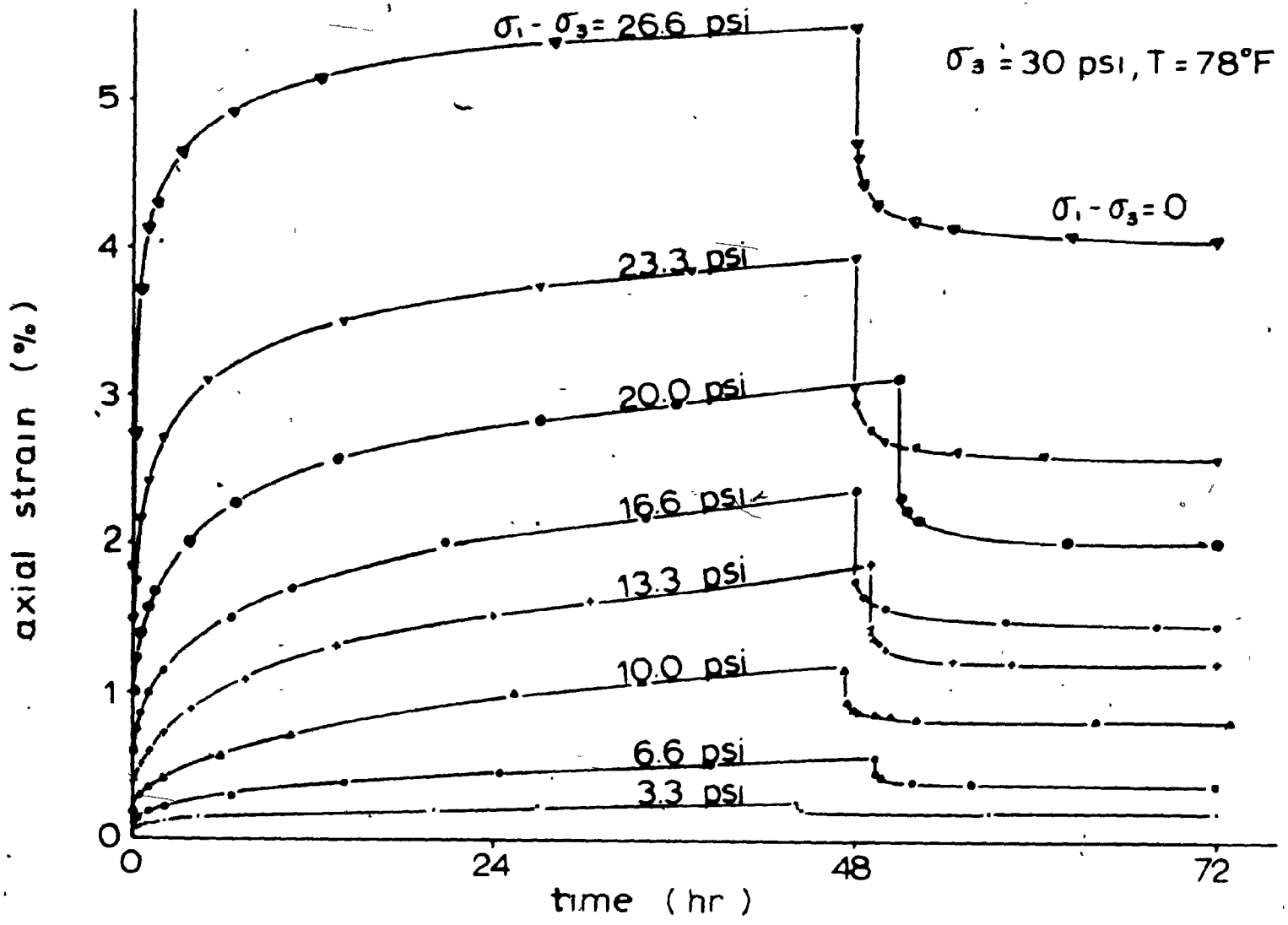

fig. B-3 family of creep curves

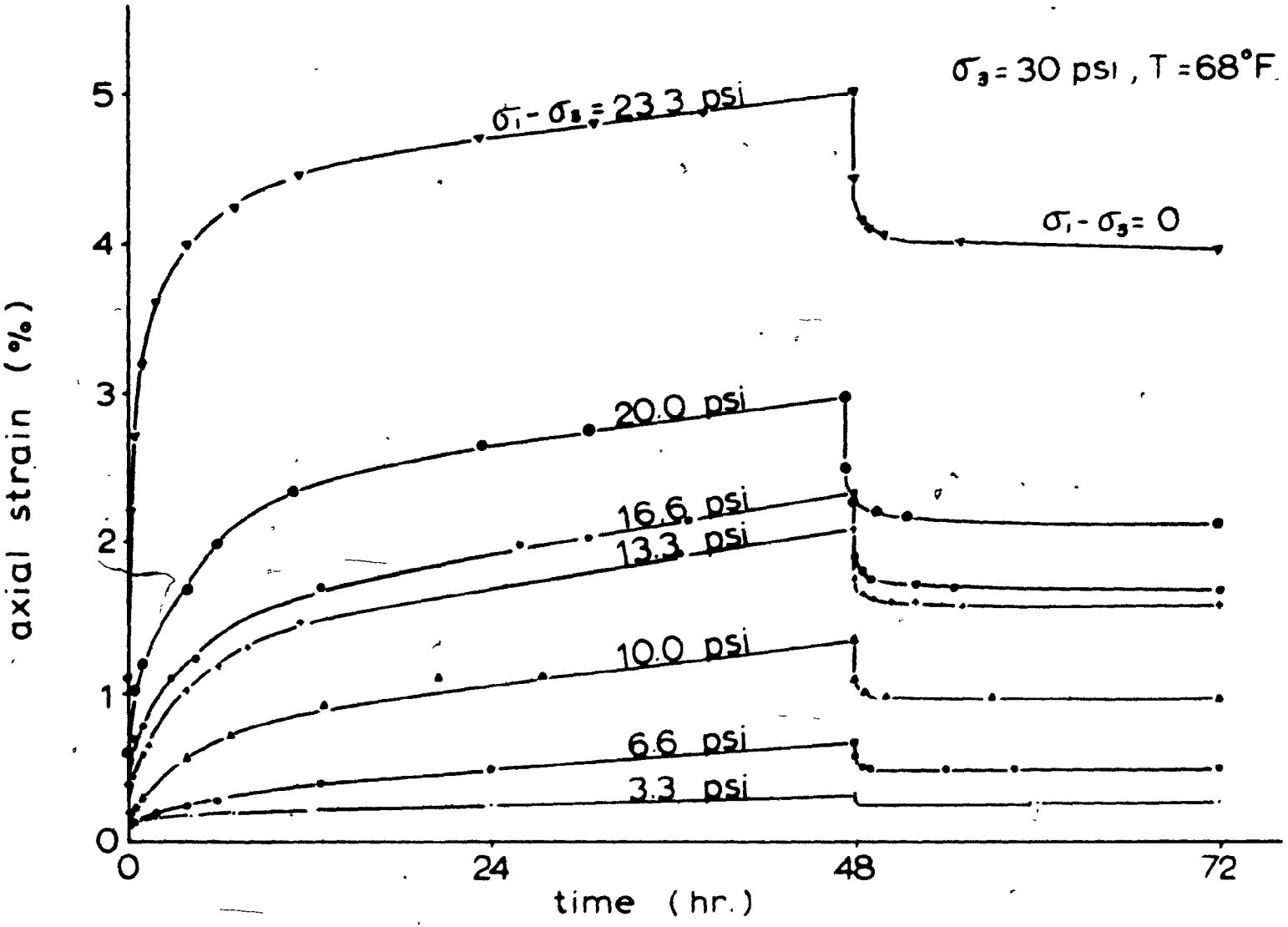

fig. B-4 family of creep curves

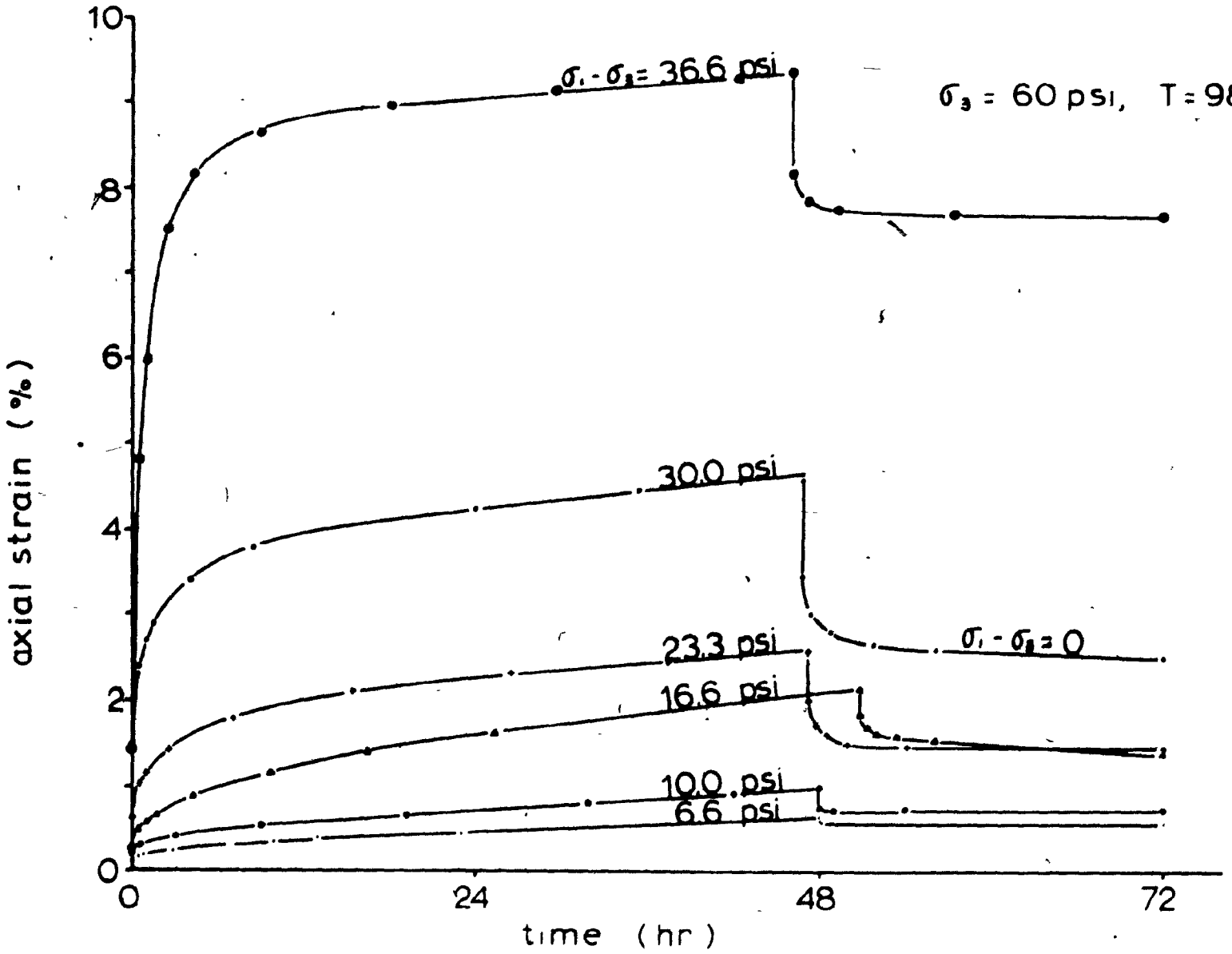

Fig B-5 family of creep curves

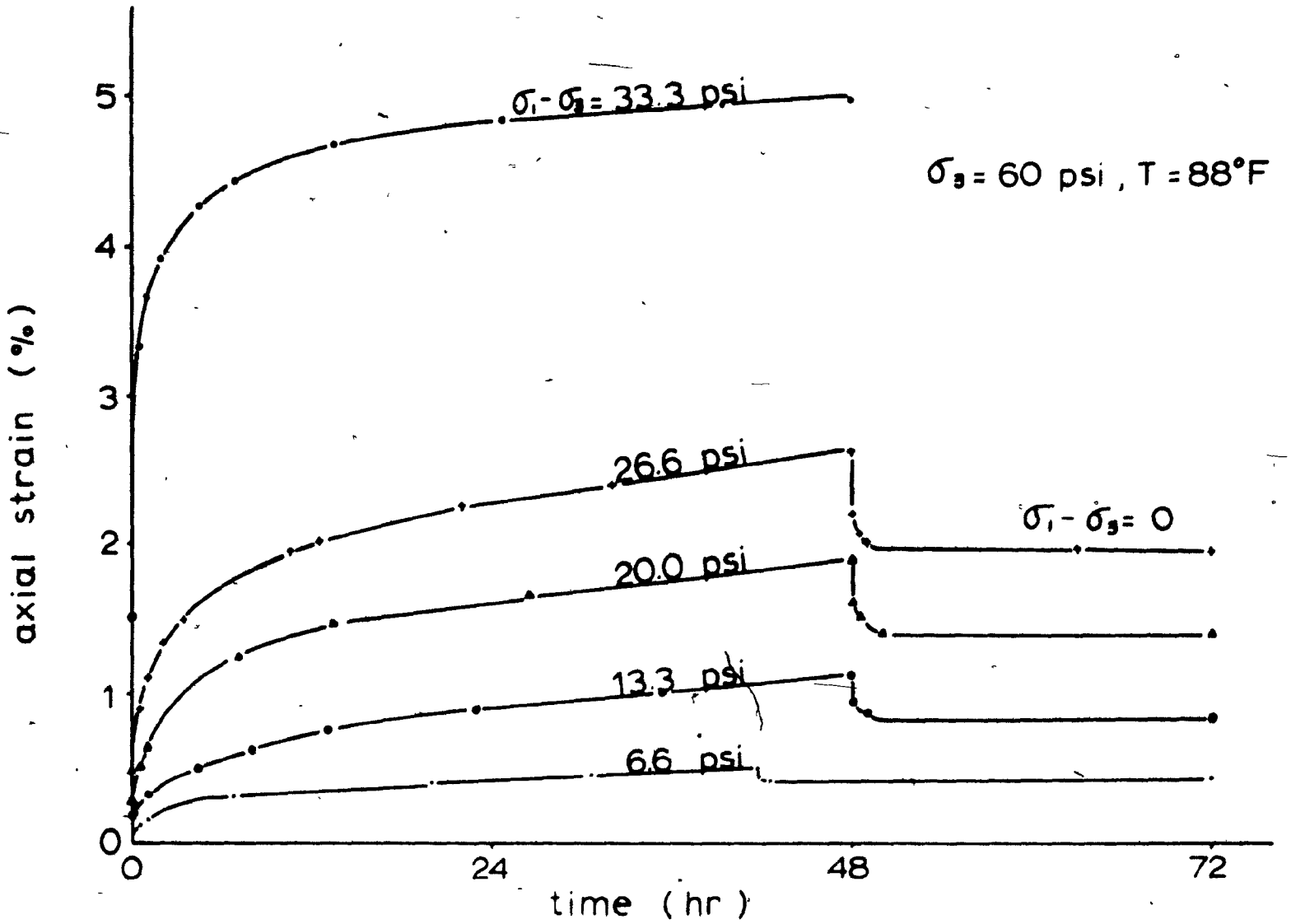

fig B-6 family of creep curves

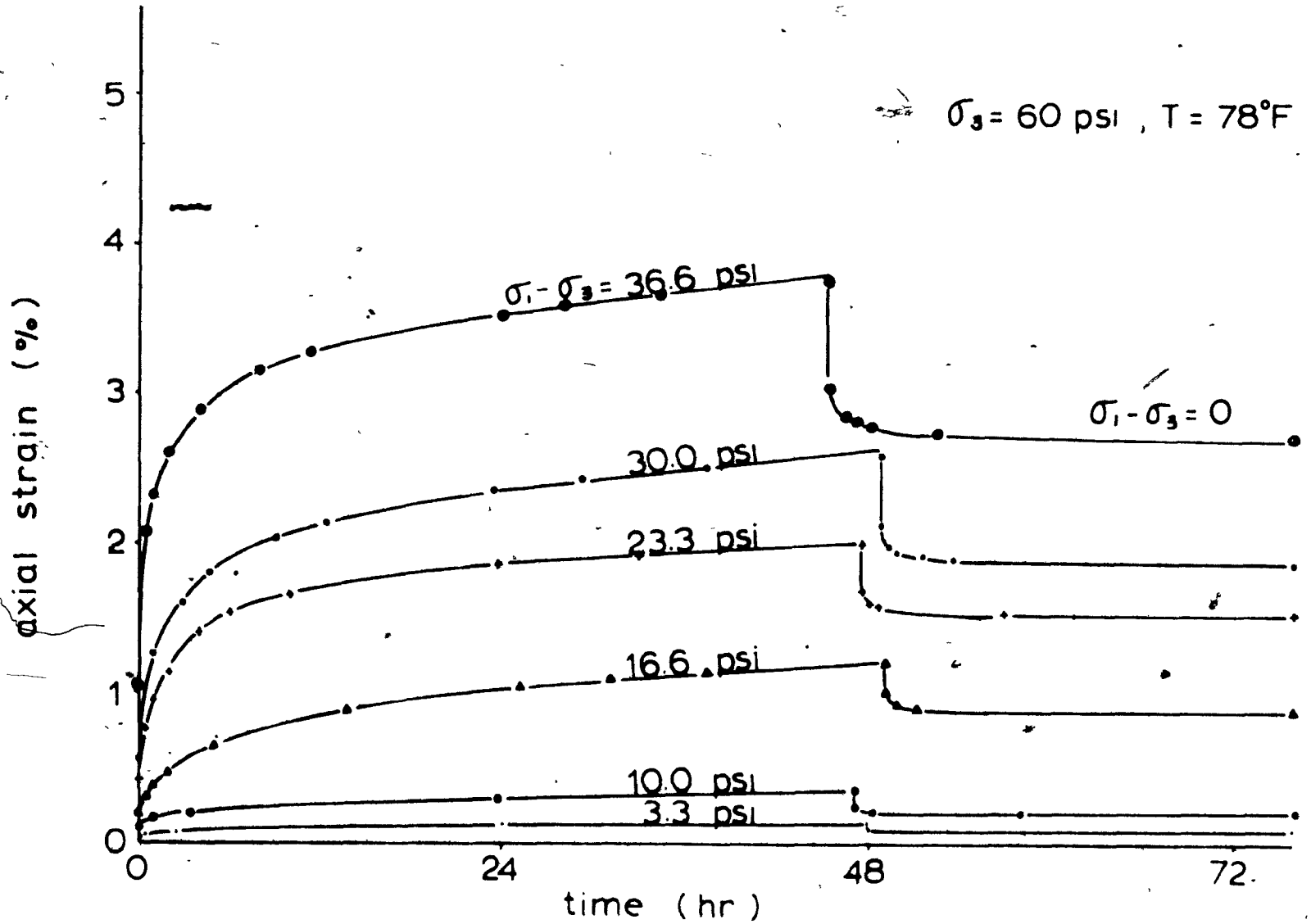

fig B-7 family of creep curves

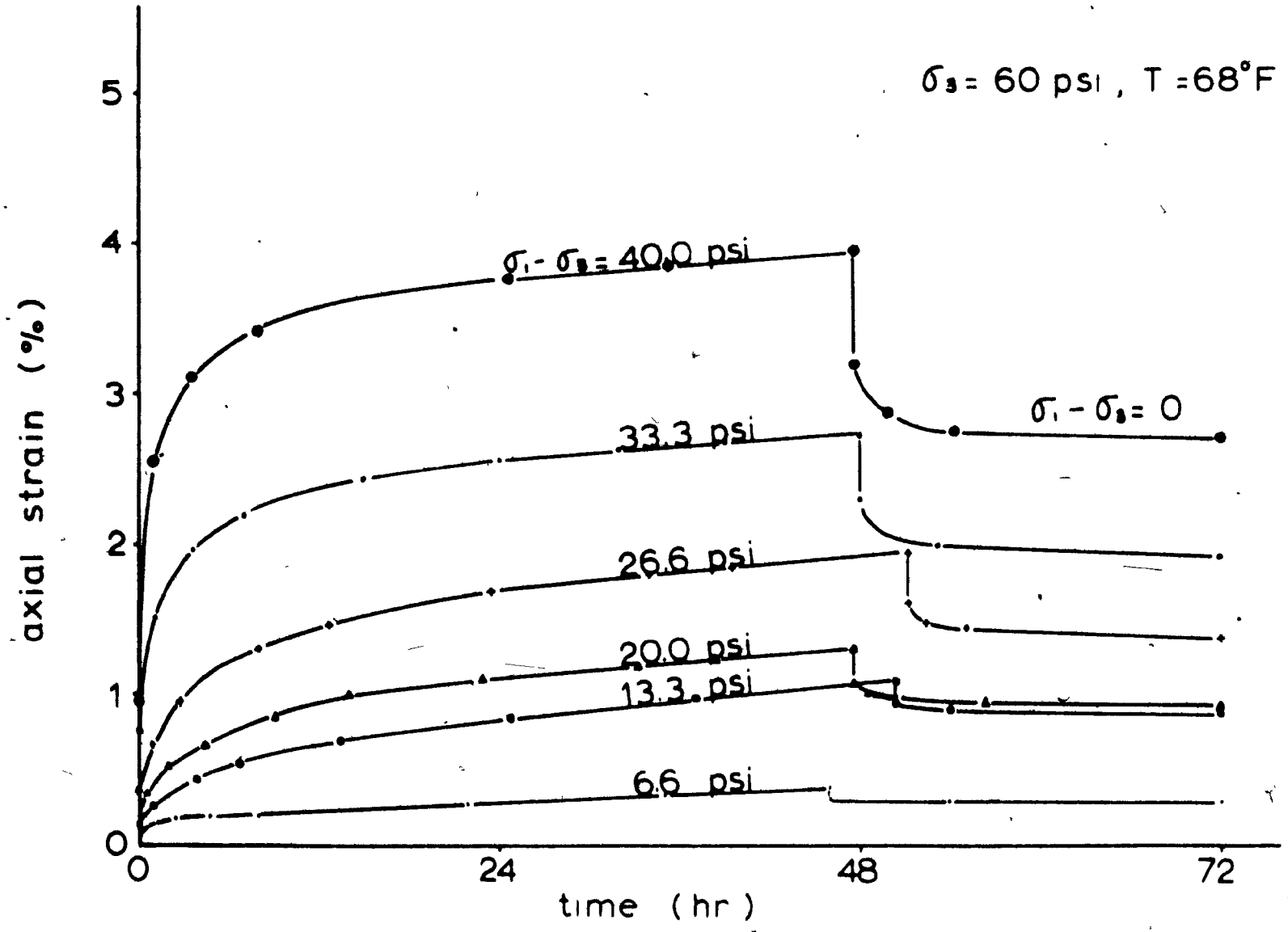

fig B-8 family of creep curves

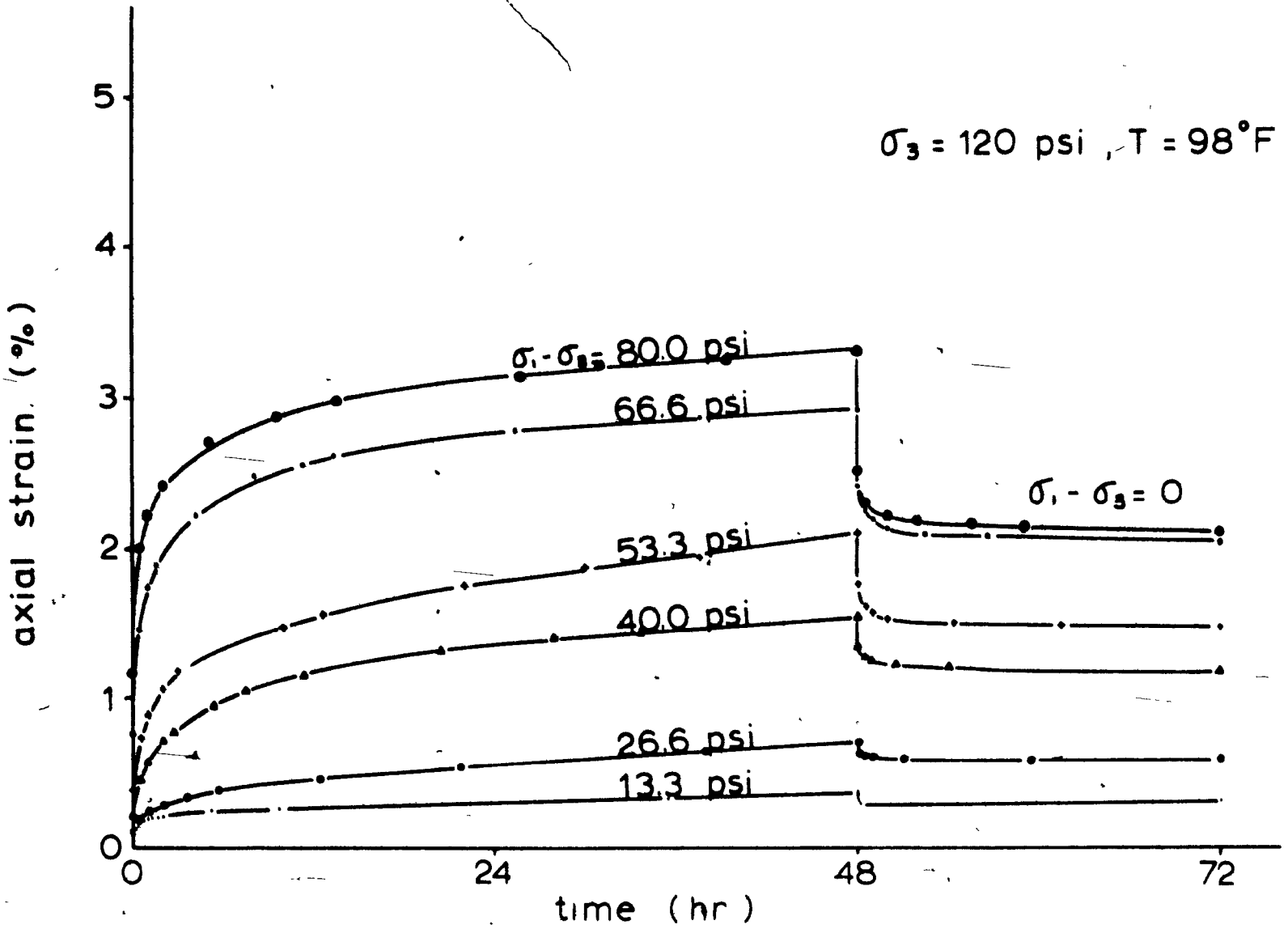

fig. B-9 family of creep curves

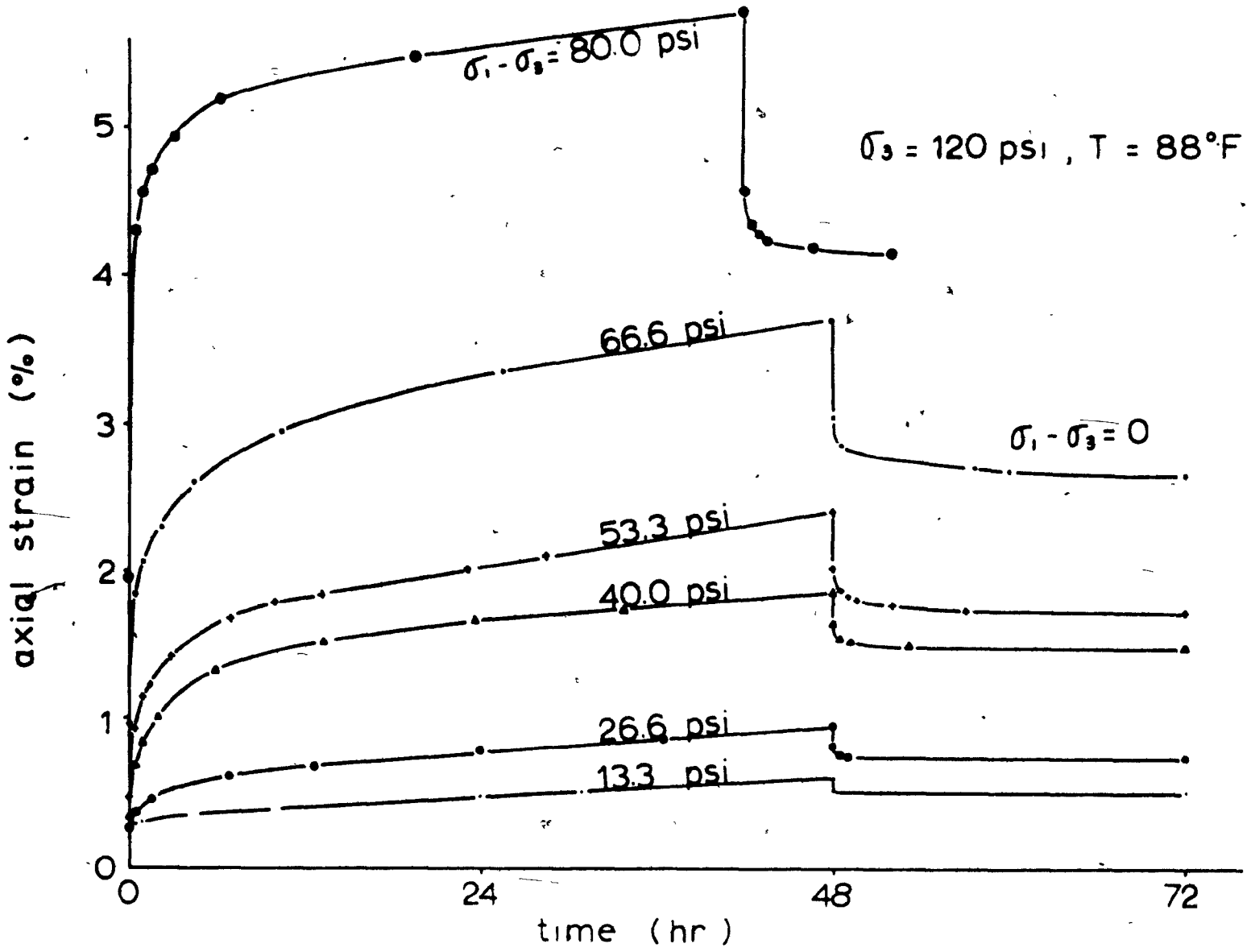

fig B-10 family of creep curves

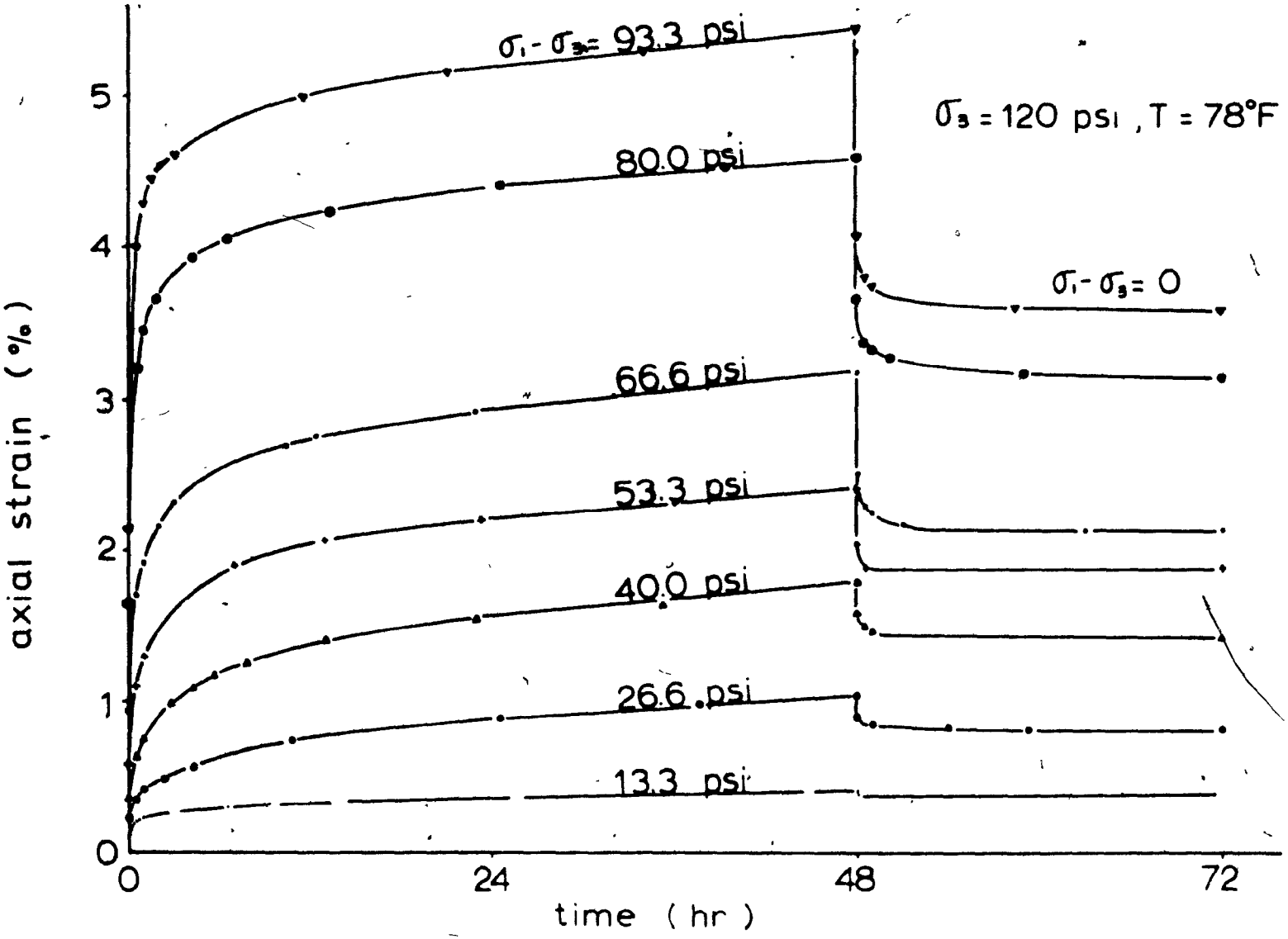

fig B-11 family of creep curves

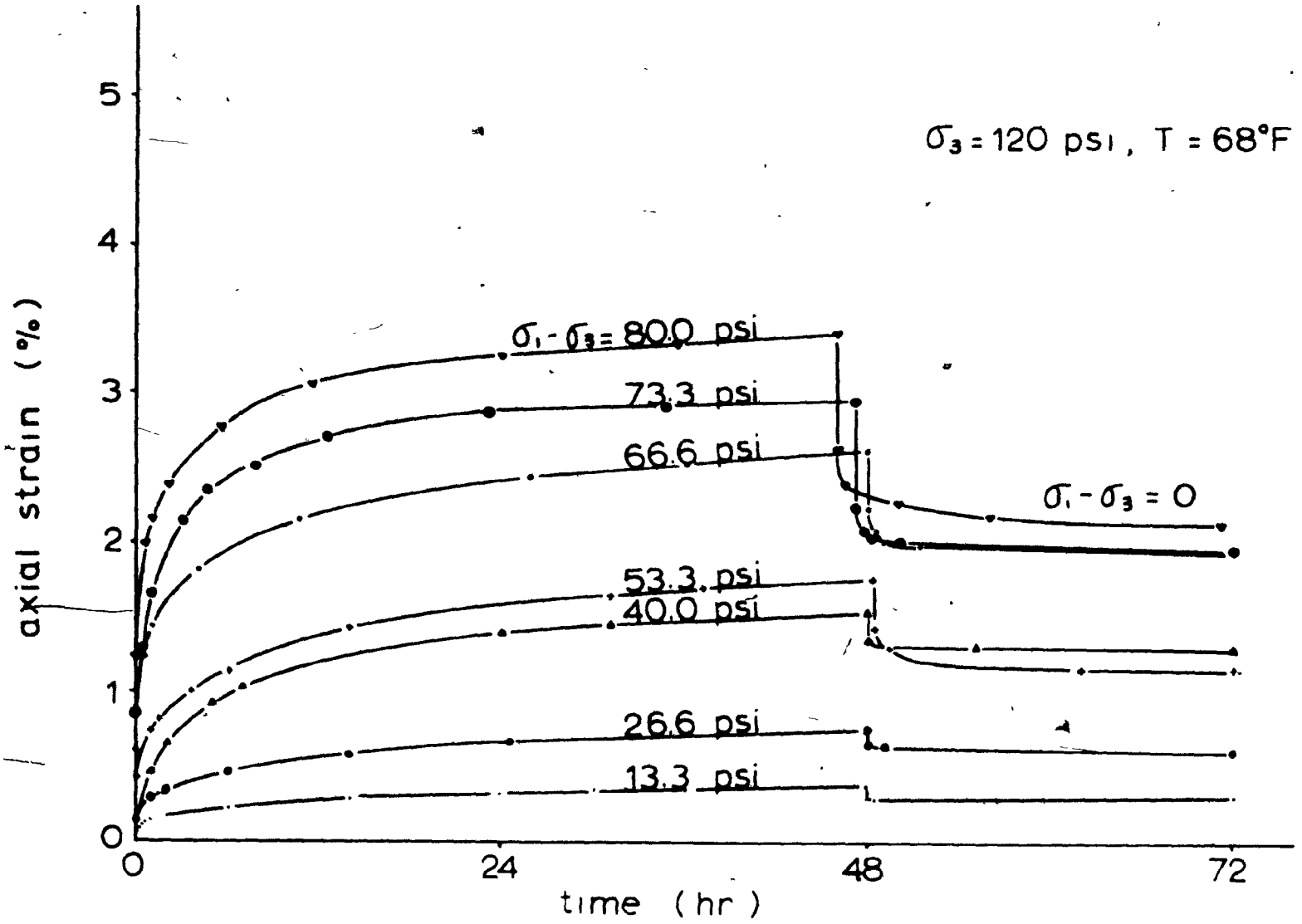

fig. B-12 family of creep curves

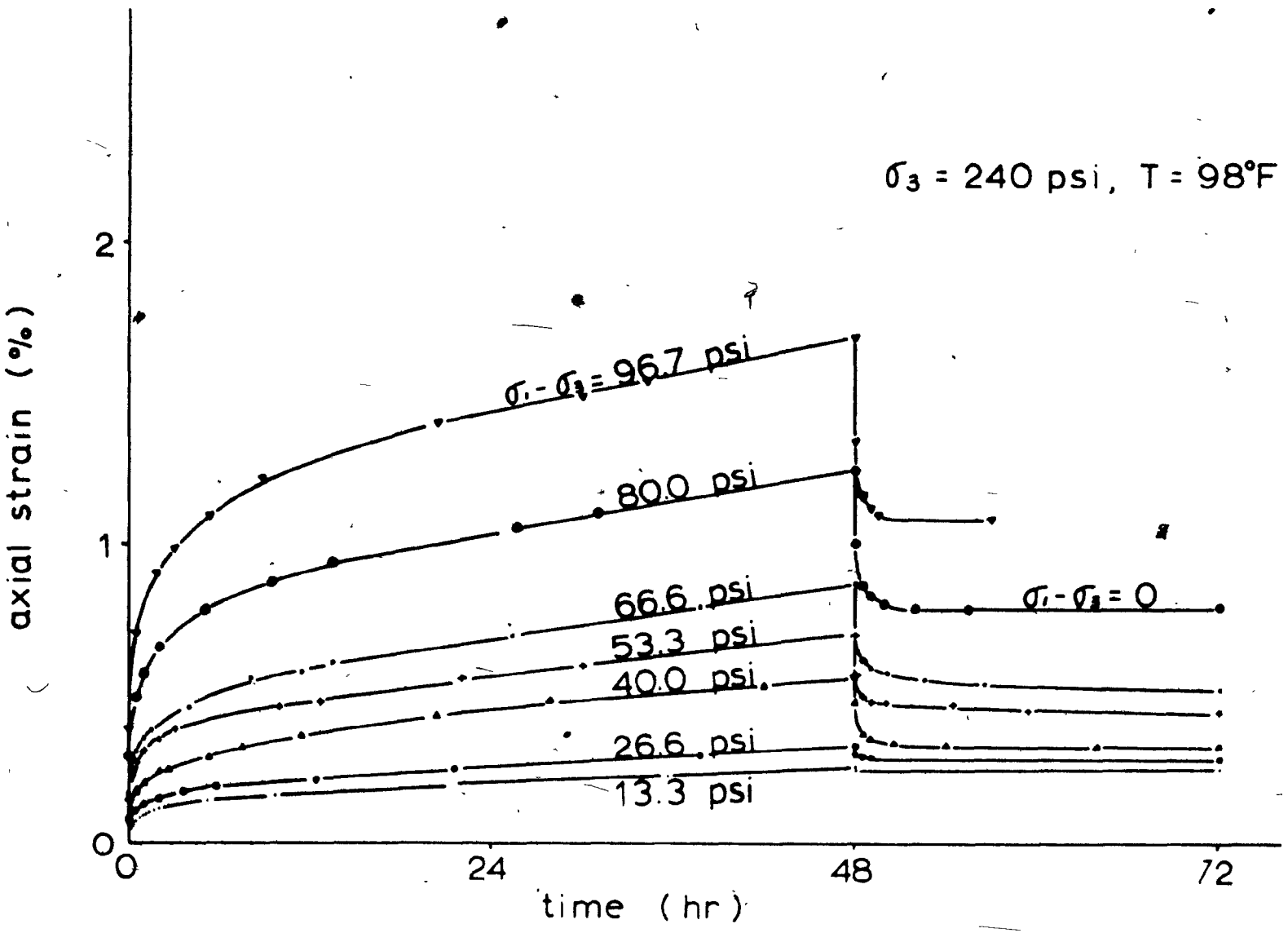

fig. B-13 family of creep curves

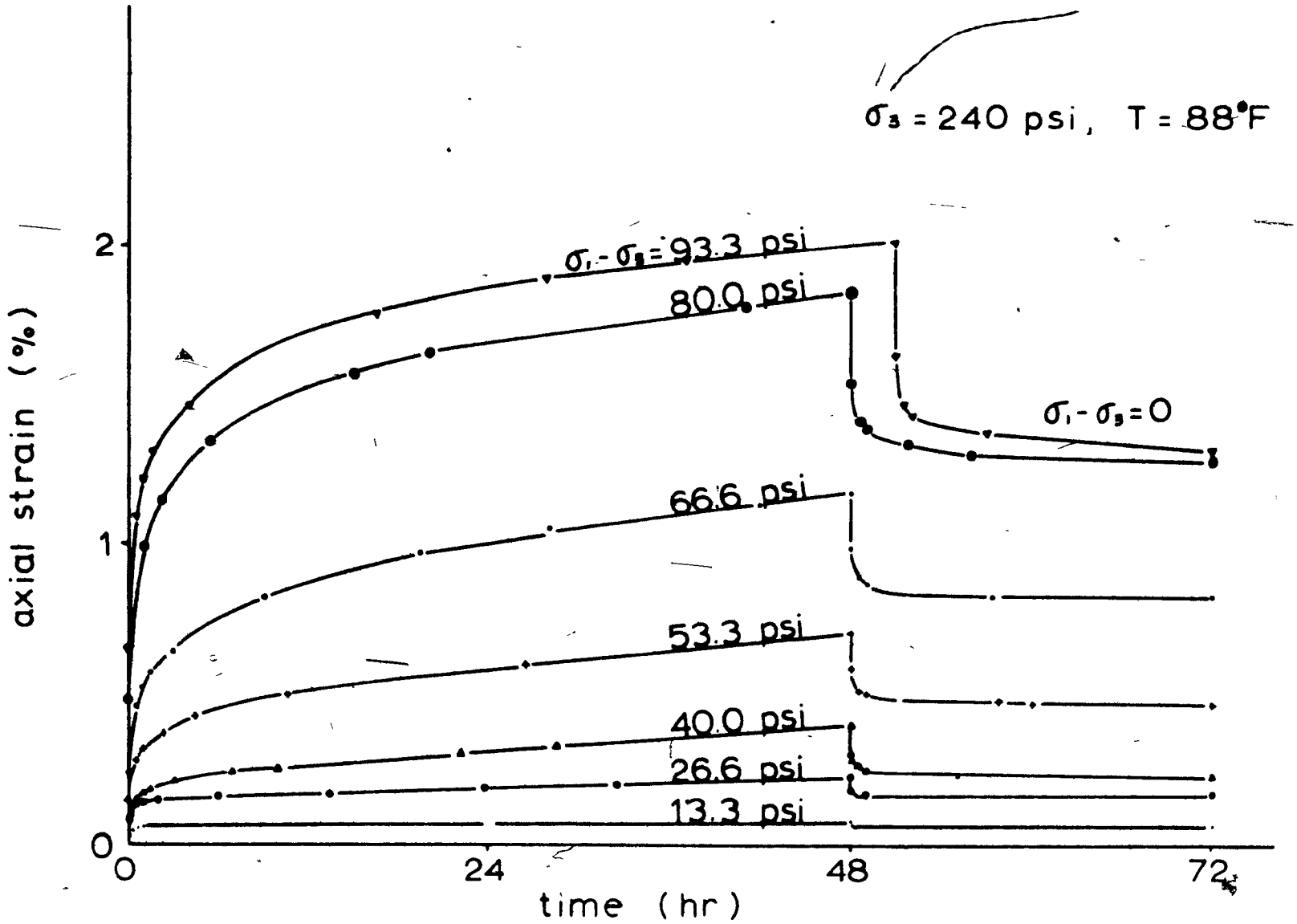

fig B-14 family of creep curves

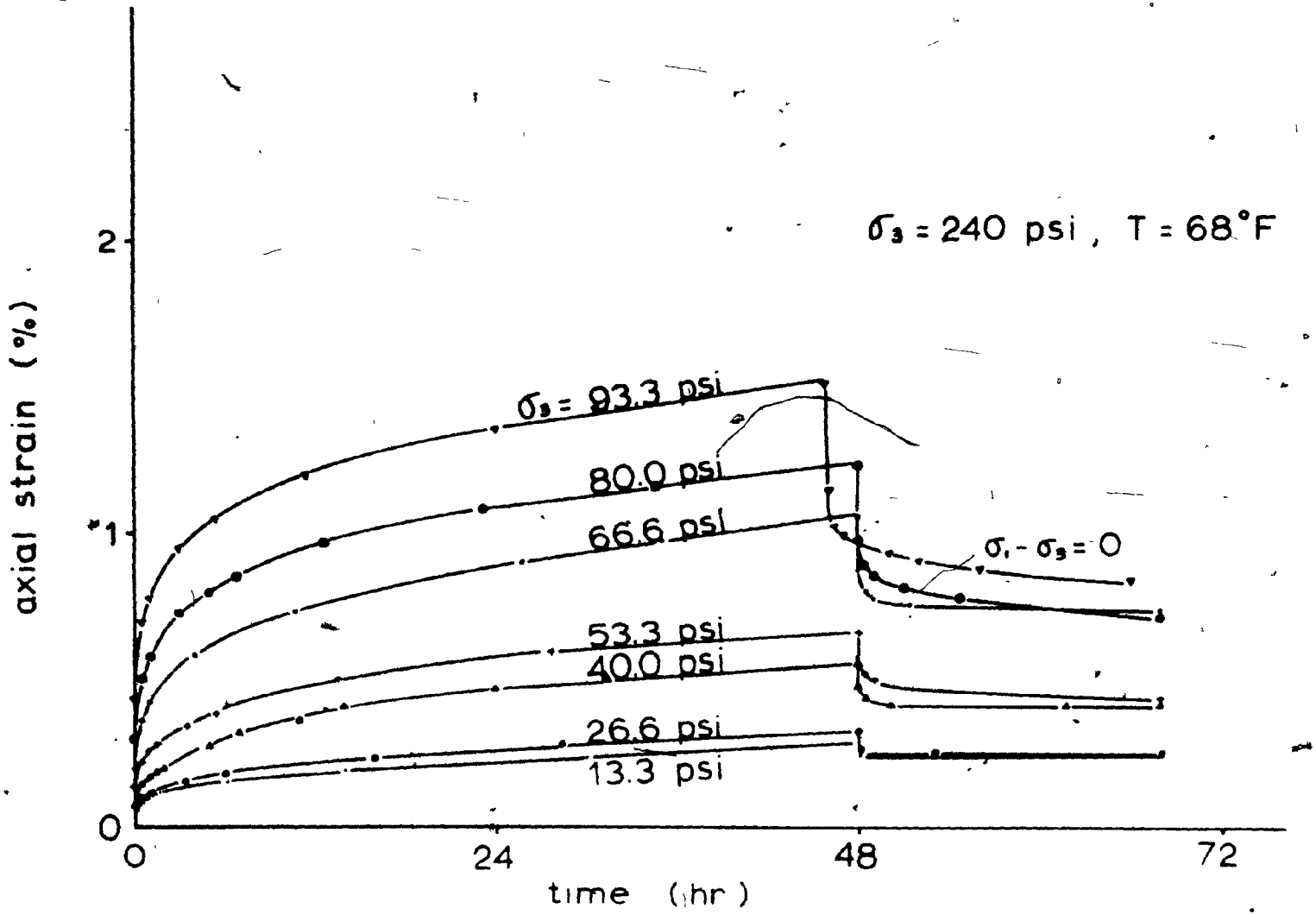

fig B-15 family of creep curves

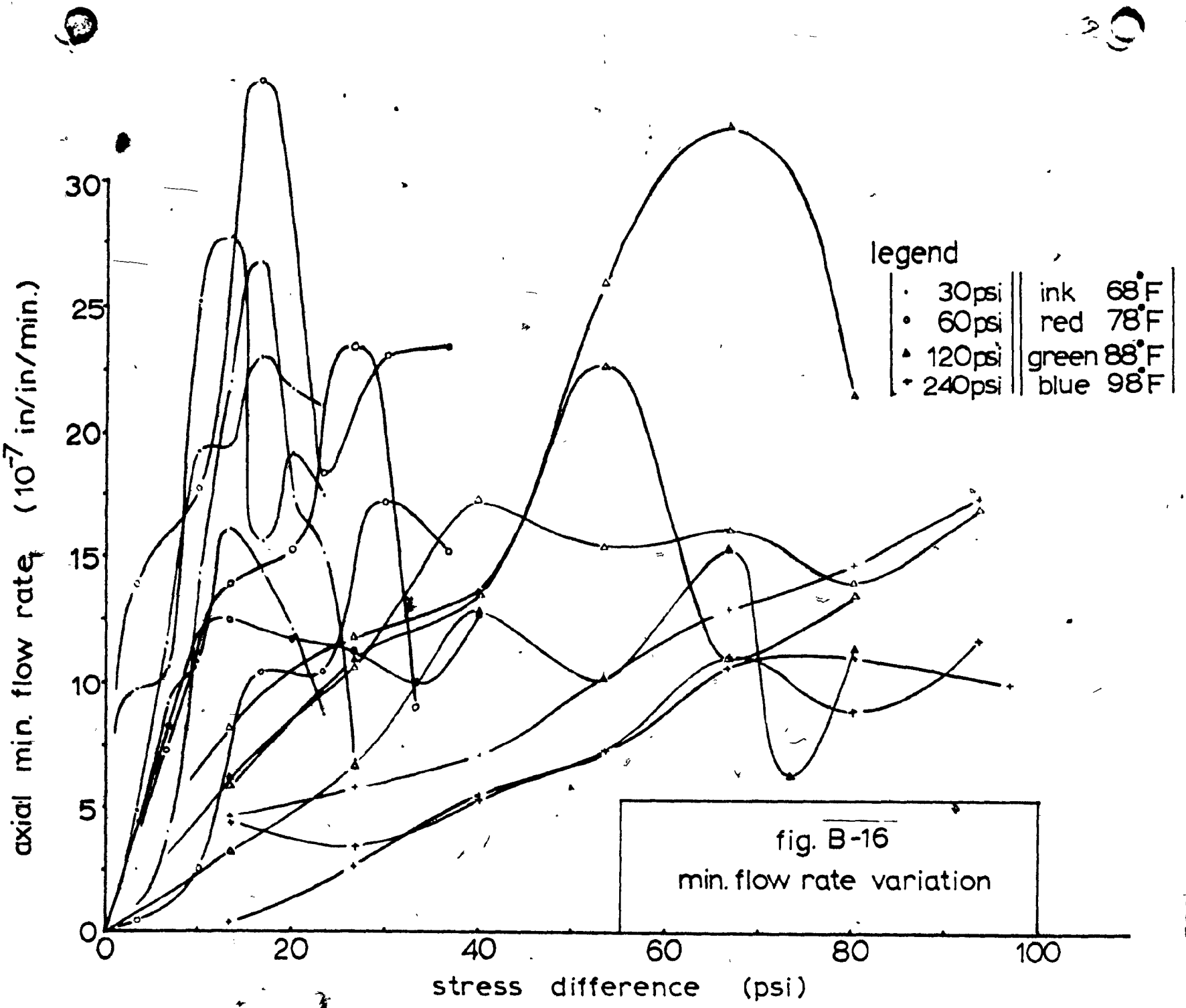

fig. B-16
min. flow rate variation

Table B-1

Unconfined Compressive Strength (psi)

temp	68°F	78°F	88°F	98°F	average
30 psi	30.0	28.0	24.5	26.5	27.25
60 psi	41.0	42.0	40.0	39.5	40.63
120 psi	90.0	115.0	115.0	105.0	106.25
240 psi	135.0	-	131.0	128.0	131.33

Table B-2

Final Water Content (%)

temp	68°F	78°F	88°F	98°F	average
30 psi	39.98	38.60	38.30	38.95	38.93
60 psi	33.40	33.90	34.00	33.13	33.61
120 psi	31.60	28.50	30.02	29.00	29.78
240 psi	26.65	-	27.52	26.60	26.92

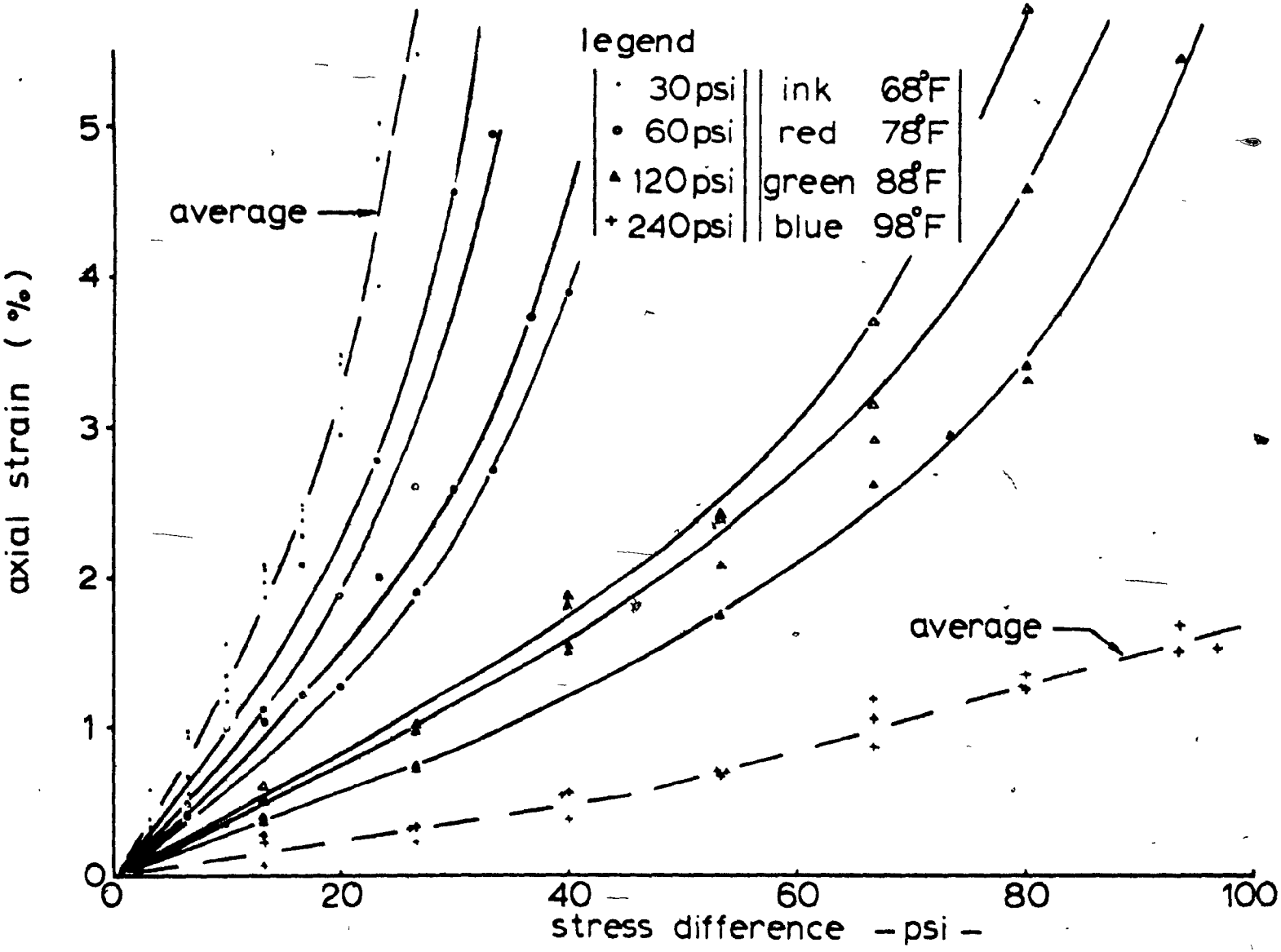

fig. B-17 stress-strain relations

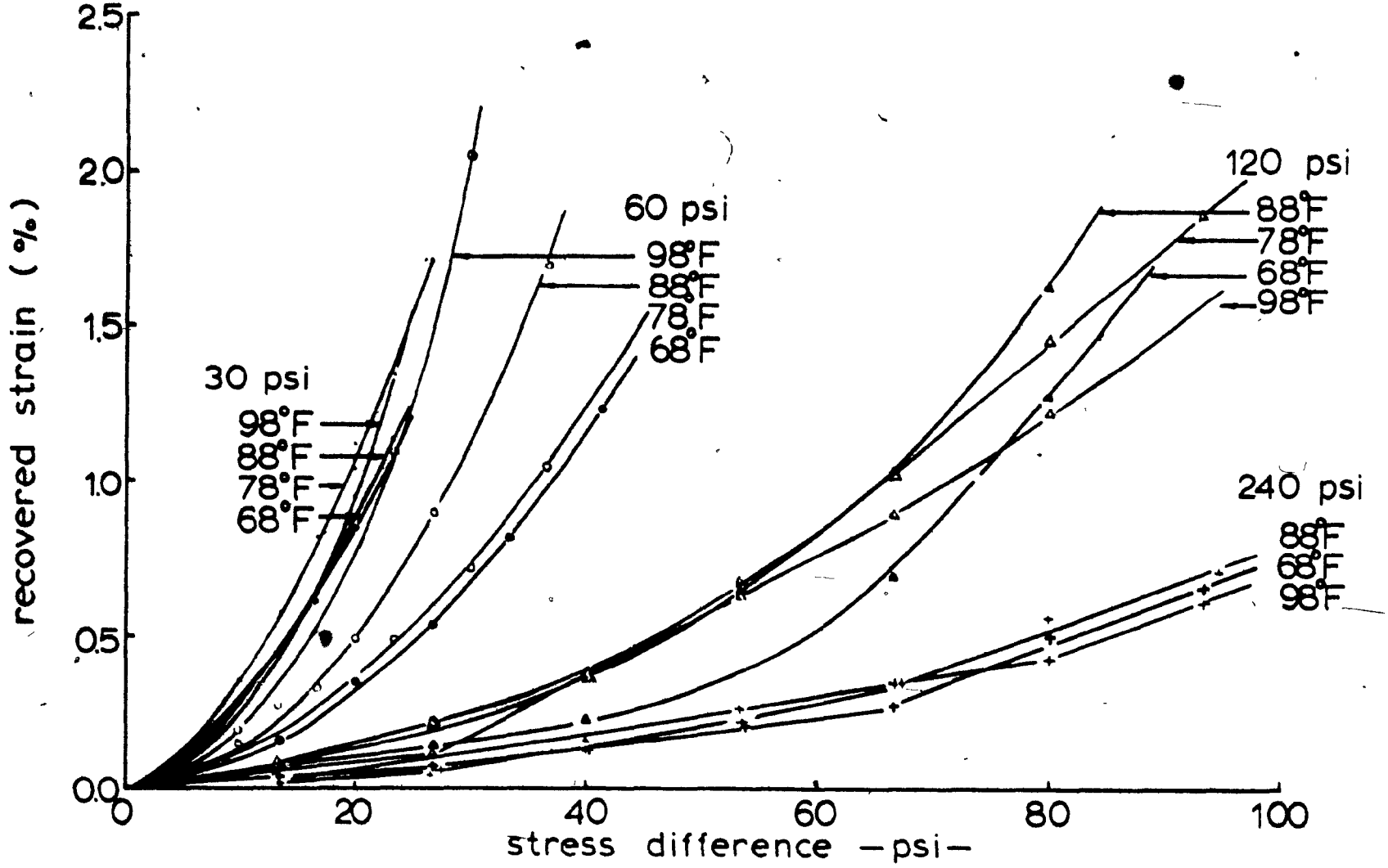

fig. B-18 recovered strain vs stress curves

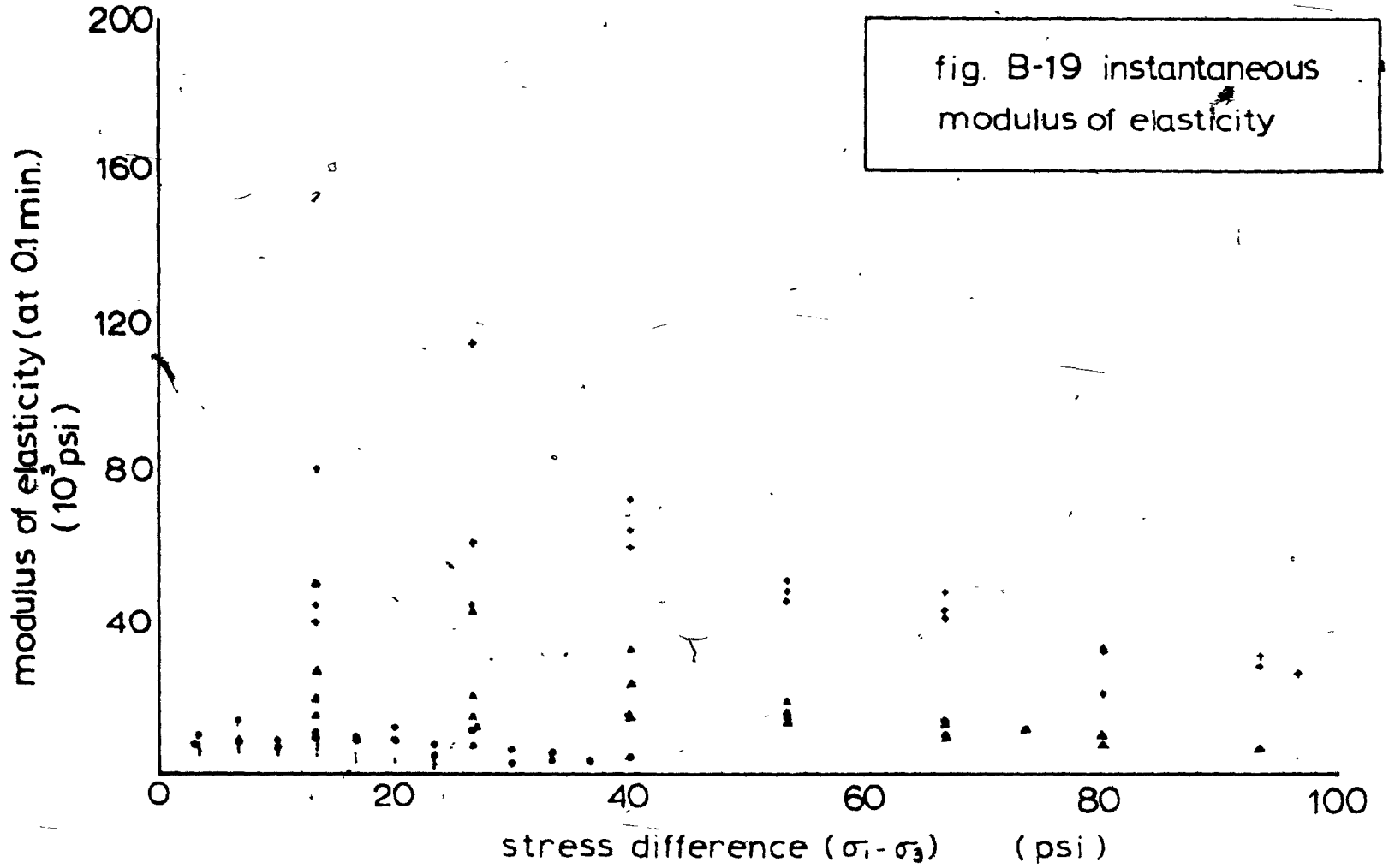

fig. B-19 instantaneous modulus of elasticity

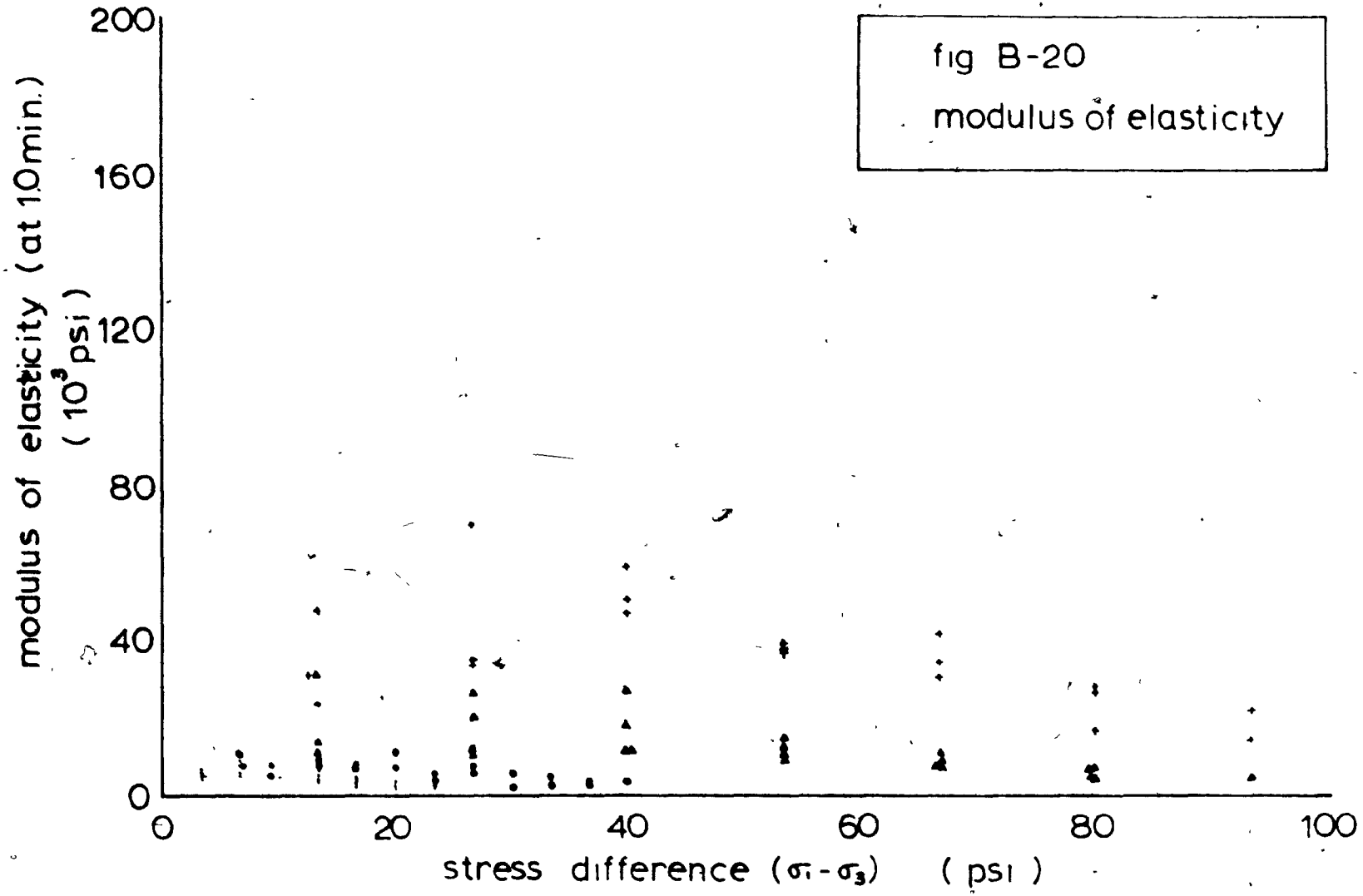

fig B-20
modulus of elasticity

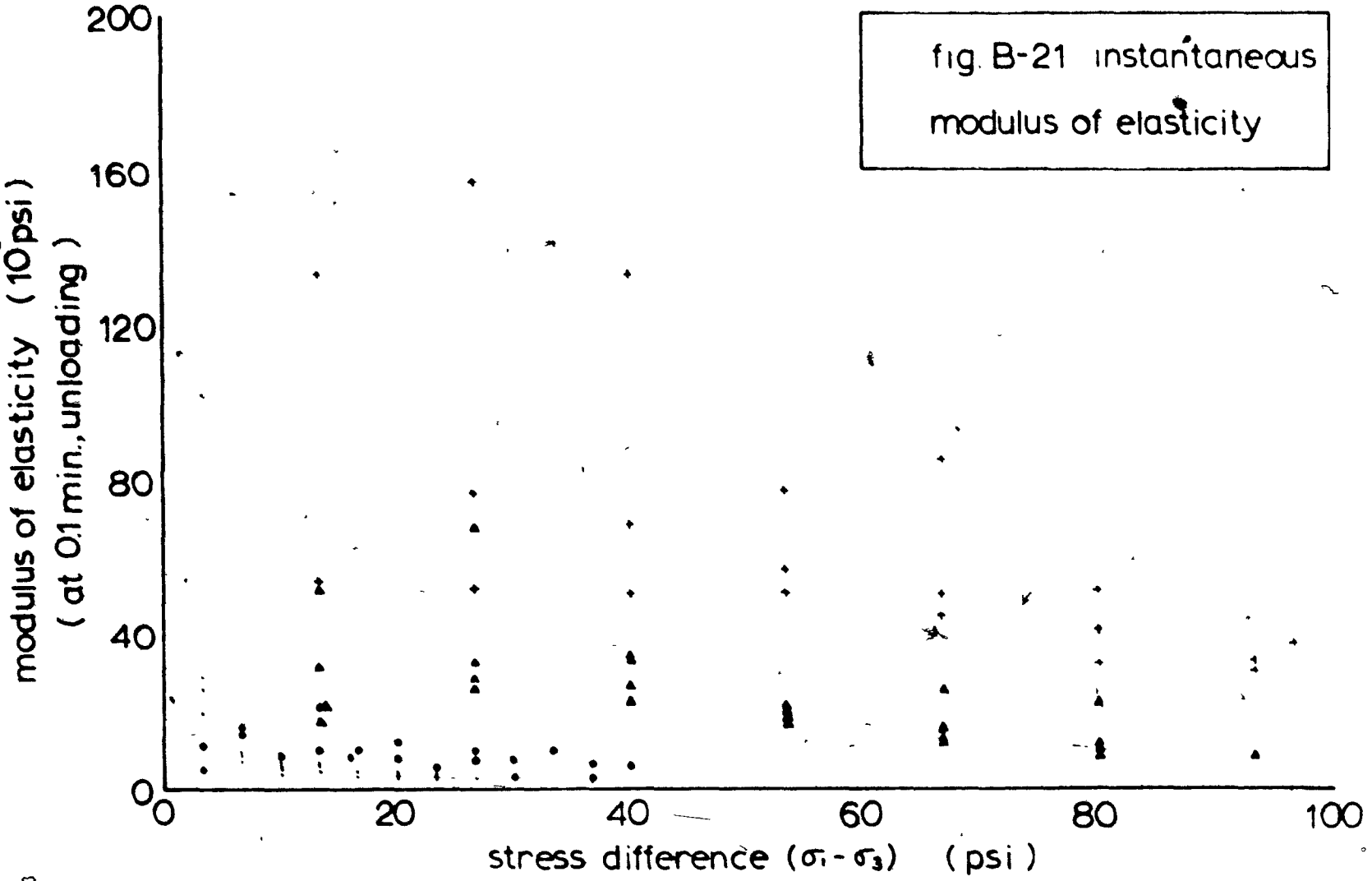

fig. B-21 instantaneous modulus of elasticity

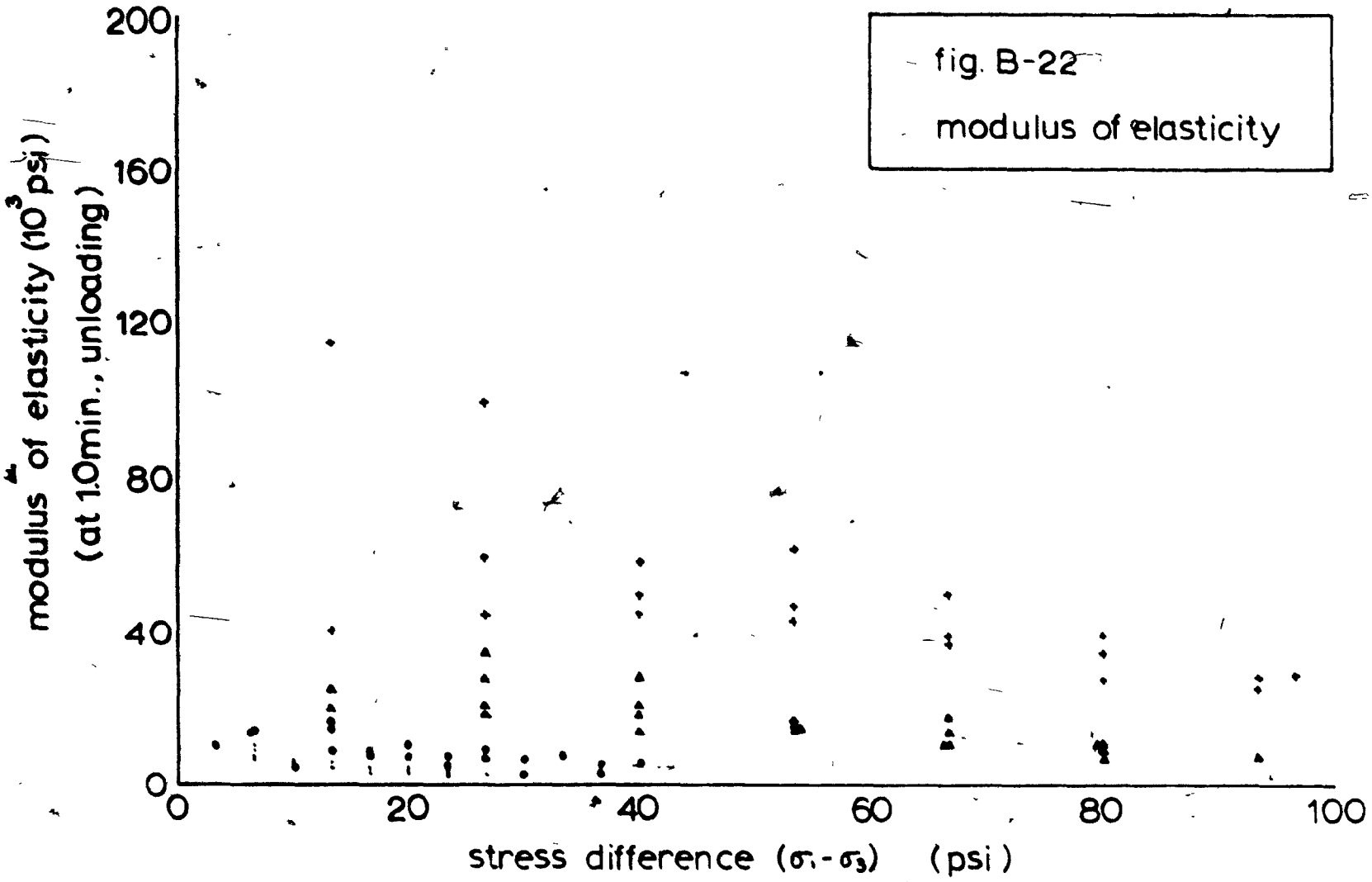
fig. B-22
modulus of elasticity
modulus of elasticity (10^3 psi)
(at 1.0min., unloading)
200
160
120
80
40
0
0
20
40
60
80
100
stress difference ($\sigma_1 - \sigma_3$) (psi)

B58

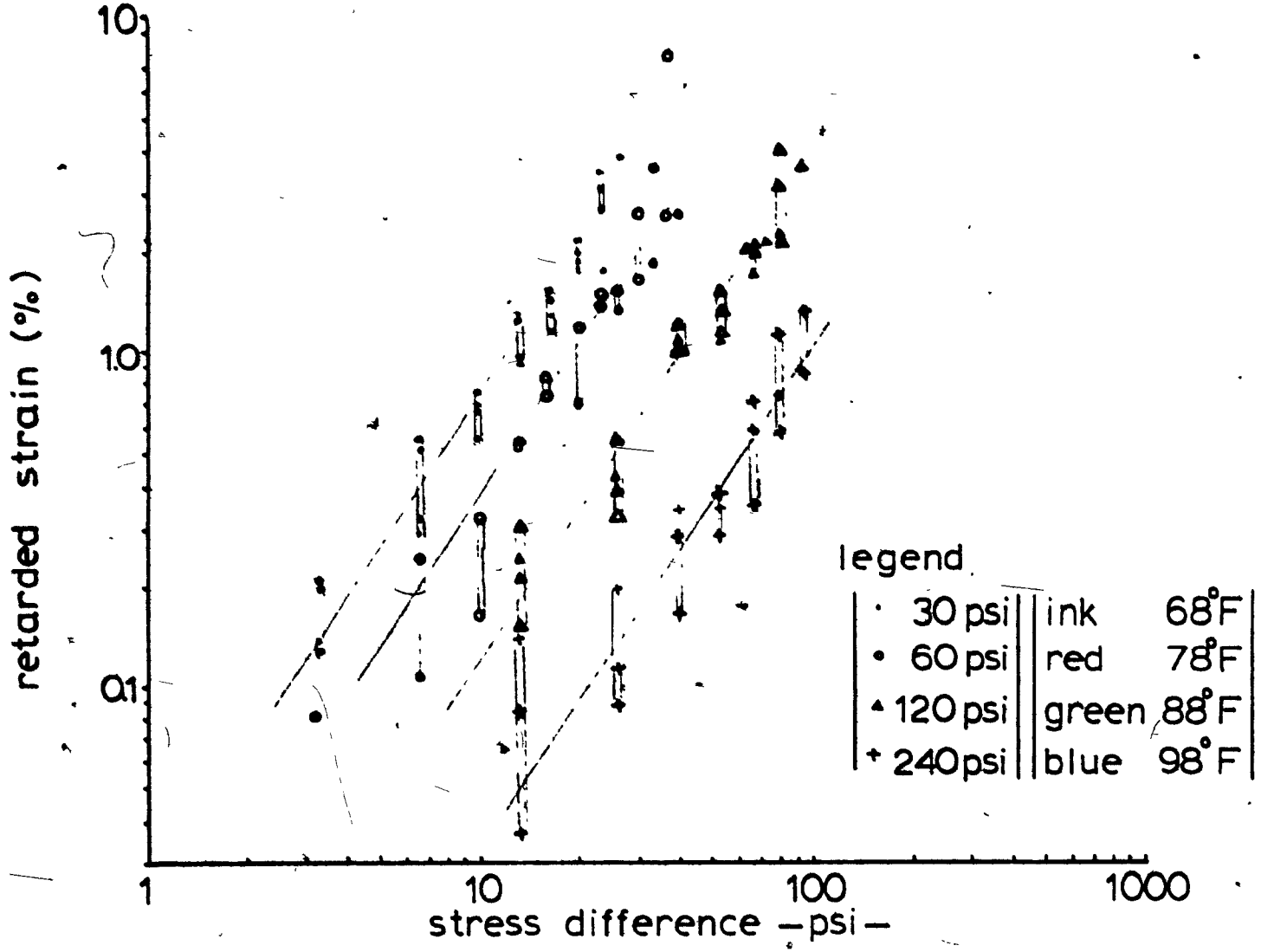

fig. B-23 relationship between stresses and retarded strain

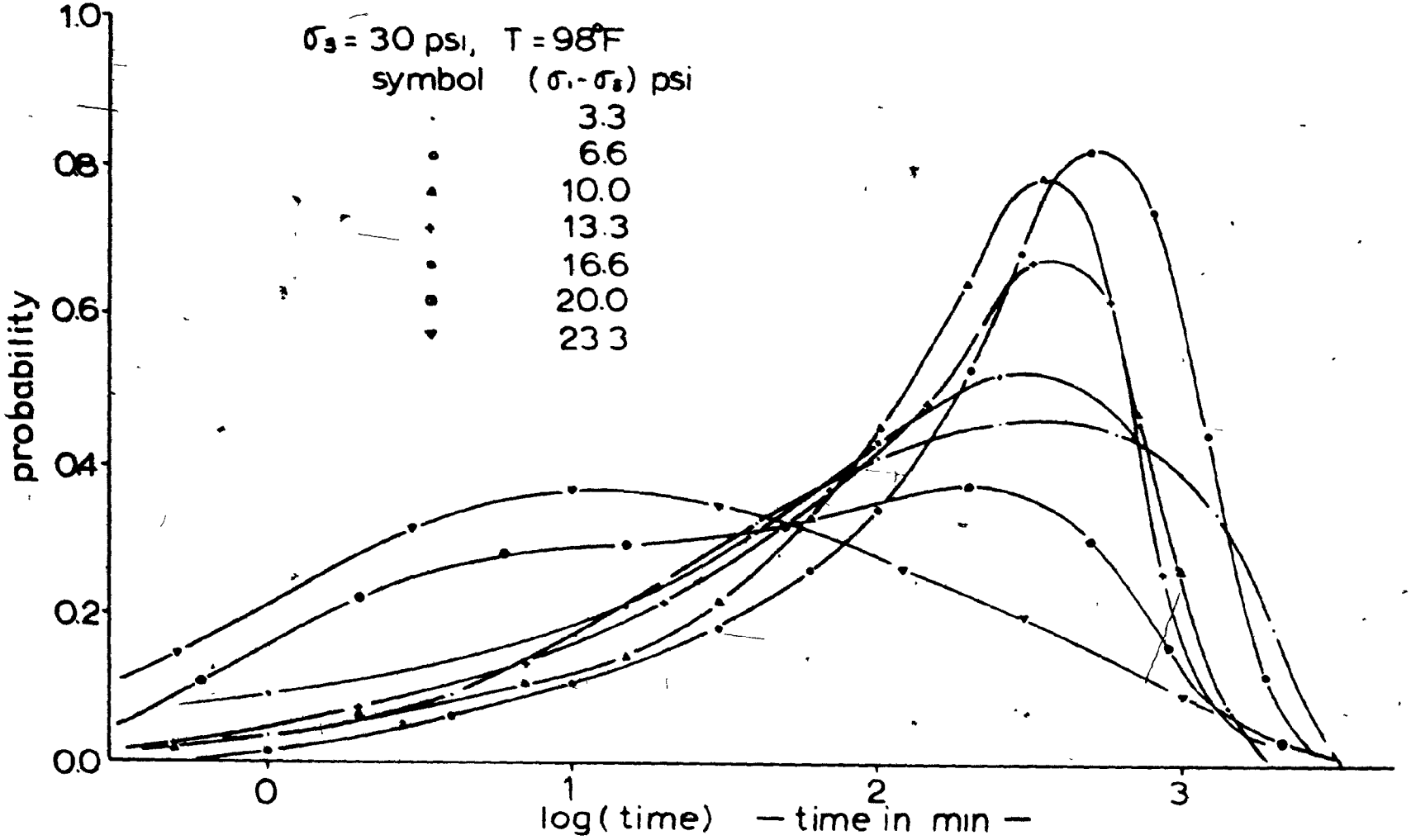

B60

fig. B-24 probability distribution curves

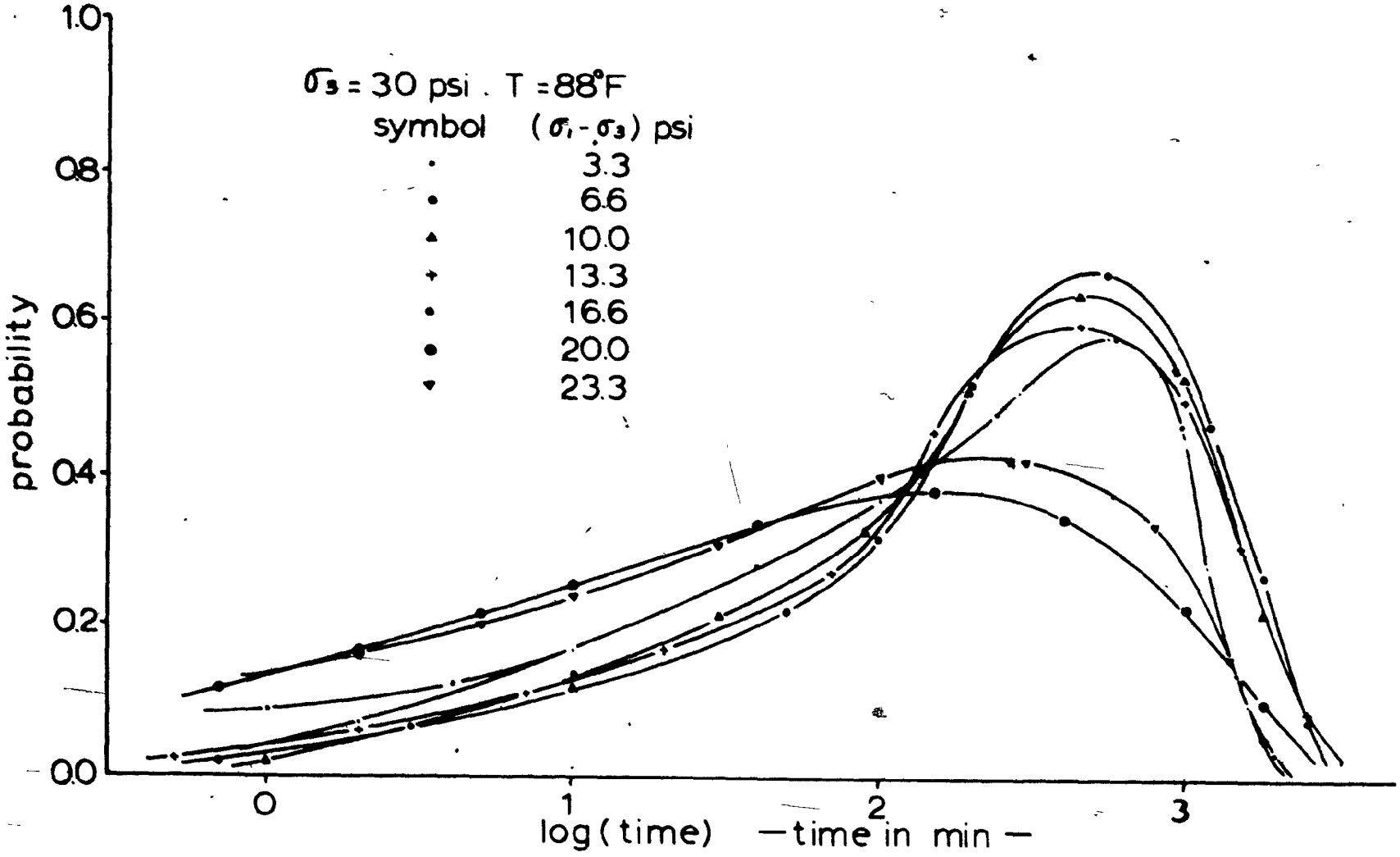

fig. B-25 probability distribution curves

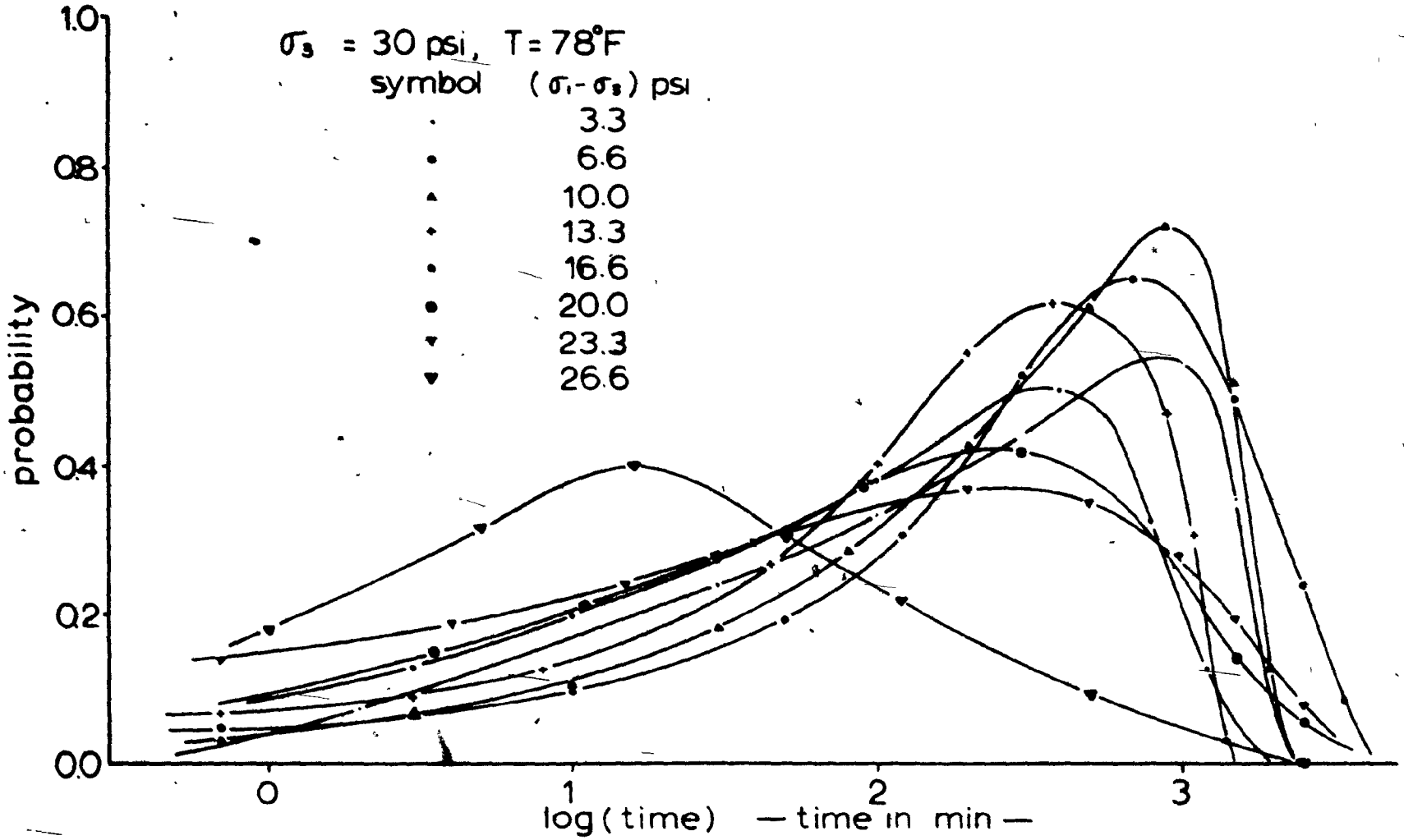

fig. B-26 probability distribution curves

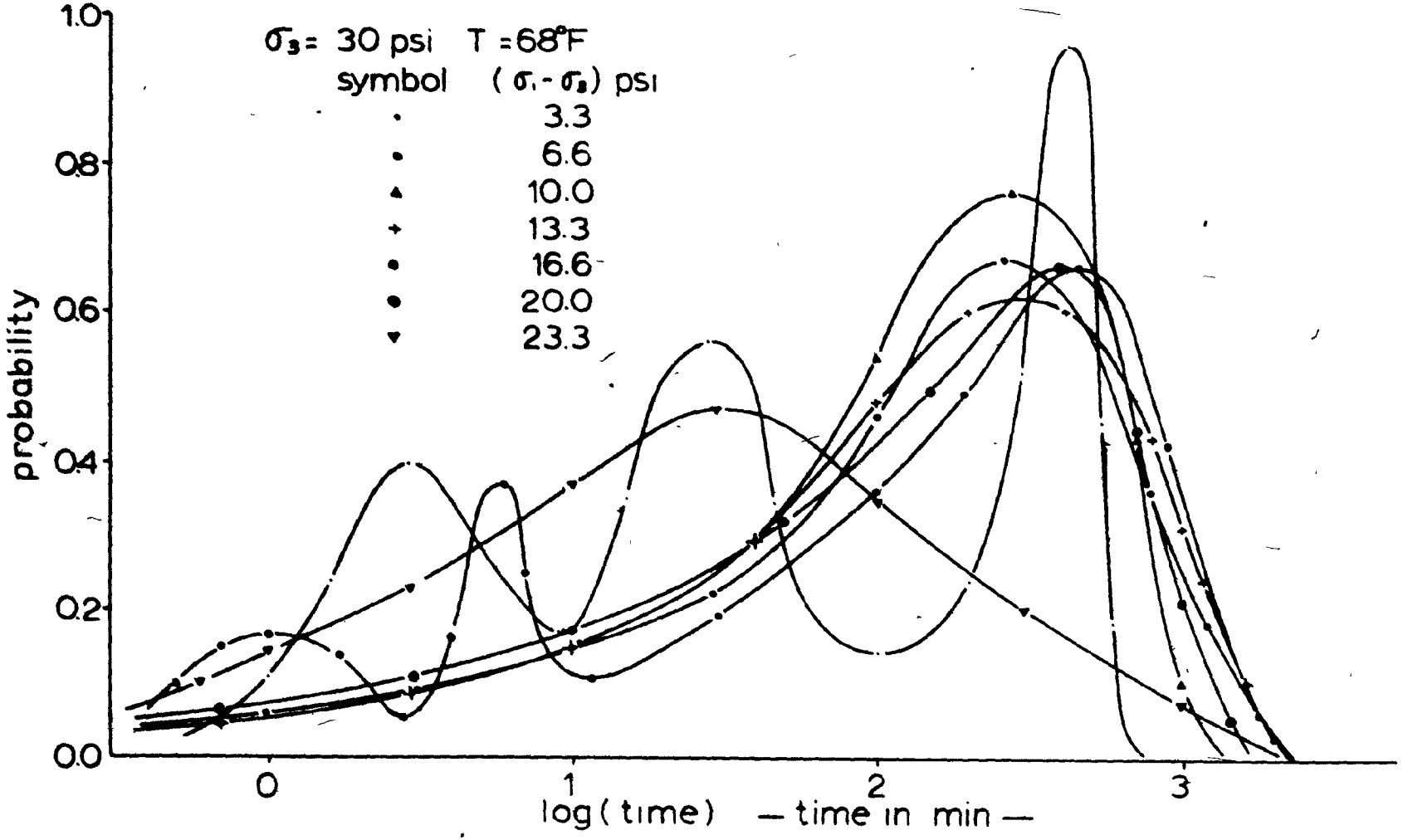

fig. B-27 probability distribution curves

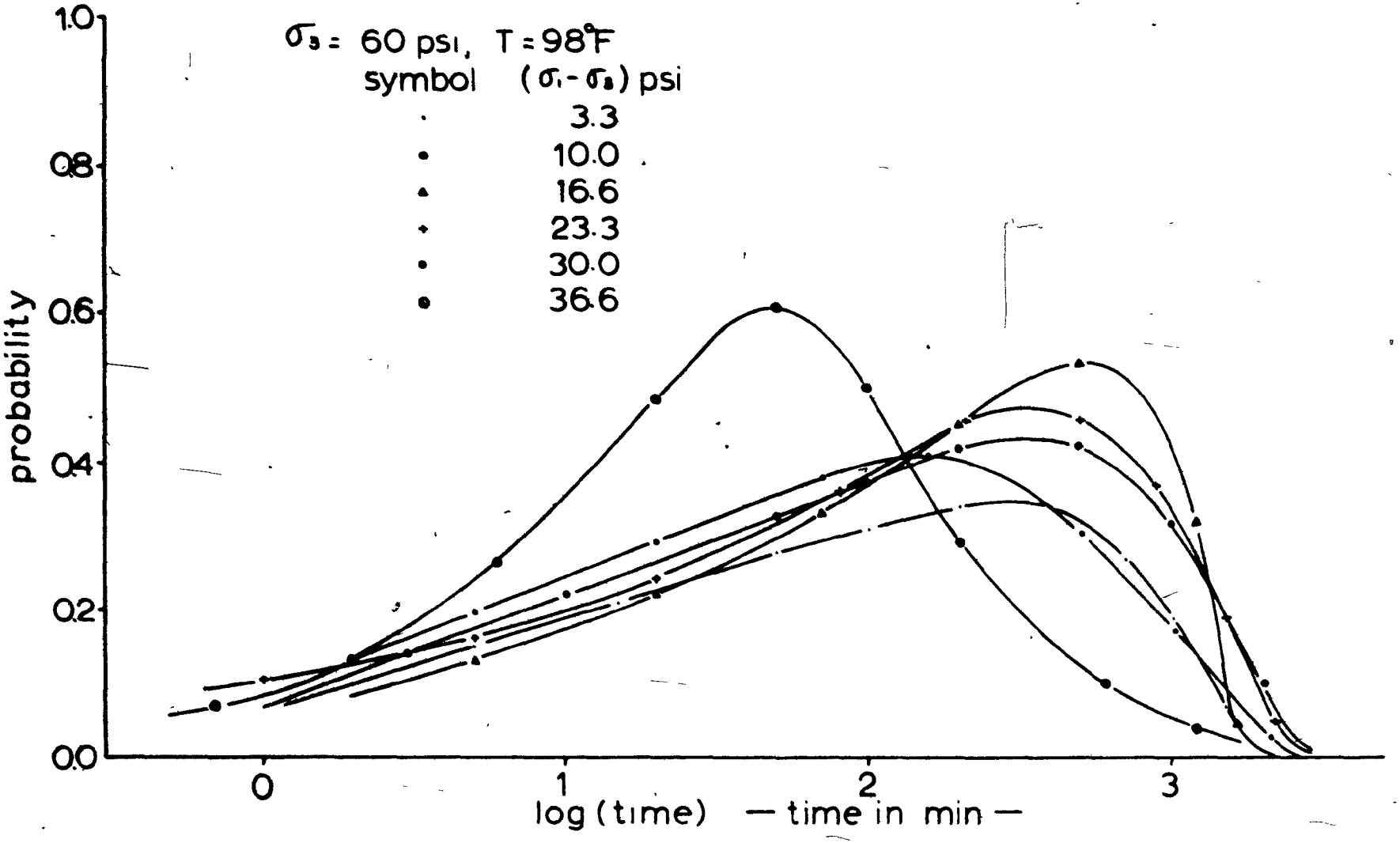

fig B-28 probability distribution curves

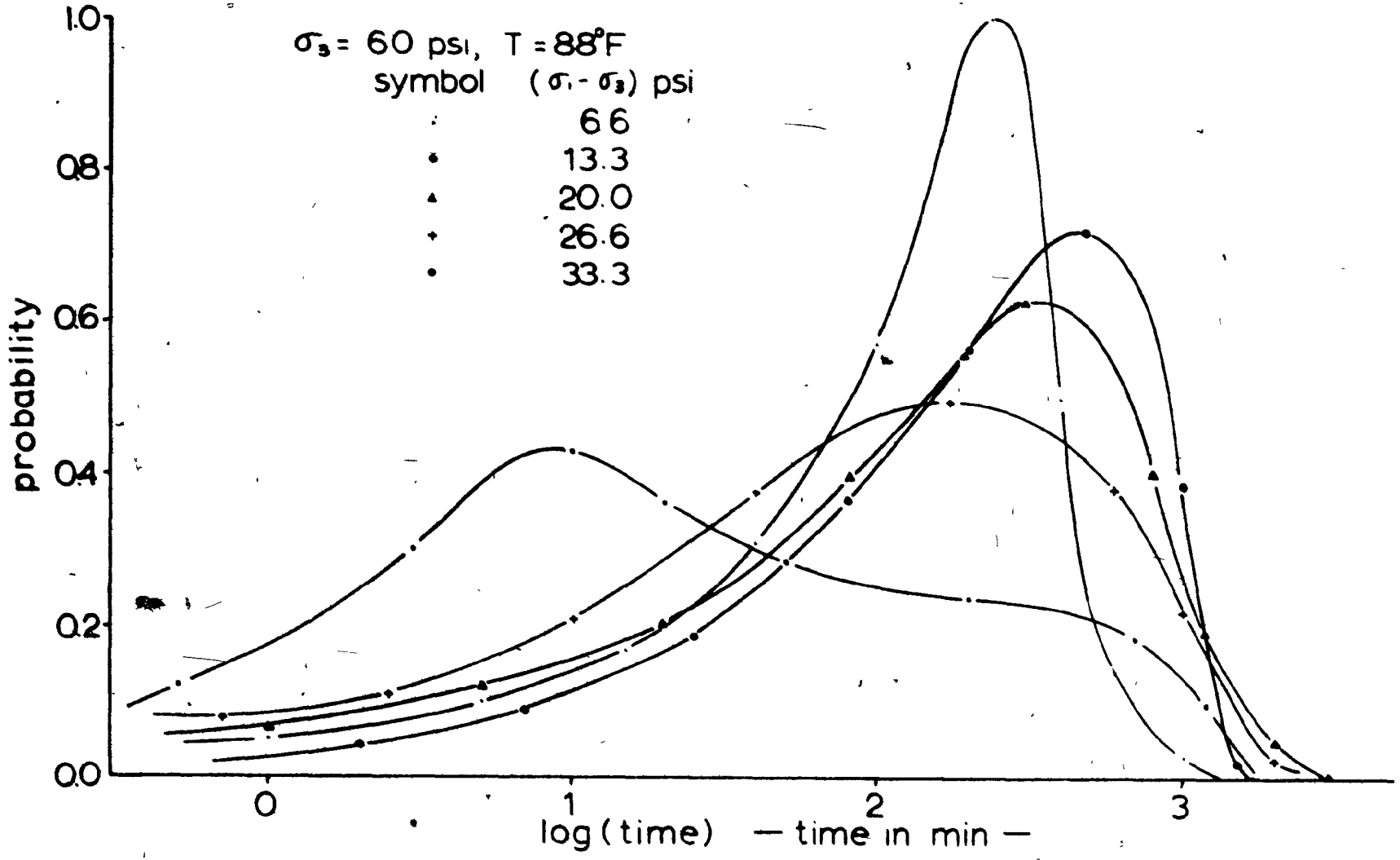

B65

fig. B-29 probability distribution curves

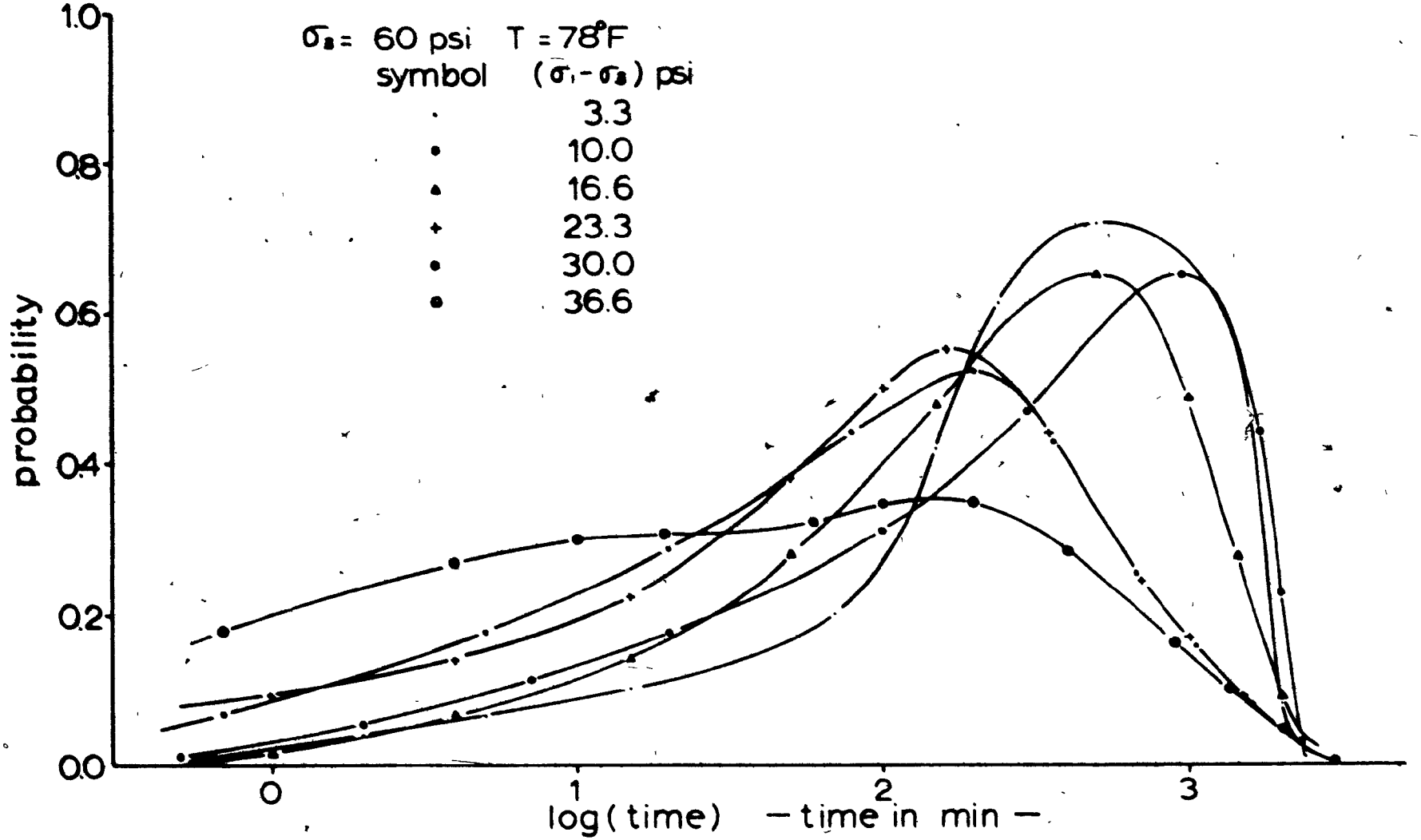

B66

fig B-30 probability distribution curves

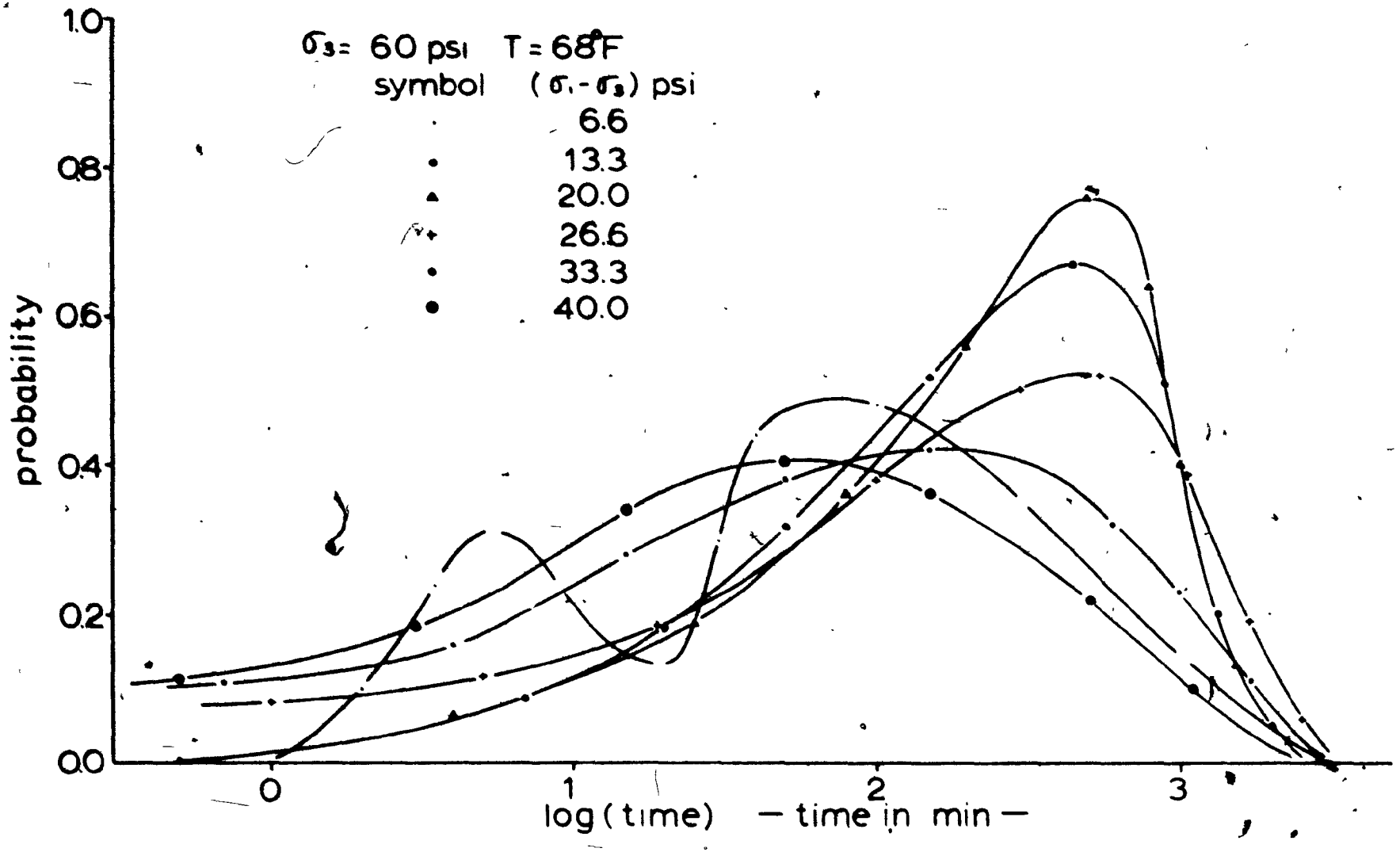

fig B-31 probability distribution curves

B67

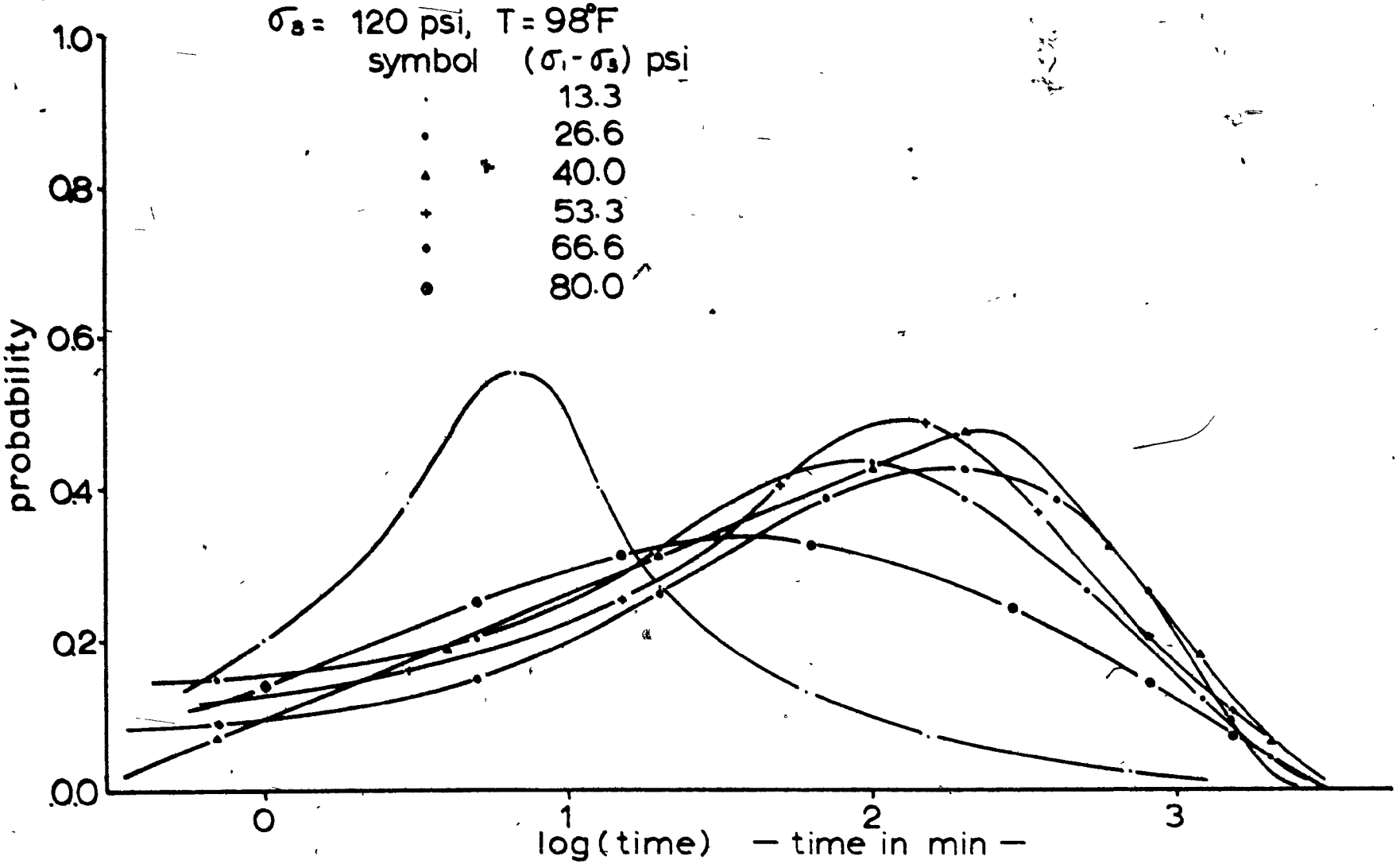

fig. B-32 probability distribution curves

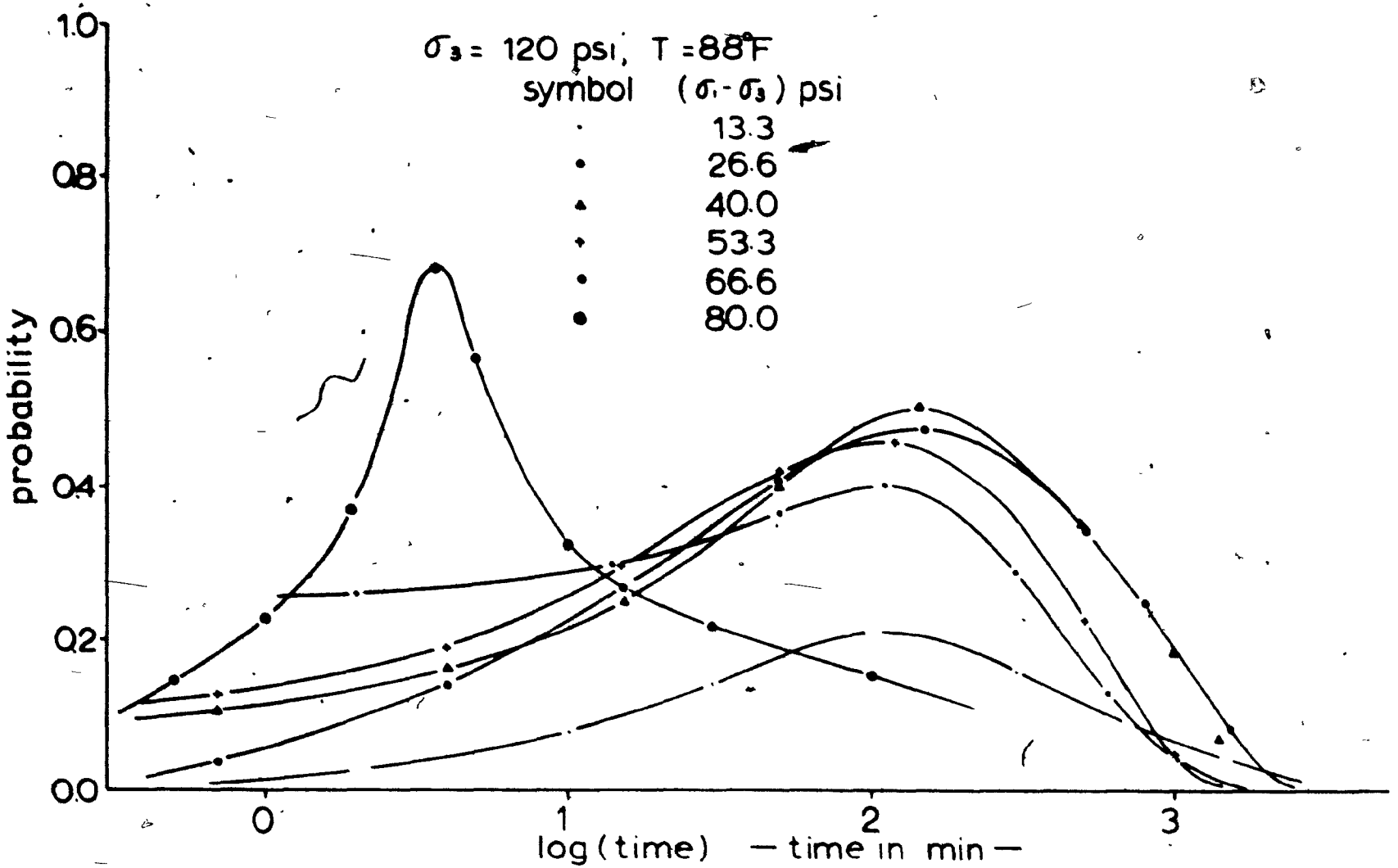

fig. B-33 probability distribution curves

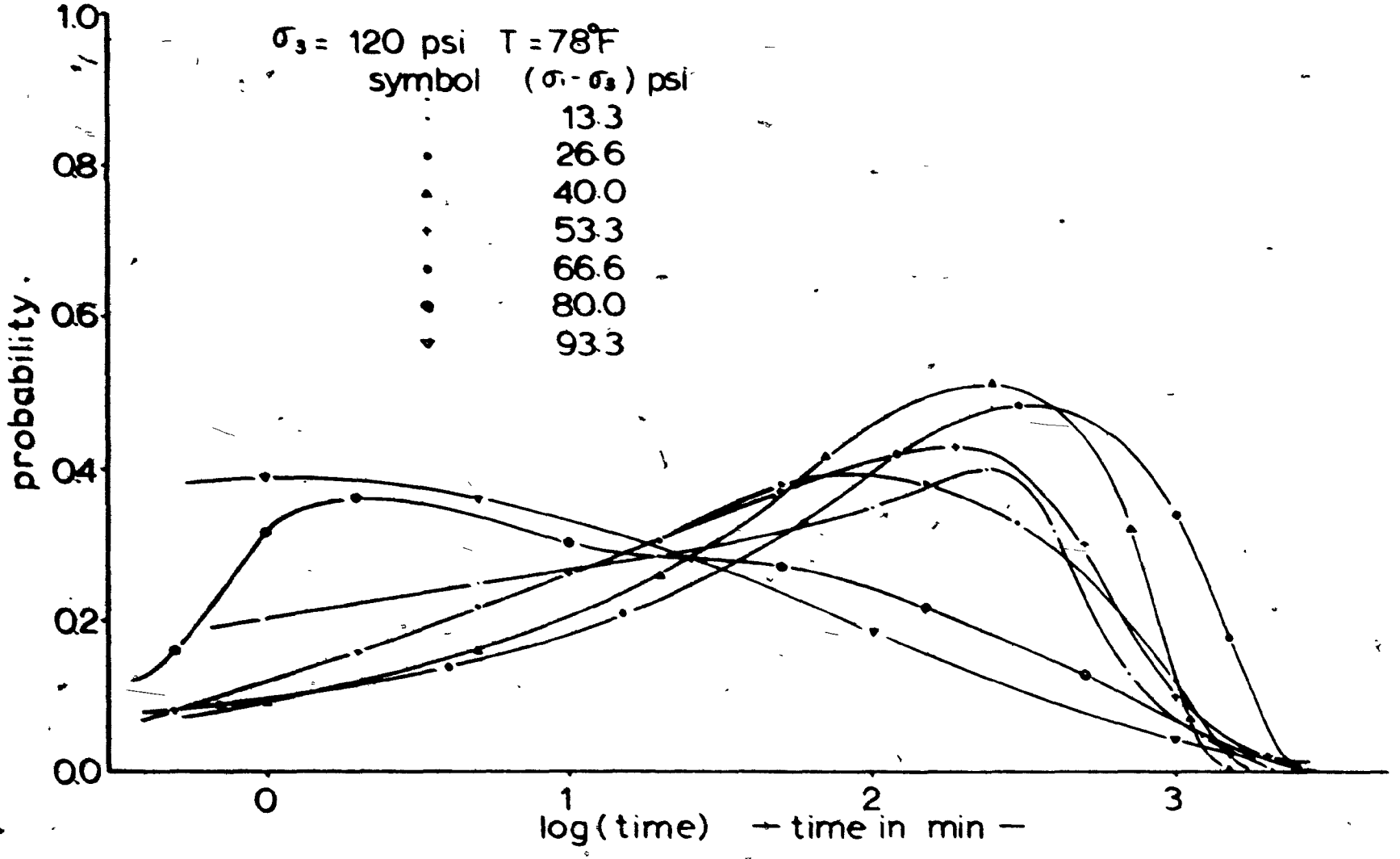

B70

fig. B-34 probability distribution curves

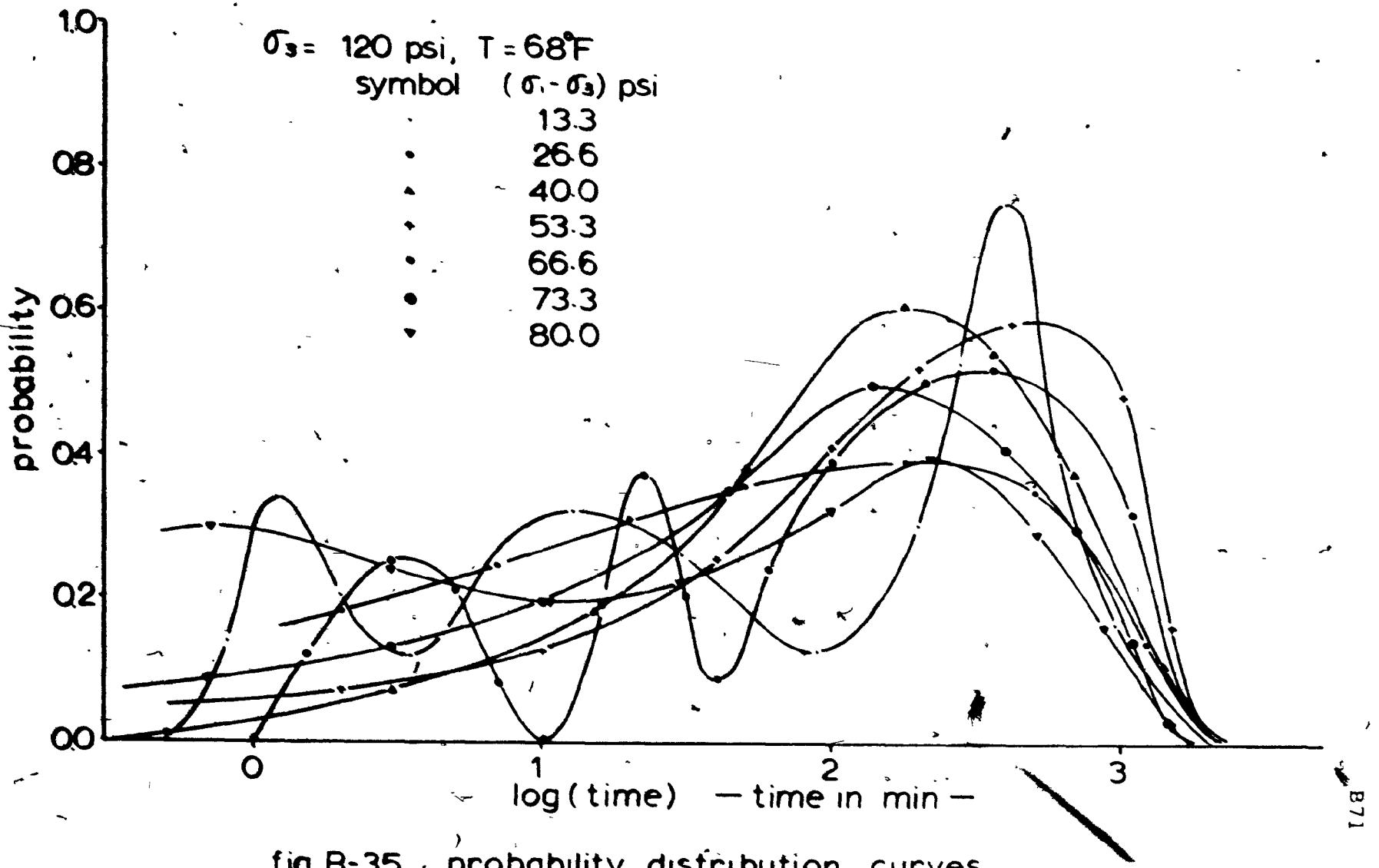

fig B-35 · probability distribution curves

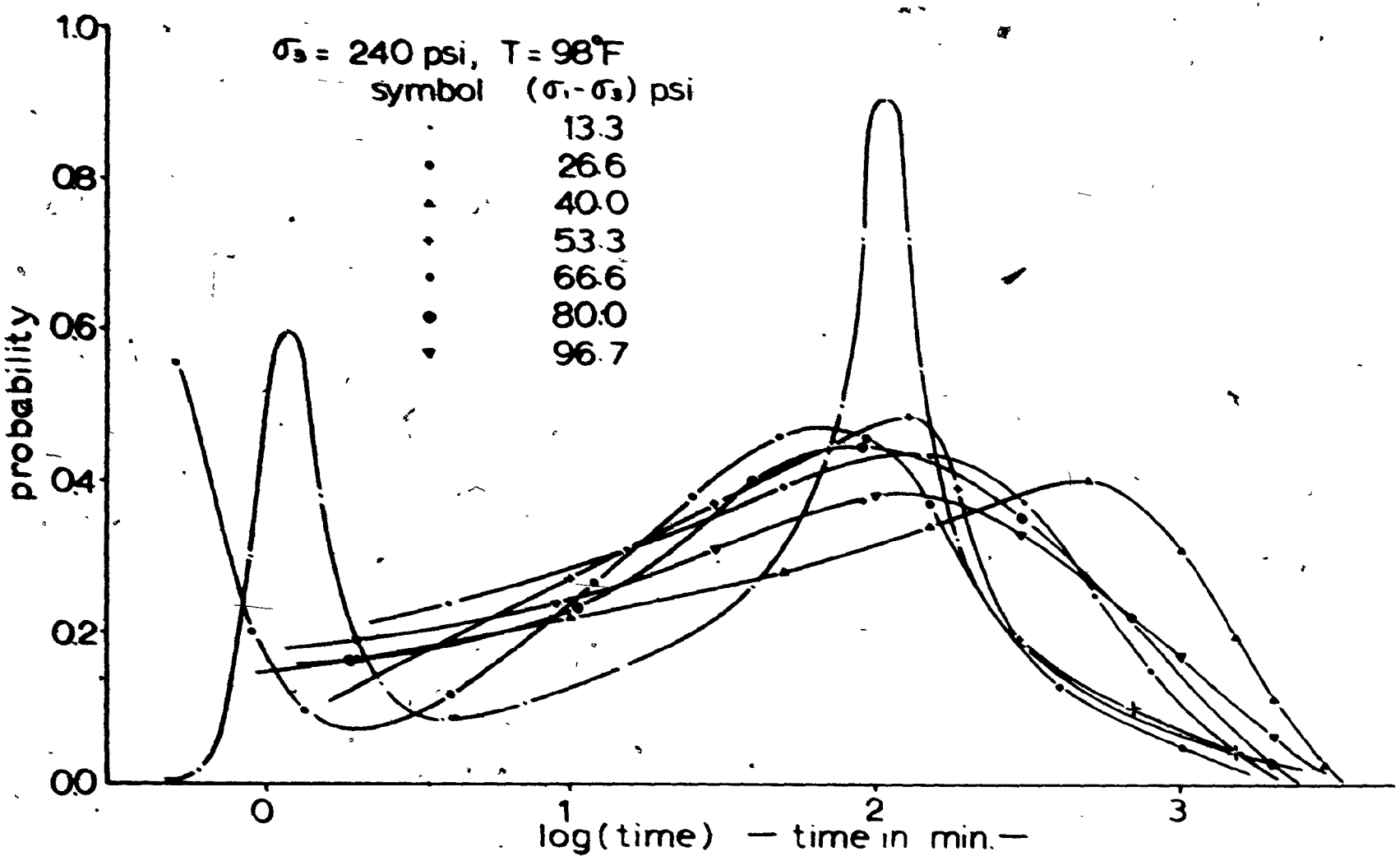

fig. B-36 probability distribution curves

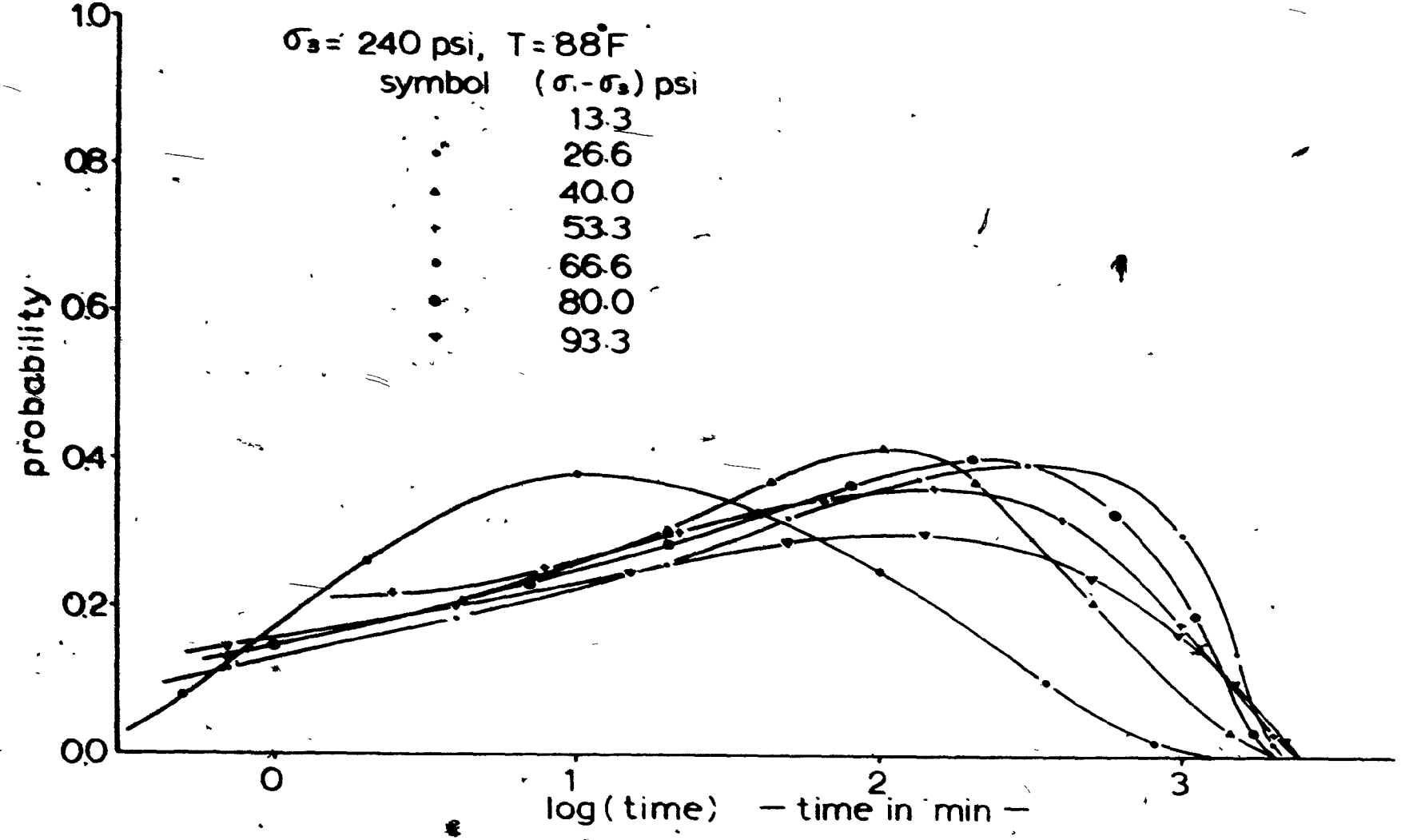

fig. B-37 probability distribution curves

B73

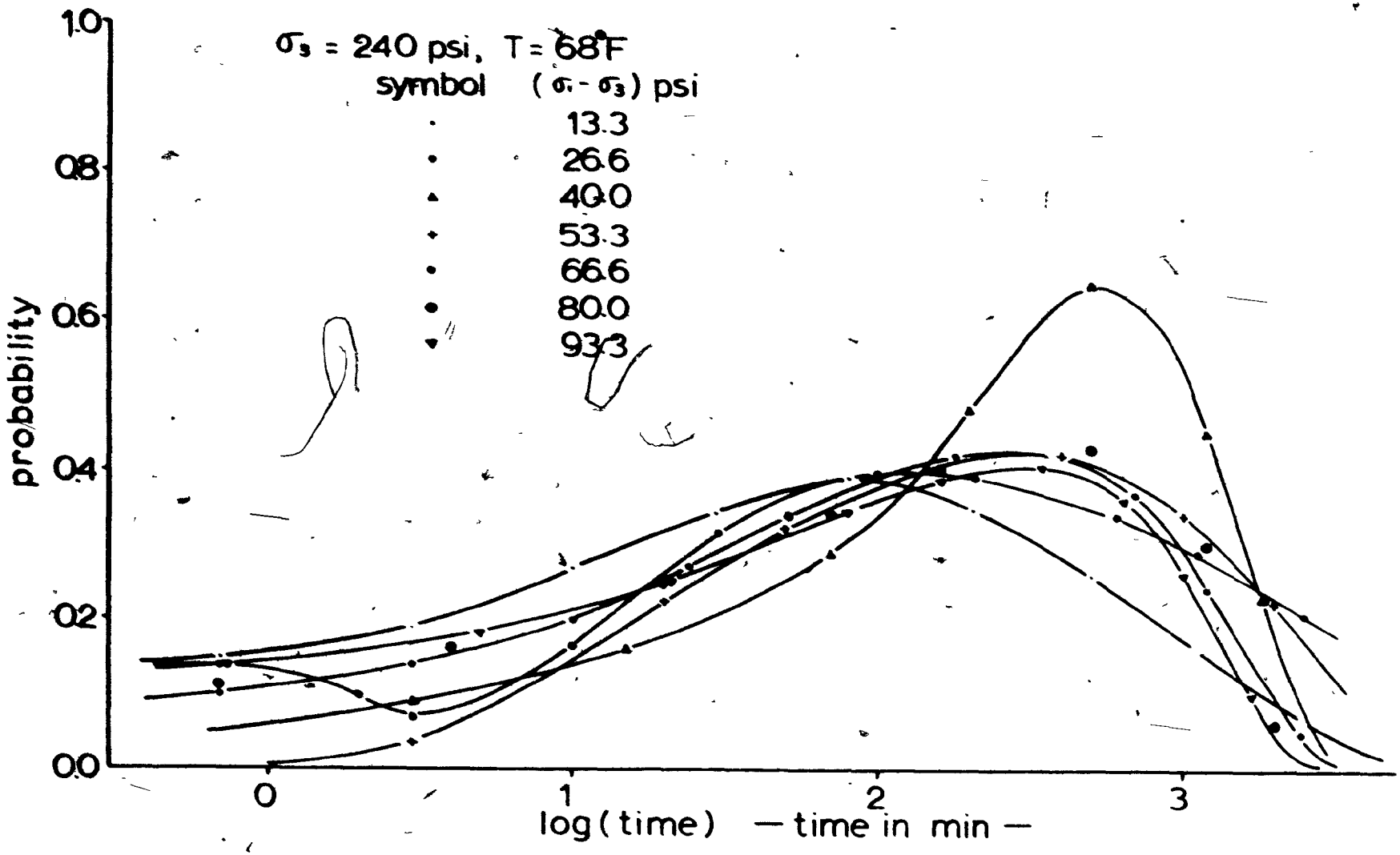

fig B-38 probability distribution curves

Table B-3a Properties of Probability Distribution Curves

Temp.	σ_3 = 30 psi: $\sigma-\sigma_3$	mode	median	mean	σ	τ	P_f	σ_3 = 60 psi: $\sigma-\sigma_3$	mode	median	mean	σ	τ	P_f
98°F	3.3	2.544	2.117	1.914	0.920	2.422	0.455	3.3	2.477	1.447	1.699	--	1.914	0.300
	6.6	2.724	2.477	2.352	0.660	2.648	0.810	10.0	2.532	1.857	1.778	1.103	2.230	0.405
	10.0	2.544	2.279	2.146	0.680	2.459	0.765	16.6	2.724	2.107	1.793	0.950	2.398	0.480
	13.3	2.544	2.155	1.973	0.815	2.380	0.610	23.3	2.518	2.000	1.732	1.150	2.312	0.450
	16.6	2.492	2.000	1.756	0.970	2.274	0.500	30.0	2.176	1.677	1.432	1.115	2.021	0.400
	20.0	2.301	1.512	1.301	1.190	1.914	0.340	36.6	1.682	1.556	1.492	0.710	1.771	0.595
	23.3	1.041	1.114	1.146	1.075	1.477	0.345							
88°F	3.3	2.748	2.161	1.869	0.880	2.447	0.510	6.6	2.389	2.076	1.924	0.715	2.255	0.920
	6.6	2.699	2.444	2.322	0.775	2.538	0.666	13.3	2.622	2.288	2.097	0.755	2.502	0.680
	10.0	2.653	2.393	2.650	0.740	2.602	0.640	20.0	2.518	2.176	2.000	0.805	2.404	0.610
	13.3	2.653	2.358	2.204	0.840	2.586	0.595	26.6	2.217	1.903	1.748	0.908	2.184	0.495
	16.6	2.744	2.167	1.881	0.935	2.447	0.510	33.3	0.930	1.161	1.278	1.035	1.525	0.315
	20.0	2.230	1.845	1.663	1.095	2.176	0.370							
	23.3	2.332	1.716	1.342	1.060	2.079	0.410							
78°F	3.3	2.944	2.100	1.681	1.030	2.443	0.435	3.3	2.741	2.525	2.415	0.740	2.708	0.720
	6.6	2.845	2.538	2.380	0.870	2.752	0.645	10.0	2.982	2.431	2.161	0.890	2.695	0.570
	10.0	2.954	2.432	2.198	0.820	2.672	0.600	16.6	2.699	2.336	2.146	0.750	2.556	0.635
	13.3	2.602	2.204	2.000	0.900	2.427	0.595	23.3	2.230	1.914	1.764	0.920	2.161	0.545
	16.6	2.544	1.919	1.613	1.000	2.240	0.445	30.0	2.301	1.851	1.644	0.945	2.140	0.500
	20.0	2.380	1.914	1.681	1.090	2.240	0.415	36.6	2.176	1.424	1.176	1.140	1.839	0.330
	23.3	2.447	1.820	1.505	1.170	2.187	0.365							
	26.6	1.230	1.255	1.267	1.080	1.591	0.340							
68°F	3.3	--	1.447	1.447	1.060	1.813	0.180	6.6	--	1.826	1.800	0.980	2.090	0.465
	6.6	--	2.204	1.964	1.070	2.455	0.590	13.3	2.654	2.312	2.146	0.700	2.518	0.650
	10.0	2.447	2.190	2.096	0.705	2.389	0.755	20.0	2.699	2.352	2.176	0.675	2.556	0.725
	13.3	2.462	2.190	2.090	0.705	2.405	0.615	26.6	2.716	2.114	1.813	1.090	2.415	0.490
	16.6	2.432	2.176	2.063	0.855	2.389	0.670	33.3	2.267	1.800	1.568	1.035	2.114	0.420
	20.0	2.602	2.114	1.863	0.842	2.358	0.580	40.0	1.778	1.519	1.398	1.088	1.845	0.405
	23.3	1.477	1.447	1.432	0.992	1.732	0.440							

Table B-3b Properties of Probability Distribution Curves

Temp.	σ_3 = 120 psi							σ_3 = 240 psi						
	$\sigma_1-\sigma_3$	mode	median	mean	σ	τ	P_c	$\sigma_1-\sigma_3$	mode	median	mean	σ	τ	P_c
98°F	13.3	0.832	0.556	0.778	--	0.833	0.550	13.3	--	1.477	1.477	1.155	1.881	0.490
	26.6	2.255	1.826	1.602	1.090	2.126	0.415	26.6	--	1.380	1.176	1.200	1.681	0.460
	40.0	2.342	1.863	1.623	0.935	2.161	0.450	40.0	2.699	1.908	1.544	1.175	2.301	0.360
	53.3	2.097	1.786	1.628	1.005	2.072	0.490	53.3	2.114	1.398	1.079	--	1.733	0.420
	66.6	1.954	1.591	1.398	1.125	1.908	0.430	66.6	2.079	1.623	1.398	0.980	1.954	0.430
	80.0	1.568	1.243	1.079	1.320	1.663	0.335	80.0	1.954	1.690	1.556	0.983	2.000	0.445
								96.7	2.079	1.602	1.362	1.150	1.954	0.375
88°F	13.3	2.041	--	--	--	0.301	--	13.3	1.903	0.954	--	--	1.447	--
	26.6	2.176	1.792	1.602	0.935	2.082	0.470	26.6	1.000	0.919	0.881	1.180	1.255	0.370
	40.0	2.161	1.845	1.699	0.965	2.120	0.500	40.0	2.041	1.602	1.398	0.985	1.892	0.410
	53.3	2.079	1.568	1.322	1.045	1.875	0.445	53.3	2.176	1.634	1.362	1.138	2.008	0.355
	66.6	2.041	1.371	1.079	1.060	1.740	0.370	66.6	2.544	1.748	1.362	1.033	2.130	0.375
	80.0	1.568	0.663	1.568	1.025	0.924	0.365	80.0	2.342	1.658	1.322	1.030	2.041	0.380
								93.3	2.146	1.322	1.301	1.478	1.785	0.295
78°F	13.3	2.371	1.380	1.000	1.190	1.813	0.330							
	26.6	2.505	2.013	1.778	1.055	2.301	0.465							
	40.0	2.398	1.881	1.623	0.990	2.158	0.490							
	53.3	2.279	1.658	1.342	1.108	1.991	0.410							
	66.6	1.954	1.447	1.204	1.150	1.813	0.390							
	80.0	0.362	0.845	1.114	1.118	1.278	0.280							
	93.3	0.000	0.778	1.146	1.033	1.161	0.315							
68°F	13.3	--	1.748	1.097	1.180	2.398	0.440	13.3	1.903	1.672	1.556	1.105	2.012	0.385
	26.6	--	2.255	1.580	1.035	2.532	0.520	26.6	--	1.982	1.924	0.973	2.352	0.390
	40.0	2.255	2.130	2.079	0.705	2.352	0.600	40.0	2.716	2.346	2.161	0.835	2.574	0.615
	53.3	2.699	2.235	2.008	0.855	2.484	0.565	53.3	2.477	2.012	1.778	0.980	2.354	0.420
	66.6	2.301	1.672	1.380	1.095	2.041	0.385	66.6	2.398	1.903	1.653	1.073	2.230	0.415
	73.3	2.176	1.826	1.653	1.065	2.097	0.490	80.0	2.602	1.903	1.568	1.115	2.255	0.410
	80.0	--	1.362	1.097	1.290	1.882	0.300	93.3	2.505	1.763	1.380	1.225	2.114	0.375

Note:

1. Results of σ_3=240 psi and T=78°F are discarded because of leakage.
2. Dimensions of $(\sigma_1-\sigma_3)$ in psi; mode, median, mean and τ are logarithm of time in minute; standard deviation in cycles; and P_c in decimals.

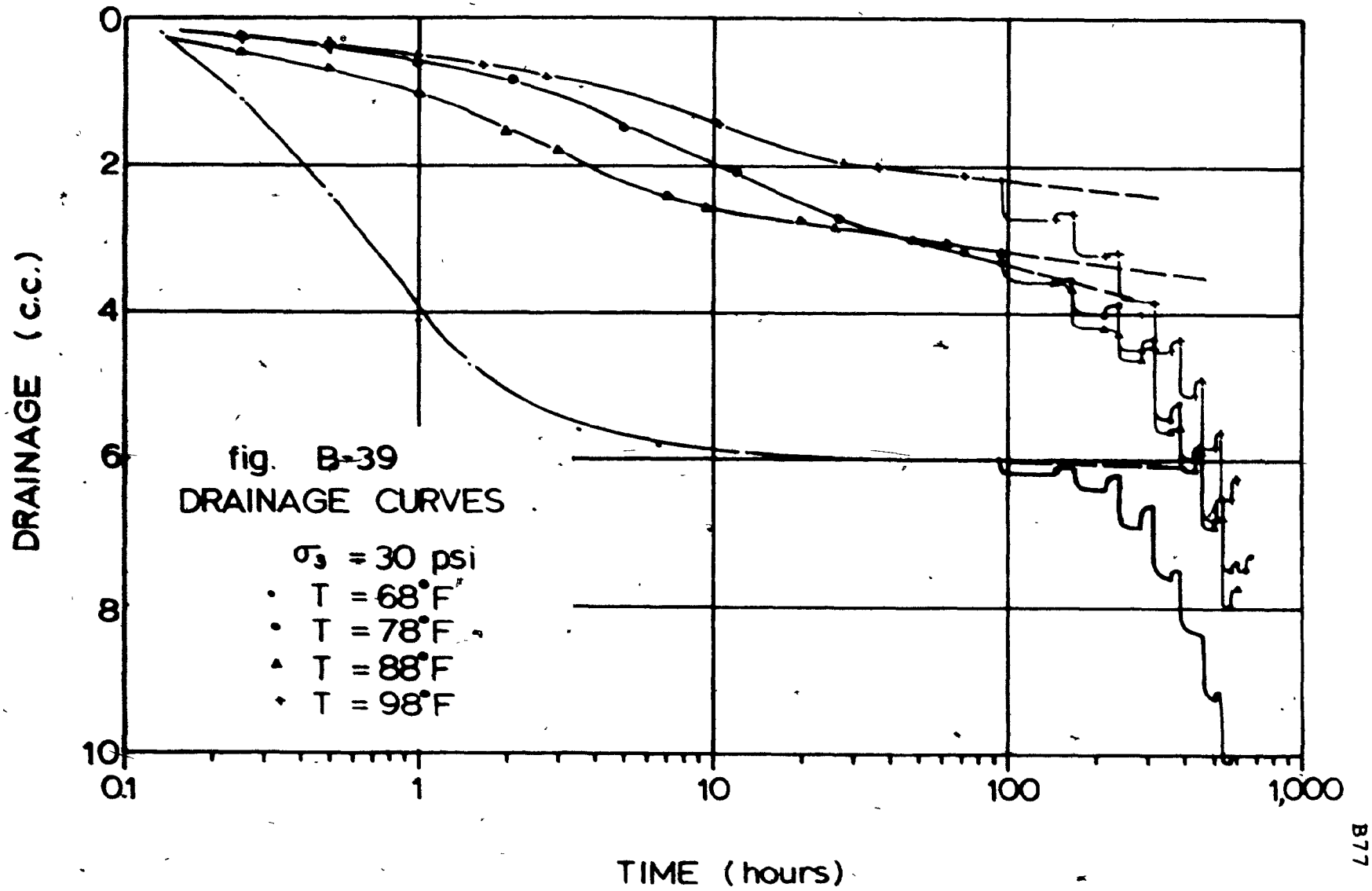
0
2
4
6
8
10
0.1
1
10
100
1,000
DRAINAGE (c.c.)
TIME (hours)
fig. B-39
DRAINAGE CURVES
σ_3 = 30 psi
T = 68°F
T = 78°F
T = 88°F
T = 98°F
877

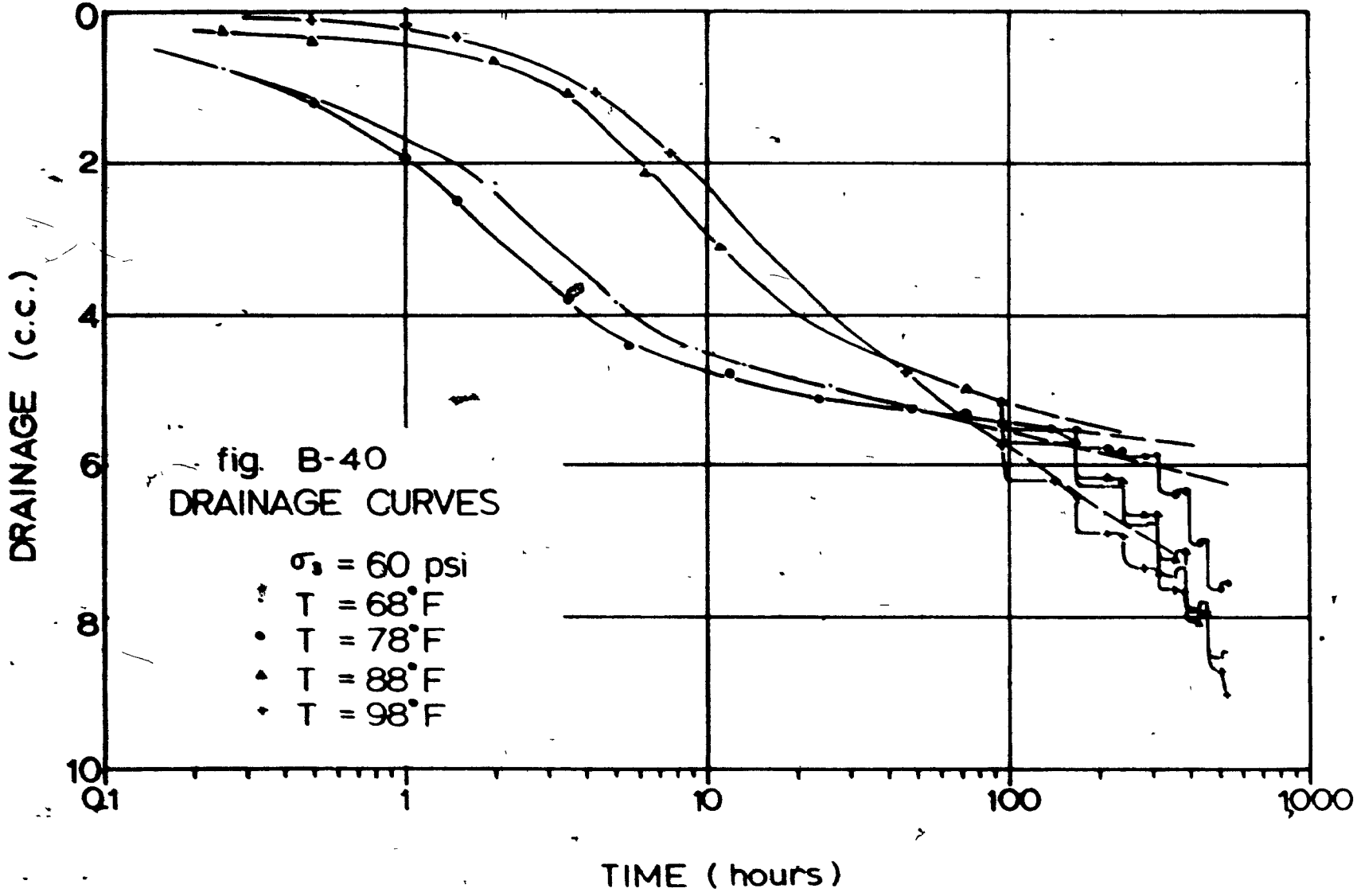
DRAINAGE (c.c.)
0
2
4
6
8
10
0.1
1
10
100
1000
TIME (hours)
fig. B-40
DRAINAGE CURVES
σ_3 = 60 psi
T = 68°F
T = 78°F
T = 88°F
T = 98°F

878

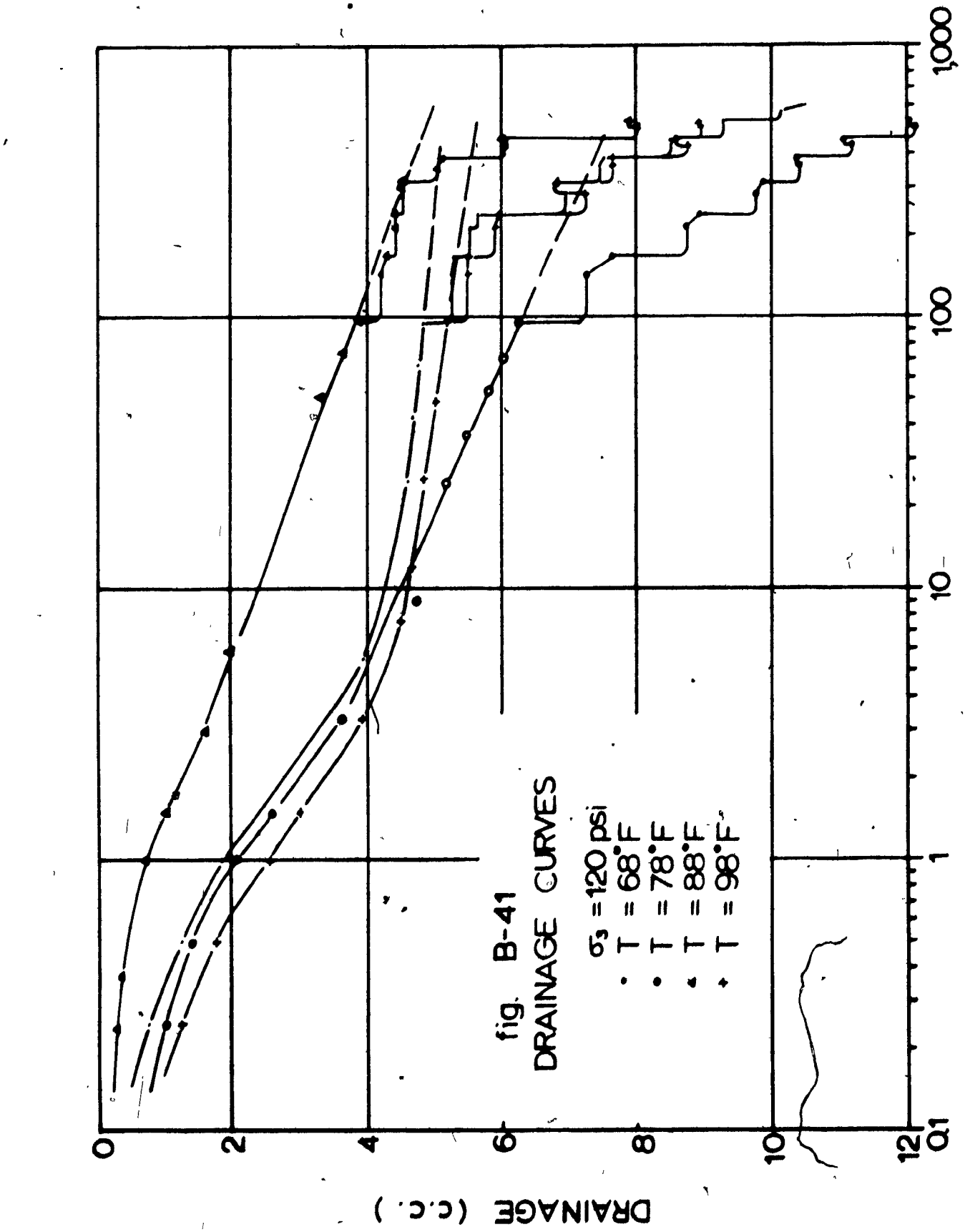

fig. B-41
DRAINAGE CURVES

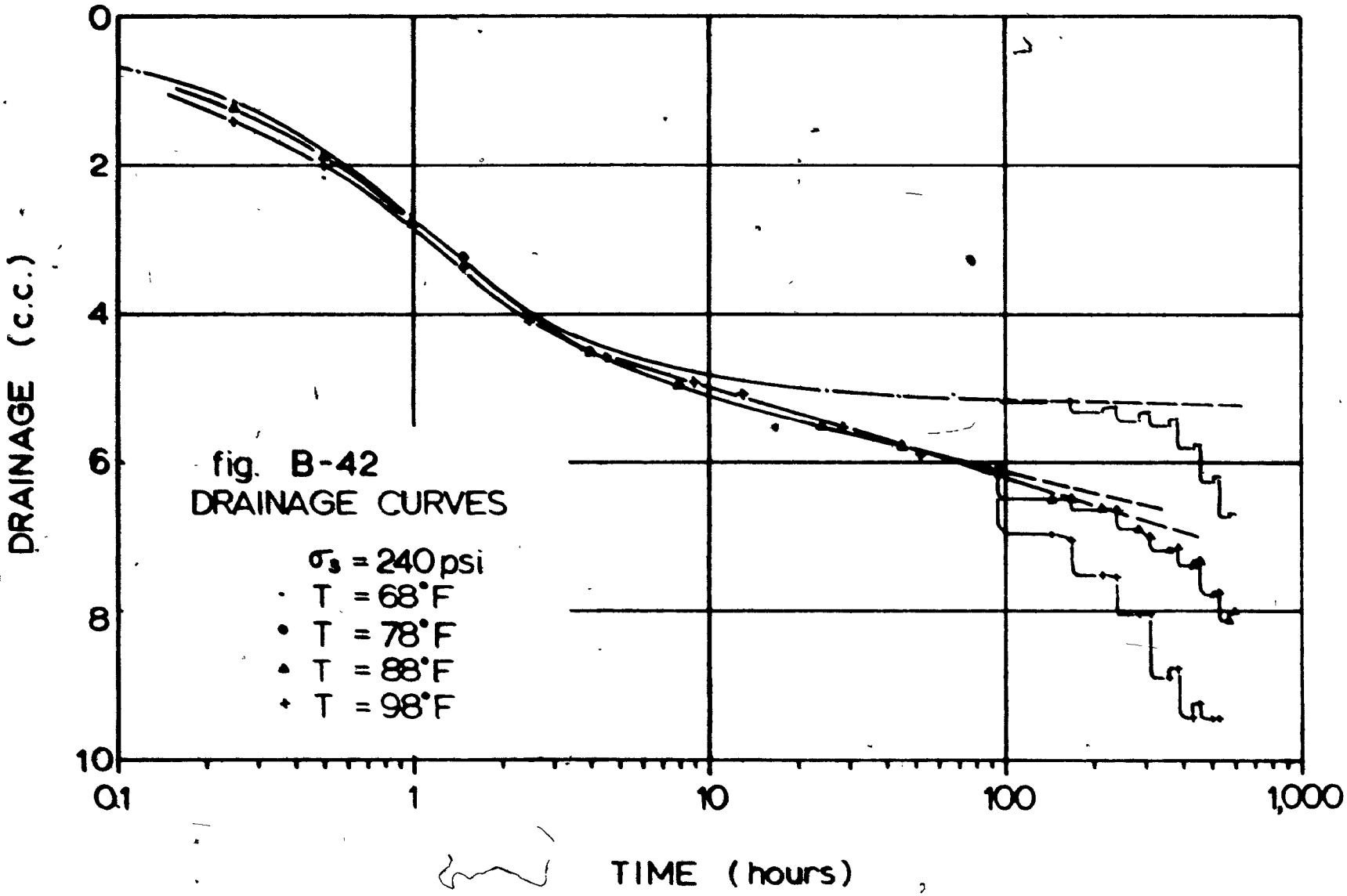

fig. B-42
DRAINAGE CURVES

880

Table P-4a: Component of Axial Strain due to Anisotropic Consolidation

σ_3 (psi)	T (°F)	stress level (%)	ε_t (%)	ΔV (c.c)	$\Delta\varepsilon_c$ (%)	$\varepsilon_t - \Delta\varepsilon_c$ (%)	$\Delta\varepsilon_c/\varepsilon_t$ (%)
30	98	12.5	0.5850	0.5	0.1415	0.4435	24.2
		24.9	0.9511	0.54	0.1528	0.7983	16.1
		37.7	1.5611	0.83	0.2349	1.3262	15.0
		50.2	1.9664	0.65	0.1840	1.7824	9.4
		62.6	2.4820	0.74	0.2094	2.2726	8.4
		75.5	3.4800	0.89	0.2519	3.2281	7.2
		87.9	4.7664	0.90	0.2547	4.5117	5.3
	88	13.5	0.365	0.40	0.1132	0.2518	31.0
		26.9	0.877	0.56	0.1585	0.7185	18.1
		40.8	1.238	0.38	0.1075	1.1305	8.7
		54.3	2.040	1.15	0.3255	1.7145	16.0
		67.8	2.440	0.40	0.1132	2.3268	4.6
		81.6	3.482	1.13	0.3198	3.1622	9.1
		95.1	3.369	1.20	0.3396	3.0294	10.1
	78	11.8	0.2591	0.24	0.0679	0.1912	26.2
		23.6	0.5592	0.51	0.1443	0.4149	25.8
		35.7	1.1677	0.62	0.1755	0.9922	15.0
		47.5	1.7600	1.07	0.3028	1.4572	17.2
		59.3	2.3600	0.92	0.2604	2.0996	11.0
		71.4	3.1200	1.10	0.3113	2.8087	10.0
		83.2	3.9396	1.00	0.2830	3.6566	7.2
		95.0	5.7422	1.02	0.2887	5.4535	5.0
	68	11.0	0.3281	0.20	0.0566	0.2715	17.3
		22.0	0.6745	0.30	0.0849	0.5896	12.6
		33.3	1.3427	0.70	0.1981	1.1441	14.8
		44.3	2.0564	1.00	0.2830	1.7734	13.8
		55.3	2.2777	0.80	0.2264	2.0513	9.9
		66.6	2.9485	0.82	0.2321	2.7464	7.9
		77.7	5.0094	1.02	0.2887	4.7207	5.8

Table B-4h: Component of Axial Strain due to Anisotropic Consolidation

σ_3 (psi)	T (°F)	stress level (%)	ε_t (%)	ΔV (c.c)	$\Delta\varepsilon_c$ (%)	$\varepsilon_t - \Delta\varepsilon_c$ (%)	$\Delta\varepsilon_c/\varepsilon_t$ (%)
60	98	8.4	0.6571	0.50	0.1415	0.5156	21.5
		25.3	1.0100	0.47	0.1330	0.8770	13.2
		42.0	2.0961	0.44	0.1245	1.9716	6.0
		59.0	2.5518	0.19	0.0538	2.4980	2.1
		75.9	4.5611	0.25	0.0708	4.4911	1.6
		92.7	9.3577	0.84	0.2377	9.1195	2.5
	88	16.5	0.4884	0.34	0.0962	0.3922	19.7
		33.3	1.1118	0.44	0.1245	0.9873	11.2
		50.0	1.8862	0.41	0.1160	1.7702	6.1
		66.5	2.6048	0.67	0.1896	2.4152	7.3
		83.3	4.9647	0.95	0.2689	4.6953	5.4
	78	7.9	0.1440	0.03	0.0085	0.1355	5.9
		23.8	0.3637	0.25	0.0708	0.2929	19.5
		39.5	1.2126	0.08	0.0226	1.1900	1.9
		55.5	2.0197	0.49	0.1387	1.8810	6.9
		77.4	2.5757	0.71	0.2009	2.3748	7.8
		87.1	3.7378	0.59	0.1670	3.5708	4.5
	68	16.1	0.3760	0.14	0.0396	0.3364	10.5
		32.4	1.0290	0.53	0.1500	0.8790	14.6
		48.8	1.2680	0.50	0.1415	1.1365	11.2
		64.9	1.9130	0.72	0.2038	1.7092	10.6
		81.2	2.7180	0.55	0.1557	2.5623	5.7
		97.6	3.9240	0.73	0.2066	3.7174	5.3

Table B-4c: Component of Axial Strain due to Anisotropic Consolidation

σ_3 (psi)	T (°F)	stress level (%)	ε_t (%)	ΔV (c.c)	$\Delta\varepsilon_c$ (%)	$\varepsilon_t - \Delta\varepsilon_c$ (%)	$\Delta\varepsilon_c/\varepsilon_t$ (%)
120	98	12.7	0.3724	0.32	0.0906	0.2818	24.3
		25.3	0.7046	0.40	0.1132	0.5914	16.1
		38.1	1.5220	1.24	0.3509	1.1711	23.1
		50.8	2.0946	0.83	0.2349	1.8591	11.2
		63.4	2.9080	1.11	0.3141	2.5939	10.8
		76.2	3.3000	0.40	0.1132	3.1868	3.4
	88	11.6	0.6157	0.27	0.0764	0.5393	4.7
		23.1	0.9682	0.15	0.0425	0.9257	4.4
		34.8	1.8640	0.08	0.0226	1.8414	1.2
		46.3	2.4005	0.45	0.1274	2.2731	5.3
		57.9	3.6981	0.94	0.2660	3.4321	7.2
		69.6	5.7706	2.01	0.5688	5.2018	9.9
	78	11.6	0.4957	0.99	0.2802	0.2155	56.6
		23.1	1.0329	1.06	0.3000	0.7329	29.0
		34.8	1.7875	0.84	0.2377	1.5498	13.3
		46.3	2.3952	0.55	0.1557	2.2395	6.5
		57.9	3.1950	0.79	0.2236	2.9714	7.1
		69.6	4.5750	1.04	0.2943	4.2816	6.4
		81.2	5.4285	0.54	0.1528	5.2757	2.8
	68	14.8	0.7687	0.44	0.1245	0.6438	33.8
		29.6	0.7552	0.24	0.0679	0.6872	9.0
		44.4	1.4784	1.28	0.3622	1.1622	23.8
		59.2	1.9602	0.63	0.1783	1.7819	10.1
		74.0	2.6172	0.99	0.2802	2.3371	10.7
		81.4	2.7519	0.75	0.2123	2.5396	7.2
		88.9	3.4041	0.87	0.2462	3.1579	7.2

Table B-44: Component of Axial Strain due to Anisotropic Consolidation

σ_3 (psi)	T (°F)	Stress level (%)	ε_{ec} (%)	ΔV (c.c)	$\Delta\varepsilon$ (%)	$\varepsilon_c - \Delta\varepsilon_c$ (%)	$\Delta\varepsilon_c/\varepsilon_c$ (%)
240	98	10.4	0.2525	0.79	0.2212	0.0300	87.6
		20.8	0.3235	0.43	0.1204	0.2000	37.2
		31.3	0.5496	0.52	0.1456	0.4040	26.5
		41.6	0.6947	0.84	0.2352	0.4595	33.9
		52.0	0.8567	0.66	0.1848	0.6721	21.5
		62.5	1.2085	0.21	0.0588	1.1497	4.9
		75.5	1.6881	0.41	0.1148	1.5733	6.8
	88	10.2	0.0730	0.36	0.1008	--	--
		20.3	0.2242	0.14	0.0392	0.1850	17.5
		30.5	0.3925	0.27	0.0756	0.3169	19.3
		40.7	0.7001	0.18	0.0504	0.6497	7.2
		50.8	1.1755	0.25	0.0700	1.1055	6.0
		61.1	1.8371	0.45	0.1260	1.7111	6.9
		71.2	2.0114	0.38	0.1064	1.9050	5.3
	68	9.9	0.2867	0.01	0.0028	0.2839	0.8
		19.7	0.3259	0.19	0.0532	0.2727	16.3
		29.6	0.5582	0.21	0.0588	0.4994	10.6
		39.5	0.6680	0.21	0.0588	0.6092	8.8
		49.3	1.0524	0.40	0.1120	0.9404	10.6
		59.3	1.2271	0.49	0.1372	1.0899	11.2
		69.1	1.4925	0.53	0.1484	1.3441	9.9